UNIVERSITY OF BERGAMO

School of Doctoral Studies

Doctoral Degree in Analytics for Economics and Business

XXXI Cycle

SSD: SECS-S/06

Mathematical methods of economy, finance, and actuarial science

MODELS AND METHODS FOR ELECTRICITY AND GAS MARKETS IN A LOW-CARBON ECONOMY

Advisor

Chiar.ma Prof.ssa Giorgia Oggioni

Doctoral Thesis

Luigi BOFFINO

Student ID 1038991

Academic year 2017/18

Contents

List of Figures

Chapter 4

Chapter 4

Chapter 5

List of Tables

Chapter 2

Chapter 3

Chapter 4

Chapter 5

Abstract

Human activity is overloading the atmosphere with carbon dioxide and other greenhouse gas emissions, which trap heat and drive up the planet temperature, resulting in a negative impact on our health, environment, and climate. Governments are considering actions to curb climate change that will significantly change both electricity and gas markets. This thesis detects these issues and proposes models and methods to analyze how electricity and gas markets can contribute to the achievement of the decarbonization targets. Among the actions carried out to reduce carbon emissions, renewable energy penetration is the most effective one. However, the integration of wind and solar power plants in electric energy systems is extremely challenging because of the uncertainty and variability that characterize their electricity production. To accommodate the stochasticity of the renewable energy production, power systems need to be more flexible. This flexibility is provided by backup capacity in the form of reserves, which are provided by dispatchable units such as thermal plants, or batteries and storage devices, which represent an environmentally friendly solution.

Considering this framework, in the first part of this thesis, two expansion planning models to efficiently integrate renewable power plants, storage units, and electric vehicles in electric energy systems are proposed. We first want to detect which are the investment choices that have to be taken by a Market Operator to deeply decarbonize electric power system. To this aim, we propose a two-stage stochastic programming model to determine the optimal mix of generation and transmission capacity to build, taking into account both technical constraints and climate-related considerations. The model uses a mix of ac and high-voltage dc transmission lines, conventional and renewable generation, and energy-storage units to meet these objectives. Short- and long-term uncertainties are modeled using operating conditions and scenarios, respectively. Secondly, we take the view of a Distribution System Operator and we propose a stochastic adaptive robust optimization approach for the expansion of a small size electricity system problem. This involves the construction of candidate renewable generating units, storage units, and charging stations for electric vehicles. In this case, long-term uncertainty is modeled using confidence bounds, while short-term uncer-

tainty is represented through a number of operating conditions.

Gas-fired power plants represent the energy choice that can help to achieve a secure, competitive, and decarbonized power systems since they can significantly contribute to emission reduction by replacing high carbon fuels in electricity generation. In addition, these units are the ideal partner for variable renewable energy, providing back up to wind and solar. In the last years, Europe has taken the lead in the decarbonization policies and has imposed a strict carbon reduction target that has to be achieved by 2050. For all these reasons, in the second part of the thesis, we focus our attention on the European gas market and we detect two important issues that can affect its stability. The first one regards the re-negotiation of the long-term gas contracts invoked by European mid-streamers and the second one concerns the security of external supply. The need of re-negotiation arises from the fact that, in Europe, gas is sold according to two main methods: oil-indexed long-term contract and hub pricing. The fall of the European gas demand combined with the increase of the US shale gas exports and the rise of liquefied natural gas availability on international markets have led to a reduction of the European gas hub prices. Since oil-indexed long-term contracts have failed to promptly adjust their positions, European gas mid-streamers asked for a re-negotiation of their existing contracts to obtain new contracts linked to hub spot prices. In this thesis, we tackle this problem by estimating the dependence risk and the optimal resource allocation of the underlying assets of a gas long-term contract through pair-vine copulas and portfolio optimization methods, using different risk measures. We also investigate the risk of external supply because Europe mainly relies on imports from economically or politically unstable countries to cover it gas demand since the local production is very limited. The analysis of the external supply risk is focused on the Italian gas market whose demand is covered by 90% by imports from foreign countries. An optimization problem that describes the equilibrium state of a gas supply chain, where producers, mid-streamers, and final consumers exchange natural gas and liquefied natural gas both with long-term contracts and on spot markets is developed for this purpose.

Chapter 1

Introduction

ENERGY is the milestone of modern society and its supply has a direct impact on the economic and social development of nations. Indeed, there is a very powerful link between economic growth and energy consumption. An optimal energy supply improves the quality of our lives, works and activities. In general, energy resources have not been in places where high consumption has developed, which implied the construction of reliable networks to transport it and stimulated cooperation between parties for energy supply. As a result energy management has now become a form of international political power. This thesis analyzes both the electricity and gas markets investigating their transformation needed to the meet carbon emission reduction goals adopted by 195 Countries in Paris in 2015, after the International Climate Conference.

In this chapter, we provide an introduction to the thesis work. First, we present an overview of the electricity market, which includes a description of the restructuring process of the electricity sector and of the structure of the electric power system, an explanation of the functioning of the principal electricity markets and a review of the most relevant market agents. Second, we present an overview of the gas market, providing a summary of the deregulation process, a description of the structure of the gas supply chain and its participants, and an explanation of the functioning of the principal gas markets. Third, we present an overview of the decarbonization process and we analyze the role played by electricity and gas in the achievement of a low-carbon economy; we also describe all the technologies used in the models developed in this thesis. Fourth, a general overview of the methodologies used in this dissertation is provided. Finally, we provide the thesis objectives and organization.

1.1 Electricity Market

1.1.1 History

The electricity market is the place where transactions involving electricity are conducted. Historically, because of its special characteristics, electricity has been regarded to be a public service. This approach justified, in the early days, a vertical integrated monopolistic structure of this sector.

In these "traditionally" regulated structures, a public institution or a single regulated company was in charge of the complete organization of the electricity supply chain, represented by generation, transmission, distribution and consumption of electric energy. Under this scheme, the relations between different electric utilities were generally characterized by voluntary cooperation in a number of areas, such as joint management of operating reserve capacity, exchange for emergency reasons and third-party use of grids for current transmission and distribution under terms negotiated by the parties concerned (see Gomez-Exposito et al. (2018)).

However, the lack of competitions often generated disparities in the cost of electricity between regions and caused technological stagnation besides influencing market transparency. For these reasons, in the 80's several regions started their restructuring process toward liberalization (see Sioshansi and Pfaffenberger (2006)). Chile is recognized as a pioneer in this process because in 1982 separated the basic activities involved in the provision of electric power. Anyway, Fischer et al. (2000) argue that the Chilean system has involved less restructuring, less competition and more regulation than first meets the eyes since, for many years, a single holding company owned the largest generating company, the primary distribution company in the Santiago region and the primary transmission company serving the largest region of the country. Similar reforms where not introduced anywhere else until 1990, when the electricity industry was much more radically transformed in England and Wales which create the first electricity pool. Shortly thereafter, it was the turn of Argentina and Norway (1991) followed by many countries of Latin America and in Europe, as well as many States of the Northern America. In all these deregulation processes, the underlying idea was always the same: unbundling generation, transmission and retailing activities.

1.1.2 Electric Power System Structure

The structure of the electricity sector can be divided into four main components: **production**, **transmission** (high voltage network), **distribution** (low voltage network), and **consumption** (see Gomez-Exposito et al. (2018); Von Meier (2006)).

Production centers generates electricity at voltage of several kilovolts ranging tipically from 6 kV to 33 kV. These values allow finding a good compromise between conductor size and insulation. In fact, the first one depends on current level, while insulation depends on the voltage level of the device. The power is then immediately transformed to voltage of hundred of kilovolts (from 132 kV to 700 kV) to optimize long-distance transmission reducing the line losses. The **transmission** grid interconnects all the major production and consumption centers forming a very dense network which ensures high reliability also in the case of failure of few lines. Electric substations represent communication nodes and can lower or increase the voltage. Moreover they are also centers where system measurement, protection, interruption and dispatch equipment are sited. **Distribution** networks are composed of low voltage transmission lines, which bring electric power to consumers adapted to their needs (from 20.000 V to 220 V). The configuration of these grids is usually radial. **Consumers** connect to the voltage level that best suits their power needs, i.e. highly energy-intensive industries connect directly to the high voltage grid while small consumers are connected to the low voltage grid. For a similar principle, generating stations with a very small output can feed their electric power directly into the distribution network. Figure 1.1 provides a scheme of the electric power system structure.

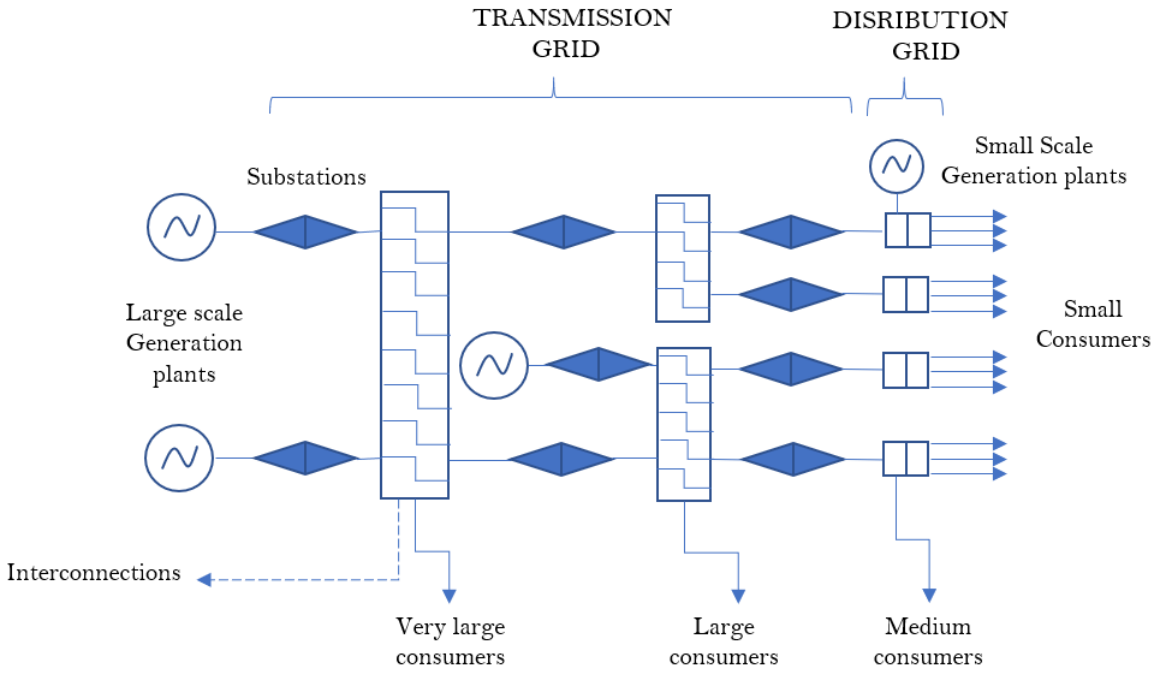

Figure 1.1: Electric Power System structure

1.1.3 Market organization

Generators, consumers and retailers can trade electricity on two main trading arenas: a **Pool** for short-term transactions and a **Futures market** for medium-term or long-term transactions (see Conejo et al. (2010)). To ensure the security of system operation and energy delivery the **Ancillary Services markets** are also needed. **Capacity market** is instead needed to provide sufficient reliable future capacity. A more detailed description of these mechanisms is provided below.

- **Pool**
  The pool includes the *day-ahead market*, *intraday market* (not in the USA) and the *balancing market*. Most of the energy is traded on the *day-ahead market* which covers the 24 hour horizon before the real time operation. The *intra-day market* generally operates after the closure of the day-ahead market and is cleared closer to delivery day. Because the forecasts on renewable sources production become more accurate when approaching to the real time operation, non-dispatchable units, mainly represented by solar and wind power plants (see Section 1.1.4), tend to rely more on the intraday market which have proven to be critical in accommodating large amounts of stochastic production (see Herrero et al. (2018)). The *balancing markets* are used to correct the real-time disparities that may arise between generation and demand due to equipment failures, load deviations or intermittent nature of some sources (e.g. wind or solar production).
  In the *day-ahead market* producers submit offers to the pool with their associated minimum selling price. At the same time, the retailers and consumers submit bids and their maximum buying price. The Market Operator collects purchase bid and sale offers and clears the day-ahead market using an appropriate market clearing procedure.
  The *day-ahead market* is cleared once a day, one day in advance and on an hourly basis. This procedure results in market clearing prices as well as production and consumption schedules. If the transmission grid is not considered in the market clearing procedure, then the resulting price is the same for all consumers and producers. Otherwise, if transmission network is taken into account, a location marginal price (LMP) is associated with each node of the power system. These prices may differ from each other due to line losses and/or congestions.
  The *intraday market* are either based on several successive auctions or on continuous trading mechanisms.
  The *balancing market* provides energy to cover both generation excess and deficit, settling deviations from the previous schedules.

- **Futures market**
  In this market the energy is traded for delivery on a specified future date that range from one week or several years in advance. In order to do this, the participants buy or sell derivative products.[1] Thus, future markets are useful if the price of electricity is highly uncertain in the pool. This is the case of the electricity pool prices, which show high volatility, high percentage of outliers and other sources of uncertainty. Within this framework the future market represent a tool to hedge against the risk for both producers and consumers. On the future market, is it possible to subscribe different types of derivative products which includes, among the others, *bilateral contracts* and *options* (see Conejo et al. (2010)).
  A *bilateral contract* is an agreement between two parties to exchange electric power under a set of specified conditions such as MW amount, time of delivery, duration, and price. Bilateral contracts can take the form of futures or forward contracts according to the market where they are traded (see El Khatib and Galiana (2007)). The former are generally traded in an exchange, and can be traded continuously up until their time of delivery. In contrast, forward contracts are typically negotiated in a Over The Counter (OTC) market directly between the load and generator with the terms of the contract remaining fixed until the time of delivery.
  An *option* is an agreement for having the choice of delivering or consuming a specified amount of electricity in a future time period. In order to subscribe such agreement it is required to pay a premium, regardless of the eventual future deliver or consumption of energy.

- **Ancillary services markets**
  The ancillary services markets provide all the services necessary for the operation of a transmission and distribution system. This markets are operated to guarantee reserve procurement and congestion management. The Network Codes[2] adopted in the European electricity market divide the ancillary services managed by the Transmission System Operator into *frequency* ancillary services, which deal with the balancing of the system and *non-frequency* ancillary services, which include voltage control and black-start capability. All these services are explained in the following:

  – Frequency containment reserves (FCR) includes operating reserves necessary

[1] A derivative is a financial security with a value that is reliant upon or derived from an underlying asset or group of assets. The derivative itself is a contract between two or more parties based upon the asset or assets. Its price is determined by fluctuations in the underlying asset. Hull and Basu (2016)

[2] See: https://www.entsoe.eu/network_codes/

for constant containment of frequency deviations (fluctuations) from nominal value in order to constantly maintain the power balance in the whole synchronously interconnected system. This category typically includes operating reserves with the activation time up to 30 seconds. Operating reserves of this category are usually activated automatically and locally.

- Frequency restoration reserves (FRR) indicate active power reserves available to restore system frequency to the nominal frequency and to restore power balance to the scheduled value. This category includes operating reserves with an activation time typically between 30 seconds up to 15 minutes (depending on the specific requirements of the synchronous area). FRR replace FCR if the frequency deviation lasts longer than 30 seconds. FRR can be distinguished between reserves with automatic activation (aFRR) and reserves with manual activation (mFRR).
- Replacement reserves (RR) indicate the active power reserves available to restore or support the required level of frequency restoration reserve (FRR) to be prepared for additional system imbalances, including generation reserves. This category includes operating reserves with activation time from 15 minutes (in Continental Europe) up to hours.
- Voltage is controlled to operate the network within the voltage ranges and to maintain voltage stability. Voltage requirements are critical to secure planning and operation of a power system within a synchronous area. Reactive power helps the power grid maintain voltage levels. The reactive power can be defined as the difference in the phase between the voltage and current, or what additional voltage would be needed to restore the system to being in phase. Reactive power and real power (the power we actually consume) are substitutes in production. Markets Operators usually require generator to produce to reactive power when requested, with any foregone real power consumption compensated based on opportunity cost.
- Black start is the capability of a power plant to start itself independent of the power grid. Some power plants have on-site generators that can be used to start the main turbine generator spinning. Others actually take electricity from the power grid for this purpose. Power plants that provide black start capability agree to keep an on-site generator or other grid-independent power source ready to operate. In the case of a large blackout, these power plants will start themselves up using their on-site generation, and feed power into the grid so that other plants can start up and restore electricity service.

- **Capacity market**
  The capacity market provides payments to power plants as an economic incentive to commit to being able to produce electricity at some point in the future, in addition to day-ahead/real-time energy and ancillary services. Capacity payments are designed to ensure that consumers continue to benefit from reliable electricity supplies at an affordable price. These payments can be received by existing power plants who promise to stay operational in the future, or by new power plants that commit to be finished with construction and operational by a certain date. Since capacity payments are received by generators regardless of whether the power plant actually produces any electricity, they represent a very attractive profit especially when market prices in the day-ahead and real-time energy markets are low.

1.1.4 Partecipants

The main agents participating in a restructured electricity market are introduced below (see Conejo et al. (2010); Shahidehpour et al. (2003)). They can be divided into non-institutional and institutional market agents. Among the non-institutional market agents we find:

- **Producers**
  These agents own generation facilities that produce electricity or interact on behalf of plant owners with the markets. They are also called generating companies (GENCOs). Besides producing electricity they are also in charge of investments, operation, and maintenance of their generation facilities with the objective of maximizing their profits. It is possible to distinguish two different types of generating units owned by producers: dispatchable and non-dispatchable ones. *Dispatchable* units, mainly represented by conventional power plants such as coal and gas-fired units, provides reserves and regulatory capacity in addition to participating to the day-ahead and intraday markets. *Non-dispatchable* units are wind and solar power plants that, which due to their uncertain and intermittent production cannot actively participate to the ancillary services markets.

- **Consumers**
  They are the end-users of the electricity. In general, large consumers can directly buy energy from the electricity markets, while small consumers mainly purchase electricity from the retailers. Their aim is to minimize their procurement costs or maximize the utility that they obtain from consuming electricity.

- **Retailers**
  They are intermediaries who trade energy between producers and consumers. They buy electricity in the pool or in the futures markets and make profit by selling it to the consumers.

Institutional markets agents include:

- **Market Operator (MO)/Power Exchange (PX)**
  It is the entity responsible for the economic management of the electricity market. It enforces the market rules and clears the markets, providing the final prices and the traded quantities.

- **Transmission System Operator (TSO)**
  It is the entity in charge of maintenance and expansion of the transmission infrastructures used to transport the electric energy. It provides grid access to the electricity market players, according to non-discriminatory and transparent rules. Generally it also manages the reserve procurement and the balancing market.

- **Independent System Operator (ISO)**
  It is the entity in charge of both the economical and technical management of the whole power system.

- **Market Regulator/National Regulatory Authority**
  It is the entity that oversees the electricity market, ensuring its competitive and adequate functioning.

In non-restructured or traditionally regulated markets, as in some parts of the USA like Southeast, Southwest (except California) and Northwest, vertically integrated utilities are still responsible for the entire flow of the electricity to consumers.[3] In other USA markets such as the PJM interconnection, the ISO-New England or the Californian CAISO, there is only a single entity, the ISO, who is in charge of both technical control and economic management of the system, while the transmission network is still owned by the vertically-integrated company. In Europe the economic management and the technical control of the power system are separated and managed by PXs and TSOs, respectively. For instance, considering the Italian electricity market GME (Gestore dei Mercati Energetici) acts as PX and Terna as TSO who is also in charge of managing the ancillary services markets (Mercato del Servizio di Dispacciamento). ARERA (Autorità di Regolazione per Energia Reti e Ambiente) is instead the Market Regulator (see GME (2009)).

[3] See: https://www.epa.gov/greenpower/us-electricity-grid-markets

1.1.5 Networks

In this thesis, we consider both transmission and distribution networks. As mentioned in Section 1.1.1, the main difference concerns the voltage, which is high in the first one while medium/low in the latter. Transmission lines can transport more electricity for longer distances with respect to distribution lines, which are shorter and transport electricity locally.

They present also a different topology. Transmission lines have usually a so-called "Network" configuration: in a network, any two points are usually connected by more than one path, meaning that some lines form loops within the system. This system is designed so that power can be injected at various locations and power can flow in different directions along the major transmission lines (bi-direction). This feature is important because since there are multiple paths for power to flow, if one transmission line is lost for any reason, all the load can still be served.
Distribution lines have usually radial configuration which means that lines branch out sequentially and power flows strictly in one direction. This property is crucial in the context of circuit protection, i.e. the interruption of circuits or isolation of sections in the event of a problem or fault. Circuit breakers can be located to isolate immediately upstream of the problem, interrupting service to all downstream components. Radial systems present also an economic advantage: smaller conductor sizes can be used toward the ends of the feeders, as the remaining load connected downstream diminishes (see Von Meier (2006)). Anyway, in the last few years Distributed Generation (DG) is being introduced on distribution networks. DG is a small-scale set of technologies (mostly renewable) dedicated to produce electricity close to final user. DG allows power loss reduction, distribution costs saving, CO_2 reduction and a decrease in the electricity prices. However, it adds production uncertainty and requires bidirectional flows and consequently new protection schemes (see Ackermann et al. (2001)).

Some differences also arise from a physical point of view. Transmission ac lines are based on a three phase supply system, i.e. three wires, mainly for an economic reason: these lines use fewer wires than common sense might suggest, and less conductor capacity than would be required to transmit an equivalent amount of power using only a single phase of ac. Distribution lines can be either three phases, in case of medium voltage or larger properties, or single phase for residential customers (see Von Meier (2006)).

Despite the fact that the transmission system is mostly ac, sometimes it is beneficial to use dc transmission. In this case, the power has to be converted both at the beginning and the tail end of the dc line through relatively costly solid-state devices called thyristors. Dc lines are used for very long distances: the technical reason is that dc

eliminates the problem of a stability limit which poses a power transmission constraint on long lines with a significant inductance. Because its effect depends on ac frequency, inductance is irrelevant for dc, and therefore only the thermal limit (determined by the resistance of the line) applies. Moreover, above a certain line length which varies according to multiple conditions, dc lines become also more economically convenient that ac line. Besides transmitting bulk power over long distances, another application for dc lines in modern power systems is to provide an intertie between two ac systems that are not synchronous, so that power can be shared between these systems. In this thesis, we include both high voltage ac and dc transmission lines. The latter become particularly useful for connecting, also trough undersea cables, large off-shore wind or solar facilities sometimes meant to represent long distance power exchanges among different States or countries.

In Europe, the TSO is responsible for building, maintaining and operating the transmission lines. Most of the European Member States have a unique TSO, which owns most of the transmission grid, but there are some exceptions. For instance, Germany has currently four different TSOs. In addition, from December 2008, the 43 different European TSOs from 36 European Countries signed in Prague a declaration of intent to create the ENTSO-E, i.e. European Network of Transmission System Operators for Electricity that is a supranational entity created to support the implementation of the EU energy and climate policy and to promote closer cooperation across Europe's TSOs. To this aim, the ENTSO-E has introduced, with guidance from the Agency for the Cooperation of Energy Regulators (ACER), the Network Codes for electricity, setting the rules for integrating renewable energy sources (RES) into the power system and creating a single and coordinated European electricity market.[4] In the USA, it is instead possible to find different Regional Transmission Operators (RTOs).

The distribution network is managed by several Distribution System Operators (DSOs), although in some cases, one of more DSOs own the majority of the distribution network. DSOs receive the bulk energy from the transmission grid and distribute it to the consumers in different locations. As for the transmission network, in Europe it exist also a European Distribution System Operators' Association (EDSO) for Smart Grids, which comprises 36 leading European DSOs. The goal is to promote smart grids to achieve the EU's ambitious energy and climate objectives to 2020 and beyond.[5]

[4] See: https://www.entsoe.eu/network_codes/
[5] See: https://www.edsoforsmartgrids.eu/

1.2 Gas Market

1.2.1 History

The natural gas industry involves activities like gas exploration and production, transportation, and delivery. All these activities require large investments and highly specific assets that once are constructed at some locations cannot be removed. Moreover, all the parties involved in these activities are interdependent. Such a complex structure exhibited scale economies, meaning that over a range of output, the per unit cost of their outputs declines as output increases. A single vertically integrated firm would have the lowest cost of production making the natural gas industry as a natural monopoly, as for the electric power industry. Due to its structure, the natural gas sector have been initially publicly owned or economically regulated by governments both in Europe and in the USA. This control has been introduced to prevent such vertically integrated firms to exercise market power to raise prices artificially (see Jess (1997)).

However, economic growth and technological improvements have reduced the importance of scale economies, lowered the cost of collecting large amounts of capital, and changed the perceptions about the potential for economic efficiency. Natural gas industry also faced a number of gas shortages and price irregularities among the different states into the 70's. As a consequence, in parallel to the electricity markets, the natural gas sector started in the 80's a restructuring process toward deregulation.
In the USA, the first step of deregulation was taken in 1978, through the legislation of the Natural Gas Policy Act (NGPA) which abolished some natural gas price ceilings. From that time on, it started a slow restructuring process culminating in the 1992 with the FERC Order 636, which introduced mandatory unbundling services in natural gas pipelines and other measures, establishing wholesale competition in the natural gas sector (see Lee (2004)).
In Europe, the deregulation process started in the early 90's. The European Commission issued in 1998 the Directive 90/30/EC concerning common rules for the internal market in natural gas. It was the first of three consecutive gas Directives imposing increasingly explicit and stringent rules to allow the development of gas markets and hubs (see Correljé (2016)). Directive 2009/73/EC, also know as Third Package,[6] unified the different national approaches, enhancing the EU-wide cooperation also through the European Network of Transmission System Operators for Gas (ENTSO-G), founded on January the first 2009, to achieve frictionless cross-border gas trade among European members. Moreover, to maintain a fully functioning and interconnected internal energy

[6] See: https://ec.europa.eu/energy/en/topics/markets-and-consumers/market-legislation

market, ENTSO-G, supported by the Agency for the Cooperation of Energy Regulators (ACER), propose a set of legally binding rules, known as gas Network Codes (see Karan and Kazdağli (2011)).

1.2.2 Gas Industry structure

The natural gas industry consists of three main segments: *up-stream*, *mid-stream*, and *down-stream* (see Correljé (2016)).

In the *up-stream* segment the exploration and the production of gas takes place. Nowdays, natural gas exploration typically begins with geologists examining the surface structure of the earth, and determining areas where it is geologically likely that gas deposits, usually coinciding with oil deposit, might exist. Then, basic seismology is used to run additional tests. As the Earth's crust is composed of different layers, each with its own properties, energy in the form of seismic waves, traveling underground, interacts differently with each of these layers helping to locate underground fossil fuel formations. It is also possible to use magnetometers to measure small differences in the magnetic field and gravimeters, which measure the difference in the gravitational field. Anyway, the best way to gain a full understanding of subsurface geology and to discover the potential natural gas deposits in a given area is to drill an exploratory well. Since this option is expensive and time consuming, it is performed only when there is an high probability to find petroleum/gas formations.
Once gas is located, it is extracted with different procedures according to the composition of the rocks where it is trapped. If the deposit is found in permeable rocks, trapped below impermeable rock, gas can be extracted by drilling down through the impermeable rock into the permeable rock. In the case where gas and oil are trapped in the spaces within impermeable shale rock these has to be fractured to get the gas out with a process known as hydraulic fracturing, commonly called fracking (see Tissot and Welte (2012)). The fluid used to create micro-fractures in the shale is a mixture of water, sand, and additives pumped at high pressure (see Vengosh et al. (2013)).
Once extracted the gas and oil are separated in the refineries, by distillation into fractions with different boiling points which are then further processed. Natural gas, as we use it, is almost entirely methane. However, when we find natural gas underground, it comes associated with a variety of other trace compounds and gases, as well as oil and water, which must be removed.

The *mid-stream* segment involves the transport of the gas to the local distribution grids and the large-scale industrial users and power plants. On a continental scale, generally, the gas is transported via high pressure transmission pipelines. Overseas the gas is transported in tankers as Liquefied Natural Gas (LNG).

A transmission pipeline is made of several components that ensure the efficiency and reliability of the system. Transmission pipes are made of strong carbon steel material and can measure from 12 to 120 centimeters in diameter, depending on their function. To ensure that the natural gas flowing through the pipeline remains pressurized, periodical compression is required along the pipe. This is accomplished by compressor stations, usually placed at 60 to 160 km intervals along the pipeline. Metering stations are also present along the pipe, measuring the gas flow. A great number of valves is present inside the pipe: they work like gateways and if open gas flows freely, otherwise they can be used to stop gas flow along a certain section of the pipe. Finally, centralized control stations collects data from the pipeline components to maintain safety and provide quick response in case of malfunctions, leaks, or any other unusual activity.
LNG is obtained by cooling down natural gas to $-160°$ Celsius. This process, although expensive is useful for transportation because LNG volume is 600 times less than that of gaseous natural gas. Liquefaction has the advantage of removing oxygen, carbon dioxide, sulfur, and water from the natural gas, resulting in LNG that is almost pure methane. It is transported by specialized tanker with insulated walls, and is kept in liquid form by auto-refrigeration. Before usage, it needs to be vaporized to gaseous form through a process call regasification. Boil-off losses usually occur during transportation and storage (see Dobrota et al. (2013); Hasan et al. (2009)), in addition to the ones associated with liquefaction and regasification phases.
Transportation of natural gas is closely linked to its storage: if not immediately required, it can be put into storage facilities for later usage. Since the consumption of natural gas is seasonal, it is usually stored during summer when the request is lower and then withdrawn in winter to meet the higher demand. Gas is usually stored underground in large reservoir that can be: depleted gas reservoir, aquifers, or salt caves. Natural gas is injected into these formations, that have been previously reconditioned to create a sort of storage vessel, building up pressure as more natural gas is added. The higher the pressure in the storage facility, the more readily gas may be extracted. Once the pressure drops to below that of the wellhead, there is no pressure differential left to push the natural gas out of the storage facility. This means that, in any underground storage facility, there is a certain amount of gas that may never be extracted. This is known as physically unrecoverable gas and it is permanently embedded in the formation. In addition to underground storage, gas can also be stored as LNG in appropriates tanks.

In the *down-stream* segment the local distribution grids deliver the gas to consumers. The distribution process is similar to the transportation one, but involves moving smaller volumes of gas at much lower pressures over shorter distances to a great number of individual users. Smaller-diameter pipes are used to transport natural gas to

individual consumers from the so-called "citygates", which are the delivery points where the natural gas is transferred from a transmission pipeline. Distributions pipes are usually made of highly advanced plastic, because of the need for flexibility, versatility and the ease of replacement.

1.2.3 Market Organization

To obtain supplies of natural gas, energy companies, storage operators, traders, and other market participants involved in all or in parts of the gas chain use the wholesale markets. This is composed by two different trading arenas: the **Spot market** for short-term transaction and the **Futures market** for medium or long-term transactions. Outside of the wholesale markets, Long-Term Contracts on OTC markets are largely diffused.

Wholesale gas trading points are usually located at physical or virtual gas hubs, where buyers and sellers can trade in natural gas. While "citigates" are distribution points for a city, a physical hub is a major shipping, distribution, and delivery point, which may have significant storage capacity, connections with onshore and offshore gas pipelines, and infrastructures to off-take or load LNG cargoes. In a physical hub, such as the Henry Hub in the USA or Zeebrugge in Belgium, traders are required to bring the gas there and parties are required to book the same quantity for both entry and exit on a point-to-point transaction mode, assuming that pre-agreed gas injected into the network at one point will be taken off at a predetermined location.
On the other side, a virtual hub is defined through a pipeline grid (interconnected pipelines with no point of origin or end) representing the entire country or a trans-regional zone, managed by a TSO. All the gas within the virtual hub can be traded, irrespective of its actual physical location. Individual buyers and sellers can book different quantities for entry and exit into the system without a predetermined destination, thus increasing the trading flexibility compared to a physical hub. For this reason, virtual hubs are generally more suitable for countries short of domestic natural gas supply and relying on various sources of supplies, including LNG imports. To be considered mature, an hub should fulfill five main requirements: liquidity, volatility, anonymity, transparency, and traded volumes. A mature hub is able to develop a reliable forward curve that can be used for risk management purposes. The final stage of maturity is when the hub is sufficient liquid to trade specific traded products such as indices pricing their physical transactions (see Heather (2015); Rademaekers et al. (2008)). In Europe, only the National Balancing Point (NBP) in the UK and the Dutch Title Transfer Facility (TTF) in the Netherlands can be considered mature with enough level of liquidity. The German hubs NetConnect Germany (NCG) and

Gaspool are closer to NBP and TTF in terms of performance transactions, while all other hubs need to be further developed (see ACER (2015)).

- **Spot Market**
  The spot market generally includes a *day-ahead* gas market, an *intraday* gas market, a *locational* market and a regulated market for the *trading of stored gas*. This is also the design applied to the Italian gas market whose details are provided in the following.
  On the *day-ahead* gas market, offers and bids related to the three gas-days after that of the trading session opening are selected. Transaction takes place in accordance with the continuous trading mode in which orders are executed according to price and time entered.
  On the *intraday* gas market, offers and bids related to the gas-day corresponding to that of trading session opening are selected. Also here, transaction takes place in accordance with the continuous trading mode.
  On the *locational* market, authorized users supply the gas TSO with quantities of gas needed to manage the physical demands within the balancing zones or deviations provided between overall injections and withdrawals on the network. The sessions of this market are held only upon request of the TSO and transactions take place in the form of auction trading.
  On the market for *trading stored gas*, all bids and offers of gas stored are traded by authorized users and by the TSO. Transactions take place in the manner of auction trading.

- **Futures Market**
  To minimize the risks inherent to spot trades, market participants sign *futures* contracts to buy and sell gas to be supplied in future months, quarters, seasons or years, at a price negotiated on the contract date. To make trading easier, these futures apply to standardized products, for example, the supply of 1 MWh for each gas day during the delivery period. Futures represent the average of the expected spot prices over a longer period, making them generally less volatile than spot products. They are used as a basis for determining the prices paid by end-consumers.
  As in the electricity market, it is also possible to buy *options*, an agreement for having the choice of delivering or consuming a specified amount of gas in a future time period. In some markets the TSO subscribes long term options to buy/sell flexible gas quantities for balancing purposes (see ENTSO-G (2012)).

- **OTC markets**
  The most common bilateral contracts on OTC markets are *Long-Term Natural*

Gas Contracts (LTCs), which commit producer and buyer over long durations, usually 20-25 years and were the most commonly used supply agreements in the gas sector, generally considered necessary to guarantee the security of supply. Historically, LTCs have been characterized by quantity and price clauses. The Take or Pay (TOP) quantity clause obligates the mid-streamer to take a certain quantity of natural gas or to pay for it. The price clause makes the LTC price linked to a bundle of oil-products (price indexation) to grant price stability to the producers and hence reduce their risk on investments. For this reason, gas infrastructures have been often developed taking into account the LTCs in place (see Abada et al. (2017)).

Considering the current organization of the gas market at international level, we can observe that LTCs dominate the Asian natural gas market, while the United States mainly trade natural gas on spot markets. Continental Europe is in the middle of a transition from LTCs to the spot pricing system, with a significant fraction of its gas supply still linked to LTCs. However, in Europe oil-indexed pricing had not reflected gas market fundamentals for some time, making the situation untenable. Mid-streamers asked for a re-negotiation of their contracts in order to link LTCs price to the spot gas prices. For this transition to be successful, there is the need of reliable markets prices which allow for both physical balancing and financial risk management on liquid trading hubs.

1.2.4 Partecipants

The main agents participating in a restructured gas supply chain are briefly introduced below and represented in Fig. 1.2 (see Holz et al. (2013); Egging (2013)).

- **Producers**
  Producers extract and refine natural gas and sell it to traders trying to maximize their profits. These agents usually own production facilities and they are also in charge of new investments, besides operation and maintenance of active production facilities.

- **Traders**
  Traders are in charge of transporting and selling natural gas to marketers. Transportation can be done via pipelines, or liquefaction, shipping and regasification infrastructures. They rent transportation capacity from the TSO to export the natural gas. They can also rent storage capacity from the Storage System Operator (SSO) to arbitrate between seasonal price variations. Their aim is to maximize their profit.

- **Transmission System Operators (TSO)**
  The TSO manages the transportation network and rents out capacity to traders.

- **Storage system Operators (SSO)**
  The SSO manages the storage capacity and rents our capacity to traders.

- **Marketers or mid-streamers**
  Marketers buy gas from the traders to supply all types of consumers which include residential/commercial, industries and power companies. Their aim is to maximize their profit.

- **Consumers**
  Consumers are the-end users of natural gas. They all buy gas from marketers. Their aim is to minimize their procurement costs or maximize the utility that they obtain from consuming gas.

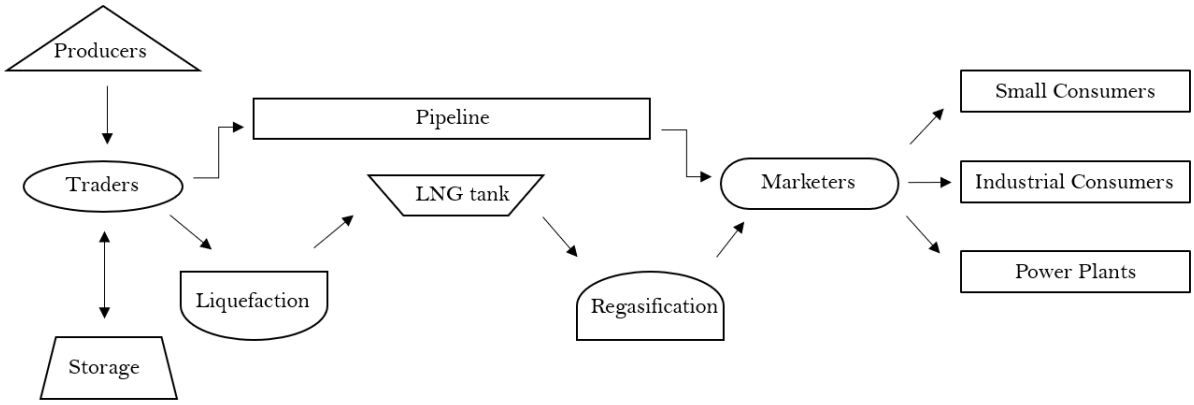

Figure 1.2: Representation of the gas supply chain participant's and interactions

1.3 Toward Decarbonization

Human activity is overloading the atmosphere with carbon dioxide and other greenhouse gas emissions, which trap heat and drive up the planet temperature, resulting in a negative impact on our health, environment, and climate. For these reasons, in December 2015, 195 countries signed the "Paris Climate Agreement", which entered into force on November 4th, 2016. The targets of this agreement are ambitious and include a long-term goal of keeping the increase in global average temperature well below 2°C by 2100, preferably below 1.5°C and of undertaking rapid reductions of emissions in accordance with the best available technologies. However, taking into account the

actual mitigation policies, the 1.5°C increase target has only 1% chance to be achieved and population growth is not a major contributing factor (see Raftery et al. (2017)). In fact, the long lifetime of CO_2, the thermal inertia of oceans and others factors are responsible for some level of natural warming, which could be enough to exceed the Paris targets (see Mauritsen and Pincus (2017)). Consequences might be serious on different levels, including premature mortality from changes in air pollution attributable to climate change (see Silva et al. (2017)).

In addition to the Paris Agreement, a number of countries and regional international organizations have adopted carbon-reduction targets of their own.

The USA were among the first Parties to deposit their instruments of ratification, acceptance, approval or accession, allowing the Agreement to enter into force. However, on June 1 2017 they announced their withdrawal and asked for a re-negotiation.[7] In spite of this, it is important to recall that according to the Article 28 of Paris Agreement the earliest date for a Party to leave the Agreement would be November 4th, 2020, upon expiry of one year from the date of receipt by the Depositary of the notification of withdrawal (see UNFCCC (2015)). Anyway, at the actual stage, the USA climate outlook is not favourable. The Russian Federation instead, has not yet ratified the Paris Agreement, delaying the adoption of ambitious climate targets and policies until at least 2019.

In the rest of the word, China joined the Paris Agreement through the so-called Nationally Determined Contribution, committing to reach a CO_2 emission peak by 2030. Although under current policies, this target will most likely be achieved, it is still not compatible with the objective of limiting global temperature increase to below 2°C. On the other side, India is making an important effort and adopted in April 2018 a very ambitious plan called National Electricity Plan (NEP) to achieve the goal of a 40% non-fossil-based power capacity by 2030 at end of this year, i.e. 12 years earlier than targeted.

In the same line, Japan is currently developing its Basic Energy Plan and long-term energy strategy. There is uncertainty around the future role of nuclear, coal and renewable energy. Coal plant construction plans remain a concern and pose a serious risk to the government's future mitigation efforts.

Canada adopted the Pan-Canadian Framework on Clean Growth and Climate containing proposals for economy-wide measures, including a carbon pricing plan and a plan to phase-out traditional coal plants. Canada's Nationally Determined Contribution target is to reduce economy-wide GHG emissions by 30% below 2005 levels by 2030, but it remains unclear if it will rely on carbon sinks in forests, soils, and wetlands to achieve its target.

[7] See: https://www.whitehouse.gov/briefings-statements/statement-president-trump-paris-climate-accord/

Finally, the European Union introduced in 2005 the European Union Emissions Trading System (EU-ETS) that is the first and largest cap-and-trade scheme applied on international scale to limit CO_2 emissions. The idea is the following: each ton of CO_2 emissions has to be covered by an allowance whose price is defined on a dedicated market. The EU-ETS went through two phases and it is now into the third one. The first phase, was a three year pilot (2005-2007) of "learning by doing" in preparation for the second phase, covering years 2008-2012. The over allocation of allowances that were assigned for free with a 95% and 90% proportions in first and second phases created some distortions reducing the direct impact of the EU-ETS on emissions. Since firms received the allowances for free they were able to generate the so-called "windfall profits" mainly in two ways: by selling the allowances on the market and by passing a significant part of the costs of CO_2 emission allowances through to product prices, resulting for example in higher electricity prices for consumers (see Sijm et al. (2006)). Despite this, the first two phases were able to generate saving on CO_2 emissions. Although disentangling the impact of the EU-ETS from other factors is complex, academic studies with both "top down", and sector-based "bottom up" evaluations attribute to this mechanism savings ranging from 2% to 4% of the total capped emissions per year (see Laing et al. (2013)). The third phase, started in 2013, substantially modifies the EU-ETS trying to overcome these drawbacks by applying a single EU-wide emission cap in place of the previous system of national caps, by enlarging the involved sectors and by significantly reducing the amount of grandfathered allowances. This is also the tendency of the announced fourth phase that is currently under discussion. The European Union has also adopted the so-called Energy Roadmap 2050, committing to reduce greenhouse gas emissions by 80%-95% relative to 1990 levels by 2050. This implies a complete transformation of the energy system: improving energy efficiency, switching to renewable energy sources which should represent at least 55% of the gross final energy consumption in 2050 (actual level is around 10%), developing efficient and economically convenient storage mechanisms, enforcing the role of gas into the transition, developing smart technologies and alternative fuels including electric vehicles. Planning plays a central role in this transformation since large share of the current energy supply capacity will come to the end of their useful life in the next years. Moreover, there is the need of improving the condition for financing in the energy sector, decreasing the costs of capital for low-carbon investment. In this sense, carbon pricing can provide an incentive although increasing the risk of carbon leakage. [8] A global effort is required and both electricity and gas market will face important transformations.

[8] Carbon leakage refers to a hypothetical situation where companies transfer production to countries with weaker climate policies in order to lower their costs.

1.3.1 Electricity role in a low-carbon energy economy

Electricity will have to play a role much greater than now in order to contribute to decarbonization. According to the EU Roadmap the biggest share energy of supply technology in 2050 should come from renewables. Renewable Energy Sources (RES) have to be employed both on large and small scale, become more efficient and create economies of scale. Many renewable based technologies such as Concentrated Solar Power (CSP) or biofuels, need further development to reduce their costs, others such as wind plants and photovoiltaic (PV) might be partially improved, for example by increasing the size of offshore wind turbines and blades to capture more wind or to improve the PV to harvest more solar power. Moreover, although renewable generation present several advantages such as unlimited resource availability all over the planet, very low production costs besides being environmentally sustainable, the operation of a renewable dominated electricity market it is not so trivial. This is due to the stochasticity that characterizes RES that makes uncertain the electricity production of such a kind of power plants (see Morales et al. (2013)). This have an effect on several floors:

- **Predictability:** first of all, when dealing with RES power production, forecasts become essential for an adequate integration of renewable power generation in electricity markets operations, since markets need be cleared in advance, while market participants shall make decisions even before that (see Section 1.1.3). An appropriate forecasting in a well-defined decision-making problem helps improving the decisions to be made, and allows controlling the risk generated by unforeseen events. Predictability has an impact on the cleared energy volumes and system prices, as well as their dynamics (see Jónsson et al. (2010)). This happens because the energy produced by RES units is commonly bid into the markets using forecasts of the future production, especially in the day-ahead and intraday markets. Indeed the potential need for balancing comes from the difference between day-ahead supply offers and actual generation. Consequently, it is not the actual renewable energy generation that drives the balancing direction, prices and quantities, but the forecasting errors instead. Moreover, since the marginal cost of renewable energy is very low, according to the so called merit-order principle, their production is scheduled before conventional production and their output directly influences the market price. As a result, in periods with high renewable power production the market price is low, while periods with low renewable power production are characterized by higher prices.

- **Variability:** renewable generation is intermittent and it is nonlinear function of the associated atmospheric variables such as solar irradiance or wind speed.

Variability from one hour to the next, but also from one day to the other, is high and these patterns contribute to shaping the evolution of the various variables in day-ahead and balancing markets. Usually, variability in renewable production is not correlated to the fluctuation of the demand and so cannot be passively absorbed by consumers. For this reason, a high degree of variability in a power system requires a high degree of flexibility that can be achieved in several ways.

- **Flexibility need:** flexibility can be achieved by operating conventional units at production levels higher or lower than their optimum in an attempt to accommodate the variability of renewable generation by ramping up or down, which sometimes implies also starting-up or shutting-down conventional units. Consequently, if large variations of renewable generation have to be accommodated by conventional generation, this may result in conventional power plants operating in a less efficient way, thus reducing the emissions savings generated with the aim of renewable production.

  Another solution to increase flexibility is the implementation of direct and indirect control initiatives.
  Direct control includes initiatives aimed at granting the TSO the right to directly modulate the demand by rationing or disconnecting single or groups of consumers. Typically, consumers involved in these strategies are protected by a contract fixing how often they can be disconnected or rationed.
  Indirect control implies the use of economic incentives so that demand for power, rather than the supply, adapts to the stochastic and variable production. In practice, this is done by broadcasting time-varying prices to the consumers (dynamic real-time pricing). This strategy is also know as demand response and requires constant communication with consumer, achievable only with an upgrade of the grid, usually associated with the notion of smart grid.

  A third way to increase flexibility is by optimally managing the reserves. Indeed, although part of the variability can be predicted, a renewable oriented power system increases the need for backup power to cope with unpredicted fluctuations of power production. This implies higher reserve availability which entails additional operating costs which can be minimized only by allocating and deploying reserves in an efficient manner.

  Finally, probably the best way to increase flexibility and facilitate the integration of RES is by developing large-scale storage capabilities. Storage plants allow shifting in time the demand by storing electricity when demand is low (and so is the price) and releasing it, during high-demand (high-price) periods. From a practical point of view this translates into increasing the consumption during

low-demand periods, allowing inflexible production units to maintain their power output or reducing the ramping of conventional units, while producing energy at high demand periods, reducing the need of reserves and the use of costly peaking power plants.[9] Even though, currently, there exist a number of energy storage technologies that can contribute to this end, it seems that further development in this field is still needed for massive electricity storage to become a reality in the required magnitude (see Pickard et al. (2009)).

In the following the different types of renewable generation and storage facilities utilized in this thesis are briefly introduced.

Wind

A wind power plant is made of several wind turbines. Each turbine is supported by a conical steel tower which is firmly anchored to the ground. In the horizontal axis wind turbines, which are the most common worldwide and also the ones we consider in this thesis, the speed of the wind rotates the blades of a rotor, producing kinetic energy. The rotor then drives a generator, contained together with other mechanical components into the nacelle, that converts the mechanical energy into electricity (see IEA (2016c)). Wind plants can be built either onshore or offshore with the latter requiring both higher investment and operation costs with respect to onshore plants. Higher investments costs depends on more expensive marine foundations, installation procedures and integration in the electrical network, while higher operation cost are due to the limited access for operations and maintenance. Anyway, offshore plants experience also higher capacity factors[10] with respect onshore plants because they can benefit from the higher wind speed, which generally increases with distance from the shore, and less turbulence, which allows the turbines to harvest the energy more effectively (see Bilgili et al. (2011)). Wind turbine prices have fallen by around half from 2009 leading to cheaper wind power globally. Moreover the global weighted average Levelized Cost Of Electricity[11] of onshore wind have dropped from USD 0.40/kWh in 1983 to USD 0.06/kWh in 2017, experiencing a 85% decline, with recent auctions in Brazil, Canada, Germany, India, Mexico and Morocco resulting in onshore wind power LCOEs as low as USD 0.03/kWh, making the technology one of the most competitive sources of new

[9] These power plant generally run only when there is a high demand, known as peak load, for electricity. They receive a higher price for supplied power with respect to base load power plants which produce a consistent amount of electricity to meet the minimum demand (base load).

[10] The capacity factor is the ratio of the actual energy produced by a turbine in a period time, to the nameplate capacity of the turbine.

[11] LCOE measures lifetime costs (including both investment and operations) divided by energy production. LCOE allows the comparison of different technologies of unequal life spans, project size, capital costs, risk, return, and capacities.

generation capacity (see IRENA (2018b)). For these reasons, this technology is considered mature with respect to other more recent types of renewables. Large amounts of wind power have been integrated into power systems worldwide resulting in a total installed capacity of 5.4 GW at the end of 2017 (see GWEC (2017)). The projection of international agencies for future development of wind technologies estimate global wind installations reaching 743GW (of which 31GW offshore) by 2020 and 2,900-5,806 GW in 2050 according to different scenarios assumptions (see GWEC (2016)).

Solar Photovoiltaic

A single Solar Photovoltaic device is known as a cell. Cells are connected together in chains to form larger units known as modules or panels which boost the power output of PV cells. Modules can be used individually, or several can be connected to form arrays. One or more arrays is then connected to the electrical grid as part of a complete PV system. Because of this modular structure, PV systems can be built to meet almost any electric power need, small or large. PV modules directly convert incident solar radiation into dc electricity, which can then be inverted to ac. PV gets its name from the process of converting light (photons) to electricity (voltage), which is called the PV effect. PV cells can be made of different materials: traditional solar cells are made from silicon and are usually flat-plat. Second-generation solar cells are called thin-film solar cells because they are made from amorphous silicon or nonsilicon materials such as cadmium telluride and are very thin and flexible. Third-generation solar cells are being made from a variety of new materials besides silicon, including solar inks using conventional printing press technologies, solar dyes, and conductive plastics. PV technology experienced a huge cost reduction in the last years with the module costs declined by 80% between the end of 2010 and the end of 2016. As a result also the weighted average LCOE cost experienced a 73% decrease to USD 0.10/kWh for new projects commissioned in 2017 (see IRENA (2018b)). At the end of 2016 the worldwide installed cumulative PV capacity was 291GW. The projection of international agencies for future development of the technology estimates the global PV installations reaching 650 GW by 2020 and 3,155-7,122 GW by 2050 according to different scenarios assumptions (see IRENA (2018a); IEA (2014a)).

Solar Thermal Electric Technology

Solar thermal electric technology, also known as Concentrated Solar Power with thermal energy storage (TES) relies on concentrating the sun's rays through the use of mirrors to create high temperature heat to drive a steam turbine. In the majority of today's systems, the sun energy is transferred to a fluid, which in turn is passed

through heat exchangers to run a traditional electricity steam cycle, similar to the one used in conventional thermal power plants. Usually, a molten salt solution is the basis for generating steam because the heat in the fluid can be stored for a period of time into specific tanks and used later to generate electricity. According to the way used to collect the heat and generate electricity it is possible to distinguish various CSP configurations. These includes parabolic through collectors, solar power tower, linear Fresnel and Dish-Stirling (see Zhang et al. (2013)). Solar power towers are currently the focal-point system currently most deployed, and also the one adopted in this thesis. CSP technology is still in its infancy in terms of deployment, although the cost have fallen between 2010 and 2017 and the estimated learning rate in the time horizon 2010-2020 is around 30%. Both investments and operating costs are expected to further decrease toward 2050. Auction results in 2016 and 2017 for projects that will be commissioned in 2020 and beyond, signed a step-change with the weighted average LCOE costs falling to between USD 0.06 and USD 0.10/kWh (see IRENA (2018b)). At the end of 2016 the worldwide installed cumulative CSP capacity was 5 GW. The projection of international agencies for future development of the technology estimates the global CSP installations reaching 12 GW by 2020 and 633-982 GW by 2050 according to different scenarios assumptions (see IRENA (2018a); IEA (2014b)).

Storage system: Batteries

Battery energy storage technologies, with their high energy densities, maturity of technology and relative ease of use represent a valuable option for small-scale energy storage. The batteries are made of stacked cells wherein chemical energy is converted to electrical energy and viceversa. The desired battery voltage as well as current levels are obtained by electrically connecting the cells in series and parallel. The batteries are rated in terms of their energy and power capacities, but they present also some other important features which differ from type to type. These are the efficiency, the life span (stated in terms of number of cycles), the operating temperature, the depth of discharge (batteries are generally not discharged completely), the rate of self-discharge and the energy density (see Divya and Østergaard (2009)). Battery storage is facing a significant development, and it is possible to distinguish many different types of batteries suitable for power system operations. These include lead-acid, sodium-sulphur, lithium-ion, nickel-cadmium, nickel-metal hybrid, and flow batteries. Lead-acid batteries are the oldest and most mature technology and have been largely implemented in power systems. The litium-ion, sodium-sulphur, nickel-cadmium and nickel-metal hybrid batteries seem to represent the leading technologies in high-power-density battery applications. Of these, litium-ion possesses the greatest potential for future development and optimization. In addition to small size and low weight the these batteries

offer the highest energy density and a storage efficiency close to 100%, but they are cost expensive. The flow batteries are also promising for applications which require long duration storages due to their non-self-discharge capability, but they offer low power density (see Nair and Garimella (2010)). In Chapter 3 we use batteries as small-scale storage solution within a small size electric energy system with electric vehicles and PV units.

Storage systems: Compressed Air Energy Storage

Compressed Air Energy Storage (CAES) represent a valid large-scale storage alternative for countries with limited water availability. At the time being, all the operating large-scale CAES plants are diabatic i.e. they allow energy exchanges with their surroundings. For this reason, diabatic CAES is considered a hybrid large-scale storage technology and uses both electricity (to compress air) and natural gas. The operation of a diabatic CAES plant can be divided into two phases. In the charging phase, that occurs during off-peak periods, CAES systems utilizes electrical energy from the grid to compress the air, that is stored at a high pressure and ambient temperature in a reservoir that can be an underground cavern, or any type of environment with similar features. The heat resultant from each compression is released in the atmosphere. In the discharging phase, a single-cycle gas turbine generator combines compressed air with natural gas in a combustion chamber. Combustion produces high-pressure gas, which is then expanded through a turbine, that drives both a generator and the input air compressor. The electricity produced is then delivered to the grid. In the last years another type of CAES, called adiabatic have been developed, although no commercial-scale operating systems exist today. Adiabatic CAES is an emission-free, pure storage technology which exploit the principle of storing the heat generated in the compression phase into dedicate thermal energy storage (TES). Then, during the discharging phase, the heat is released into the compressed air increasing its temperature with no need to burn gas and so avoiding CO_2 emissions. Additional details for these technologies, including investments and operation costs are given in Chapter 2.

1.3.2 Gas role in a low-carbon economy

In recent years technology advances such as horizontal drilling and hydraulic fracturing have unlocked gas resources in unconventional reservoirs, such as tight sands, coal bed methane, and shale rock rich in organic materials. The USA have been the forerunners of this new exploration process which is now applied internationally. As a result, unconventional gas should account for nearly half of the growth in global gas production to 2035, with China, USA and Australia as majors contributors. Consequently, gas

resource estimates have increased sharply, and natural gas has now the potential to shed the supply, price volatility, and energy security concerns that have surrounded it during the last few decades (see Flavin and Kitasei (2010)). In addition to that, natural gas is the only fossil fuel for which global demand is expected to grow, showing that it fares well under different policy conditions (see IEA (2016d, 2018)). The prospect of more abundant and economical gas supplies, together with the increasing urgency of the climate problem, is drawing more attention to the role that natural gas will play in the transition to a low-carbon power sector. More specifically, the role of gas will be critical for several reasons (see Holz et al. (2013)). In the short-medium term natural gas will substitute other fossil fuels with a relatively higher carbon content per generated energy, particularly coal. This could help reducing emissions with existing technologies until at least 2030-2035 according to the forecasts of the EU Roadmap 2050. This effect may be intensified by the advantages provided by gas-fired power plants, which present lower investment costs, are rather quickly built and relatively flexible. And it is thanks to this flexibility that gas-fired power plants can play a balancing role in an increasingly intermittent electricity system, acting as backup units. Other sectors than electricity generation, i.e. transportation and heating may be affected as well. Moreover the development of the Carbon Capture and Sequestration mechanism (CCS), which can cover a broad range of technologies, represent an important option to transform the production from natural gas plants in low-carbon production and pursuing decarbonization targets. CCS is currently considered to be technically feasible at commercial scale, with both large-scale and small-scale projects operating all over the world (see Gibbins and Chalmers (2008)). In the following we provide a brief description of this technology, which is also included as possible option in the long-term investment model developed in Chapter 2. Anyway, to keep its competitiveness as fuel for electricity generation, natural gas management has to be improved. First the gas market needs more integration, liquidity, storage capacity and diversity of supply sources. In particular, the latter is fundamental for non-producing countries which are constantly exposed to the risk of supply failure due to economical and political reasons. This aspect is analyzed in Chapter 5 of this thesis. In addition, LTCs may continue to be necessary to guarantee investments in both up-stream and mid-stream segments, but more flexibility in the price formula is required. There is the need of moving away from pure oil-indexation, opening to gas spot prices as possible underlying of these long-term contract. This aspect is developed in Chapter 4 of this thesis.

Carbon Capture and Sequestration

Carbon Capture and Sequestration is a technology that can capture up to 90% of the CO_2 emissions produced from the use of fossil fuels in electricity generation and industrial processes, preventing the carbon dioxide from entering the atmosphere. The CCS chain consists of three parts: capturing the carbon dioxide, transporting the carbon dioxide, and securely storing underground the carbon dioxide emissions in depleted oil and gas fields or deep saline aquifer formations. Capture technologies separate carbon dioxide from gases in electricity generation and may be done in at least three different ways: pre-combustion capture, post-combustion capture and oxy-fuel combustion. A pre-combustion system involves first converting solid, liquid or gaseous fuel into a mixture of hydrogen and carbon dioxide using processes such as gasification or reforming. The CO_2 is then captured. In the post-combustion CO_2 is captured from the exhaust of a combustion process in several ways which include absorbing it in a suitable solvent, using high pressure membrane filtration, with the aim of adsorption/desorption processes or cryogenic separation. In the process of oxy-fuel combustion the oxygen required is separated from air prior to combustion and the fuel is combusted in oxygen diluted with recycled flue-gas rather than by air. This oxygen-rich, nigtrogen-free atmosphere results in final flue-gases consisting mainly of CO_2 and water, so producing a more concentrated CO2 stream for easier purification. Fossil Fuel power plants can be built with the carbon capture technology integrated, or can be built "carbon capture ready", which allows the plant to have carbon capture capabilities in the future. The cost of CCS is expected to decrease in the long-run as a result of research and development activities, and the building of economies of scale. Anyway also in this case, higher carbon prices are needed to push companies to invest in CCS (see Holz et al. (2013)).

1.4 Thesis Motivations and Objectives

The issues discussed in Section 1.3 has motivated the work carried out in this thesis, whose aim is to develop different modeling frameworks to represent the transition of electricity and gas markets toward a low-carbon economy. The thesis is divided into two main parts:

- In the first part, two planning models to efficiently integrate renewable and storage units in electric energy systems are proposed. Among the actions carried out to mitigate greenhouse gas emissions, increasing RES penetration is one of the most important. Anyway, renewable generation implies dealing with production variability and uncertainty, which represent a challenge for the power system.

Therefore, more backup capacity is needed. Possible solutions include increasing reserves, which are supplied by dispatchable units such as thermal plants. An alternative is the integration of storage capacity, which provides flexibility to system and represents an environmentally friendly solution. The objectives of this first part include:

- Developing an accurate modeling of multi-scale uncertainties, i.e. short-term uncertainty, able to represent daily variability of several factors including renewable energy production, and long-term uncertainty, which pertains to future projections. The problem is tackled by applying two different methodologies: stochastic programming and robust optimization.
- Integrating and adequately representing daily operations of different types of storage facilities, which help providing flexibility to the system.
- Correctly taking into account realistic network constraints by representing the topology of the system under study. Lines capacity availability is usually a concern because power production centers are located away from demand centers. We seek to develop models which allow lines expansion.

These topics are investigated in Chapters 2 and 3. The specific objectives of these two chapters include:

- To develop a two-stage stochastic programming investment model for generation- and transmission-capacity planning decisions taking into account decarbonization targets to be achieved by 2050 that is the considered reference year. Investment decisions are taken at the first stage, whereas operating decisions are taken at the second stage.
- To represent two types of climate policies: an explicit cap on carbon emission and a carbon price. In this way our model can represent capacity expansion under current European climate policy and policies that have been contemplated in the United States.
- To investigate how different technologies can contribute to the decarbonization of the energy sector. This includes the use of renewable technologies, such as wind and concentrating solar power (CSP), nuclear generation, and fossil-fueled generation with carbon capture and sequestration (CCS) systems. To allow both ac and high-voltage dc (HVDC) transmission lines, as well as energy-storage technologies to be built.
- To incorporate a novel representation of the operation of TES included into CSP plants in a long-term investment model.

  - To examine the impacts of a variety of policy and technical factors on power system decarbonization. Specifically, to study the effects of environmental policies, technology improvements, and transmission-network congestion. We also want to examine the trade-off between the use of wind and solar generation for decarbonization.
  - To develop an Adaptive Robust Optimization model for planning investments in a Small Size Electric Energy System (SSEES).
  - To model investments in PV power plants, storage units, charging stations for Electric Vehicles (EVs), and network lines in an integrate framework;
  - To study the changes in the investment decisions on the basis of the impact of long-term uncertainty, the central planner's revenues accruing from selling electricity to EVs at charging stations, the degree of autonomy of SSEES from the main grid, and the possibility of expanding the network.
  - To conduct an ex-post analysis on the amount of CO_2 saved with the utilization of EVs in order to evaluate the benefits of progressive road-transport decarbonization.

- In the second part, we analyze both the possible re-negotiation of the natural gas LTCs in the European market, characterized by an hybrid price system where also purchases of spot gas are allowed, and the security of supply of the Italian gas market. Gas is the less pollutant fossil fuel and will play an important role in the medium term, as explained in Section 1.3.2. A significant fraction of European gas supply depends on imports from foreign countries and, in addition, is linked to LTCs. The fall of the European natural gas demand, combined with the increase of the oil price, favored the emergence of a gas volume bubble that caused significant losses for most of the European mid-streamers because natural gas prices at the hubs were considerably lower with respect to the ones they were comminted to pay because of LTCs. This situation instilled in the downstream part of the industry the idea of indexing contracts on gas spot prices rather than oil-based commodities. At this light also the issue of the security of supply of importing countries deserves attention. These topics are investigated in Chapters 4 and 5. Chapter specific objectives of this second part include:

  - To study via Pair-Copula Constructions (PCC), the dependence risk structure across the underlyings of LTCs on natural gas.
  - To develop an integrated framework that combines vine copula and optimization techniques traditionally used in the contest of portfolio management.

- To address the debate over oil/spot indexation of European LTCs by defining the optimal composition of the assets traditionally used to price these contracts.
- To develop an optimization model that describes the equilibrium state of the natural gas supply chain where natural gas producers, mid-streamers, and consumers can sell and buy both natural gas and LNG through LTCs or/and on spot market.
- To study the risk of external gas supply by directly integrating new risk indicators in our model.
- To investigate different degrees of mid-streamers' flexibility by comparing a situation where they fully accomplish the LTC volume requirements with a case where they behave in a more flexible way.

1.5 Methodologies

The methodologies used in this dissertation are briefly revised below.

1.5.1 Optimization Problems

An optimization problem (OP) or mathematical programming problem consists in maximizing or minimizing a certain objective function subject to different restrictions, typically in the form of equality or inequality constraints. In general, an optimization problem can be formulated as follows (see Gabriel et al. (2013)):

$$\begin{aligned} \underset{x}{\text{minimize}} \quad & f(x) \\ \text{subject to} \quad & h(x) = 0 \\ & g(x) \leq 0 \end{aligned}$$

where $x \in \mathbb{R}^n$ is the optimization variable vector, $f(x) : \mathbb{R}^n \to \mathbb{R}$ is the objective function to be minimized, $h(x) : \mathbb{R}^n \to \mathbb{R}^{m_e}$ are the function for the equality constraints and $h(x) : \mathbb{R}^n \to \mathbb{R}^{m_t}$ for the inequality constraints. The set of solution meeting both $h(t) = 0$ and $g(x) \leq 0$ constitutes the feasible region. A solution within the feasible region is a feasible solution, while the feasible solution minimizing the objective function is the optimal solution.

The joint consideration of several interrelated optimization problems i where $i = 1, ..., n$, constitutes an equilibrium problem of the form:

$$\begin{aligned} \underset{x^i}{\text{minimize}} \quad & f^i(x^1, ..., x^n) \\ \text{subject to} \quad & h^i(x^1, ..., x^n) = 0 \\ & g^i(x^i, ..., x^n) \leq 0 \end{aligned}$$

where the vector $x^i \in \mathbb{R}^{n^i}$ includes the set of optimization variables of problem i. By setting $n_o = \sum_{i=1}^{n} n^i$ it is possible to define the objective functions and the constraints of the problem i as follows: $f^i : \mathbb{R}^{n_o} \to \mathbb{R}$, $h^i : \mathbb{R}^{n_o} \to \mathbb{R}^{m_e^i}$ and $g^i : \mathbb{R}^{n_o} \to \mathbb{R}^{m_i^i}$. The Karush-Kuhn-Tucker (KKT) conditions are a set of complementarity conditions which should be satisfied by the optimal solution of an optimization problem. KKT condition are a natural way to cast these types of equilibrium problems. A complementarity condition between a vector of non-negative variables $\mu \in \mathbb{R}^{m_t}$ and a function $g(x)$ can be defined as:

$$g(x) \leq 0 \qquad \mu^\intercal g(x) = 0 \qquad \mu \leq 0$$

which can be written more compactly as

$$0 \leq \mu \perp g(x) \leq 0$$

where $\perp$ indicates complementarity, i.e. $\mu^\intercal g(x) = 0$.
In order to meaningfully formulate KKT conditions associated to an optimization or equilibrium problem constraint qualification is required. KKT conditions can be necessary, but not sufficient conditions, i.e., solutions meeting them are not necessarily optimal but optimal solutions need to meet them. If the objective function of the related optimization problem is continuously differentiable and the set constituted by the constraints is convex, the solution is guaranteed to be optimal (sufficiency condition). KKT conditions are first-order conditions, i.e., conditions that are formulated using first derivative vectors and matrices (gradients and Jacobians). The Langrangian function of the single optimization problem previuosly defined is:

$$\mathcal{L} = f(x) + \lambda^\intercal h(x) + \mu^\intercal g(x)$$

where $f(x), h(x), g(x)$ are aasumed to be continuously differentiable in the feasible region. The associated KKT conditions are

$$\nabla_x f(x) + \lambda^\intercal \nabla_x h(x) + \mu^\intercal \nabla_x g(x) = 0$$

$$
\begin{aligned}
h(x) &= 0 \\
g(x) &\leq 0 \\
\mu^{\intercal} g(x) &= 0 \\
\mu &\geq 0
\end{aligned}
$$

where $\lambda \in \mathbb{R}^{m_e}$ and $\mu \in \mathbb{R}^{m_t}$ are Lagrange multiplier vectors associated with equality and inequality constraints, respectively, and ∇_x denotes the gradient with respect to the variable vector x. Note the the last three constraint can be expressed in compact form as stated above. In this dissertation we solve an equilibrium problem defined by jointly solving the KKT conditions of several single optimization problems each one modeling the behavior of a specific market player within the gas market.

1.5.2 Stochastic Programming

Most decision-making problems can be adequately formulated as optimization problems. If the input data of an optimization problem are well-defined and deterministic, its optimal solution is achieved by solving the problem. Anyway, when dealing with decision making problems in the real word, a common issue is the lack of perfect information. This happens in several fields, such as engineering, economics, finances, etc. However, decisions need to be made even with lack of perfect information. This is what motivates the use of stochastic programming models for decision making under uncertainty. Indeed, uncertain input data can be described through probability functions. In such a situation, possible solutions include substituting the uncertain input data by their corresponding expected values, which results in a well defined and deterministic optimization problem. However, solving such a problem may lead to a solution that, once implemented, does not result in the best outcome. Alternatively, the probability distribution of input data can be approximated by a collection of plausible sets of input data with associated probabilities of occurrence. Doing so, it is possible to formulate a *stochastic* optimization problem to achieve a solution that is the best in some sense considering all possible values of the uncertain parameters.
The main drawback of stochastic programming is the size of the resulting problem, which usually leads to computational intractability. Moreover, as stated above, it is clear that stochastic programming relies on the knowledge of the probabilistic distribution of the uncertain parameters, which are usually represented with the aim of scenarios. Therefore adequate generation techniques are needed to achieve a good representation, and further, efficient scenario reduction techniques to attain computational tractability without loosing important information (see Birge and Louveaux (1997); Kall et al. (1994); Prékopa (2013)). In this dissertation, a two-stage mixed-

integer linear stochastic programming model is proposed. A general two-stage linear stochastic programming problem is formulated as follows:

$$\begin{aligned} \underset{x}{\text{minimize}} \quad & c^{\mathrm{T}}x + \mathbb{E}_{\xi}\{Q(x,\xi)\} \\ \text{subject to} \quad & Ax = b \\ & x \geq 0 \end{aligned}$$

where $Q(x,\xi)$ is the optimal value of the second-stage problem:

$$\begin{aligned} \underset{y}{\text{minimize}} \quad & q(\xi)^{\mathrm{T}}y \\ \text{subject to} \quad & T(\xi)x + W(\xi)y = h(\xi) \\ & y \geq 0 \end{aligned}$$

This model can be applied to problems that deal with "here-and-now" decisions, which have to be taken on the basis of prior existing information about future situations without additional observations. The first-stage decisions do not depend on the scenario that will actually occur in the future. The second-stage decisions occur after the uncertainty realization and are the resources that can be used for each possible future scenario. The decisions taken depend on the future realization of the scenario, for this reason are called "wait-and-see". In this formulation $x \in \mathbb{R}^n$ is the first-stage decision variable vector, $y \in \mathbb{R}^n$ is the second-stage decision variable vector, and $\xi(q,T,W,h)$ contains the data of the second-stage problem. The "here-and-now" decision, x, is made at the first stage, before the realization of the uncertain data ξ is known. At the second stage, after the realization of ξ becomes available, an appropriate optimization problem is solved. At the first stage, the cost c^{T}, plus the expected cost of the optimal second-stage decision, $\mathbb{E}_{\xi}\{Q(x,\xi)\}$ are optimized. The second-stage problem can be viewed as an optimization problem which describes a supposedly optimal behavior when the uncertain data ξ are revealed. Matrices T and M are called technological and recourse matrices, respectively.

1.5.3 Adaptive Robust Optimization

Robust optimization is widely used to solve optimization problems under uncertainty. With respect to stochastic programming, it has the advantage of eliminating the need of scenario generation, and therefore reducing potential computational intractability.

Indeed, instead of seeking to immunize the solution in some probabilistic sense to stochastic uncertainty, with robust optimization the decision-maker constructs a solution that is feasible for any realization of the uncertainty in a given set. The uncertain parameters are kept within robust sets, which are easier to construct with respect to scenarios. By considering the worst possible realization, the optimal solution is obtained, although this might sometimes lead to too conservative results (see Ben-Tal et al. (2009); Bertsimas et al. (2011)). The adaptive robust optimization formulation originates from the need of adequately represent a decision sequence in which *(1)* decision are made under uncertainty, *(2)* uncertainty realization is considered, *(3)* corrective actions can be made. A general adaptive robust optimization problem is formulates as follows:

$$
\begin{array}{llll}
\min\limits_{x} & \max\limits_{u} & \min\limits_{y} & f(\mathbf{x},\mathbf{u},\mathbf{y}) \\
 & & \text{s.t.} & \\
 & & \mathbf{h}^C(\mathbf{x},\mathbf{u},\mathbf{y}) = 0 & \\
 & & \mathbf{g}^C(\mathbf{x},\mathbf{u},\mathbf{y}) \leq 0 & \\
 & & \mathbf{y} \in \mathcal{Y} & \\
 & \text{s.t.} & & \\
 & \mathbf{u} \in \mathcal{U} & & \\
\text{s.t.} & & & \\
\mathbf{h}^I(\mathbf{x}) = 0 & & & \\
\mathbf{g}^I(\mathbf{x}) \leq 0 & & & \\
\mathbf{x} \in \mathcal{X} & & &
\end{array}
$$

Objective function $f(\mathbf{x},\mathbf{u},\mathbf{y})$ represents the minimization of the total cost, including investment and operating costs. The investment decision variables are gathered in vector x, and depend on the so called expansion constraints. The entries of vector u are variables describing the uncertain parameters and $\mathcal{U}$ represent the uncertainty set which defines variability limits of uncertain parameters. Similarly, the entries of vector y are the operating decision variables. Note that $\mathcal{U}$ defines the feasibility set, which includes constraints related to the system operation and system limits. The worst case realization of the uncertainty and the successive adaptive actions are considered in the $max - min$ right-hand-side problem, while the min left-hand-side problem seeks minimum total cost.

1.5.4 Pair-Copulas Construction

Copulas are functions that join or couple multivariate distribution functions to their one-dimensional marginal distribution functions. Alternatively, copulas are multivariate distributions functions whose one-dimensional margins are uniform on the interval [0,1]. In a sense, every joint distribution function implicitly contains both a description of the marginal behaviour of individual variables and a description of their dependency structure. Copulas provide a way of isolating the description of their dependency structure. In particular, the copula approach allows capturing the complex dependency patterns of multivariate data, such as asymmetry and dependence in the extremes which cannot be captured by multivariate normal or student-t distributions.

The following theorem (Sklar) holds (see Sklar (1959)):

$$F(x_1, ..., x_d) = C(F_1(x_1), ..., F_d(x_d))$$
$$f(x_1, ..., x_d) = c(F_1(x_1), ..., F_d(x_d))f_1(x_1)...f_d(x_d)$$

where $F(x_1, ..., x_d)$ and $f(x_1, ..., x_d)$ are the joint distribution and density function, respectively. $F_i(x_i)$ and $f_i(x_i)$ for $i = 1, ..., d$ are the marginal distribution and density function, respectively. $c(u_1, ...u_d) := \frac{\partial^d}{\partial u_1 ... \partial u_d}$ is the copula density function.

While there exists a multitude of bivariate copulas, the class of multivariate copulas is still quite restricted. Hence, if the dependency structures of different pairs of variables in a multivariate problem are very different, not even the copula approach will allow for the construction of an appropriate model. It has been proved that under some regularity conditions a multivariate density can be expressed as a product of bivariate copulas, acting on several different conditional probability distributions. This has allowed formulating an approach finalized to the probabilistic construction of multivariate distribution functions based on pair-copulas, namely pair-copula construction (PCC). Many PCC's are feasible and, for this reason, there exist graphical structures to organize them. PCC allows exploiting the advantages of using copulas, providing additional flexibility by modeling conditional pairs.

1.6 Thesis Organization

This document is structured according to the following chapters:

Chapter 1 In this chapter we first present an overview of the electricity market, which includes a description of the restructuring process of the electricity sector and of the structure of the electric power system, an explanation of the function-

ing of the principal electricity markets and a review of the most relevant market agents. Second, we describe the gas market, providing a summary of its deregulation process, a description of the structure of the gas supply chain and of its participants, and an explanation of the functioning of the principal gas markets. Third, we present an overview of the decarbonization process and we analyze the role played by electricity and gas to meet low-carbon economy targets. We also describe all the technologies used in this thesis. Fourth, a general overview of the methodologies used in this dissertation is provided. Finally, we provide the thesis objectives.

Chapter 2 presents a two-stage stochastic optimization model to determines the optimal mix of generation and transmission capacity that needs to be built in order to serve future demands at least cost, while respecting both technical and environmental constraints. The model uses a mix of ac and high-voltage dc transmission lines, conventional and renewable power plants, and energy-storage units to meet these objectives. Short- and long-term uncertainties are modeled using operating conditions and scenarios, respectively. A case study and a sensitivity analysis are provided to show how the proposed model works.

Chapter 3 proposes a stochastic adaptive robust optimization approach for the expansion planning problem of a small size electric energy system. This involves the construction of candidate renewable generating units, network lines, storage units, and charging stations for electric vehicles. Short- and long-term uncertainties are modeled using operating conditions and confidence bounds, respectively. A case study is used to illustrate the effectiveness of the proposed technique, while an an ex-post decarbonization analysis is conducted to evaluate the environmental impact of the integration of electric vehicles in the energy system.

Chapter 4 originates from the European debate concerning oil versus gas indexation of long-term natural gas contracts. The dependence risk and the optimal resource allocation of the underlying assets of a gas long-term contract are estimated through pair-vine copulas and portfolio optimization methods with respect to different risk measures, respectively. Both spot gas prices traded at the hub and oil-based commodities are considered as possible underlyings of the LTCs. Results can provide concrete indications for practitioners in the field..

Chapter 5 analyzes the security of external supply of the Italian gas market that mainly relies on natural gas imports to cover its internal demand. An optimization problem, which describes the equilibrium state of a gas supply chain where producers, mid-streamers, and final consumers exchange natural gas and LNG,

is developed. Both long-term contracts and spot pricing systems are considered. Mid-streamers are assumed to be exposed to the external supply risk, which is estimated with indicators that we develop starting from those already existing in the literature. In addition, different degrees of mid-streamers' flexibility are investigated by comparing a situation where mid-streamers fully satisfy the long-term contract volume clause to a case where the fulfillment of this volume clause is not mandatory.

Chapter 2

A Two-Stage Stochastic Optimization Planning Framework to Deeply Decarbonize Electric Power Systems

This chapter is based on the article:

Boffino L., A. J. Conejo , R. Sioshansi, G. Oggioni.
A Two-Stage Stochastic Optimization Framework for Planning Deeply Decarbonized Electric Power Systems
which is currently under review in Energy Economics

In 2015, 195 countries signed the Paris Agreement under the United Nations Framework Convention on Climate Change. To achieve the ambitious greenhouse gas-reduction targets therein, the electric power sector must be fundamentally transformed. To this end, we develop in this chapter a two-stage stochastic optimization model. The proposed model determines the optimal mix of generation and transmission capacity to build to serve future demands at least cost, while respecting technical constraints and climate-related considerations. The model uses a mix of ac and high-voltage dc transmission lines, conventional and renewable generation, and energy-storage units to meet these objectives. Short- and long-term uncertainties are modeled using operating conditions and scenarios, respectively.

We demonstrate the model using a case study that is based on the Texas power system, with 2050 as the target year of the analysis. We include explicit carbon-emissions constraints. Doing so allows us to examine the effect of carbon-reduction targets and deep

decarbonization of electricity production on investment decisions. As expected, we find that thermal-dominated power systems must transition toward having a renewable-dominated generation mix.

The model developed in this chapter have been implemented in GAMS and solved with CPLEX.

2.1 Introduction

As a result of concerns surrounding climate change, 195 countries signed the Paris Agreement under the United Nations Framework Convention on Climate Change in 2015. The agreement includes ambitious climate-related goals, which necessitate rapid and substantive declines in carbon emissions and the carbon-intensity of human activity. Moreover, a number of countries and regional international organizations have adopted carbon-reduction targets of their own. For instance, the European Union has adopted the so-called Energy Roadmap 2050, which includes targets to reduce greenhouse gas emissions by 80%–95% relative to 1990 levels by 2050.

Electricity production represents a major source of anthropogenic carbon emissions. Thus, the electric power system must play a substantive role in these reductions. Greater use of renewable energy sources, such as wind and solar, is one possible means of decarbonizing electricity production. However, the real-time availability of weather-dependent renewable energy sources is variable and uncertain. This gives rise to challenges in relying on such energy sources in place of dispatchable (e.g., thermal) generation. Spatial disaggregation of renewables and energy storage are possible means to mitigate these issues that are caused by resource variability and uncertainty.

There are a number of works in the literature that examine decarbonization pathways for electric power systems and the role of renewables therein. Di Sbroiavacca et al. (2016) show how climate-related goals and carbon reductions could be achieved in the Argentinean electricity sector. Along the same lines, Calderón et al. (2016) examine decarbonization of the Colombian power system. They find that absent climate policy, CO_2 emissions will increase for the foreseeable future with no stabilization. They further show that carbon-reduction goals can be achieved with greater use of renewable resources. Qi et al. (2016) examine how the carbon-intensity of electricity production in China was reduced between 2005 and 2013. The aim of this analysis is to better inform future policy designs for further decarbonization of the Chinese power system.

Although these works demonstrate that renewables can play a significant role in decarbonizing electricity production, renewables create planning and operating challenges. As an example, Graf and Marcantonini (2017) conduct an empirical study of the operation of the Italian power system, using historical data from between 2005

and 2014. They show that renewables did displace thermal generation during this period, thereby reducing emissions. However, they also find that the variability in real-time renewable output increases cycling of thermal plants, reducing their operating efficiencies and slightly increasing their emissions rates. There is, nevertheless, a net emissions reduction from renewables during this period, as the former effect far outweighs the latter.

Expanding upon the findings of Graf and Marcantonini (2017), achieving deep decarbonization of electricity production requires major changes in the generation mix. One must go beyond simply adding more renewables to a power system. Instead, the balance of the system must become more flexible to accommodate the variability of real-time renewable availability. Furthermore, as discussed by Denholm et al. (2010), energy storage is expected to have a growing role as renewables constitute a larger portion of the generation mix. This is because energy storage provides significant flexibility in shifting renewable generation through time, thereby managing its variability.

This work adds to this existing literature by developing a modeling methodology to make generation- and transmission-planning decisions with decarbonization targets. Our model is formulated as a two-stage stochastic optimization problem wherein generation- and transmission-capacity planning decisions are made in the first stage. The second stage represents system operations during a set of representative operating days. These operating days implicitly capture short-term/small-scale uncertainties, such as load and renewable-supply variability. Long-term/large-scale uncertainties, such as changes in generation-fuel prices or load growth, are captured explicitly through scenarios that define the second stage of the stochastic optimization model.

Our model is formulated from the perspective of a central planner (e.g., an integrated-resource planning process that is undertaken by an electric utility or a regulator). A number of jurisdictions have restructured electricity markets in place, meaning that this type of central-planning process does not occur. Our model is, nevertheless, of value in such settings, as it can provide guidance on long-term planning decisions. Moreover, our modeling methodology provides insights as to how investments should be made in a perfectly competitive restructured market.

We focus our model development on representing two types of climate policies. One is an explicit cap on carbon emissions while the other is a carbon price. In this way our model can represent capacity expansion under current European climate policy and policies that have been contemplated in the United States. Our model is also designed to accommodate a variety of technical approaches to decarbonization. This includes the use of renewable technologies, such as wind and concentrating solar power (CSP), nuclear generation, and fossil-fueled generation with carbon capture and sequestration (CCS) systems. Our model allows both ac and high-voltage dc (HVDC) transmission

lines, as well as energy-storage technologies to be built. We allow for standalone energy storage and integrating thermal energy storage (TES) into CSP plants.

We demonstrate our model using a case study that is based on the Texas electric power system, using 2050 as the target planning year. Given the long planning horizon, we can treat the system as having no generation capacity (insomuch as existing capacity today will likely be retired by 2050) but having existing transmission capacity (as such assets are long-lived). By changing the stringency of the decarbonization targets, we examine how the generation and transmission mixes change. We also examine a number of sensitivity cases, which show the impacts of changes in technology development and transmission congestion on the decarbonization pathway of the system. Although our results are specific to our Texas-based case study, we make a number of qualitative observations that are likely broadly applicable. Moreover, our modeling framework is sufficiently generic that it can be applied to determining a decarbonization pathway for any power system.

Our work makes two primary contributions to the existing literature. First, we propose a stochastic optimization framework that represents multi-scale uncertainties, ac and HVDC transmission, renewable generators, and energy-storage facilities. We also incorporate a novel representation of the operation of TES that is incorporated into CSP plants in our model. Second, through our case study and sensitivity analyses, we examine the impacts of a variety of policy and technical factors on power system decarbonization. Specifically, we study the effects of environmental policies, technology improvements, and transmission-network congestion. We also examine tradeoffs between the use of wind and solar generation for decarbonization.

The remainder of this chapter is organized as follows. Section 2.2 details the proposed planning model. Section 2.3 summarizes our case-study data, providing more details on the technology options that are modeled in our analysis. Section 2.4 summarizes our case-study results in a base case while Section 2.5 provides the results of our sensitivity analyses. Section 2.6 concludes.

2.2 Model

Our model follows the approach that is used by Liu et al. (2018b) in representing capacity-planning decisions. More specifically, we use a static two-stage stochastic investment model. The first stage concerns all of the generation- and transmission-investment decisions. The second stage captures all of the operating conditions. Long-term/large-scale uncertainties are represented explicitly in scenarios that define the second stage while short-term/small-scale uncertainties are represented implicitly via different representative operating conditions.

We proceed in this section by first providing model notation, which is then followed by a detailed model formulation. We then further describe the technical and economic features that are captured in the model.

2.2.1 Model Notation

Indexes

c	Index of thermal generation units.
g	Index of wind generation units.
k	Index of CSP generation units.
l	Index of existing and candidate transmission lines.
n	Index of power system nodes.
o	Index of operating conditions.
ref	Index for reference node.
s	Index of standalone energy-storage units.
t	Index of time periods within an operating condition.
w	Index of scenarios.
τ	Index of final time period within an operating condition.

Sets

$\zeta^s(l)$	Sending-end node of transmission line l.
$\zeta^r(l)$	Receiving-end node of transmission line l.
Ω_n^C	Set of thermal units that are located at node n.
Ω_n^G	Set of wind units that are located at node n.
Ω_n^K	Set of CSP units that are located at node n.
Ω^{L+}	Set of candidate transmission lines.
Ω_a^{L+}	Set of candidate ac transmission lines.
Ω_n^S	Set of energy-storage units that are located at node n.

We divide the transmission lines into existing and candidate lines. This is because of our assumption that transmission-infrastructure investments are sufficiently long-lived that transmission corridors that are existing today are still operational in the future target year of the analysis (i.e., 2050 in our case study). We further subdivide the transmission lines into two technology types—ac and HVDC. The reason for this division is that power flows along the two types of lines are modeled differently. We model

power flows along ac transmission lines using a linear approximation of Kirchhoff's laws. Power flows along HVDC lines are represented using a 'pipeline assumption,' whereby power flows can be directed along each line. This is because each HVDC line is a radial connection between a single point in the ac network to a candidate wind or CSP site.

We assume that there are no existing generation or energy-storage units in the target year of the analysis. This is because such assets are too short-lived for units that are operational today to be available in the target year. Thus, all thermal, wind, CSP, and energy-storage units are in actuality candidate units that must be built to be available for operational use. As we further detail below, we model two types of energy-storage units. One are TES systems, which are directly integrated into CSP plants and can only be used to store thermal energy that is produced by the solar field of the respective CSP. The other are standalone energy-storage units, which can be used to store electrical energy from any source. The index, s, corresponds to such standalone energy-storage units.

Parameters

$b_{k,o,t}$	Hour-t capacity factor of CSP unit k in operating condition o [p.u.].
B_l	Susceptance of transmission line l [S].
$\bar{c}_k$	Energy-storage capacity of TES system of CSP unit k [h].
$\bar{c}_s$	Energy-storage capacity of energy-storage unit s [h].
$f_{g,o,t}$	Hour-t capacity factor of wind unit g in operating condition o [p.u.].
$F_l^{\max}$	Capacity of transmission line l [MW].
I_c^C	Investment cost of thermal unit c [$/MW].
$I^{C,\max}$	Investment budget for building thermal units [$].
I_g^G	Investment cost of wind unit g [$/MW].
$I^{G,\max}$	Investment budget for building wind units [$].
I_k^K	Investment cost of CSP unit k [$/MW].
$I^{K,\max}$	Investment budget for building CSP units [$].
I_l^L	Investment cost of candidate transmission line l [$].
$I^{L,\max}$	Investment budget for building candidate transmission lines [$].
I_s^S	Investment cost of energy-storage unit s [$/MW].
$I^{S,\max}$	Investment budget for building energy-storage units [$].
M	A large fixed constant.
$P_{n,o,w,t}^{D,\max}$	Hour-t load at node n in operating condition o of scenario w [MW].

$\bar{P}_c^{C,\max}$ Maximum capacity of thermal unit c that can be built [MW].

$\bar{P}_g^{G,\max}$ Maximum capacity of wind unit g that can be built [MW].

$\bar{P}_k^{K,\max}$ Maximum capacity of CSP unit k that can be built [MW].

$\bar{P}_s^{S,\max}$ Maximum capacity of energy-storage unit s that can be built [MW].

β_k Hourly energy-retention rate of TES system in CSP unit k [p.u.].

$\bar{\epsilon}$ Carbon-emissions limit [t].

ϵ_c Carbon-emissions rate of thermal unit c [t/MWh].

ϵ_s Carbon-emissions rate of energy-storage unit c [t/MWh].

η_k^K Charging efficiency of TES system in CSP unit k [p.u.].

η_s^S Roundtrip efficiency of energy-storage unit s [p.u.].

κ_c^C Production cost of thermal unit c [$/MWh].

κ^D Load-shedding cost [$/MWh].

κ_g^G Production cost of wind unit g [$/MWh].

κ_k^K Production cost of CSP unit k [$/MWh].

$\kappa_k^{K,P}$ Charging cost of TES system of CSP unit k [$/MWh].

$\kappa_k^{K,T}$ Discharging cost of TES system of CSP unit k [$/MWh].

$\kappa_s^{S,P}$ Charging cost of energy-storage unit s [$/MWh].

$\kappa_s^{S,T}$ Discharging cost of energy-storage unit s [$/MWh].

ξ_c^d Ramp-down limit of thermal unit c [MW/h].

ξ_c^u Ramp-up limit of thermal unit c [MW/h].

ρ_o Weight of operating condition o [days].

ϕ_w Probability of scenario w.

χ Carbon-emissions price [$/t].

Decision Variables

$p_{c,o,w,t}^C$ Hour-t production level of thermal unit c in operating condition o of scenario w [MW].

$p_c^{C,\max}$ Capacity of thermal unit c that is built [MW].

$p_{n,o,w,t}^D$ Hour-t load at node n that is shed in operating condition o of scenario w [MW].

$p_{g,o,w,t}^G$ Hour-t production level of wind unit g in operating condition o of scenario w [MW].

$p_g^{G,\max}$ Capacity of wind unit g that is built [MW].

$p^{K}_{k,o,w,t}$ Hour-t production level of CSP unit k in operating condition o of scenario w [MW].

$p^{K,\max}_{k}$ Capacity of CSP unit k that is built [MW].

$p^{L}_{l,o,w,t}$ Hour-t power flow through transmission line l in operating condition o of scenario w [MW].

$p^{S,\max}_{s}$ Capacity of energy-storage unit s that is built [MW].

x^{L}_{l} Binary variable that equals 1 if candidate transmission line l is built and equals 0 otherwise.

$\gamma^{K,L}_{k,o,w,t}$ Ending hour-t state of charge (SOC) of TES system in CSP unit k in operating condition o of scenario w [MWh].

$\gamma^{K,P}_{k,o,w,t}$ Hour-t charging rate of TES system in CSP unit k in operating condition o of scenario w [MW].

$\gamma^{K,T}_{k,o,w,t}$ Hour-t discharging rate of TES system in CSP unit k in operating condition o of scenario w [MW].

$\gamma^{S,L}_{s,o,w,t}$ Ending hour-t SOC of energy-storage unit s in operating condition o of scenario w [MWh].

$\gamma^{S,P}_{s,o,w,t}$ Hour-t charging rate of energy-storage unit s in operating condition o of scenario w [MW].

$\gamma^{S,T}_{s,o,w,t}$ Hour-t discharging rate of energy-storage unit s in operating condition o of scenario w [MW].

$\theta_{n,o,w,t}$ Hour-t phase angle at node n in operating condition o of scenario w [rad].

2.2.2 Model Formulation

Our proposed two-stage stochastic planning model is formulated as:

$$\begin{aligned}\min\ & \sum_{c} I^{C}_{c} p^{C,\max}_{c} + \sum_{g} I^{G}_{g} p^{G,\max}_{g} + \sum_{k} I^{K}_{k} p^{K,\max}_{k} + \sum_{l\in\Omega^{L+}} I^{L}_{l} x^{L}_{l} + \sum_{s} I^{S}_{s} p^{S,\max}_{s} \qquad (2.1)\\ & + \sum_{w,o,t} \phi_w \rho_o \left\{ \sum_{c} \left(\kappa^{C}_{c} + \chi\epsilon_c\right) p^{C}_{c,o,w,t} + \sum_{n} \kappa^{D} p^{D}_{n,o,w,t} + \sum_{g} \kappa^{G}_{g} p^{G}_{g,o,w,t} + \sum_{k} \left(\kappa^{K}_{k} p^{K}_{k,o,w,t} \right.\right.\\ & \left.\left. + \kappa^{K,P}_{k} \gamma^{K,P}_{k,o,w,t} + \kappa^{K,T}_{k} \gamma^{K,T}_{k,o,w,t}\right) + \sum_{s} \left[\kappa^{S,P}_{s} \gamma^{S,P}_{s,o,w,t} + \left(\kappa^{S,T}_{s} + \chi\epsilon_s\right) \gamma^{S,T}_{s,o,w,t}/\eta^{S}_{s}\right] \right\}\\ \text{s.t. } & 0 \le p^{C,\max}_{c} \le \bar{P}^{C,\max}_{c}, \quad \forall c \qquad (2.2)\\ & 0 \le p^{G,\max}_{g} \le \bar{P}^{G,\max}_{g}, \quad \forall g \qquad (2.3)\\ & 0 \le p^{K,\max}_{k} \le \bar{P}^{K,\max}_{k}, \quad \forall k \qquad (2.4)\\ & 0 \le p^{S,\max}_{s} \le \bar{P}^{S,\max}_{s}, \quad \forall s \qquad (2.5)\end{aligned}$$

$$x_l^L \in \{0,1\}, \quad \forall l \in \Omega^{L+} \tag{2.6}$$

$$\sum_c I_c^C p_c^{C,\max} \leq I^{C,\max} \tag{2.7}$$

$$\sum_g I_g^G p_g^{G,\max} \leq I^{G,\max} \tag{2.8}$$

$$\sum_k I_k^K p_k^{K,\max} \leq I^{K,\max} \tag{2.9}$$

$$\sum_s I_s^S p_s^{S,\max} \leq I^{S,\max} \tag{2.10}$$

$$\sum_{l \in \Omega^{L+}} I_l^L x_l^L \leq I^{L,\max} \tag{2.11}$$

$$\sum_{w,o,t} \phi_w \rho_o \left(\sum_c \epsilon_c p_{c,o,w,t}^C + \sum_s \epsilon_s \gamma_{s,o,w,t}^{S,T} \right) \leq \bar{\epsilon} \tag{2.12}$$

$$\begin{aligned} &\sum_{c \in \Omega_n^C} p_{c,o,w,t}^C + \sum_{g \in \Omega_n^G} p_{g,o,w,t}^G + \sum_{k \in \Omega_n^K} \left(p_{k,o,w,t}^K - \gamma_{k,o,w,t}^{K,P} + \gamma_{k,o,w,t}^{K,T} \right) - \sum_{s \in \Omega_n^S} \left(\gamma_{s,o,w,t}^{S,P} - \gamma_{s,o,w,t}^{S,T} / \eta_s^S \right) \\ &\quad + \sum_{l,\zeta^r(l)=n} p_{l,o,w,t}^L - \sum_{l,\zeta^s(l)=n} p_{l,o,w,t}^L = P_{n,o,w,t}^{D,\max} - p_{n,o,w,t}^D, \quad \forall n,o,w,t \end{aligned} \tag{2.13}$$

$$0 \leq p_{c,o,w,t}^C \leq p_c^{C,\max}, \quad \forall c,o,w,t \tag{2.14}$$

$$-\xi_c^d \leq p_{c,o,w,t}^C - p_{c,o,w,t-1}^C \leq \xi_c^u, \quad \forall c,o,w,t>1 \tag{2.15}$$

$$0 \leq p_{g,o,w,t}^G \leq f_{g,o,t} p_g^{G,\max}, \quad \forall g,o,w,t \tag{2.16}$$

$$0 \leq p_{k,o,w,t}^K + \gamma_{k,o,w,t}^{K,P} \leq b_{k,o,t} p_k^{K,\max}, \quad \forall k,o,w,t \tag{2.17}$$

$$0 \leq \gamma_{k,o,w,t}^{K,P} \leq b_{k,o,t} p_k^{K,\max}, \quad \forall k,o,w,t \tag{2.18}$$

$$0 \leq p_{k,o,w,t}^K + \gamma_{k,o,w,t}^{K,T} \leq p_k^{K,\max}, \quad \forall k,o,w,t \tag{2.19}$$

$$0 \leq \gamma_{k,o,w,t}^{K,T} \leq p_k^{K,\max}, \quad \forall k,o,w,t \tag{2.20}$$

$$\gamma_{k,o,w,t}^{K,L} = \beta_k \gamma_{k,o,w,t-1}^{K,L} + \eta_k^K \gamma_{k,o,w,t}^{K,P} - \gamma_{k,o,w,t}^{K,T}, \quad \forall k,o,w,t \tag{2.21}$$

$$0 \leq \gamma_{k,o,w,t}^{K,L} \leq \bar{c}_k p_k^{K,\max}, \quad \forall k,o,w,t \tag{2.22}$$

$$0 \leq \gamma_{s,o,w,t}^{S,P} \leq p_s^{S,\max}, \quad \forall s,o,w,t \tag{2.23}$$

$$0 \leq \gamma_{s,o,w,t}^{S,T} / \eta_s^S \leq p_s^{S,\max}, \quad \forall s,o,w,t \tag{2.24}$$

$$\gamma_{s,o,w,t}^{S,L} = \gamma_{s,o,w,t-1}^{S,L} + \gamma_{s,o,w,t}^{S,P} - \gamma_{s,o,w,t}^{S,T}, \quad \forall s,o,w,t \tag{2.25}$$

$$0 \leq \gamma_{s,o,w,t}^{S,L} \leq \bar{c}_s p_s^{S,\max}, \quad \forall s,o,w,t \tag{2.26}$$

$$\gamma_{s,o,w,\tau}^{S,L} \geq \gamma_{s,o,w,0}^{S,L} = 0.5 p_s^{S,\max}, \quad \forall s,o,w \tag{2.27}$$

$$-F_l^{\max} \leq p_{l,o,w,t}^L \leq F_l^{\max}, \quad \forall l \notin \Omega^{L+}, o,w,t \tag{2.28}$$

$$-F_l^{\max} x_l^L \leq p_{l,o,w,t}^L \leq F_l^{\max} x_l^L, \quad \forall l \in \Omega^{L+}, o,w,t \tag{2.29}$$

$$p_{l,o,w,t}^L = B_l \cdot \left(\theta_{\zeta^s(l),o,w,t} - \theta_{\zeta^r(l),o,w,t} \right), \quad \forall l \notin \Omega^{L+}, o,w,t \tag{2.30}$$

$$-\left(1-x_l^L\right)M \leq p_{l,o,w,t}^L - B_l \cdot \left(\theta_{\zeta^s(l),o,w,t} - \theta_{\zeta^r(l),o,w,t}\right) \leq \left(1-x_l^L\right)M, \quad \forall l \in \Omega_a^{L+}, o, w, t \tag{2.31}$$

$$-\pi \leq \theta_{n,o,w,t} \leq \pi, \quad \forall n, o, w, t \tag{2.32}$$

$$\theta_{\text{ref},o,w,t} = 0, \quad \forall o, w, t \tag{2.33}$$

$$0 \leq p_{n,o,w,t}^D \leq P_{n,o,w,t}^{D,\max}, \quad \forall n, o, w, t. \tag{2.34}$$

Objective function (2.1) consists of total investment and expected operation cost of the power system. We assume that the investment-cost parameters, I_c^C, I_g^G, I_k^K, I_l^L, I_s^S, are annualized to make the investment and operations costs comparable to one another. Otherwise, the costs would be skewed because the investments are long-lived while operations may only be modeled over a short duration (e.g., for a single representative year in our case study). The simplest way to annualize the investment costs is to multiply the overnight cost of building each technology by:

$$\frac{i \cdot (1+i)^y}{(1+i)^y - 1},$$

where y is the assumed lifetime of the asset and i is the real interest rate.

Operating costs are computed under each hour of each operating condition of each scenario. These operating costs include the costs of producing energy from the thermal, wind, and CSP units, the cost of operating the TES that is embedded in the CSP units and the standalone energy-storage units, and the cost of any load curtailment.

We also include operating costs that are associated with CO_2 emissions (e.g., due to a Pigouvian-tax or cap-and-trade policy). We assume two possible sources of CO_2 emissions—thermal generators and standalone energy-storage units. Any fossil-fueled thermal generator that does not have a CCS system incorporated in it will release CO_2. The standalone energy-storage technology that we focus on in our case study is diabatic compressed-air energy storage (CAES). As discussed by Succar et al. (2006); Greenblatt et al. (2007); Succar and Williams (2008), diabatic CAES is in actuality a hybrid energy-storage system that combusts natural gas during the discharging cycle. Thus, we allow for cases in which the use of the energy-storage technology can result in CO_2 emissions. We also examine, in one of our sensitivity cases in Section 2.5.4, the viability of adiabatic CAES, which is a pure energy-storage technology, the use of which does not entail any direct CO_2 emissions.

The model has two types of constraints. Constraints (2.2)–(2.12) pertain to the first (investment) stage while the remaining pertain to the second (operating) stage. Constraints (2.2)–(2.5) impose capacity limits on how much thermal, wind, CSP, and energy-storage capacity can be built at each candidate location. These constraints may reflect land-use, resource, or other physical limitations on the deployment of these

units. Constraints (2.6) impose the binary nature of transmission-expansion decisions, which have this 'lumpy' nature. Constraints (2.7)–(2.11) impose budget constraints on the investment decisions.

Constraint (2.12) imposes an expected carbon-emissions limit (e.g., due to a cap-and-trade system limiting total system emissions). As such, our model captures two common means of imposing carbon-emissions limits. One is an explicit limit, as imposed by constraint (2.12), while the other is a more implicit cost or tax on carbon emissions, which is captured in objective function (2.1). In practice, policy makers often focus on implementing one of these types of policy mechanisms as opposed to both.

Constraints (2.13) impose nodal load balance in each operating period. Constraints (2.14) and (2.15) impose capacity and ramping limits, respectively, on the operation of the thermal units. Constraints (2.16) impose capacity constraints on the output of the wind units. The energy that is available to be produced in each operating period is represented using a capacity factor, which captures the impact of weather conditions. The same approach is used to represent the impact of weather on energy that is available from CSP plants.

Constraints (2.17)–(2.22) pertain to the operation of the CSP units. We model the CSP units by adapting the methodology that is developed by Sioshansi and Denholm (2010a,b). Constraints (2.17) restrict the total amount of energy that each CSP unit produces and stores in its TES system to be no greater than the amount of energy that is collected by the unit's solar field. The energy that is collected by a CSP plant's solar field is thermal. As such, we apply the assumed powerblock efficiency to convert the thermal energy into the equivalent amount of electrical energy that would be produced by the CSP unit when the stored energy is discharged. Doing so allows for more streamlined modeling of the CSP unit and its integrated TES system within a planning model. Constraints (2.18) ensure that the TES system does not store more than its power capacity allows. Constraints (2.19) limit the total production of each CSP unit, either by using energy directly from its solar field or from its TES system, to be no greater than the power capacity of its powerblock. Constraints (2.20) limit the amount of energy that is discharged from the TES system based on its power capacity. Constraints (2.21) define how the SOC of the TES system in each CSP unit evolves from one operating period to the next. Finally, constraints (2.22) impose energy limits on the SOC of the TES system in each CSP unit.

Constraints (2.23)–(2.26) pertain to the operation the standalone energy-storage units. Constraints (2.23)–(2.24) impose power-capacity limits on the charging and discharging, respectively, of energy-storage units. Constraints (2.25) define how the SOC of each energy-storage unit changes from one operating period to the next and

constraints (2.26) impose energy limits on the SOC. Constraints (2.27) fix the SOC of each energy-storage unit at the beginning of each operating condition (which are taken to be representative operating days in our case study) to 50% of its energy capacity. It further requires that the SOC at the end of each operating condition to be above this level. Graves et al. (1999) suggest this as a heuristic technique to ensure that a model does not fully deplete energy storage at the end of each operating horizon. The modeling of the standalone energy-storage units is based on the work of Drury et al. (2011), who develop an optimization model that is tailored to CAES.

Constraints (2.28) impose power-flow limits on each existing transmission line while constraints (2.29) do the same for candidate lines. These latter constraints also force the power flow on a candidate transmission line that is not built to equal zero, which is a physical requirement. Constraints (2.30) define power flows on existing transmission lines in terms of differences in the phase angles at the two ends of the line. Constraints (2.31) define power flows on candidate transmission lines analogously. These latter constraints are written in this inequality form to allow the flows on a candidate transmission line that is not built to equal zero without forcing the phase angles at the two ends of that line to equal one another. This is a standard approach to modeling power flows with binary transmission-investment decisions. Conejo et al. (2016) provide further details on how these constraints are modeled. Power flows in HVDC lines are not modeled using phase angles. Rather, because these lines are radial connections to distant candidate wind or CSP sites, their power flows can be set arbitrarily within their bounds without impacting power flows elsewhere in the network. Constraints (2.32) impose limits on the phase angles and constraints (2.33) fix the phase angles at the reference node to be zero.

Finally, constraints (2.34) limit the amount of load that is curtailed at each node to be no greater than the nodal demand.

Our proposed capacity-expansion model is a mixed-integer linear optimization problem. Thus, it can be tractably solved using off-the-shelf commercial software tools, such as CPLEX or Gurobi. Although we have a stochastic optimization problem, explicit non-anticipativity constraints are not needed. This is because the investment decisions (i.e., $p_c^{C,\max}$, $p_g^{G,\max}$, $p_k^{K,\max}$, $p_s^{S,\max}$, and x_l^L) are defined so as not to depend on the realization of the second-stage scenarios, w. The proposed model can also be used in a rolling-horizon fashion over time, whereby future scenarios are periodically updated (e.g., the model can be re-run every year with updated scenarios of future conditions). Domínguez et al. (2015) argue that using a two-stage stochastic planning model in such a manner can yield solutions that are similar to those that are achieved using a more computationally costly multi-period model.

2.3 Case-Study Data

Our case study considers the 28-node system, which is a modified version of the IEEE 24-node test system, that is shown in Figure 2.1. Generating and energy-storage units are labeled in the figure based on how they are indexed in the model formulation (i.e., c, g, k, and s for thermal, wind, CSP, and standalone energy-storage units, respectively). Existing transmission lines are indicated by solid lines whereas candidate ac lines are indicated by dashed lines. Dotted lines indicate candidate HVDC lines. Loads are indicated by arrows. The topology of the network and other system data are adapted from the Electric Reliability Council of Texas (ERCOT) power system. We focus our case study on ERCOT because it a mostly electrically isolated power system (with the exception of some limited dc tie lines to neighboring interconnects) with substantial load and potential for the deployment of wind and CSP.

Twenty-four of the nodes represent the center of the network where the loads and most of the candidate generating and energy-storage units are located. As such, these nodes are connected by existing ac lines and candidate ac lines can be built to reinforce connections within the center of the network. The remaining nodes are isolated and can be connected to the center of the network with candidate HVDC lines. Two of the nodes are candidate locations for offshore wind generators while the other two are candidate locations for CSP plants.

Our case study includes 63 candidate units: 40 thermal, 11 onshore wind, two offshore wind, two CSP, and eight standalone energy-storage units. Additional candidate CSP units are considered in one of the sensitivity cases that is examined in Section 2.5.3. We consider ten different thermal generation technologies: advanced pulverized coal units (with and without CCS), conventional natural gas-fired combined cycle (NGCC) units, advanced NGCC units (with and without CCS), conventional and advanced natural gas-fired combustion turbines (CT), integrated gasification combined cycle (IGCC) units (with and without CCS), and advanced nuclear units. This represents generating technologies that, as reported by the United States Energy Information Administration (EIA),[1] are available today or that are anticipated to be commercially available by the target year of our analysis (2050).

Table 2.1 summarizes the cost, maximum-capacity, and emissions-rate data for the thermal units, which are obtained from the EIA. All of the technologies are assumed to be able to ramp over their full output range, with the exception of nuclear units, which are assumed to have no ramping capability. Instead, nuclear units are assumed to continuously operate at their installed capacity as must-run units. The operating costs that are reported in Table 2.1 are computed using projections of future fuel prices

[1] https://www.eia.gov/analysis/studies/powerplants/capitalcost/

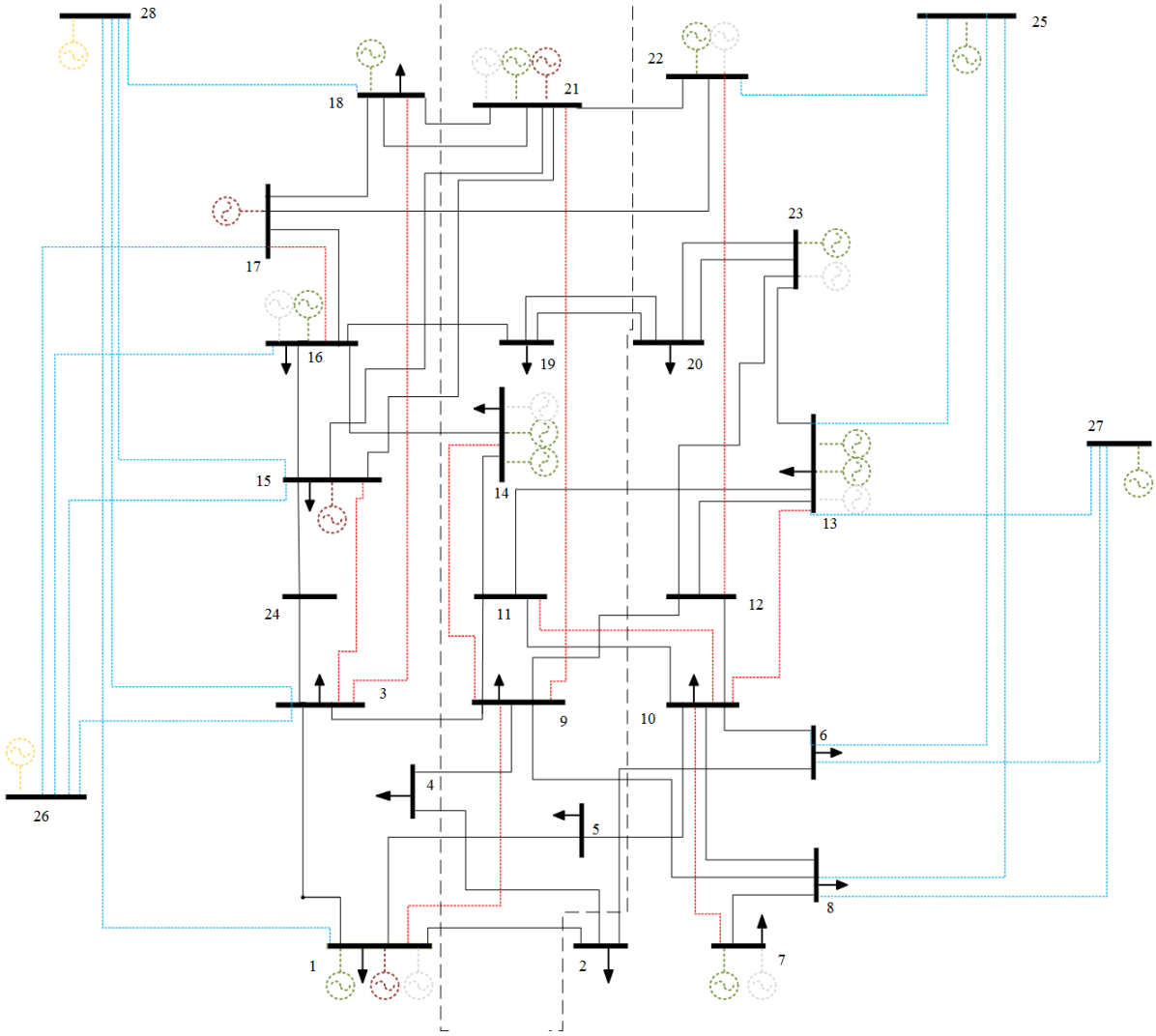

Figure 2.1: 28-Node Network Diagram

that are published by IEA (2017). The maximum capacity for each technology that is reported in Table 2.1 is the total amount that can be installed across all of the candidate locations where that technology can be built. There are 11 candidate locations, which are in the center of the test system, for onshore wind. Conversely, offshore wind can only be built at two nodes that are isolated from the center of the system. Onshore wind has investment costs that range between \$1970/kW and \$2100/kW and operating costs that range between \$2.00/MWh and \$2.71/MWh. A maximum of 7700 MW of wind can be built at the onshore sites (See Table 2.2). Up to 4000 MW of offshore wind can be built. These units have higher investment costs that range between \$2900/kW and \$3190/kW, which reflects the greater complexity that installing offshore wind entails (See Table 2.3). These units also have higher

Table 2.1: Data For Candidate Thermal Units

Technology	Investment Cost [$/kW]	Operating Cost [$/MWh]	Maximum Capacity [MW]	ϵ_c
Advanced Pulverized Coal Without CCS	2933	25.95	3800	0.841
Advanced Pulverized Coal With CCS	5227	38.15	3800	0.112
Conventional NGCC	917	46.82	2880	0.374
Advanced NGCC Without CCS	1023	42.69	2400	0.341
Advanced NGCC With CCS	2095	52.91	2160	0.041
Conventional CT	973	81.97	1600	0.576
Advanced CT	676	70.14	2400	0.518
IGCC Without CCS	3784	26.19	3800	0.743
IGCC With CCS	6599	33.22	3000	0.097
Advanced Nuclear	5530	16.06	4800	0.000

operating costs that range between $4.85/MWh and $5.35/MWh, which reflects the greater challenges in their operation and maintenance. One of the candidate offshore wind units is closer to the shore, which results in its having a lower investment cost (and a lower cost for building the associated HVDC line that connects it to the center of the network). The other offshore wind unit is further from the shore, giving it a higher average capacity factor and lower operating cost . Investment and operating costs of the wind units are obtained from the EIA and the work of Krohn et al. (2009).

Table 2.2: Technical Characteristics of Onshore-Wind Units

Node	Maximum Capacity [MW]	Operating Cost [$/MWh]	Investment Cost [$/kW]
1	700	2.71	2005
7	700	2.15	2022
13	700	2.06	1980
13	700	2.05	2010
14	700	2.10	1990
14	700	2.21	2020
16	700	2.04	2040
18	700	2.00	2100
21	700	2.04	2000
22	700	2.55	1970
23	700	2.02	1980

Up to 2000 MW total of CSP capacity can be built across the two candidate locations. We assume that the solar field of each CSP plant is scaled to maintain a solar multiple of 2.0. A CSP plant with a solar multiple of 2.0 is sized to provide sufficient thermal energy to operate the powerblock at its rated capacity with a direct normal irradiance of 950 W/m^2, a 5-m/s wind speed, and a 25-C ambient temperature. We, furthermore, assume that each CSP plant has a TES system with $\bar{c}_k = 4$ hours

Table 2.3: Technical Characteristics of Offshore-Wind Units

Node	Maximum Capacity [MW]	Operating Cost [$/MWh]	Investment Cost [$/kW]
25	2000	4.85	3190
27	2000	5.35	2900

of storage capacity. This means that a fully charged TES system can be discharged and operated at its nameplate capacity for four consecutive hours.[2] Operating and investment costs for the CSP units are obtained from version 2017.1.17 of the System Advisor Model (SAM). Blair et al. (2014) provide a general overview and description of this software tool. We assume power-tower CSP systems with investment costs ranging between $3272/kW and $3599/kW and generation costs ranging between $3.80/MWh and $4.00/MWh. The TES systems in the CSP plants are assumed to have operating costs of $0.1400/MWh in charging mode and $0.1549/MWh in discharging mode. We assume that the TES systems have a 99% roundtrip efficiency and 0.1% hourly thermal-energy losses, meaning that we have $\eta_k^K = 0.99$ and $\beta_k = 0.999$ for all k. As with the offshore wind units, one of the candidate CSP units is assumed to be closer to a load pocket in the system, meaning that this unit has a lower cost of being connected to the system with HVDC lines. However, this unit has a lower average capacity factor than the other CSP unit (see Table 2.4).

Table 2.4: Technical Characteristics of CSP Units

Node	Maximum Capacity [MW]	Generation Cost [$/MWh]	TES-Discharging Cost [$/MWh]	TES-Charging Cost [$/MWh]	Investment Cost [$/kW]
26	1000	4.00	0.1400	0.1549	3272
28	1000	3.80	0.1400	0.1549	3599

We consider CSP, as opposed to photovoltaic (PV) solar, because CSP is a relatively dispatchable renewable resource owing to the low cost and high efficiency of integrating TES into a CSP plant. Madaeni et al. (2012) show that this characteristic of CSP gives it considerable value for grid-integration purposes. Moreover, Liu et al. (2018b) conduct a long-term generation- and transmission-planning study of the ERCOT system, considering wind and PV solar as renewable-energy resources. They find that relatively little PV solar is built, by virtue of its relatively high energy cost, which is driven by its investment cost and low capacity factor. These properties of

[2] In actuality, a fully charged TES system would operate very slightly below 100% of its nameplate capacity in the fourth hour. The reason for this is that the TES system incurs very slight thermal-energy losses from one hour to the next. Thus, the four-hour definition is based on an assumption of no thermal-energy losses.

CSP *vis-à-vis* PV solar are consistent with the solar-insolation conditions of our case study.

We model a single standalone energy-storage technology, which is diabatic CAES. Diabatic CAES is a hybrid energy-storage technology that uses both electricity (to compress air) and natural gas (when stored energy is discharged). When charged, electricity is used to drive a compressor, which injects pressurized air into a reservoir. When discharged, the compressed air is withdrawn from the reservoir and combined with natural gas in an open-cycle combustion turbine. Combustion produces high-pressure gas, which is expanded through a turbine, that drives both an electric generator and the air compressor. The benefit of using the compressed air in the discharging phase is that the combustion turbine has a heat rate of approximately 4200 BTU/kWh,[3] which is half that of a conventional CT. Because diabatic CAES is a hybrid energy-storage technology, only 0.7 MWh of stored electric energy must be used to discharge 1 MWh of electricity. Adiabatic CAES, further details of which are given in Section 2.5.4, is considered in one of the sensitivity cases. Adiabatic CAES is a pure energy-storage technology, which does not entail the combustion of any fossil fuel when discharged.

Sioshansi et al. (2011) note that CAES is an attractive large-scale energy-storage technology with long life expectancy, low investment and maintenance costs, and reasonable roundtrip efficiency. Moreover, Succar and Williams (2008) find that many areas of the world that are potentially well suited for the deployment of CAES are also wind-rich. This includes ERCOT. This can be contrasted with the (currently) more commonly used pumped hydroelectric storage (PHS) technology, which requires access to water and reservoirs at different elevations. Water is scarce and the requisite geological formations are lacking in many wind-rich areas of the world, including in Texas.

We model eight candidate CAES units (see Table 2.5). Each CAES unit is assumed to have a fixed $\bar{c}_s = 10$ hours of storage capacity. Each CAES units can be built with up to 350 MW of power capacity. We take operating and investment costs and physical properties of the CAES plants from the work of Das et al. (2011). We assume that the investment costs range between \$550/kW and \$610/kW and that each CAES unit has an operating cost of \$0.50/MWh when charging energy. The discharging costs range between \$28.33/MWh and \$28.79/MWh, which primarily reflect the cost of natural gas. Each CAES unit is also assumed to have a carbon-emissions rate of 0.259 t/MWh and an efficiency of $\eta_s^S = 0.7$ (based on the characteristic that only 0.7 MWh of stored energy must be used to discharge 1 MWh of electricity).

The transmission system consists of 38 existing lines, which range in capacity from

[3]We report this heat rate in imperial (as opposed to SI) units, as BTU/kWh is still the most commonly used unit of generator efficiency in the United States.

Table 2.5: Technical Characteristics of Diabatic-CAES Units

Node	Maximum Capacity [MW]	Discharging Cost [$/MWh]	Charging Cost [$/MWh]	Investment Cost [$/kW]	Carbon-Emissions Rate of Discharging [t/MWh]
1	350	28.79	0.5	571	0.259
7	350	28.71	0.5	560	0.259
13	350	28.33	0.5	599	0.259
14	350	28.47	0.5	550	0.259
16	350	28.55	0.5	605	0.259
21	350	28.66	0.5	610	0.259
22	350	28.75	0.5	589	0.259
23	350	28.41	0.5	600	0.259

200 MW to 800 MW and have an average capacity of about 440 MW. These existing lines are all ac and connect the nodes in the center of the network (see Table 2.6). Ten candidate ac lines, with capacities ranging between 400 MW and 800 MW, can be added to create further links amongst the nodes in the center of the network (see Table 2.7). There are a further 15 candidate HVDC lines, which only connect one of the four remote nodes to one of the nodes in the center of the network (see Table 2.8) . Each of the distant nodes has multiple candidate HVDC lines with which it can be connected to the main grid, indicating that a particular offshore-wind or CSP project has multiple potential points of interconnection with the main network. Eight of the HVDC lines have a 2-GW capacity while the remainder have a 1-GW capacity. Transmission-investment costs are obtained from the work of Vaillancourt (2014).

We annualize the investment costs by assuming a 25-year depreciation period and a 10% real interest rate. This yields an 11% cost-annualization rate.

We model different load and wind- and solar-availability conditions using scenarios and operating conditions. Specifically, we represent operations in the target year through a set of operating conditions, which are indexed by o in the model. Each operating condition is taken to be a representative day, which is modeled at hourly time steps (i.e., the index, t, corresponds to the 24 hours of each representative day). We use the scenarios, which are indexed by w in the model, to capture uncertainty in long-term demand growth between today and 2050.

To capture correlations in wind and solar availabilities and load, the operating-condition data are all obtained using historical data from the year 2012. Historical load data are obtained from ERCOT and scaled to obtain reference loads for the system. These reference loads are then apportioned to the nodes (see Figure 2.1) based on the historical distribution of loads to different zones of the ERCOT network.

Wind-speed data are obtained from the Wind Integration National Dataset (WIND) Toolkit. Draxl et al. (2015b,a) provide details and meteorological validation of the WIND Toolkit. Wind speeds are used to determine the real-time availability of wind

Table 2.6: Technical Characteristics of Existing Transmission Lines

From Node	To Node	Reactance [p.u.]	Flow Limit [MW]
1	2	0.014	450
1	3	0.211	220
1	5	0.085	510
1	23	0.087	600
2	4	0.127	220
2	6	0.192	220
3	9	0.119	400
3	24	0.084	400
4	9	0.104	220
5	10	0.088	220
6	10	0.061	200
7	8	0.061	320
8	9	0.165	220
8	10	0.165	220
9	11	0.084	320
9	12	0.084	250
10	11	0.084	230
10	12	0.084	200
11	13	0.048	400
11	14	0.042	320
12	13	0.048	400
12	23	0.097	600
14	16	0.059	600
15	16	0.071	600
15	21	0.049	600
15	21	0.049	600
15	24	0.052	310
16	17	0.026	800
16	19	0.023	600
17	18	0.014	600
17	22	0.105	600
18	21	0.026	600
18	21	0.026	600
19	20	0.040	600
19	20	0.040	600
20	23	0.022	600
20	23	0.022	600
21	22	0.068	600

Table 2.7: Technical Characteristics of Candidate ac Transmission Lines

From Node	To Node	Reactance [p.u.]	Flow Limit [MW]	Investment Cost [$ million]
1	9	0.026	600	210
3	15	0.026	600	200
3	18	0.049	400	312
7	10	0.026	600	201
9	14	0.026	600	190
9	21	0.049	400	315
10	11	0.026	600	180
10	13	0.026	600	195
12	22	0.049	400	290
16	17	0.026	800	190

power, which is represented in the model through the capacity factors, $f_{g,o,t}$. King et al. (2014) validate the use of the WIND Toolkit for this type of simulation. We collect wind-speed data for 33 onshore locations and for the representative southwestern Texas offshore location. The wind-speed data are then processed using SAM, assuming the power curve of a 2-MW Vestas V80/2000 wind turbine with an 80-m hub height to generate hourly wind-availability data. Wind-availability profiles for the 13 candidate wind locations are obtained by spatial averaging of the profiles from the locations in the WIND Toolkit that are used.

Solar availabilities are simulated using SAM, based on weather data that are obtained from the National Solar Radiation Database (NSRDB). Sengupta et al. (2014b,a) provide details and validation of the NSRDB data. We only consider two candidate CSP plants in our base case. As such, we use NSRDB data for five locations that are in relatively close proximity to one another to simulate the solar-availability of each CSP plant (i.e., we use NSRDB data for 10 locations total). We use SAM to simulate the operation of a standard power-tower CSP plant with a 110-MW powerblock, a solar multiple of 2.0, and a TES system with 100 hours of storage capacity. From this simulation, we can determine the maximum amount of thermal energy that is captured by the CSP plant in each hour (i.e., the 100-hour TES system ensures that no thermal energy is curtailed in the SAM simulation due to power constraints on the operation of the plant). We then use the assumed 41.2% average efficiency of the CSP plant's powerblock to convert the simulated thermal energy that is captured by the solar field in each hour to the amount of equivalent electrical energy that would be produced by the powerblock. We finally normalize the potential electrical output by the 110-MW nameplate capacity of the powerblock to obtain hourly capacity factors for each CSP plant that is simulated in SAM. We again use spatial averaging to convert these capacity factors to the capacity factors for each of the two candidate CSP plants that are

Table 2.8: Technical Characteristics of Candidate HVDC Transmission Lines

From Node	To Node	Flow Limit [MW]	Investment Cost [$ million]
25	6	2000	684.0
25	8	2000	817.5
25	13	2000	589.5
25	22	2000	503.5
26	3	1000	503.5
26	15	1000	551.0
26	16	1000	589.0
26	17	1000	617.5
27	6	2000	532.0
27	8	2000	551.0
27	13	2000	503.5
28	1	1000	817.5
28	3	1000	684.0
28	15	1000	589.5
28	18	2000	503.5

used in our planning model. Depending on ambient whether conditions, the capacity factor of a CSP plant can be greater than unity in some hours, indicating that the solar field collects more thermal energy than can be utilized by the powerblock. Such excess energy can be stored in the TES system.

Once we have a full set of load and wind- and solar-availability data for the year, we use k-means clustering to reduce the full year into a set of representative operating days. Thus, we obtain our final set of operating conditions (i.e., the set over which the index, o, in our model is defined) from this process. MacQueen (1967) is a formative work that describes the k-means clustering algorithm, while Baringo and Conejo (2013); Liu et al. (2018a) describe its use in obtaining operating conditions that represent the load, wind, and solar patterns of the year and respect their auto- and cross-correlations. The k-means clustering algorithm provides 15 clusters, each of which gives one representative day for the planning model (i.e., our planning model has 15 day-long operating conditions). The load, wind, and solar data for the operating condition that is used to represent each cluster are obtained from the day within the cluster that is closest to the cluster centroid. We assign a weight to the representative day (i.e., the value of ρ_o in the planning model) that is equal to the number of days within its associated cluster. This clustering results in the system having a peak load of 3.1 GW in the base scenario of the scenario tree.

We consider an additional source of long-term uncertainty, which is demand growth. Demand growth is represented explicitly via second-stage scenarios. We assume that

with probability 0.5 the demands are equal to the values that are obtained from the k-means clustering. With probability 0.3 demands are assumed to grow an additional 5% relative to this baseline value and with probability 0.2 demands are 3% lower. One reason for modeling uncertain demand growth is that it 'forces' the model to build sufficient capacity to serve higher-than-expected demands. This excess capacity that the demand-growth scenarios engender can be analogized to planning-reserve margins, which are normally enforced as constraints in deterministic capacity-expansion models. A benefit of modeling demand-growth scenarios (as opposed to planning-reserve margins) is that the objective function takes into account the expected cost of operating the system under higher-demand scenarios. Deterministic models that include planning-reserve constraints do not normally internalize the cost of operating the excess capacity that is built to provide the reserves (in the event that these units are needed to serve higher-than-expected demand). As such, the investments that are given by deterministic planning models with planning-reserve constraints tend to be skewed toward technologies that are overly costly to operate.

The online supplementary material includes tables that further detail our case-study data, which are excluded here for sake of brevity. All of the cases are programmed using version 21.1.2 of the GAMS mathematical programming language. They are solved using the hybrid branch-and-bound and cutting-plane algorithm in version 12.5.1.0 of the CPLEX solver on a system with Windows 10, a 2.6-GHz processor, and 8 GB of RAM.

2.4 Base-Case Results

Figure 2.2 summarizes the mix of generation and energy-storage units that are built under a variety of cases with different carbon-emissions limits imposed on the system. The first case that is shown in the figure is a 'business-as-usual' (BAU) case, in which constraint (2.12) is relaxed and there is no carbon-emissions limit. The remaining cases impose constraint (2.12), with progressively more aggressive carbon-emissions limits that are defined as reductions relative to the BAU case. The final bar in figure 2.2 is labeled '100% Reduction'. With our case-study data and the technologies that we consider, complete decarbonization of the power system is extremely costly. As such, we allow minuscule carbon emissions in the base case and in all of the sensitivity cases that are considered in Section 2.5. In all of the cases, carbon emissions are reduced by at least 99.7% relative to the BAU case. We, nevertheless, refer to these cases as having 100% carbon reductions. We do not impose a carbon tax in any of these cases, because we assume that explicit carbon-emissions limits are used as the policy mechanism to achieve decarbonization.

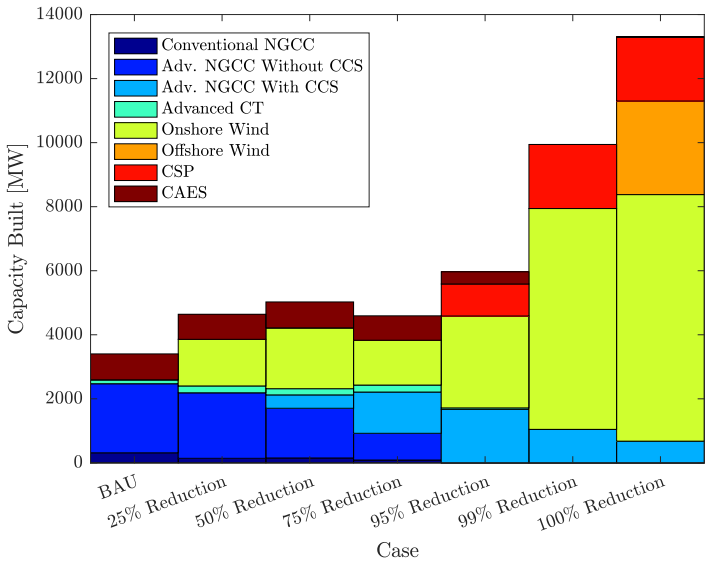

Figure 2.2: Capacity Built In Business-As-Usual Case and with Different Carbon-Emissions Reductions Relative to Business-As-Usual Case

The BAU case yields investments solely in thermal and energy-storage units. This shows that absent any policy mechanism interalizing the social cost of carbon, thermal generation is the lowest-cost source of energy. Among the thermal-generation technologies that are available, natural gas-fired units are favored over other generating fuels. Most of the generating capacity in the BAU case is baseload NGCC, with some CAES and advanced CT capacity being built to serve on-peak loads.

As the carbon-emissions limit is enforced and made more stringent, the investment mix changes in a number of ways. 25% carbon-emissions reductions are achieved through greater investments in onshore wind. 50% and 75% carbon-emissions reductions are achieved using onshore wind and by shifting the thermal generation mix toward having CCS. As the thermal-generation mix shifts toward using CCS, there is still a preference for natural gas over coal as a generation fuel. These results show that onshore wind is initially the lowest-cost source of carbon abatement. CCS is only employed with more stringent carbon-reduction goals, once the prime onshore-wind resources are exploited. Greater carbon-emissions reductions beyond 75% require the use of CSP and offshore wind. This shows that the higher cost of these units, along with the cost of the HVDC connectors that are required to deliver their generation to load, makes these technologies quite expensive. As such, these units are only used with highly aggressive carbon-reduction targets. The fact that offshore wind and CSP are only built to achieve carbon-emissions reductions beyond 75% also implies that HVDC lines are only built with these aggressive carbon-reduction goals.

Interestingly, we find that the role of CAES in providing system flexibility dimin-

ishes as the carbon-reduction target gets more aggressive. This is because of the carbon emissions that are associated with discharging CAES. As the carbon-emissions limit gets tighter, CAES is replaced with CSP (which has TES incorporated in it) as the primary source of supply-side flexibility. This diminishing use of CAES as the carbon-emissions limit becomes more stringent results in increasing wind-curtailment rates. Unlike onshore wind and CSP, offshore wind is only used in the most extreme case in which carbon emissions must be fully eliminated. The 'low priority' for building offshore wind stems from its relatively high cost, inflexibility (as TES cannot be incorporated in wind units), and it having little to no advantage over onshore wind in terms of real-time availability. Indeed, the only major benefit to offshore is that its availability is more stable. The distribution of hourly capacity factors of onshore wind has more extremes compared to offshore wind.

Figure 2.2 also shows that as the carbon-emissions limit gets more stringent, the total installed capacity increases considerably (e.g., from 3.4 GW in the BAU case to 13 GW to achieve 100% carbon-emissions reductions). This is because of the lower capacity factor of wind and solar resources compared to dispatchable thermal generation. The 100%-carbon-reduction case results in a very small amount of NGCC with CCS being built. These units have lower emissions rates than CAES and operate only in a small handful of hours when CSP and wind plants are not fully able to serve the load. These small number of hours in which the NGCC units operate give the minuscule carbon emissions in the 100%-carbon-reduction case.

Although nuclear generation has no direct carbon emissions, nuclear capacity is not built in any of the carbon-reduction cases that we examine. This shows that nuclear is an uneconomic generation source in our case study, despite having no carbon footprint. One may attribute the lack of nuclear capacity to its extremely inflexible ramping capability that we assume. However, if it is sufficiently inexpensive, nuclear could be built to serve off-peak loads only, even without the capability to ramp. Doing so would result in the plant having a 100% capacity factor, as it would operate constantly. Moreover, the availability of low-cost CAES could allow even more nuclear capacity to be built to serve on-peak loads. Sioshansi et al. (2012) note that this use of energy storage (i.e., to store nuclear generation overnight to serve on-peak loads) was the major rationale for developing PHS in the United States in the 1970s. The fact that nuclear is not built in any of the cases that we model, even for these limited uses, show that there are substantively lower-cost energy sources, even when seeking carbon-free electricity.

Figure 2.3 summarizes annual expected operating and investment costs of the system with the different carbon-reduction targets. As expected, enforcing and tightening constraint (2.12) increases overall costs. Although the BAU case is the least costly,

it is interesting to note that the system can achieve non-trivial carbon-emissions reductions with relatively small overall cost increases relative to BAU. For instance, 25% carbon-emissions reductions can be achieved with only an 8% increase in total expected system costs. On the other hand, complete decarbonization of the electricity sector can be much more costly. 99% emissions reductions increase total expected system costs by 126% (relative to BAU) while complete decarbonization increases costs by 216%.

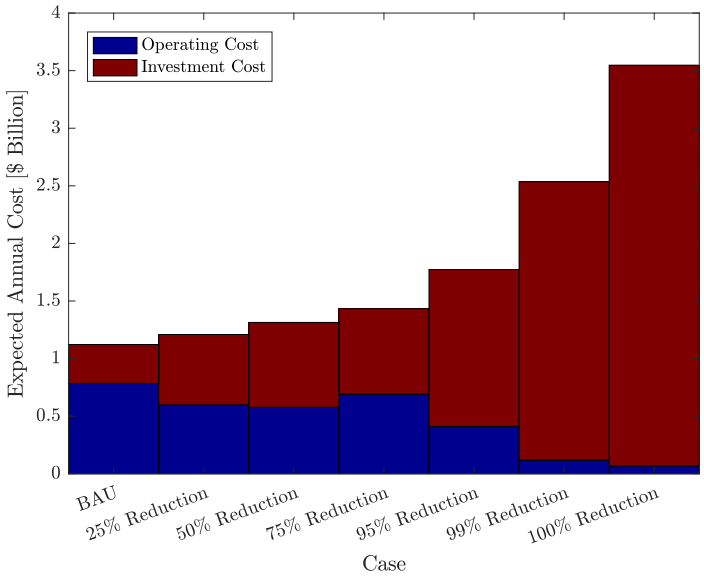

Figure 2.3: Expected Annual Operating and Investment Costs In Business-As-Usual Case and With Different Carbon-Emissions Reductions Relative to Business-As-Usual Case

A question that these cost results raise is what is the optimal level of decarbonization, taking into account its costs and benefits. The United States Environmental Protection Agency (EPA) produced estimates of the social cost of carbon in 2050, under different discount rates and carbon-impact scenarios.[4] We can assess the socially optimal level of carbon reduction by relaxing constraint (2.12) and setting χ (i.e., the carbon-emissions price) equal to a given social-cost-of-carbon estimate in objective function (2.1). Doing so drives the investment model to tradeoff the estimated social cost of carbon against the direct cost of achieving carbon reductions. The EPA estimates a social cost of carbon that ranges between \$69/t and \$212/t. These estimates correspond to socially optimal carbon-reduction levels that range between 25% and 85% (relative to the BAU case).

[4]These estimates, which were produced by the EPA under the administration of President Barack Obama, are archived and publicly available at https://19january2017snapshot.epa.gov/climatechange/social-cost-carbon_.html.

2.5 Sensitivity Analyses

This section presents results of four sensitivity analyses, in which we examine the impacts of different case-study assumptions on the design, cost, and operation of the power system. The first sensitivity case considers improvements in the generation, energy-storage, and HVDC technologies. The second examines the impacts of increased transmission congestion. The third examines the impacts of relaxing land-use restrictions on building CSP plants. The fourth sensitivity case considers adiabatic CAES as an alternative to diabatic CAES.

2.5.1 Technology Improvement

Our first sensitivity case considers three different technology improvements. The first are efficiency and investment-cost improvements in CSP plants. Lilliestam et al. (2017) examine the historical cost-reduction trajectory of CSP. They find that although CSP has not enjoyed, to date, the same cost-reductions that PV solar has, it is beginning to achieve more aggressive cost reductions. Contemporaneously, Turchi et al. (2013); Neises and Turchi (2014) examine the use of supercritical carbon dioxide power cycles in the power blocks of CSP plants. They find that doing so can achieve powerblock efficiencies that are greater than 50%, as opposed to efficiencies ranging between 35% and 45% for the subcritical Rankine cycles that are used in CSP plants today. Based on these findings, we consider a sensitivity case in which the investment costs of CSP plants are 25% lower than in the base case and their efficiencies (which are used to convert the thermal energy that is gathered by the solar fields into electricity-out capacity factors) are increased to 55%.

The second technology improvement involves offshore wind. IEA (2016b) finds that offshore wind is costly relative to onshore wind, but that there is potential for this cost difference to be closed. Moreover, offshore wind also suffers from the need for radial HVDC lines to connect generating units to load pockets. Thus, we consider a sensitivity case in which the investment costs of offshore wind plants are reduced 35% (making their costs comparable to onshore wind) and the cost of HVDC lines are reduced an average of 63%, relative to the base case (see Table 2.9.

The final technology improvement that we consider is a 10% investment-cost reduction for CAES. This reflects the impacts of learning, which can reduce investment costs as CAES plants are developed around the world in the coming years.

Figure 2.4 summarizes the capacity of generating and energy-storage units that are built under the technology-improvement sensitivity cases. The bars in the figure are grouped into four sets of three, each of which corresponds to a different technology-improvement case. The first three sets of bars correspond to one of the three technology

Table 2.9: Investment Costs of Candidate HVDC Transmission Lines

From Node	To Node	Investment Cost [$ million]
25	6	304.0
25	8	437.0
25	13	209.0
25	22	123.5
26	3	123.5
26	15	171.0
26	16	209.0
26	17	237.5
27	6	152.0
27	8	171.0
27	13	123.5
28	1	437.5
28	3	304.5
28	15	209.0
28	18	123.5

improvements (e.g., CSP, offshore wind, or CAES) occurring individually. The fourth set of three bars correspond to a case in which all three of the technology improvements occur simultaneously. For each of the four technology-improvement cases, we examine investment decisions under a BAU case and in cases in which carbon emissions are limited to being 50% and 95% less than in the BAU case.[5]

The figure shows that in all of the technology-improvement cases that we examine, none of the renewable technologies are cost-competitive with thermal generation in a BAU case. This indicates that further technology improvements and cost reductions would be needed to make the renewable technologies that we examine cost-competitive with thermal generation in a BAU case. However, if CAES achieves the investment-cost reductions that we examine here, there is a 15% increase in installed CAES capacity in the BAU case. This increased CAES investment comes with the exact same reduction in CT capacity, meaning that CAES is being used to displace this expensive peaking capacity.

The technology-improvement cases that we examine result in some changes in the generation mix as carbon-emissions limits are imposed. Reducing carbon emissions by 50% in any of three individual technology-improvement sensitivity cases gives investment mixes that are similar to that in the base case. In all of these cases, there is investment in onshore wind, which displaces thermal generation, to acheive the requisite

[5]The carbon-emissions limits are defined, in all of the sensitivity cases in this section, relative to the carbon emissions in the corresponding BAU case.

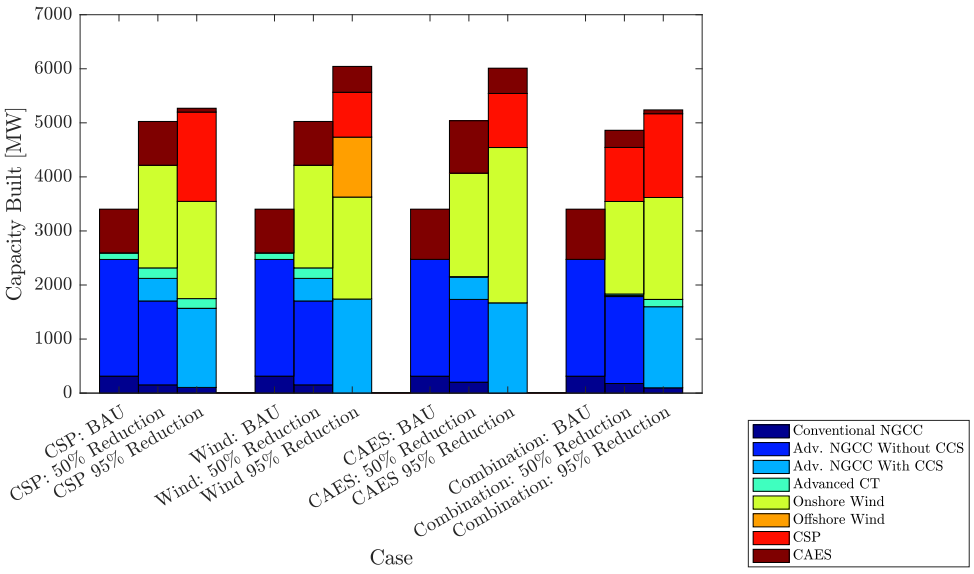

Figure 2.4: Capacity Built In Business-As-Usual Case and with Different Carbon-Emissions Reductions Relative to Business-As-Usual Case Under Technology-Improvement Sensitivity Analysis

carbon reductions. However, the investments are different with 50% carbon-emissions reductions in the 'combined' technology-improvement sensitivity case. The combined case sees less onshore-wind and CAES investments and greater CSP capacity compared to the three individual technology-improvement sensitivity cases. This is due to the combined impact of higher CSP efficiency and lower CSP- and HVDC-investment costs, which make CSP an economic alternative to onshore wind. Moreover, because CSP has integrated TES, the flexibility that this affords reduces the need for CAES. In sum, the CSP displaces close to 200 MW of onshore wind and 500 MW of thermal capacity, relative to the base case.

These trends continue with a 95%-emissions-reduction target. In all of the sensitivity cases, except for the case in which offshore wind *only* achieves technology improvements, CSP has a greater role in decarbonizing the generation mix. Compared to the base case, the combined and CSP-only technology-improvement sensitivity cases see nearly 1 GW less onshore-wind, 300 MW less CAES, and 600 MW more CSP investments. The fact that 1 GW of wind can be displaced by 600 MW of CSP capacity further illustrates the flexibility benefit that the TES, which is integrated into the CSP plants, provides. When the system relies on wind for decarbonization in the base case, greater capacity must be built to manage the variability in real-time wind availability. The TES systems in the CSP plants reduce the need for such oversizing, as the TES can be used to mitigate the impacts of variable solar availability.

The sensitivity case in which offshore wind *only* has technology improvements re-

sults in 1.1 GW of offshore wind being built in place of about 200 MW of CSP (relative to the base case) to achieve 95% emissions reductions. This can be contrasted with the base case, in which offshore wind is only built to achieve complete decarbonization, due to its relatively high cost. Interestingly, no offshore wind is built to achieve 95% emissions reductions in the combined technology-improvement case. This is because, although offshore wind is economically viable in the combined technology-improvement case, so too is CSP, which is less costly and more flexible than offshore wind.

Figure 2.5 summarizes the annual expected operating and investment costs of the system under the four technology-improvement sensitivity cases. The figure shows that these sensitivity cases yield mixed cost savings. For instance, the combined technology-improvement cases reduces the cost of achieving 50% and 95% emissions reductions by 22% and 33%, respectively, relative to the base case. The case in which CSP *only* has technology improvements reduces the cost of achieving these emissions reductions by 6% and 22%. This can be contrasted with a case in which offshore wind *only* has technology improvements, which only yields an 8% reduction in the cost of achieving 95% emissions reductions. This follows from the results that are summarized in Figure 2.4—the combined and CSP-only technology-improvement sensitivity cases yielded the most notable differences in the generation mix.

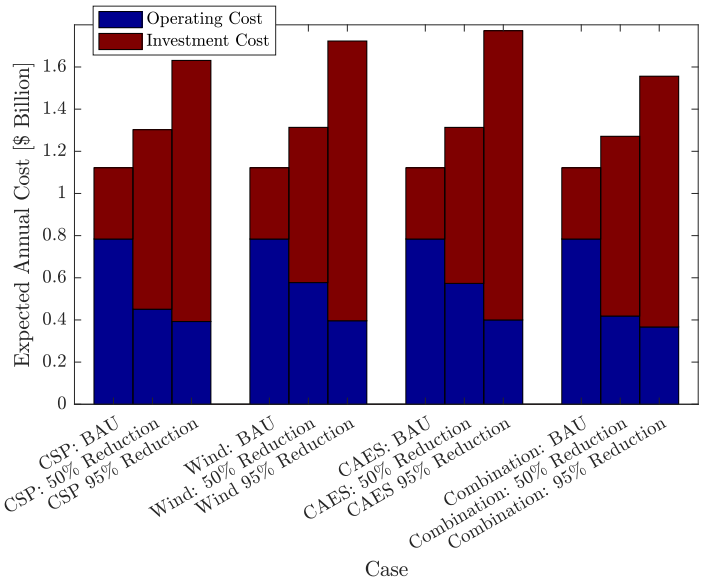

Figure 2.5: Expected Annual Operating and Investment Costs In Business-As-Usual Case and With Different Carbon-Emissions Reductions Relative to Business-As-Usual Case Under Technology-Improvement Sensitivity Analysis

2.5.2 Transmission Congestion

Our second sensitivity analysis considers the impacts of diminished transmission capacity, which can result from smaller-sized transmission equipment being installed and land-use or other restrictions on building candidate lines. We consider a case in which the transmission capacity of all existing and candidate lines is reduced by 25%. We further assume that five of the candidate ac lines, which are close to load pockets in the transmission network, are no longer available to be built.

Figure 2.6 shows the mix of generation and CAES units that are built in the transmission-congestion sensitivity case with different emissions-reduction targets. Overall, the transmission-congestion sensitivity case results in greater transmission investments and requires more generation and CAES capacity to be built, relative to the base case. The base case does not require new transmission builds until reducing carbon emissions by 95%. Moreover, these transmission builds in the base case are primarily to deliver energy from remote renewable units to loads. Conversely, the transmission-congested sensitivity case requires transmissions builds even in the BAU case. These transmission builds are needed simply to avoid load curtailment. The 99%-carbon-reduction case requires more than double the transmission investment relative to the base case.

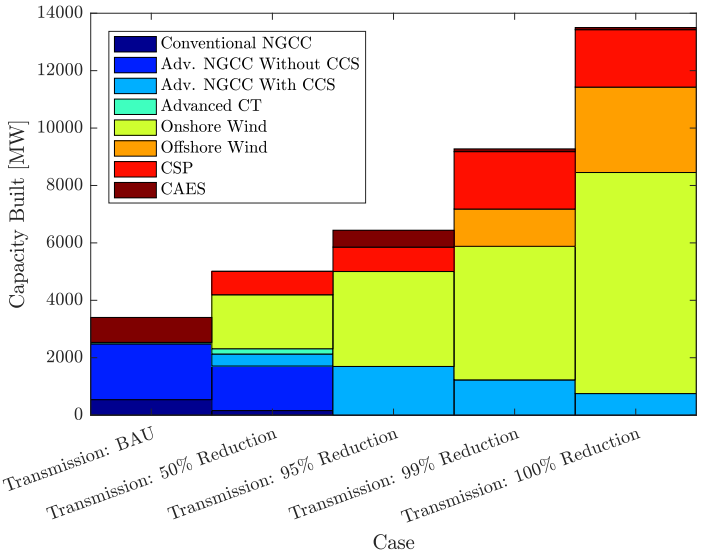

Figure 2.6: Capacity Built In Business-As-Usual Case and with Different Carbon-Emissions Reductions Relative to Business-As-Usual Case Under Transmission-Congestion Sensitivity Analysis

The generation and CAES units are more dispersed throughout the transmission network than in the base case. Dispersing the energy-production and -storage capacities across the network provides greater flexibility in having energy available in

congested load pockets. One benefit of renewable units in this regard is that they are fairly dispersed within the network. As such, renewable and CAES units are jointly able to provide a great deal of congestion relief. One interesting observation regarding the operation of the system in the transmission-constrained case is that some hours see simultaneous charging and discharging of energy-storage units at different locations in the network. This is inefficient, insomuch as energy is lost when it is stored. Simultaneous charging and discharging of energy storage is nonetheless necessary, because load peaks and troughs occur at different times at different locations. As such, absent transmission capacity, excess energy must be stored at some nodes in the network despite stored energy being discharged to serve load elsewhere in the network.

2.5.3 Land Use

The purpose of the land-use sensitivity case is to further explore the economic competitiveness of CSP relative to onshore wind. Our base case places CSP at a competitive disadvantage compared to onshore wind, because CSP can only be connected to the network via radial HVDC transmission lines. As such, CSP bears an additional cost compared to onshore wind, which can use existing transmission corridors and can, in some cases, be co-located with load. The land-use sensitivity case explores the competitiveness of CSP independent of transmission-interconnection costs, by allowing CSP plants to be built at each node where onshore wind can be. These additional candidate CSP plants are assumed to have the same cost and technical characteristics as the CSP units in the base case (see Table 2.10).

We use weather data for 18 additional locations, which correspond to the nodes where onshore wind can be built, to simulate real-time availability of the added candidate CSP plants. We also consider a sensitivity case, which removes the land-use restrictions on building CSP plants and which assumes that CSP achieves the technology improvements that are outlined in Section 2.5.1 (see Table 2.11).

Figure 2.7 summarizes the generation and energy-storage capacities that are built with different emissions-reductions targets under the two land-use sensitivity cases. The first set of six bars corresponds to a case in which *only* land-use restrictions on the deployment of CSP are relaxed. The second set of six bars corresponds to a case in which land-use restrictions are relaxed and the CSP-technology improvements that are outlined in Section 2.5.1 are assumed. The first set of bars shows that even without the cost of interconnecting with the transmission network, CSP is not cost competitive with onshore-wind units. Indeed, the only difference in CSP investments that results from relaxing land-use restrictions is that slightly more capacity is built to achieve 99% emissions reductions. In fact, we find that with land-use restrictions CSP is only built when the capacity to build onshore wind at a particular node is exhausted.

Table 2.10: Technical Characteristics of Additional CSP Units in Land-Use Sensitivity Case

Node	Maximum Capacity [MW]	Generation Cost [$/MWh]	TES-Discharging Cost [$/MWh]	TES-Charging Cost [$/MWh]	Investment Cost [$/kW]
1	350	3.86	0.14	0.1549	3507
7	350	3.87	0.14	0.1549	3442
13	350	3.86	0.14	0.1549	3336
13	350	3.81	0.14	0.1549	3471
14	350	3.88	0.14	0.1549	3513
14	350	3.85	0.14	0.1549	3350
16	350	3.87	0.14	0.1549	3239
18	350	3.85	0.14	0.1549	3345
21	350	3.82	0.14	0.1549	3432
22	350	3.83	0.14	0.1549	3222
23	350	3.89	0.14	0.1549	3417
26	1000	4.00	0.14	0.1549	3599
28	1000	3.80	0.14	0.1549	3272

The second set of six bars in Figure 2.7 shows that this result is reversed if land-use restrictions are relaxed *and* CSP achieves technology improvements. Considerably more CSP capacity is built under these assumptions compared to the base case (and the land-use-*only* sensitivity case) to achieve carbon-emissions reductions between 25% and 95%. Interestingly, the amount of CSP capacity that is built to achieve 99% carbon-emissions reductions is the same with and without the CSP-technology improvements. This suggests that with 99%-carbon-emissions reductions, the CSP that is built is solely driven by the emissions constraint and not by the economics of the technology.

The findings of this sensitivity case are consistent with current experience in the deployment of renewable energy sources. Although CSP has a flexibility benefit relative to wind (and PV solar) that stems from the ability to integrate low-cost TES, CSP has seen little deployment compared to wind. This is largely because CSP is considerably more expensive to build (even when neglecting transmission-interconnection costs). However, our sensitivity cases in which CSP achieves technology improvements (both the case examined here and those in Section 2.5.1) reveal that CSP has the potential to become highly competitive with wind.

2.5.4 Adiabatic CAES

This sensitivity case considers the use of adiabatic CAES as an alternative to diabatic CAES. Unlike diabatic CAES, adiabatic CAES is a pure energy-storage technology. The primary difference between diabatic- and adiabatic-CAES systems is the treatment

Table 2.11: Technical Characteristics of Additional CSP Units in Land-Use Sensitivity Case With Technology Improvements

Node	Maximum Capacity [MW]	Generation Cost [$/MWh]	TES-Discharging Cost [$/MWh]	TES-Charging Cost [$/MWh]	Investment Cost [$/kW]
1	350	3.86	0.14	0.1549	2630
7	350	3.87	0.14	0.1549	2581
13	350	3.86	0.14	0.1549	2502
13	350	3.81	0.14	0.1549	2603
14	350	3.88	0.14	0.1549	2634
14	350	3.85	0.14	0.1549	2512
16	350	3.87	0.14	0.1549	2429
18	350	3.85	0.14	0.1549	2508
21	350	3.82	0.14	0.1549	2574
22	350	3.83	0.14	0.1549	2416
23	350	3.89	0.14	0.1549	2562
26	1000	4.00	0.14	0.1549	2699
28	1000	3.8	0.14	0.1549	2454

of the waste heat that is produced when air is compressed in the storage cycle. In a diabatic-CAES system, the waste heat is exhausted to the atmosphere. As such, a diabatic-CAES system must combust natural gas as a heat source when expanding the compressed air in the discharging cycle. An adiabatic-CAES system, conversely, stores the waste heat (often in a dedicated TES system). This stored heat is then combined with the compressed air during the discharging cycle, alleviating the need to use natural gas. This makes adiabatic CAES considerably less costly to operate than diabatic CAES. Moreover, adiabatic CAES involves no direct carbon emissions, unlike a diabatic-CAES system, which emits carbon when combusting the natural gas in the discharging cycle. Hartmann et al. (2012); Barnes et al. (2015); Barbour et al. (2015); Liu and Wang (2016); Sciacovelli et al. (2017) provide further details regarding the technical properties and viability of adiabatic CAES.

The adiabatic-CAES sensitivity case assumes that this technology is available in place of diabatic CAES. It is difficult to estimate the technical characteristics of adiabatic CAES, because no commercial-scale systems exist today. Indeed, the DOE Global Energy Storage Database[6] lists the 500 kW Pollegio-Loderio Tunnel Demonstration Plant in Switzerland as the only operational adiabatic CAES plant as of July, 2018. Thus, we rely on current and future estimates of the capabilities of these plants in modeling the adiabatic-CAES sensitivity case.

We assume that the adiabatic-CAES plants have the $\bar{c}_s = 10$ hours of storage capacity and that each unit can have up to 350 MW of power capacity built. The

[6] https://www.energystorageexchange.org/

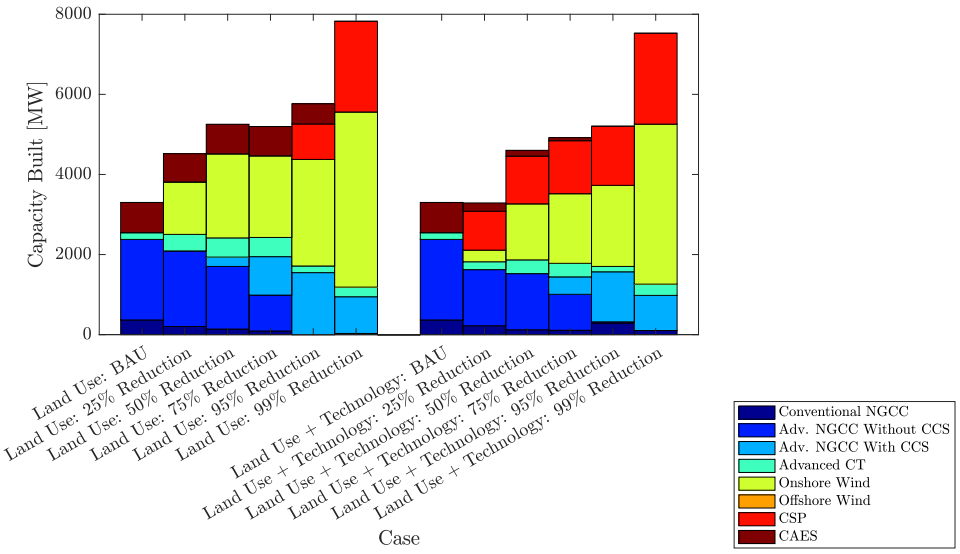

Figure 2.7: Capacity Built In Business-As-Usual Case and with Different Carbon-Emissions Reductions Relative to Business-As-Usual Case Under Land-Use Sensitivity Analysis

adiabatic-CAES units are assumed to have efficiencies of $\eta_s^S = 1.33$, which means that 1.33 MWh of energy must be stored to later discharge 1 MWh of electricity. η_s^S being greater than 1 reflects the fact that adiabatic CAES is a pure energy-storage technology, meaning that electricity is lost in the storage cycle. However, the benefit of this energy loss is that the adiabatic-CAES units have zero carbon emissions.

We consider two sets of investment and operating costs for the adiabatic-CAES plants. The first set, which reflect current cost estimates, assumes investment costs ranging between \$1187/kW and \$1210/kW and charging and discharging costs of \$14/MWh and \$17/MWh, respectively (see Table 2.12).

Table 2.12: Technical Characteristics of Adiabatic-CAES Units With High Costs

Node	Maximum Capacity [MW]	Discharging Cost [\$/MWh]	Charging Cost [\$/MWh]	Investment Cost [\$/kW]
1	350	14	17	1198
7	350	14	17	1187
13	350	14	17	1199
14	350	14	17	1210
16	350	14	17	1195
21	350	14	17	1205
22	350	14	17	1189
23	350	14	17	1200

The second set, which reflect possible future cost reductions, assumes investment costs ranging between \$594/kW and \$605/kW and charging and discharging costs of \$12/MWh and \$13/MWh, respectively (see Table 2.13).

Table 2.13: Technical Characteristics of Adiabatic-CAES Units With Low Costs

Node	Maximum Capacity [MW]	Discharging Cost [\$/MWh]	Charging Cost [\$/MWh]	Investment Cost [\$/kW]
1	350	11.5	12.5	599
7	350	11.5	12.5	593
13	350	11.5	12.5	599
14	350	11.5	12.5	605
16	350	11.5	12.5	597
21	350	11.5	12.5	602
22	350	11.5	12.5	504
23	350	11.5	12.5	600

Figure 2.8 summarizes the generation and energy-storage capacities that are built in the adiabatic-CAES sensitivity case with different emissions-reduction targets. The first set of bars correspond to a case with high investment and operating costs for adiabatic CAES, whereas the second set correspond to lower future cost projections. Interestingly, we find that adiabatic CAES is a considerably less desirable energy-storage technology compared to diabatic CAES. The base case and other sensitivity cases result in some diabatic CAES being built, except with extremely high emissions-reduction targets. This is because once the emissions-reduction target is sufficiently stringent, the carbon emissions that are associated with discharging diabatic CAES makes it use infeasible.

Adiabatic CAES relaxes the impact of the emissions-reduction constraint on the use of CAES. However, adiabatic CAES is more costly than diabatic CAES. This cost disadvantage overwhelms the zero-emissions benefit of adiabatic CAES, except in the extreme case of full decarbonization. With full decarbonization, about 10 MW and 500 MW of adiabatic CAES is built with high and low costs, respectively, as opposed to no diabatic CAES in the base case.

2.6 Discussion and Conclusions

This work presents a two-stage stochastic optimization model that can be used for long-term power system-expansion planning. We pay particular attention to modeling carbon-emissions limits and decarbonization of electricity production. This can

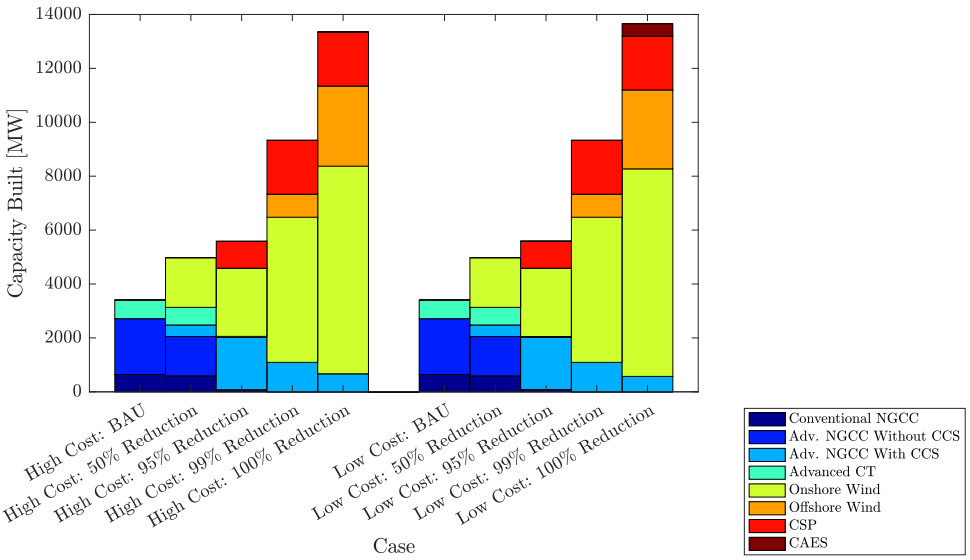

Figure 2.8: Capacity Built In Business-As-Usual Case and with Different Carbon-Emissions Reductions Relative to Business-As-Usual Case Under Adiabatic-CAES Sensitivity Analysis

be achieved in our model using two policy mechanisms: either *via* an explicit carbon-emissions constraint or by pricing carbon (e.g., Pigouvian taxes on emissions). Our model and case study consider three technical options for decarbonization—renewable energy sources, nuclear generators, and fossil-fueled plants with integrated CCS systems.

Weather-dependent renewable generators raise modeling, planning, and operating challenges, because their real-time resource availability is uncertain and variable. As such, we include energy-storage technologies in the model as a flexibility source for mitigating these characteristics of renewables. We focus on two energy-storage technologies—CAES and TES integrated in CSP plants—in our case study, which can be widely deployed in high-renewable-penetration scenarios. The real-time variability of renewable availability is captured in our model using a variety of different operating conditions. These operating conditions capture the range of weather conditions over the course of a year, which can give different load levels and wind and solar availabilities. Large-scale uncertainties, such as long-term load growth, are captured explicitly through second-stage scenarios in the scenario tree.

We demonstrate our model and analyze decarbonization pathways using a detailed case study that is based on the ERCOT system. We find that absent any policy mechanism that internalizes the societal cost of carbon, the power system will maintain a fossil-fueled generation mix with some CAES to alleviate the need to build peaking generation capacity. Natural gas is preferred to coal as a generation fuel, given its

anticipated low cost and the high efficiency of NGCC units. This system design holds regardless of potential future cost reductions in renewable and CAES technologies.

As the social cost of carbon is internalized (we do this in our case study *via* explicit carbon-emissions limits) the system moves away from natural gas-fired generators toward onshore-wind capacity. Moreover, portions of the natural gas-fired fleet uses CCS for modest carbon-emissions limits. As the carbon-emissions limits become very stringent, fossil-fueled generation is essentially completely phased out of the system. CAES is also phased out, because of the carbon emissions that are associated with the combustion of natural gas in the discharging cycle. The flexibility that CAES affords is instead provided by CSP plants, which have TES incorporated in them. Finally, achieving complete decarbonization of the electric power system calls upon the use of offshore wind, which tends to be more costly than onshore with only marginal relative improvements in its capacity factor. Interestingly, nuclear is not used for decarbonization purposes, given its very high cost.

Achieving modest decarbonization targets yields relatively small expected power system-cost increases. Indeed, we find that for the range of social costs of carbon that were published by the EPA, reducing carbon emissions by between 25% and 85% (relative to a BAU case) is socially optimal. One of the challenges in setting carbon policy is that the social costs of climate change are difficult to estimate *a priori*. Thus, it may prove robust against the potential for catastrophic impacts of climate change to set decarbonization targets that are toward the upper end of this range.

Under current estimates of costs and technical characteristics, onshore wind is the most attractive renewable-energy technology that we consider. We find, however, that if CSP achieves its projected cost reductions and efficiency gains and if transmission-interconnection costs are reduced, CSP can become an extremely competitive alternative to onshore wind. Moreover, the inherent flexibility of CSP alleviates the need to build standalone energy-storage capacity. Offshore wind is generally not competitive with onshore wind and CSP. This is because of its relatively high investment and operating costs and the need to build radial HVDC lines to connect it to load centers. For these reasons, offshore wind is normally only built if all other renewable-energy sources are exhausted.

Diabatic CAES is an economically feasible alternative to PHS, which is currently the most widely deployed energy-storage technology. This is an important finding, because many parts of the world lack either the water or geological formations that are necessary for the deployment of PHS. CAES, on the other hand, has the potential to be deployed in many renewable-rich regions. The major difficulty that diabatic CAES raises is the emission of carbon that is associated with the discharging cycle. Adiabatic CAES, which is a technology that is currently in the demonstration phase,

holds the potential to mitigate the carbon-emissions issue of diabatic CAES. However, our adiabatic-CAES sensitivity case reveals that with current and future projections of technology costs, adiabatic CAES is not an economic source of supply-side flexibility. Our findings suggest that adiabatic CAES will require further development to become a viable alternative to diabatic CAES, except under extreme carbon-reduction targets.

Chapter 3

An adaptive robust optimization approach for expansion planning of a small size electric energy system with electric vehicles and renewable units

This chapter is based on the article:
Boffino L., L. Baringo, G. Oggioni.
An adaptive robust optimization approach for expansion planning of a small size electric energy system with electric vehicles and renewable units
which is currently submitted to the European Journal of Operational Research

In this chapter we propose a stochastic adaptive robust optimization approach for the expansion planning problem of a small size electricity system. This involves the construction of candidate renewable generating units, network lines, storage units, and charging stations for electric vehicles. The problem is formulated under the perspective of a central planner, which aims at determining the expansion plan that minimizes both investment and operation costs, including the power exchanged with the transmission system. We consider both short- and long-term uncertainties that are modeled in different way. In particular, short-term uncertainties in the demand variability, in the production of stochastic units, and in the price of electricity withdrawn from or injected into the transmission system are modeled through a number of operating conditions. Long-term uncertainties in the future peak demands, in the future value of electricity exchanged with the transmission grid, and in the number of electric vehicles

are modeled using confidence bounds. A case study, based on a four-node network, is used to illustrate the effectiveness of the proposed technique and to analyze the relationship between the optimal expansions decisions, the revenues from selling electricity to the electric vehicles, and the degree of independence from the transmission system. Moreover, an ex-post decarbonization analysis is conducted to evaluate the environmental impact of the adoption of electric vehicles.

The model developed in this chapter have been implemented in GAMS and solved with CPLEX.

3.1 Introduction

The implementation of the Energy Roadmap 2050 (see EU Commission (2011a)) commits Europe to reducing greenhouse gas (GHG) emissions to 80-95% below 1990 levels by 2050. This target can be accomplished thanks to the full decarbonization of energy systems, the transition towards low- and zero-emission vehicles, and investments in efficient technologies. This is a direct consequence of the fact that the energy sector is the main responsible of carbon emissions followed by transport sector that generates around a quarter of the European GHG emissions. It is clear that, in the future, a large share of the planned GHG emissions reductions should come from road transport. However, while GHG emissions from energy and industrial sectors have been reduced in recent decades, those from transport have significantly increased. For instance, emissions from road transport are today around 17% above 1990 levels.

For this reason, the European Commission outlined in a White Paper issued in 2011 (see EU Commission (2011b)) a roadmap for the transport sector to achieve a 60% reduction in its GHG emissions levels compared with those of 1990 by 2050.

This White Paper shows how the transition to a more sustainable transport system can be addressed by reducing the European dependence on oil to both lower GHG emissions and improve energy security. In particular, it describes goals for a competitive and efficient transport system, including benchmarks, such as halving the utilization of conventionally fuelled cars in urban transport by 2030 and phasing them out entirely in cities by 2050. More recently, the European Commission has published a guideline for low-emission mobility that highlights the importance of removing obstacles to the transport electrification to move towards low and zero-emission vehicles and increase the supply of low-emission alternative fuels, such as renewable electricity (see EU Commission (2016)).

The direct consequence of the implementation of these policies put forward by the European Commission would be a progressively increasing penetration of electric vehicles (EVs) in the coming years. This may impose additional challenges to small

size electric energy systems (SSEESs) that are already stressed by the uncertainty and variability of the renewable generating units.

This work focuses on these aspects and proposes an expansion planning model for a SSEES considering the perspective of a central planner. This operator can invest in storage and renewable (photovoltaic or PV) units in addition to charging stations for EVs. It can also decide to reinforce existing lines or build new ones. Storage units are considered to compensate for the variability of the electricity production from PV power plants; network line expansion increases system adequacy and reliability taking into consideration the fact that electricity is required both by consumers and EVs. Demand is located in each node of the network and is supplied either by the electricity produced by PV plants, the storage units, or by that withdrawn from the transmission grid (main grid in the following) with which the SSEES is connected. Note that we also allow the SSEES to sell electricity to the main grid in the case where its electricity production exceeds the local needs.

These storage, renewable, charging station, and line (SRC&L) investment decisions are taken on the basis of two degrees of uncertainty: a short-term one that describes the daily variability of the residential demand, the production of the stochastic PV units, and the price of electricity exchanged with the main grid; and a long-term one that regards the future peak demand, the future price of the electricity exchanged with the main grid, and the future number of EVs. The short-term uncertainty is modeled through a set of operating conditions. Each operating condition is taken to be a representative day, which is modeled at hourly time steps (see Section 3.2.2).

On the other side, two methods are generally considered in the technical literature to deal with medium- and long-term uncertainty in this type of decision-making problems. One of them is stochastic programming (see, e.g., Birge and Louveaux (1997)) that models uncertain parameters using a set of scenarios. The main drawback of this approach is that its accuracy strongly depends on the knowledge of the probability distribution of uncertain parameters and on the number of scenarios. On the one hand, for a long-term planning problem such as the one considered in this work, it is not straightforward to have a good forecast of probability distributions of uncertain parameters. Moreover, increasing the number of scenarios may result in an intractable problem. The other option used in the technical literature is robust optimization (see Bertsimas and Sim (2004)) that ensures worst case protection within confidence bounds.

For these reasons, we decide to model the long-term uncertainty in the aforementioned parameters using confidence bounds whose construction is generally much simpler than generating scenarios.

More precisely, we apply an Adaptive Robust Optimization (ARO) framework (see

Bertsimas and Brown (2009); Bertsimas et al. (2011)) that gives the possibility to model decision making under recourse. This approach is in general based on a three-level problem formulation that in the case of the expansion model considered in this work can be summarized as follows:

- In the first level, the central planner minimizes the expansion costs considering as variables those associated with the investments or expansion decisions.
- The second level identifies the worst uncertain realization of the (long-term) parameters in the plausible confidence bounds (note that the variables of this level are those modeling the uncertain parameters).
- In the third level, the market planner minimizes the operation costs taking as given the values of the first and the second level variables.

This three-level ARO formulation has been proposed for different problems such as energy and reserve dispatch in electricity markets (see, e.g., Zugno and Conejo (2015)), offering strategy of a virtual power plant in the day-ahead market (see Baringo and Baringo (2017)), generation and transmission expansion problem (see, e.g., Baringo and Baringo (2018)) and transmission expansion problems (see, e.g., Jabr (2013); Ruiz and Conejo (2015); Mínguez and García-Bertrand (2016); Zhang and Conejo (2018)).

In this context, the contributions of this work are fourfold:

1. To model investments in PV power plants, storage units, charging stations, and network lines in an integrate framework;
2. To develop an ARO model describing investments in a SSEES where both short-term and long-term uncertainties are considered;
3. To evaluate how investment decisions vary on the basis of the impact of long-term uncertainty, the central planner's revenues accruing from selling electricity to EVs at charging stations, the degree of autonomy of SSEES from the main grid, and the possibility of expanding the network.
4. To conduct an ex-post analysis on the amount of CO_2 saved with the utilization of EVs to evaluate whether the environment can benefit from the progressive decarbonization of the road-transport.

The rest of the chapter is organized as follows. Section 3.2 describes the formulation of the expansion planning problem applied to a SSEES, starting from a deterministic approach and then transforming it into an ARO problem. Section 3.3 illustrates the method used to solve the ARO model, while Section 3.4 describes the case study and the considered input data. Section 3.5 is devoted to the analysis of the obtained results. Finally, Section 3.6 concludes with some final remarks.

3.2 Problem Formulation

In this section, we describe the formulation of the proposed SRC&L expansion model applied to a SSEES. For the sake of clarity, we first provide a deterministic instance of the problem that only accounts for the short-term uncertainty, while the future peak demand, the price of the electricity interchanged with the main grid, and the number of EVs are considered known parameters. The long-term uncertainty of these parameters is then characterized and the problem is formulated using an ARO model.

3.2.1 Notation

We here list the indexes, the sets, the parameters, and the variables used in our models.

Indexes

c	Charging stations.
o	Operating conditions.
l	Demands.
ℓ	Lines.
n	Nodes.
r	Renewable (PV) units.
s	Storage units.
t	Hours.
v	Iterations.

Sets

$r(\ell)/s(\ell)$	Receiving/sending-end node of the ℓth line.
Ψ_n^{C}	Charging stations located at node n.
Ψ_n^{G}	Connection to the main grid located at node n.
Ψ_n^{R}	Renewable units located at node n.
Ψ_n^{S}	Storage units located at node n.
$\Psi^{\mathrm{L+}}$	Set of candidate lines.

Parameters

B_ℓ Susceptance of the ℓth line [S].

C_{ot}^{E} Cost of the power used to charge EVs in hour t of operating condition o [$/kW].

$\tilde{C}_{ot}^{\mathrm{G}}$ Forecast value of the price of power exchanged with the main grid in hour t of operating condition o [$/kW].

$\hat{C}_{ot}^{\mathrm{G}}$ Maximum increase of the price of power exchanged with the main grid in hour t of operating condition o [$/kW].

C_{lot}^{LS} Load-shedding cost of demand l in hour t of operating condition o [$/kW].

C_{c}^{IC} Annualized investment cost in charging station c [$].

C_{r}^{IR} Annualized investment cost in renewable unit r [$].

C_{s}^{IS} Annualized investment cost in storage unit s [$].

C_{ℓ}^{IL} Annualized investment cost in candidate line ℓ [$].

$\overline{C}^{\mathrm{I}}$ Annualized investment budget [$].

$\underline{E}_{s}^{\mathrm{S}}/\overline{E}_{s}^{\mathrm{S}}$ Minimum/Maximum energy that can be stored in storage unit s [kWh].

$\underline{G}/\overline{G}$ Minimum/Maximum power that can be exchanged with the main grid [kW].

K_{lot}^{D} Demand factor of load l in hour t of operating condition o [pu].

K_{cot}^{EV} EV availability factor in charging station c in hour t of operating condition o [pu].

K_{rot}^{R} Capacity factor of renewable unit r in hour t of operating condition o [pu].

N_{o}^{D} Number of days grouped in operating condition o [days].

$\tilde{N}_{co}^{\mathrm{EV}}$ Forecast number of electric vehicles in charging station c in operating condition o.

$\hat{N}_{co}^{\mathrm{EV}}$ Maximum increase in the number of EVs in charging station c operating condition o.

$\overline{P}_{c}^{\mathrm{C}}$ Charging capacity of charging station c.

$\tilde{P}_{l}^{\mathrm{D}}$ Forecast peak load of demand l [kW].

$\hat{P}_{lot}^{\mathrm{D}}$ Maximum increase of the peak load of demand l [kW].

P_{co}^{EV} Maximum demand in charging station c in operating condition o [kW].

P_{co}^{EVmax} Maximum daily demand in charging station c in operating condition o [kW].

$\overline{P}_{\ell}^{\mathrm{L}}$ Capacity of line ℓ [kW].

$\overline{P}_{r}^{\mathrm{R}}$ Capacity of renewable unit r [pu].

$\overline{P}_{s}^{\mathrm{SC}}$ Charging capacity of storage unit s [kW].

$\overline{P}_{s}^{\mathrm{SD}}$ Discharging capacity of storage unit s [kW].

η_s^{SC} Charging efficiency of storage unit s [%].

η_s^{SD} Discharging efficiency of storage unit s [%].

Uncertain Variables

$\overline{c}_{ot}^{\mathrm{G}}$ Price of the power exchanged with the main grid in hour t of operating condition o [$/kW].

$\overline{p}_l^{\mathrm{D}}$ Peak load of demand l [kW].

$\overline{n}_{co}^{\mathrm{EV}}$ Number of EV in charging station c in operating condition o.

Optimization Variables

e_{sot}^{S} Energy stored in storage unit s in hour t of operating condition o [kWh].

p_{cot}^{C} Charging power in charging station c in hour t of operating condition o [kW].

p_{got}^{G} Power exchanged with the main grid g in hour t of operating condition o [kW].

$p_{\ell ot}^{\mathrm{L}}$ Power flow through line ℓ in hour t of operating condition o [kW].

p_{lot}^{LS} Load shed by demand l in hour t of operating condition o [kW].

p_{rot}^{R} Power from renewable unit r in hour t of operating condition o [kW].

p_{sot}^{SC} Charging power of storage unit s in hour t of operating condition o [kW].

p_{sot}^{SD} Discharging power of storage unit s in hour t of operating condition o [kW].

x_c^{C} Integer variable representing the number of charging stations c that are built.

x_r^{R} Integer variable representing the number of renewable units r that are built.

x_s^{S} Integer variable representing the number of storage units s that are built.

x_ℓ^{L} Binary variable that is equal to 1 if the ℓth candidate line is built, 0 otherwise.

δ_{not} Voltage angle at node n in hour t of operating condition o [rad].

3.2.2 Planning horizon and short-term uncertainty characterization

The expansion problem is solved for a long-term planning horizon, e.g., 30 years. In order to represent the uncertainty in the demand, production of PV units, price of electricity exchanged with the main grid, and EV behavior, this planning horizon is represented by a single target year. In turn, this target year is represented by a set of operating conditions, each one taken to be a representative day. Each of these representative days represents the daily variability of the consumers' demand,

the production of the stochastic PV units, and the price of the electricity exchanged with the main grid on a 24 hours horizon.

To obtain the operating conditions, we use historical data and a modified version of the K-means clustering technique proposed by Baringo and Conejo (2013). This method groups together historical data that are similar while maintaining the information and auto- and cross-correlation among them. In particular, each operating condition indexed by o comprises the 24 hours of the representative day which are indexed by t. The number of operating conditions should be selected so that the expansion outcome does not change if such number is increased. In addition, the clustering technique assigns to each operating condition a weight (N_o^{D}) that depends on the number of historical data that are grouped in the cluster defining each operating condition.

3.2.3 Deterministic model

The expansion planning considering a deterministic approach is formulated as the following mixed-integer linear programming (MILP) model:

$$\min_{\Phi^{\mathrm{D}}} \sum_{s} C_s^{\mathrm{IS}} x_s^{\mathrm{S}} + \sum_{r} C_r^{\mathrm{IR}} x_r^{\mathrm{R}} + \sum_{c} C_c^{\mathrm{IC}} x_c^{\mathrm{C}} + \sum_{\ell \in \Psi^{\mathrm{L+}}} C_\ell^{\mathrm{IL}} x_\ell^{\mathrm{L}} + \\ + \sum_{o} N_o^{\mathrm{D}} \left[\sum_{t} \left(\sum_{g} \tilde{C}_{ot}^{\mathrm{G}} p_{got}^{\mathrm{G}} + \sum_{l} C_l^{\mathrm{LS}} p_{lot}^{\mathrm{LS}} - \sum_{c} C_{ot}^{\mathrm{E}} p_{cot}^{\mathrm{C}} \right) \right] \tag{3.1a}$$

subject to

$$x_s^{\mathrm{S}} \in \mathbb{Z}^+, \quad \forall s, \tag{3.1b}$$

$$x_r^{\mathrm{R}} \in \mathbb{Z}^+, \quad \forall r, \tag{3.1c}$$

$$x_c^{\mathrm{C}} \in \mathbb{Z}^+, \quad \forall c, \tag{3.1d}$$

$$x_\ell^{\mathrm{L}} \in \{0,1\}, \quad \forall \ell \in \Psi^{\mathrm{L+}}, \tag{3.1e}$$

$$x_\ell^{\mathrm{L}} = 1, \quad \forall \ell \notin \Psi^{\mathrm{L+}}, \tag{3.1f}$$

$$\sum_{s} C_s^{\mathrm{IS}} x_s^{\mathrm{S}} + \sum_{r} C_r^{\mathrm{IS}} x_r^{\mathrm{R}} + \sum_{c} C_c^{\mathrm{IS}} x_c^{\mathrm{C}} + \sum_{\ell \in \Psi^{\mathrm{L+}}} C_\ell^{\mathrm{IL}} x_\ell^{\mathrm{L}} \leq \overline{C}^{\mathrm{I}}, \tag{3.1g}$$

$$\sum_{g \in \Psi_n^{\mathrm{G}}} p_{got}^{\mathrm{G}} + \sum_{r \in \Psi_n^{\mathrm{R}}} p_{rot}^{\mathrm{R}} + \sum_{s \in \Psi_n^{\mathrm{S}}} p_{sot}^{\mathrm{SD}} \eta_s^{\mathrm{SD}} - \sum_{\ell | s(\ell) = n} p_{\ell ot}^{\mathrm{L}} + \sum_{\ell | r(\ell) = n} p_{\ell ot}^{\mathrm{L}} \\ = \sum_{l \in \Psi_n^{\mathrm{L}}} \left(\tilde{P}_l^{\mathrm{D}} K_{lot}^{\mathrm{D}} - p_{lot}^{\mathrm{LS}} \right) + \sum_{s \in \Psi_n^{\mathrm{S}}} p_{sot}^{\mathrm{SC}} + \sum_{c \in \Psi_n^{\mathrm{C}}} p_{cot}^{\mathrm{C}}, \quad \forall n, \forall o, \forall t, \tag{3.1h}$$

$$p_{\ell ot}^{\mathrm{L}} = x_\ell^{\mathrm{L}} B_\ell \left(\delta_{s(\ell)ot} - \delta_{r(\ell)ot} \right), \quad \forall \ell, \forall o, \forall t, \tag{3.1i}$$

$$-\overline{P}^{\mathrm{L}}_{\ell} \leq p^{\mathrm{L}}_{\ell ot} \leq \overline{P}^{\mathrm{L}}_{\ell}, \quad \forall \ell, \forall o, \forall t, \tag{3.1j}$$

$$-\pi \leq \delta_{not} \leq \pi, \quad \forall n, \forall o, \forall t, \tag{3.1k}$$

$$\delta_{not} = 0, \quad n\text{: ref.}, \forall o, \forall t, \tag{3.1l}$$

$$\underline{G} \leq p^{\mathrm{G}}_{got} \leq \overline{G}, \quad \forall g, \forall o, \forall t \tag{3.1m}$$

$$0 \leq p^{\mathrm{LS}}_{lot} \leq \tilde{P}^{\mathrm{D}}_{l} K^{\mathrm{D}}_{lot} \quad \forall l, \forall o, \forall t, \tag{3.1n}$$

$$0 \leq p^{\mathrm{R}}_{rot} \leq K^{\mathrm{R}}_{rot} \overline{P}^{\mathrm{R}}_{r} x^{\mathrm{R}}_{r}, \quad \forall r, \forall o, \forall t, \tag{3.1o}$$

$$e_{sot} = e_{so,t-1} + p^{\mathrm{SC}}_{sot} \eta^{\mathrm{SC}}_{s} \Delta t - p^{\mathrm{SD}}_{sot} \Delta t, \quad \forall s, \forall o, \forall t \tag{3.1p}$$

$$\underline{E}^{\mathrm{S}}_{s} x^{\mathrm{S}}_{s} \leq e_{sot} \leq \overline{E}^{\mathrm{S}}_{s} x^{\mathrm{S}}_{s}, \quad \forall s, \forall o, \forall t, \tag{3.1q}$$

$$0 \leq p^{\mathrm{SC}}_{sot} \leq \overline{P}^{\mathrm{SC}}_{s} x^{\mathrm{S}}_{s}, \quad \forall s, \forall o, \forall t, \tag{3.1r}$$

$$0 \leq p^{\mathrm{SD}}_{sot} \leq \overline{P}^{\mathrm{SD}}_{s} x^{\mathrm{S}}_{s}, \quad \forall s, \forall o, \forall t, \tag{3.1s}$$

$$0 \leq p^{\mathrm{C}}_{cot} \leq \overline{P}^{\mathrm{C}}_{c} x^{\mathrm{C}}_{c}, \quad \forall c, \forall o, \forall t, \tag{3.1t}$$

$$0 \leq p^{\mathrm{C}}_{cot} \leq \tilde{N}^{\mathrm{EV}}_{co} P^{\mathrm{EV}}_{co} K^{\mathrm{EV}}_{cot}, \quad \forall c, \forall o, \forall t, \tag{3.1u}$$

$$\sum_{t} p^{\mathrm{C}}_{cot} \leq \tilde{N}^{\mathrm{EV}}_{co} P^{\mathrm{EVmax}}_{co}, \quad \forall c, \forall o, \tag{3.1v}$$

where set $\Phi^{\mathrm{D}} = \left\{ x^{\mathrm{S}}_{s}, \forall s;\ x^{\mathrm{R}}_{r}, \forall r;\ x^{\mathrm{C}}_{c}, \forall c;\ x^{\mathrm{L}}_{\ell}, \forall \ell \in \Psi^{\mathrm{L+}};\ p^{\mathrm{G}}_{ot}, \forall o, \forall t;\ p^{\mathrm{R}}_{rot}, \forall r, \forall o, \forall t;\ p^{\mathrm{SD}}_{sot}, p^{\mathrm{SC}}_{sot}, e_{sot}, \forall s, \forall o, \forall t;\ p^{\mathrm{L}}_{\ell ot}, \forall \ell, \forall o, \forall t;\ p^{\mathrm{LS}}_{lot}, \forall l, \forall o, \forall t;\ p^{\mathrm{C}}_{cot}, \forall c, \forall o, \forall t;\ \delta_{not}, \forall n, \forall o, \forall t \right\}$ includes the optimization variables of problem (3.1).

Problem (3.1) is driven by the minimization of both investment and operating costs. Objective function (3.1a) includes the following terms:

1. Term $\sum_{s} C^{\mathrm{IS}}_{s} x^{\mathrm{S}}_{s} + \sum_{r} C^{\mathrm{IR}}_{r} x^{\mathrm{R}}_{r} + \sum_{c} C^{\mathrm{IC}}_{c} x^{\mathrm{C}}_{c} + \sum_{\ell \in \Psi^{\mathrm{L+}}} C^{\mathrm{IL}}_{\ell} x^{\mathrm{L}}_{\ell}$ represents the annualized investment costs in storage, renewable units, charging stations, and candidate lines.

2. Terms $\sum_{t} \left(\sum_{g} \tilde{C}^{\mathrm{G}}_{ot} p^{\mathrm{G}}_{got} + \sum_{l} C^{\mathrm{LS}}_{l} p^{\mathrm{LS}}_{lot} \right), \forall o$, include the costs (revenues) of the power bought (sold) from the main grid and the load-shedding cost. No charges are foreseen for the solar PV power production. Note that p^{G}_{got} is a free variable: when it is positive, it indicates the amount of electricity that the SSEES withdraws from the main grid, if negative it stands for the amount of power that the SSEES sells back to the main grid.

3. Terms $\sum_{t} \sum_{c} C^{\mathrm{E}}_{ot} p^{\mathrm{C}}_{cot}, \forall o$, represent the revenues achieved by selling energy to EVs through charging stations.

Note that terms in items 2 and 3 depend on operating conditions o and are multiplied by factor N^{D}_{o} to make investment and operating costs comparable.

Constraints of the problem can be classified into two groups. Constraints (3.1b)-(3.1g) are investment constraints, while (3.1h)-(3.1v) are operating constraints.

Constraints (3.1b), (3.1c), and (3.1d) are declarations of integer variables representing the investment in storage, PV, and charging units, respectively. Note that these variables identify the number of plants that can be built. We fix, "a priori", the capacity of these units and the investments costs indicated in the objective function are proportional to the capacity that the specific unit can assume. Binary variables x_ℓ^{L} defined in constraints (3.1e) indicate whether the candidate line ℓ is built ($x_\ell^{\mathrm{L}} = 1$) or not ($x_\ell^{\mathrm{L}} = 0$). On the other side, these binary variables are equal to 1 for existing lines as imposed by constraints (3.1f). Constraint (3.1g) represents the investment budget. Constraints (3.1h) impose the power balance at each node. These conditions state that the amount of electricity exchanged with main grid in addition to the power produced by PV installations, discharged from the storage units and adjusted by the flows with the other nodes has to be equal to the sum of consumers' demand corrected by possible load shedding and the electricity required by charging storage units to supply EVs. Equations (3.1i) define the power flow through lines using a dc power flow formulation (see Conejo and Baringo (2018)). These power flows are limited by the capacity of lines using equations (3.1j). Constraints (3.1k) and (3.1l) bound voltage angles and fix to zero the voltage angle at the reference node, respectively. Constraints (3.1m) limit the power that can be exchanged with the main grid. Constraints (3.1n) and (3.1o) limit the load shed and the production of renewable units, respectively. In particular, the load shedding has to be lower than the consumers' demand that is computed as the product between the peak demand parameter $\tilde{P}_l^{\mathrm{D}}$ and the load factor K_{lot}^{D} computed through the operating conditions. Conditions (3.1o) have been constructed in a similar way. The term $K_{rot}^{\mathrm{R}} \overline{P}_r^{\mathrm{R}} x_r^{\mathrm{R}}$ identifies the maximum electricity production of these stochastic units. In particular, the solar availability factor K_{rot}^{R} is multiplied by $\overline{P}_r^{\mathrm{R}} x_r^{\mathrm{R}}$ that indicates the total capacity of the PV units installed in a node of the SSEES. This is obtained by the product between the investment variable x_r^{R} and the assumed "a priori" capacity $\overline{P}_r^{\mathrm{R}}$ that is attributed to each PV unit. Equations (3.1p)-(3.1s) model the working of storage units. Constraints (3.1p) define the energy evolution in storage units. Equations (3.1q) impose bounds on the energy stored. Constraints (3.1r) and (3.1s) limit the charging and discharging powers, respectively. The bounds of constraints (3.1q)-(3.1s) are obtained by multiplying the investment variables x_s^{S}, which express the number of storage stations to be built, by ad hoc parameters. Finally, equations (3.1t)-(3.1v) model the charging stations. Constraints (3.1t), (3.1u), and (3.1v) impose limits on the charging power in charging stations depending on the charging capacity, EV hourly demand, and EV daily demand, respectively. The bounds of constraints (3.1t) are computed as the product between the number of charging stations

constructed x_c^{C} and the "a priori" capacity assigned to each charging unit identified by the parameter $\overline{P}_c^{\mathrm{C}}$. Constraints (3.1u), and (3.1v) impose limits on the charging power in charging stations depending on the EV hourly demand, and EV daily demand, respectively.

Long-term uncertainty characterization: uncertainty set

In the deterministic problem (3.1), the peak demand, the number of EVs, and the price of the power exchanged with the main grid are assumed to be known at the time of making the expansion decisions. However, when these decisions are made, this information is not known by the expansion planner. Therefore, it is also necessary to represent the long-term uncertainty in the decision making problem in order to obtain informed expansion decisions.

For the problem considered, uncertainty in the peak demand, the price of the power exchanged with the main grid, and the number of EVs is modeled by decision variables that take values within known confidence bounds:

$$\overline{c}_{ot}^{\mathrm{G}} \in \{\tilde{C}_{ot}^{\mathrm{G}} - \hat{C}_{ot}, \tilde{C}_{ot}^{\mathrm{G}} + \hat{C}_{ot}^{\mathrm{G}}\}, \quad \forall o, \forall t, \tag{3.2a}$$

$$\overline{p}_l^{\mathrm{D}} = \{\tilde{P}_l^{\mathrm{D}} - \hat{P}_l^{\mathrm{D}}, \tilde{P}_l^{\mathrm{D}} + \hat{P}_l^{\mathrm{D}}\}, \quad \forall l, \tag{3.2b}$$

$$\overline{n}_{co}^{\mathrm{EV}} = \{\tilde{N}_{co}^{\mathrm{EV}} - \hat{N}_{co}^{\mathrm{EV}}, \tilde{N}_{co}^{\mathrm{EV}} + \hat{N}_{co}^{\mathrm{EV}}\}, \quad \forall c, \forall o. \tag{3.2c}$$

In the proposed ARO model, we identify the worst-case uncertainty realization given the expansion decisions, i.e., that uncertainty realization that maximizes the operation cost. For the uncertainty set considered in this work, this worst-case realization corresponds to a vertex of the polyhedron representing the uncertainty set (see Jiang et al. (2014)). Thus, it is possible to use the following equivalent binary-variable-based set:

$$\Omega = \{\overline{c}_{ot}^{\mathrm{G}} = \tilde{C}_{ot}^{\mathrm{G}} + u^{\mathrm{G}} \hat{C}_{ot}^{\mathrm{G}}, \quad \forall o, \forall t, \tag{3.3a}$$

$$\overline{p}_l^{\mathrm{D}} = \tilde{P}_l^{\mathrm{D}} + u_l^{\mathrm{D}} \hat{P}_l^{\mathrm{D}}, \quad \forall l, \tag{3.3b}$$

$$\overline{n}_{co}^{\mathrm{EV}} = \tilde{N}_{co}^{\mathrm{EV}} - u_c^{\mathrm{EV}} \hat{N}_{co}^{\mathrm{EV}}, \quad \forall c, \forall o, \tag{3.3c}$$

$$u^{\mathrm{G}} \leq \Lambda^{\mathrm{G}}, \tag{3.3d}$$

$$\sum_l u_l^{\mathrm{D}} \leq \Lambda^{\mathrm{D}}, \tag{3.3e}$$

$$\sum_c u_c^{\mathrm{EV}} \leq \Lambda^{\mathrm{EV}}, \tag{3.3f}$$

$$u^{\mathrm{G}} \in \{0, 1\}, \tag{3.3g}$$

$$u_l^{\mathrm{D}} \in \{0, 1\}, \quad \forall l, \tag{3.3h}$$

$$u_c^{\mathrm{EV}} \in \{0,1\}, \quad \forall c\}. \tag{3.3i}$$

Constraints (3.3a), (3.3b), and (3.3c) expressed the price of the power bought from the main grid, the peak demand, and the number of EVs in terms of the forecast and fluctuation levels of the corresponding uncertain variables, respectively. Note that from the point of view of the central planner, the worst possible long-term outcomes are represented by an increase in the cost of the power bought from the main grid (3.3a), a raise of the peak demand (3.3b), together with a decrease in the number of the EVs in the network (3.3c). While the interpretation of the first two constraints is trivial, constraint (3.3c) deserves an explanation: according to our assumptions, the central planner is in charge of building charging stations in the system and receives a compensation when these charging stations are used. Therefore, a long-term decrease in the number of EVs implies in turn a lower EVs' electricity demand, which translates into a reduction of the central planner's potential revenues. Constraints (3.3d), (3.3e), and (3.3f) allow controlling the robustness in the solution through the so-called uncertainty budgets Λ^{G}, Λ^{D}, and Λ^{EV}. If these uncertainty budgets are equal to 0, it means that the corresponding uncertain variable is equal to its forecast value, i.e., we disregard uncertainty. As we increase the value of these uncertainty budgets, we allow the corresponding uncertain variables to deviate from its forecast value, i.e., we consider a comparatively more robust solution. Finally, constraints (3.3g), (3.3h), and (3.3i) define binary variables.

3.2.4 Stochastic Adaptive Robust Optimization Model

The proposed ARO model is formulated as a trilevel programming problem. The first level determines the expansion decisions minimizing both the expansion and the operation costs. Given these expansion decisions, the second level identifies the worst-case realization of peak demands, number of EVs, and the price of the electricity exchanged with the main grid that maximize the operation costs. Finally, the third level models the operation of the SSEES minimizing the operation cost for given first- and second-level decisions. The proposed trilevel programming problem is formulated as follows:

$\min_{\Phi^{\mathrm{L1}}}$

$$\sum_s C_s^{\mathrm{IS}} x_s^{\mathrm{S}} + \sum_r C_r^{\mathrm{IR}} x_r^{\mathrm{R}} + \sum_c C_c^{\mathrm{IC}} x_c^{\mathrm{C}} + \sum_{\ell \in \Psi^{\mathrm{L+}}} C_\ell^{\mathrm{IL}} x_\ell^{\mathrm{L}}$$

$$+ \max_{\Phi^{\mathrm{L2}} \in \Omega} \quad \min_{\Phi_{ot}^{\mathrm{L3}} \in \Xi(\cdot)}$$

$$\sum_o N_o^{\mathrm{D}} \left[\sum_t \left(\sum_g \bar{c}_{ot}^{\mathrm{G}} p_{got}^{\mathrm{G}} + \sum_l C_l^{\mathrm{LS}} p_{lot}^{\mathrm{LS}} - \sum_c C_{ot}^{\mathrm{E}} p_{cot}^{\mathrm{C}} \right) \right] \tag{3.4a}$$

subject to

$$\text{Constraints (3.1b)} - \text{(3.1g)}. \tag{3.4b}$$

Problem (3.4) involves three nested optimization problems:

1. The first level associated with the expansion decisions, i.e., variables in set $\Phi^{\text{L1}} = \{x^{\text{S}}_s, \forall s;\ x^{\text{R}}_r, \forall r;\ x^{\text{C}}_c, \forall c;\ x^{\text{L}}_\ell, \forall \ell \in \Psi^{\text{L+}}_n\}$.

2. The second level related to the worst-case realization of the value of the electricity exchanged with the main grid, the peak demand, the number of EVs, i.e., variables in set $\Phi^{\text{L2}} = \{\overline{c}^{\text{G}}_{ot}, \forall o, \forall t;\ \overline{p}^{\text{D}}_l, \forall l;\ \overline{n}^{\text{EV}}_{co}, \forall c, \forall o\}$.

3. The third level modeling the reaction of the SSEES against first- and second-level decisions, i.e., variables in set $\Phi^{\text{L3}}_{ot} = \{e^{\text{S}}_{sot}, \forall s;\ p^{\text{C}}_{cot}, \forall c;\ p^{\text{G}}_{got};\ p^{\text{LS}}_{lot}, \forall l;\ p^{\text{L}}_{\ell ot}, \forall \ell;\ p^{\text{R}}_{rot}, \forall r;\ p^{\text{SC}}_{sot}, \forall s;\ p^{\text{SD}}_{sot}, \forall s;\ \delta_{not}, \forall n\}, \forall o, \forall t$.

Problem (3.4) is driven by the minimization of the worst-case expansion and operation costs (3.4a) subject to the expansion constraints (3.4b) described in Section 3.2.3. In problem (3.4), Ω and Ξ are the uncertainty and the feasibility sets, respectively. Uncertainty set Ω is described in Section 3.2.3, while set Ξ identifies the feasible space of the third-level optimization variables as explained in Section 3.2.4.

Definition of the Feasibility Sets

Given first- and second-level decision variables, set Ξ models the feasible space of third-level optimization variables:
$\Xi\left(x^{\text{S}}_s, \forall s; x^{\text{R}}_r, \forall r; x^{\text{C}}_c, \forall c; x^{\text{L}}_\ell, \forall \ell \in \Psi^{\text{L+}}; \overline{c}^{\text{G}}_{ot}, \forall o, \forall t; \overline{p}^{\text{D}}_{lot}, \forall l, \forall o, \forall t; \overline{n}^{\text{EV}}_{co}, \forall c, \forall o\right) = \{\Phi^{\text{L3}}_{ot} :$

$$\sum_{g\in\Psi^{\text{G}}_n} p^{\text{G}}_{got} + \sum_{r\in\Psi^{\text{R}}_n} p^{\text{R}}_{rot} + \sum_{s\in\Psi^{\text{S}}_n} p^{\text{SD}}_{sot}\eta^{\text{SD}} - \sum_{\ell|s(\ell)=n} p^{\text{L}}_{\ell ot} + \sum_{\ell|r(\ell)=n} p^{\text{L}}_{\ell ot}$$
$$= \sum_{l\in\Psi^{\text{L}}_n} \left(k^{\text{D}}_{ot}\overline{p}^{\text{D}}_{lot} - p^{\text{LS}}_{lot}\right) + \sum_{s\in\Psi^{\text{S}}_n} p^{\text{SC}}_{sot} + \sum_{c\in\Psi^{\text{C}}_n} p^{\text{C}}_{cot} \ : \lambda_{not}, \quad \forall n, \forall o, \forall t, \tag{3.5a}$$

$$p^{\text{L}}_{\ell ot} = x^{\text{L}}_\ell B_\ell \left(\delta_{s(\ell)ot} - \delta_{r(\ell)ot}\right) \ : \varphi^{\text{L}}_{\ell ot}, \quad \forall \ell, \forall o, \forall t, \tag{3.5b}$$

$$-\overline{P}^{\text{L}}_\ell \le p^{\text{L}}_{\ell ot} \le \overline{P}^{\text{L}}_\ell \ : \underline{\mu}^{\text{L}}_{\ell ot}, \overline{\mu}^{\text{L}}_{\ell ot}, \quad \forall \ell, \forall o, \forall t, \tag{3.5c}$$

$$-\pi \le \delta_{not} \le \pi \ : \underline{\mu}^{\text{A}}_{not}, \overline{\mu}^{\text{A}}_{not}, \quad \forall n, \forall o, \forall t, \tag{3.5d}$$

$$\delta_{not} = 0 \ : \xi_{not}, \quad n\text{: ref.}, \forall o, \forall t, \tag{3.5e}$$

$$\underline{G} \le p^{\text{G}}_{got} \le \overline{G} \ : \underline{\mu}_{got}, \overline{\mu}_{got} \quad \forall g, \forall o, \forall t \tag{3.5f}$$

$$0 \le p^{\text{LS}}_{lot} \le \overline{p}^{\text{D}}_l k^{\text{D}}_{lot} \ : \underline{\mu}^{\text{D}}_{lot}, \overline{\mu}^{\text{D}}_{lot}, \quad \forall l, \forall o, \forall t, \tag{3.5g}$$

$$0 \le p^{\text{R}}_{rot} \le K^{\text{R}}_{rot}\overline{P}^{\text{R}}_r x^{\text{R}}_r \ : \underline{\mu}^{\text{R}}_{rot}, \overline{\mu}^{\text{R}}_{rot}, \quad \forall r, \forall o, \forall t, \tag{3.5h}$$

$$e_{sot} = e_{so,t-1} + p^{\mathrm{SC}}_{sot}\eta^{\mathrm{SC}}_{s}\Delta t - p^{\mathrm{SD}}_{sot}\Delta t \ : \varphi^{E}_{sot}, \quad \forall s, \forall o, \forall t, \tag{3.5i}$$

$$\underline{E}^{\mathrm{S}}_{s}x^{\mathrm{S}}_{s} \leq e_{sot} \leq \overline{E}^{\mathrm{S}}_{s}x^{\mathrm{S}}_{s} \ : \underline{\mu}^{\mathrm{E}}_{sot}, \overline{\mu}^{\mathrm{E}}_{sot}, \quad \forall s, \forall o, \forall t, \tag{3.5j}$$

$$0 \leq p^{\mathrm{SC}}_{sot} \leq \overline{P}^{\mathrm{SC}}_{s}x^{\mathrm{S}}_{s} \ : \underline{\mu}^{\mathrm{SC}}_{sot}, \overline{\mu}^{\mathrm{SC}}_{sot}, \quad \forall s, \forall o, \forall t, \tag{3.5k}$$

$$0 \leq p^{\mathrm{SD}}_{sot} \leq \overline{P}^{\mathrm{SD}}_{s}x^{\mathrm{S}}_{s} \ : \underline{\mu}^{\mathrm{SD}}_{sot}, \overline{\mu}^{\mathrm{SD}}_{sot}, \quad \forall s, \forall o, \forall t, \tag{3.5l}$$

$$0 \leq p^{\mathrm{C}}_{cot} \leq x^{\mathrm{C}}_{c}\overline{P}^{\mathrm{C}}_{c} \ : \underline{\mu}^{\mathrm{C}}_{cot}, \overline{\mu}^{\mathrm{C}}_{cot}, \quad \forall c, \forall o, \forall t, \tag{3.5m}$$

$$0 \leq p^{\mathrm{C}}_{cot} \leq \overline{n}^{\mathrm{EV}}_{co}P^{\mathrm{EV}}_{co}K^{\mathrm{EV}}_{cot} \ : \underline{\mu}^{\mathrm{EV}}_{cot}, \overline{\mu}^{\mathrm{EV}}_{cot}, \quad \forall c, \forall o, \forall t, \tag{3.5n}$$

$$\sum_{t} p^{\mathrm{C}}_{cot} \leq \overline{n}^{\mathrm{EV}}_{co}P^{\mathrm{EVmax}}_{co} \ : \varphi^{EV}_{co}, \quad \forall c, \forall o \tag{3.5o}$$

}.

Note that the feasibility set Ξ is parameterized in terms of first- and second-level decision variables. Constraints (3.5a)-(3.5n) are identical to constraints (3.1h)-(3.1v). Finally, observe that the dual variables are provided following a colon.

3.3 Solution Procedure

The ARO problem (3.4) is solved using a column-and-constraint generation algorithm (see Zeng and Zhao (2013)) which is based on the iterative solution of a master problem and a subproblem. Figure 3.1 summarizes the master and the subproblem that are described in details in the following sections.

3.3.1 Master problem

The master problem at iteration υ is provided below:

$\min_{\Phi^{\mathrm{M}}}$

$$\sum_{s} C^{\mathrm{IS}}_{s}x^{\mathrm{S}}_{s} + \sum_{r} C^{\mathrm{IR}}_{r}x^{\mathrm{R}}_{r} + \sum_{c} C^{\mathrm{IC}}_{c}x^{\mathrm{C}}_{c} + \sum_{\ell \in \Psi^{\mathrm{L+}}} C^{\mathrm{IL}}_{\ell}x^{\mathrm{L}}_{\ell} + \theta \tag{3.6a}$$

subject to

$$\text{Constraints (3.1b)} - \text{(3.1g)} \tag{3.6b}$$

$$\theta \geq \sum_{o} N^{\mathrm{D}}_{o}\left[\sum_{t}\left(\overline{c}^{\mathrm{G}(\upsilon')}_{ot}\sum_{g} p^{\mathrm{G}}_{got\upsilon'} + \sum_{l} C^{\mathrm{LS}}_{l}p^{\mathrm{LS}}_{lot\upsilon'} - \sum_{c} C^{\mathrm{E}}_{ot}p^{\mathrm{C}}_{cot\upsilon'}\right)\right],$$

$$\forall \upsilon' \leq \upsilon, \tag{3.6c}$$

$$\sum_{g \in \Psi^{\mathrm{G}}_{n}} p^{\mathrm{G}}_{got\upsilon'} + \sum_{r \in \Psi^{\mathrm{R}}_{n}} p^{\mathrm{R}}_{rot\upsilon'} + \sum_{s \in \Psi^{\mathrm{S}}_{n}} p^{\mathrm{SD}}_{sot\upsilon'}\eta^{\mathrm{SD}}_{s} - \sum_{\ell | s(\ell)=n} p^{\mathrm{L}}_{\ell ot\upsilon'} + \sum_{\ell | r(\ell)=n} p^{\mathrm{L}}_{\ell ot\upsilon'}$$
$$= \sum_{l \in \Psi^{\mathrm{L}}_{n}}\left(K^{\mathrm{D}}_{lot}\overline{p}^{\mathrm{D}(\upsilon')}_{l} - p^{\mathrm{LS}}_{lot\upsilon'}\right) + \sum_{s \in \Psi^{\mathrm{S}}_{n}} p^{\mathrm{SC}}_{sot\upsilon'} + \sum_{c \in \Psi^{\mathrm{C}}_{n}} p^{\mathrm{C}}_{cot\upsilon'},$$

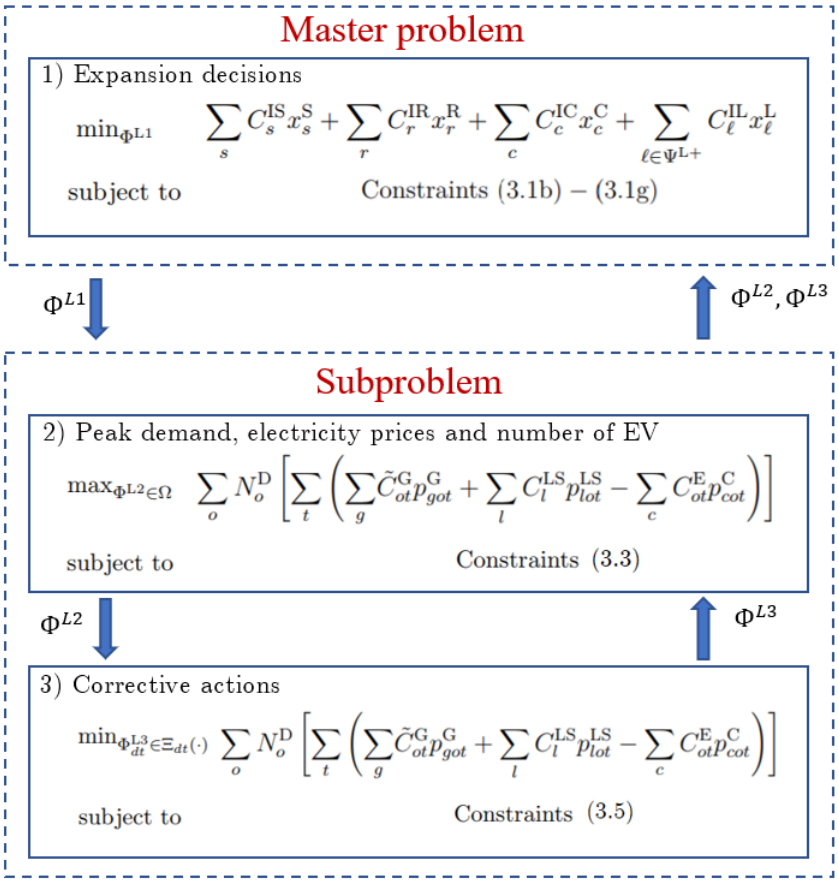

Figure 3.1: Iterative solution approach of the ARO problem

$$\forall n, \forall o, \forall t, \forall \upsilon' \leq \upsilon, \tag{3.6d}$$

$$p_{\ell o t \upsilon'}^L = x_\ell^L B_\ell \left(\delta_{s(\ell) o t \upsilon'} - \delta_{r(\ell) o t \upsilon'} \right), \quad \forall \ell, \forall o, \forall t, \forall \upsilon' \leq \upsilon, \tag{3.6e}$$

$$-\overline{P}_\ell^L \leq p_{\ell o t \upsilon'}^L \leq \overline{P}_\ell^L, \quad \forall \ell, \forall o, \forall t, \forall \upsilon' \leq \upsilon, \tag{3.6f}$$

$$-\pi \leq \delta_{n o t \upsilon'} \leq \pi, \quad \forall n, \forall o, \forall t, \forall \upsilon' \leq \upsilon, \tag{3.6g}$$

$$\delta_{n o t \upsilon'} = 0, \quad n\text{: ref.}, \forall o, \forall t, \forall \upsilon' \leq \upsilon, \tag{3.6h}$$

$$\underline{G} \leq p_{g o t \upsilon'}^G \leq \overline{G}, \quad \forall g, \forall o, \forall t, \forall \upsilon' \leq \upsilon, \tag{3.6i}$$

$$0 \leq p_{l o t \upsilon'}^{LS} \leq K_{lot}^D \overline{P}_l^{D(\upsilon')}, \quad \forall l, \forall o, \forall t, \forall \upsilon' \leq \upsilon \tag{3.6j}$$

$$0 \leq p_{r o t \upsilon'}^R \leq K_{rot}^R \overline{P}_r^R x_r^R, \quad \forall r, \forall o, \forall t, \forall \upsilon' \leq \upsilon, \tag{3.6k}$$

$$e_{s o t \upsilon'} = e_{s o, t-1, \upsilon'} + p_{s o t \upsilon'}^{SC} \eta_s^{SC} \Delta t - p_{s o t \upsilon'}^{SD} \Delta t, \quad \forall s, \forall o, \forall t, \forall \upsilon' \leq \upsilon, \tag{3.6l}$$

$$\underline{E}_s^S x_s^S \leq e_{s o t \upsilon'} \leq \overline{E}_s^S x_s^S, \quad \forall s, \forall o, \forall t, \forall \upsilon' \leq \upsilon, \tag{3.6m}$$

$$0 \leq p_{s o t \upsilon'}^{SC} \leq \overline{P}_s^{SC} x_s^S, \quad \forall s, \forall o, \forall t, \forall \upsilon' \leq \upsilon, \tag{3.6n}$$

$$0 \leq p_{s o t \upsilon'}^{SD} \leq \overline{P}_s^{SD} x_s^S, \quad \forall s, \forall o, \forall t, \forall \upsilon' \leq \upsilon, \tag{3.6o}$$

$$0 \leq p^{\mathrm{C}}_{cotv'} \leq x^{\mathrm{C}}_{c}\overline{P}^{\mathrm{C}}_{c}, \quad \forall c, \forall o, \forall t, \forall v' \leq v, \tag{3.6p}$$

$$0 \leq p^{\mathrm{C}}_{cotv'} \leq \overline{n}^{\mathrm{EV}(v')}_{co} P^{\mathrm{EV}}_{co} K^{\mathrm{EV}}_{cot}, \quad \forall c, \forall o, \forall t, \forall v' \leq v, \tag{3.6q}$$

$$\sum_{t} p^{\mathrm{C}}_{cotv'} \leq \overline{n}^{\mathrm{EV}(v')}_{co} P^{\mathrm{EVmax}}_{co}, \quad \forall c, \forall o, \forall v' \leq v. \tag{3.6r}$$

where variables in set $\Phi^{\mathrm{M}} = \{\Phi^{\mathrm{L1}};\ \theta;\ e^{\mathrm{S}}_{sotv'},\ \forall o,\ \forall t,\ \forall s,\ \forall v' \leq v;\ p^{\mathrm{C}}_{cotv'},\ \forall c,\ \forall o,\ \forall t,\ \forall v' \leq v;\ p^{\mathrm{G}}_{gotv'},\ \forall g,\ \forall o,\ \forall t,\ \forall v' \leq v;\ p^{\mathrm{LS}}_{lotv'},\ \forall l,\ \forall o,\ \forall t,\ \forall v' \leq v;\ p^{\mathrm{L}}_{\ell otv'},\ \forall \ell,\ \forall o,\ \forall t,\ \forall v' \leq v;\ p^{\mathrm{R}}_{rotv'},\ \forall r,\ \forall o,\ \forall t,\ \forall v' \leq v;\ p^{\mathrm{SC}}_{sotv'},\ \forall s,\ \forall o,\ \forall t,\ \forall v' \leq v;\ p^{\mathrm{SD}}_{sotv'},\ \forall s,\ \forall o,\ \forall t,\ \forall v' \leq v;\ \delta_{notv'},\ \forall n,\ \forall o,\ \forall t,\ \forall v' \leq v\}$ are the optimization variables of master problem (3.6).

Master problem (3.6) is a relaxed version of the trilevel problem (3.4) in which auxiliary variable θ iteratively approximates the worst-case value of the second-level objective function. Therefore, the size of master problem (3.6) increases with the number of iterations. Finally, note that parameters with superscript (v') refer to the optimal values of variables yielded by the subproblem at iteration v'.

3.3.2 Subproblem

At each iteration v, master problem (3.6) provides the expansion decisions. Given these decisions, the subproblem formulated below determines the worst-case uncertainty realization:

$\max_{\Phi^{\mathrm{L2}} \in \Omega} \quad \min_{\Phi^{\mathrm{L3}}_{ot} \in \Xi(\cdot)}$

$$\sum_{o} N^{\mathrm{D}}_{o} \left[\sum_{t} \left(\sum_{g} \overline{C}^{\mathrm{G}}_{ot} p^{\mathrm{G}}_{got} + \sum_{l} C^{\mathrm{LS}}_{l} p^{\mathrm{LS}}_{lot} - \sum_{c} C^{\mathrm{E}}_{ot} p^{\mathrm{C}}_{cot} \right) \right] \tag{3.7a}$$

Subproblem (3.7) is a bilevel model whose lower-level problem is continuous and linear on its decisions variables. Thus, the lower-level problem can be replaced by its dual constraints. Moreover, using the strong duality equality, we can replace the objective function of the subproblem by the dual lower-level objective function (see Bertsimas and Sim (2003)). As a result, the subproblem is finally formulated as the following single-level problem:

$\max_{\Phi^{\mathrm{L2}}, \Phi^{\mathrm{L3}}_{ot}}$

$$\begin{aligned}
\sum_{o} \Bigg\{ \sum_{t} \Bigg[& \lambda_{not} \sum_{l \in \Psi^{\mathrm{L}}_{n}} K^{\mathrm{D}}_{lot} \overline{p}^{\mathrm{D}}_{l} - \sum_{\ell} \overline{P}^{\mathrm{L}}_{\ell} (\underline{\mu}^{\mathrm{L}}_{\ell ot} + \overline{\mu}^{\mathrm{L}}_{\ell ot}) - \sum_{n} \pi (\underline{\mu}^{\mathrm{A}}_{not} + \overline{\mu}^{\mathrm{A}}_{not}) \\
& \sum_{g} \underline{G} \underline{\mu}^{\mathrm{G}}_{got} - \sum_{g} \overline{G} \overline{\mu}^{\mathrm{G}}_{got} - \sum_{l} K^{\mathrm{D}}_{lot} \overline{p}^{\mathrm{D}}_{l} \overline{\mu}^{\mathrm{D}}_{lot} - \sum_{r} K^{\mathrm{R}}_{rot} \overline{P}^{\mathrm{R}}_{r} x^{\mathrm{R}(v)}_{r} \overline{\mu}^{\mathrm{R}}_{rot} \\
& - \sum_{s} \overline{E}^{\mathrm{S}}_{s} x^{\mathrm{S}(v)}_{s} \overline{\mu}^{\mathrm{E}}_{sot} + \sum_{s} \underline{E}^{\mathrm{S}}_{s} x^{\mathrm{S}(v)}_{s} \underline{\mu}^{\mathrm{E}}_{sot} - \sum_{s} \overline{P}^{\mathrm{SC}}_{s} x^{\mathrm{S}(v)}_{s} \overline{\mu}^{\mathrm{SC}}_{sot}
\end{aligned}$$

$$- \sum_{s} \overline{P}_{s}^{\mathrm{SD}} x_{s}^{\mathrm{S}(\upsilon)} \overline{\mu}_{sot}^{\mathrm{SD}} - \sum_{c} \overline{P}_{c}^{\mathrm{C}} x_{c}^{\mathrm{C}(\upsilon)} \overline{\mu}_{cot}^{\mathrm{C}} - \sum_{c} \overline{n}_{co}^{\mathrm{EV}} P_{co}^{\mathrm{EV}} K_{cot}^{\mathrm{EV}} \overline{\mu}_{cot}^{\mathrm{EV}} \Bigg] - \sum_{c} \overline{n}_{co}^{\mathrm{EV}} P_{co}^{\mathrm{EVmax}} \varphi_{co}^{\mathrm{EV}} \Bigg\} \tag{3.8a}$$

subject to

$$\text{Constraints (3.3)} \tag{3.8b}$$

$$N_{o}^{\mathrm{D}} \overline{c}_{ot}^{\mathrm{G}} = \lambda_{n(g)ot} - \overline{\mu}_{got}^{\mathrm{G}} + \underline{\mu}_{got}^{\mathrm{G}}, \quad \forall g, \forall o, \forall t, \tag{3.8c}$$

$$N_{o}^{\mathrm{D}} C_{l}^{\mathrm{LS}} = \lambda_{n(l)ot} - \overline{\mu}_{lot}^{\mathrm{D}} + \underline{\mu}_{lot}^{\mathrm{D}}, \quad \forall l, \forall o, \forall t, \tag{3.8d}$$

$$- N_{o}^{\mathrm{D}} C_{ot}^{\mathrm{E}} = -\lambda_{n(c)ot} + \underline{\mu}_{cot}^{\mathrm{C}} - \overline{\mu}_{cot}^{\mathrm{C}} + \underline{\mu}_{cot}^{\mathrm{EV}} - \overline{\mu}_{cot}^{\mathrm{EV}} - \varphi_{co}^{\mathrm{EV}}, \quad \forall c, \forall o, \forall t, \tag{3.8e}$$

$$- \lambda_{s(\ell)ot} + \lambda_{r(\ell)ot} + \varphi_{\ell ot}^{\mathrm{L}} + \underline{\mu}_{\ell ot}^{\mathrm{L}} - \overline{\mu}_{\ell ot}^{\mathrm{L}} = 0, \quad \forall \ell, \forall o, \forall t, \tag{3.8f}$$

$$\lambda_{n(r)ot} + \underline{\mu}_{rot}^{\mathrm{R}} - \overline{\mu}_{rot}^{\mathrm{R}} = 0, \quad \forall r, \forall o, \forall t, \tag{3.8g}$$

$$\lambda_{n(s)ot} \eta_{s}^{\mathrm{SD}} + \varphi_{sot}^{\mathrm{E}} \Delta t + \underline{\mu}_{sot}^{\mathrm{SD}} - \overline{\mu}_{sot}^{\mathrm{SD}} = 0, \quad \forall s, \forall o, \forall t, \tag{3.8h}$$

$$- \lambda_{n(s)ot} - \varphi_{sot}^{\mathrm{E}} \eta^{\mathrm{SC}} \Delta t + \underline{\mu}_{sot}^{\mathrm{SC}} - \overline{\mu}_{sot}^{\mathrm{SC}} = 0, \quad \forall s, \forall o, \forall t, \tag{3.8i}$$

$$\varphi_{sot}^{\mathrm{E}} - \varphi_{so,t-1}^{\mathrm{E}} + \underline{\mu}_{sot}^{\mathrm{E}} - \overline{\mu}_{sot}^{\mathrm{E}} = 0, \quad \forall s, \forall o, \forall t \tag{3.8j}$$

$$- \sum_{\ell | s(\ell)=n} x_{\ell}^{\mathrm{L}(\upsilon)} B_{\ell} \varphi_{\ell ot}^{\mathrm{L}} + \sum_{\ell | r(\ell)=n} x_{\ell}^{\mathrm{L}(\upsilon)} B_{\ell} \varphi_{\ell ot}^{\mathrm{L}} + \underline{\mu}_{not}^{\mathrm{A}} - \overline{\mu}_{not}^{\mathrm{A}} = 0, \quad \forall o, \forall t, \forall n \setminus n : \text{ref.}, \tag{3.8k}$$

$$- \sum_{\ell | s(\ell)=n} x_{\ell}^{\mathrm{L}(\upsilon)} B_{\ell} \varphi_{\ell ot}^{\mathrm{L}} + \sum_{\ell | r(\ell)=n} x_{\ell}^{\mathrm{L}(\upsilon)} B_{\ell} \varphi_{\ell ot}^{\mathrm{L}} + \underline{\mu}_{not}^{\mathrm{A}} - \overline{\mu}_{not}^{\mathrm{A}} + \xi_{not} = 0, \quad \forall o, \forall t, n : \text{ref.}, \tag{3.8l}$$

$$\underline{\mu}_{\ell ot}^{\mathrm{L}}, \overline{\mu}_{\ell ot}^{\mathrm{L}} \geq 0, \quad \forall \ell, \forall o, \forall t \tag{3.8m}$$

$$\underline{\mu}_{not}^{\mathrm{A}}, \overline{\mu}_{not}^{\mathrm{A}} \geq 0, \quad \forall n, \forall o, \forall t, \tag{3.8n}$$

$$\underline{\mu}_{got}^{\mathrm{G}}, \overline{\mu}_{got}^{\mathrm{G}} \geq 0, \quad \forall g, \forall o, \forall t, \tag{3.8o}$$

$$\underline{\mu}_{lot}^{\mathrm{D}}, \overline{\mu}_{lot}^{\mathrm{D}} \geq 0, \quad \forall l, \forall o, \forall t, \tag{3.8p}$$

$$\underline{\mu}_{rot}^{\mathrm{R}}, \overline{\mu}_{rot}^{\mathrm{R}} \geq 0, \quad \forall r, \forall o, \forall t, \tag{3.8q}$$

$$\underline{\mu}_{sot}^{\mathrm{E}}, \overline{\mu}_{sot}^{\mathrm{E}} \geq 0, \quad \forall s, \forall o, \forall t, \tag{3.8r}$$

$$\underline{\mu}_{sot}^{\mathrm{SC}}, \overline{\mu}_{sot}^{\mathrm{SC}} \geq 0, \quad \forall s, \forall o, \forall t, \tag{3.8s}$$

$$\underline{\mu}_{sot}^{\mathrm{SD}}, \overline{\mu}_{sot}^{\mathrm{SD}} \geq 0, \quad \forall s, \forall o, \forall t, \tag{3.8t}$$

$$\underline{\mu}_{cot}^{\mathrm{C}}, \overline{\mu}_{cot}^{\mathrm{C}} \geq 0, \quad \forall c, \forall o, \forall t, \tag{3.8u}$$

$$\underline{\mu}_{cot}^{\mathrm{EV}}, \overline{\mu}_{cot}^{\mathrm{EV}} \geq 0, \quad \forall c, \forall o, \forall t, \tag{3.8v}$$

$$\varphi_{co}^{\mathrm{EV}} \geq 0, \quad \forall c, \forall o. \tag{3.8w}$$

3.3.3 Algorithm

Given the master problem (3.6) and subproblem (3.7), the column-and-constraint generation algorithm works as follows:

1. Initialize the iteration counter ($\upsilon \leftarrow 0$), select the convergence tolerance (ϵ), and set the lower bound (LB) and upper bound (UB) to $-\infty$ and $+\infty$, respectively.
2. Solve master problem (3.6).
3. Update the lower bound using equation (3.9) below:

$$\text{LB} = z^{\text{M}*} \tag{3.9}$$

   where $z^{\text{M}*}$ is the optimal value of the objective function (3.6a).
4. Set $x_s^{\text{S}(\upsilon)} = x_s^{\text{S}*}$, $\forall s$; $x_r^{\text{R}(\upsilon)} = x_r^{\text{R}*}$, $\forall r$; $x_c^{\text{C}(\upsilon)} = x_c^{\text{C}*}$, $\forall c$; and $x_\ell^{\text{L}(\upsilon)} = x_\ell^{\text{L}*}$, $\forall \ell$, where $x_c^{\text{C}*}$, $\forall c$; $x_r^{\text{R}*}$, $\forall r$; $x_s^{\text{S}*}$, $\forall s$; and $x_\ell^{\text{L}*}$, $\forall \ell$, denote the optimal values of these variables yielded by the solution of the master problem (3.6) in Step 2.
5. Solve subproblem (3.8).
6. Update the upper bound using equation (3.10) below:

$$\text{UB} = \min\{\text{UB}, \sum_s C_s^{\text{IS}} x_s^{\text{S}(\upsilon)} + \sum_r C_r^{\text{IR}} x_r^{\text{R}(\upsilon)} + \sum_c C_c^{\text{IC}} x_c^{\text{C}(\upsilon)} + \sum_{\ell \in \Psi^{\text{L}+}} C_\ell^{\text{IL}} x_\ell^{\text{L}(\upsilon)} + z^{\text{S}*}\} \tag{3.10}$$

   where $z^{\text{S}*}$ is the optimal value of the objective function (3.8a).
7. If $\text{UB} - \text{LB} < \epsilon$, the algorithm stops. The optimal expansion decisions are $x_r^{\text{R}*}$, $\forall r$; $x_s^{\text{S}*}$, $\forall s$; $x_c^{\text{C}*}$, $\forall c$; and $x_\ell^{\text{L}*}$, $\forall \ell$. Otherwise, go to step 8.
8. Update the iteration counter $\upsilon \leftarrow \upsilon + 1$.
9. Set $\overline{p}_l^{\text{D}(\upsilon)} = \overline{p}_l^{\text{D}}$, $\forall l$; $\overline{c}_{ot}^{\text{G}(\upsilon)} = \overline{c}_{ot}^{\text{G}*}$, $\forall o$, $\forall t$; and $\overline{n}_{co}^{\text{EV}(\upsilon)} = \overline{n}_{co}^{\text{EV}*}$, $\forall c$, $\forall o$, where $\overline{p}_l^{\text{D}}$, $\forall l$; $\overline{c}_{ot}^{\text{G}*}$, $\forall o$, $\forall t$; and $\overline{n}_{co}^{\text{EV}*}$, denote the optimal values of these variables yielded by the solution of the subproblem (3.8) in Step 5.
10. Go to step 2.

3.4 Case Study

The proposed ARO model is analyzed using the four-node test system depicted in Figure 3.2. In this SSEES, residential demand load is located in all nodes and can be

served using electricity produced by the PV and storage units, or by purchasing it from the main grid with which node 1 is connected. Charging stations, PV and storage units can be built either at node 2 or at node 3. The "a priori" assumed capacity of storage, PV, and charging units are reported in Table 3.1. We assume that a candidate charging stations have a capacity of 3.3 kW, while 10 kW is the capacity of each candidate PV unit. Batteries are assumed to have charging and discharging capacity equal to 10 kW and can store energy up to 10 hours. The charging and discharging efficiencies are set equal to 0.9. The investment costs for PV units, charging stations, and battery are taken from Fu et al. (2017); Pandžić et al. (2015); Smith and Castellano (2015) respectively. These investment costs are reported in Table 3.1 and are proportioned with the "a priori" capacities assumed for each candidate installation.

Note that investment costs reported in Table 3.1 have to be annualized to make them comparable with operations costs. In our analysis, we apply a 10% rate for the annualization of these investment costs. Finally, we consider that it is possible to build up to 10000 storage units, 10000 PV plants and 10000 charging stations.

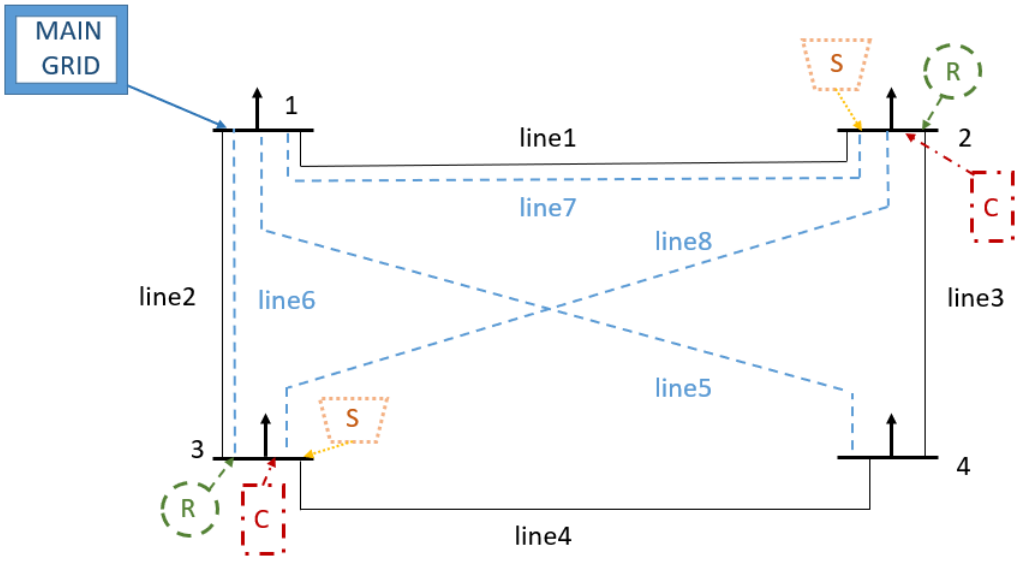

Figure 3.2: Four-bus system

Candidate units	Capacity [kW]	Investment Cost [$]
Storage unit	10	7000
PV plant	10	21400
Charging station	3.3	3000

Table 3.1: Data for candidate units.

Following Sun et al. (2015), we consider EVs with a 0.33 kWh/mi energy rating,

a 24 kWh battery capacity, and a maximum charging rate equal to 3.3 kW. All EVs can charge immediately after the arrival, i.e. we do not assume any smart charging strategy. The possible departure and arrival locations of EVs are "home" (identified by node 3) and "work" (corresponding to node 2), where these can be charged by connecting to the dedicated stations. To characterize EV travel behavior, the 2009 National Household Travel Survey (NHTS) for the Texas State is used.[1]

In particular, we assume that the typical behavior of EV drivers is approximately similar to combustion vehicles. Looking at the complete data set, it is possible to notice that the vehicle path changes according to the day of the week; for this reason we separate these data into two categories: weekend and working days. By combining data for "departure", "arrival", and "time of the trip" of the single vehicle, we obtain data for parking time in both the locations considered, i.e. "work" and "home". We estimate the percentage of battery discharging during the trip by considering the "miles run" data. We assume that vehicles are always charged when parked until the battery is full or they leave for another location. In this way, we obtain the EV electricity demand for each vehicle during a 24 hour horizon. We group the data in order to obtain four hourly different EVs demand profiles, i.e. "work" and "home" during week days and weekend. We then divide each profile by the the respective EV peak demand to obtain the factor K_{cot}^{EV}. Moreover, we construct the parameter P_{cot}^{EVmax} that limits the daily EV demand considering that the battery has to stop charging when full.

Historical load data are obtained from the Electric Reliability Council of Texas (ERCOT)[2] and scaled to obtain reference loads for the system. These reference loads are then apportioned to the nodes based on the historical distribution of loads of the North Central Zone of Texas, which is the area with the highest demand. The considered average peak load values $\tilde{P}_l^{\mathrm{D}}$ for the system are 380 kW for node 1, 420 kW for node 2, 750 kW for node 3, and 480 kW for node 4. To determine the price of the power exchanged with the main grid, we use historical day-ahead electricity prices for the ERCOT North Central load zone. Solar data are obtained from version 2017.1.17 of the System Advisor Model (SAM),[3] based on weather data from the National Solar Radiation Database (NSRDB).[4] To maintain the correlation between solar and load data, PV power production data refers to the North Central Zone of Texas. More specifically, PV power production data are obtained as average production of 12 different locations within the considered zone. This allows us to obtain a power production which is not influenced by extremely favorable/disadvantageous solar conditions pertaining specific plants. Finally, in order to maintain correlation among electricity prices, loads and

[1] Data available at https://nhts.ornl.gov/
[2] Data available at www.ercot.com
[3] Data available at https://sam.nrel.gov/
[4] Data available at https://rredc.nrel.gov/solar/old_data/nsrdb/

solar production, all these data pertain to the same year, i.e., 2015. All these data are used to compute the operating conditions used to estimate the short-term uncertainty.

We consider a total of 10 operating conditions, that are further subdivided to represent working days and weekends. As explained above, each operating condition has a weight assigned during the clustering procedure. The total weight of the subset of operating conditions pertaining working days is equal to the number of working days in a year, i.e. 261. On the other side, the total weight of the operating conditions related to weekends is 104, namely the global number of Saturdays and Sundays in a year. This differentiation is introduced to deal with the different time of travel and arrival/departure profiles of the EVs during working days and weekends.

To model the long-term uncertainty, we assume that the price of the electricity exchanged with the main grid and the peak demand can increase respectively up to 25% and 50% in the long term with respect to their expected values, respectively. The possibility of a 25% reduction in the number of EV is instead assumed in the long run. Since loads are located in all nodes, the demand uncertainty budget Λ^{D} can range from 0 to 4. For the same principle, since there is only one connection to the main grid, the grid uncertainty budget Λ^{G} can range from 0 to 1 and, because there are only two possible locations for charging stations, the EV uncertainty budget Λ^{EV} can range from 0 to 2.

In addition to the already existing lines 1-4, the candidate lines 5-8 can be built. In particular, lines 6 and 7 are reinforcement lines, while lines 5 and 8 establish new connections between the nodes. Line data are reported in Table 3.2.

Line	From Node	To Node	Reactance [p.u.]	Flow Limit [kW]	Investment Cost [$]
1	1	2	0.097	1000	–
2	1	3	0.097	1000	–
3	2	4	0.097	1000	–
4	3	4	0.097	1000	–
5	1	4	0.097	550	10500
6	1	3	0.097	550	8000
7	1	2	0.097	550	8000
8	2	3	0.097	550	10500

Table 3.2: Flow limits and investments costs for candidate lines of the SSES network

Parameter C^{E}_{ot}, which identifies the revenues that the central planner gets from selling electricity to EVs, is assumed to be twice (unless otherwise specified) the forecast price of the power exchanged with the main grid $\tilde{C}^{\mathrm{G}}_{ot}$. The latter ranges from a minimum of 13$/kWh to a maximum of 203$/kWh according to the operating condition and hour of the day. Note that, in most of the analyzed cases illustrated in the following section, the central planner withdraws electricity from the grid. Finally, load shedding cost is

set equal to 1000 $/kWh.

3.5 Results

This section describes the results of our analysis. As indicated above, we evaluate how investment decisions change depending on the considered long-term uncertainty, the central planner's revenues accruing from selling electricity to EVs, the degree of independency of the SSEES from the main grid, and the possibility of expanding the network. Finally, we provide an ex-post estimation of the amount of CO_2 emissions saved thanks to the penetration of renewable energy and EVs.

Note that analysis of each impact listed above entails some modifications of the general ARO model presented in Section 3.2 as explained in the following.

3.5.1 Impact of the long-term uncertainty

In this case, we investigate how the investment choices change when setting different values of uncertainty budgets that regulate the worst possible realizations of some long-term parameters. This evaluation is conducted considering the following assumptions:

- No limits on the power exchanged with the main grid is imposed, namely constraint (3.5f) is relaxed.
- No line expansion is allowed so that the network only accounts for already existing lines 1-4. We denote this four-line network as "4L".

In addition, taking as reference the above assumptions, we run two sets of simulations:

1. The capacity limits of the existing lines in the "4L" network are those indicated in Table 3.2. We indicate this case as "4L.F.C.", namely "four-line network, full line capacity".

2. We reduce the capacity of the existing lines of the "4L" network by 20% as compared to the values reported in Table 3.2. We indicate this case as "4L.80%F.C.", namely "four-line network, 80% of the full line capacity".

We start our analysis by setting Λ^{G}, Λ^{L}, or Λ^{EV} equal to zero, meaning that long-term uncertainty in the peak demand, the value of the electricity exchanged with the main grid, and the number of EVs is not considered and that the model reduces to the deterministic form described in Section 3.2.3. Note that this directly descends from the construction of uncertainty set Ω defined by constraints (3.3a)-(3.3i). Table 3.3 reports the results for the deterministic case.

Deterministic	# Charging stations		Solar Capacity (kW)		Storage Capacity (kW)		Total Cost ($)	
	4L.F.C.	4L.80%F.C.	4L.F.C.	4L.80%F.C.	4L.F.C.	4L.80%F.C.	4L.F.C.	4L.80%F.C.
Λ^{G}, Λ^{L}, $\Lambda^{EV} = 0$	91	85	0	0	0	70	221,520	228,026

Table 3.3: Results for the deterministic case

Simulations for case "4L.F.C" show that there is no network congestion. However, congestion appears in the implementation of the "4L.80%F.C." scenario. This is a common trend underlying results in Sections 3.5.1-3.5.3. In the "4L.F.C." case, PV and storage units are not built since the consumers' and EVs' demand can be directly satisfied by the electricity withdrawn from the main grid. The central planner only invests in charging stations because they represent a source of revenues. The situation changes under the "4L.80%F.C." case. The appearance of congestion limits the access to the main grid and therefore the system needs the construction of 70 kW of storage capacity to accommodate the short-term uncertainty. Investments in charging stations remain even though the number of charging stations built is reduced with respect to the "4L.F.C." case. This is due to the fact that the load shedding cost term C_l^{LS} in the objective function (3.4a) gives priority to the consumers, i.e., the electricity drained from the main grid is firstly used to satisfy residential demand because there is a penalty in case of unserved demand, then the excess is sold to the EV owners. As expected, congestion increases the total costs of the SSEES, implying a reduction of its efficiency. Note that in both cases, electricity is only withdrawn from the main grid and it is not sold back.

	# Charging stations		Solar Capacity (kW)		Storage Capacity (kW)		Total Cost ($)	
Λ^{G}	4L.F.C.	4L.80%F.C.	4L.F.C.	4L.80%F.C.	4L.F.C.	4L.80%F.C.	4L.F.C.	4L.80%F.C.
0	64	61	0	770	330	460	318,325	453,454
1	59	28	0	770	330	460	403,243	526,463

Table 3.4: Impact of the long-term uncertainty of the value of the electricity from the main grid on investment decisions

As soon as the values the uncertainty budget Λ^{G}, Λ^{L}, or Λ^{EV} differ from zero, long-term uncertainties are considered. Table 3.4 illustrates the changes in the optimal expansion decisions for different values of the uncertainty budget Λ^{G}. For this analysis, we fix $\Lambda^{L} = 2$ and $\Lambda^{EV} = 1$, meaning that the peak load can increase in up to the two nodes which represent the worst possible outcomes for the system, and the number of EVs can decrease in one location.When $\Lambda^{G} = 0$, we assume that the value of the electricity exchanged with the main grid does not deviate from its average in the long-run, i.e. we measure the effect of the uncertainty in the peak demand and EVs only. The obtained results differ from those reported in Table 3.3. In particular, the number

of charging stations reduces, the storage units are built even in absence of congestion to compensate the increased demand and PV plants are installed when congestion appears to maintain the system balance. This situation is exacerbated when $\Lambda^{G} = 1$, i.e., when we assume that the price of the electricity exchanged with the main grid can increase in the long run. This leads to a further drop of investments in charging stations due to the reduction of the revenues generated from selling electricity. Thus, total costs increase compared to the deterministic case.

The optimal expansion decisions for different values of the uncertainty budget Λ^{L} are reported in Table 3.5. In this case, we set $\Lambda^{G} = 1$ and $\Lambda^{EV} = 1$. We notice that the uncertainty in the peak demand has a major impact on the expansion decisions. In the "4L.F.C." configuration, when $\Lambda^{L} = 0$, storage capacity is not required. Anyway, the total cost is higher with respect to the deterministic case because of the nonzero values of the other two uncertainty budgets. Setting $\Lambda^{L} = 1$ indicates that an increase of the peak demand at node 3, the node with highest peak demand, is the worst possible realization of the uncertain variable. A 170 kW storage capacity is required, while there is a decrease in the amount of charging stations built. The total cost increases by 21.5% with respect to the $\Lambda^{L} = 0$ "4L.F.C." simulation. By setting $\Lambda^{L} = 2$, loads at nodes 3 and 4 result to be the worst possible demand realizations for the system. In this case, 330 kW of storage capacity are built. Further increasing the uncertainty in the peak demand by setting $\Lambda^{L} = 3$ and $\Lambda^{L} = 4$ stimulates investment also in PV (50 kW), and increases the investments in storage units, especially when the system is congested. This has an impact on the total costs, which become 60% higher than the $\Lambda^{L} = 0$ "4L.F.C." case.

As already observed, the congestion leads to higher total costs and to the installation of storage and solar capacity with lower level of uncertainty with respect to the non congested case. Interestingly in the congested case, when $\Lambda^{L} = 3$ and $\Lambda^{L} = 4$, the system starts both purchasing and selling electricity to the main grid and installing a considerable amount of solar capacity to counteract congestion. Note that the proportion of the power sold to the main grid comes from the PV units, but it remains lower than the amount that is withdrawn. However, this partially helps to abate the total cost of the system.

Table 3.6 reports the results for different values of the uncertainty budget Λ^{EV}. We fix $\Lambda^{G} = 1$ and $\Lambda^{L} = 2$ in this case. As it can be noticed, the variation of Λ^{EV} has a limited impact on the total cost, which however remains higher than in the deterministic case. The trend of investment decisions is similar to that observed in Table 3.4.

	# Charging stations		Solar Capacity (kW)		Storage Capacity (kW)		Total Cost ($)	
Λ^{L}	4L.F.C.	4L.80%F.C.	4L.F.C.	4L.80%F.C.	4L.F.C.	4L.80%F.C.	4L.F.C.	4L.80%F.C.
0	63	60	0	0	0	70	296,632	300,760
1	60	56	0	360	170	330	360,256	421,514
2	59	28	0	770	330	460	403,243	526,463
3	58	80	50	9630	390	510	446,411	2,194,878
4	58	80	50	9630	390	510	474,884	2,223,352

Table 3.5: Impact of the long-term uncertainty of peak demand on investment decisions

	# Charging stations		Solar Capacity (kW)		Storage Capacity (kW)		Total Cost ($)	
Λ^{EV}	4L.F.C.	4L.80%F.C.	4L.F.C.	4L.80%F.C.	4L.F.C.	4L.80%F.C.	4L.F.C.	4L.80%F.C.
0	77	35	0	770	330	460	402,007	525,863
1	59	28	0	770	330	460	403,243	526,463
2	58	28	0	770	330	460	403,261	526,463

Table 3.6: Impact of the long-term uncertainty of the number of EVs on investment decisions

3.5.2 Impact of the revenues associated with EVs

In this section, we evaluate how the central planner's investment choices change depending on the revenues that it gets from supplying electricity to EVs through charging stations. We take into consideration the following assumptions:

- No limits on the power exchange with the main grid is imposed, namely constraint (3.5f) is relaxed.
- No line expansion is allowed so that the network only accounts for already existing lines 1-4.
- We take as reference the "4L.F.C." case.
- Uncertainty budgets are fixed to $\Lambda^{\mathrm{G}} = 1$, $\Lambda^{\mathrm{L}} = 2$, and $\Lambda^{\mathrm{EV}} = 1$.

In general, charging stations are built only if they represent a profit for the central planner, i.e., when the difference between the revenues that it obtains from selling electricity to EV owners through charging stations and the electricity provision costs is high enough to cover part or all investment costs in charging stations. We recall that the electricity provided to the charging stations derives either from the main grid, the PV units, or the storage units. Since the solar power is assumed to be freely generated, it becomes crucial the margin between the price applied to the electricity sold to the EVs' owners C^{E}_{ot} and the forecast price of the power exchanged with the main grid $\tilde{C}^{\mathrm{G}}_{ot}$. For this reason, we conduct a sensitivity analysis on the values assumed by parameter C^{E}_{ot} compared to $\tilde{C}^{\mathrm{G}}_{ot}$. The range of values is reported in Table 3.7.

Values of C^{E}_{ot}	# Charging Stations	Solar Capacity (kW)	Storage Capacity (kW)	Total Cost ($)
$C^{\mathrm{E}}_{ot} = 1.5\tilde{C}^{\mathrm{G}}_{ot}$	0	0	330	408,474
$C^{\mathrm{E}}_{ot} = 1.8\tilde{C}^{\mathrm{G}}_{ot}$	17	0	330	407,375
$C^{\mathrm{E}}_{ot} = 2\tilde{C}^{\mathrm{G}}_{ot}$	59	0	330	403,243
$C^{\mathrm{E}}_{ot} = 2.5\tilde{C}^{\mathrm{G}}_{ot}$	71	0	340	387,038
$C^{\mathrm{E}}_{ot} = 3\tilde{C}^{\mathrm{G}}_{ot}$	73	0	370	369,482
$C^{\mathrm{E}}_{ot} = 5\tilde{C}^{\mathrm{G}}_{ot}$	104	0	420	292,490
$C^{\mathrm{E}}_{ot} = 6.5\tilde{C}^{\mathrm{G}}_{ot}$	115	10	440	231,679

Table 3.7: Impact of the revenues associated with EVs on investment decisions

When the value of C^{E}_{ot} 50% higher than that of $\tilde{C}^{\mathrm{G}}_{ot}$ there is no installation of charging stations, which start to be built when this gap is equal to 80%, i.e C^{E}_{ot}=1.8 $\tilde{C}^{\mathrm{G}}_{ot}$. From this point on, there is a progressive increasing trend in investments in charging units as far as C^{E}_{ot} doubles the value of $\tilde{C}^{\mathrm{G}}_{ot}$. The relation between these two parameters also affects the investments in storage units whose total capacity amounts to 330 kW till the proportion is equal to 2, i.e. C^{E}_{ot}=2 $\tilde{C}^{\mathrm{G}}_{ot}$ and then starts increasing for higher ratios. Moreover, the raise of the revenues from EVs implies a reduction of the total costs. It is remarkable the case C^{E}_{ot}=6.5 $\tilde{C}^{\mathrm{G}}_{ot}$, where the revenues are so consistent that it becomes convenient investing in a PV plant to provide additional power to charging stations.

3.5.3 Impact of the degree of dependency of SSEES from the main grid

This section is devoted to the analysis of the impact that the dependency of the SSEES from the main grid has on the expansion decisions. The illustrated results are based on these assumptions:

- No line expansion is allowed so that the network only accounts for already existing lines 1-4.
- We take as reference the "4L.F.C." case.
- Uncertainty budgets are fixed to $\Lambda^{\mathrm{G}} = 1$, $\Lambda^{\mathrm{L}} = 2$, and $\Lambda^{\mathrm{EV}} = 1$.

In order to detect the level of SSEES dependence on the main grid, we first run the ARO model considering the conditions listed above and assuming that constraint (3.5f) is relaxed. From this, we obtain that the maximum power purchased from the main grid is 2250 kW. We take 2250 kW as reference and then we re-run the ARO model by making constraint (3.5f) active and attributing different values to upper and lower bound $\overline{G}$ and $\underline{G}$, respectively. In particular, since in almost all the previous simulations

the system is only importing power from the main grid, here we are interested in addressing how expansion decisions change when the maximum amount of electricity drainable from the main grid reduces. For this reason, we assume that parameter $\overline{G}$ can take the values of 2000 kW, 1800 kW, 1600 kW, 1400 kW, corresponding to a reduction of 11%, 20%, 29%, and 38% of the reference amount withdrawn, respectively, and we fix the lower bound $\underline{G}$, i.e. the minimum hourly amount of electricity that can sold to the grid, to -2000 kW in all the following simulations.

$\overline{G}$	# Charging Stations	Solar Capacity (kW)	Storage Capacity (kW)	Total Cost ($)
No limits	59	0	330	403,243
2000 kW	58	0	520	411,538
1800 kW	36	530	530	490,368
1600 kW	20	1,230	710	606,605
1400 kW	135	32,760	870	41,557,144

Table 3.8: Impact of the limits of the power purchased from main grid on investment decisions

The results of this analysis are reported in Table 3.8, where row "No limits" reports the expansion decisions taken by the central planner when it can freely withdraw electricity from the main grid. The general trend, observed when the supply from the main grid is set equal either to 2000 kW, 1800 kW or 1600 kW, is that central planner prefers to invest more in PV and storage units, while reducing the number of charging stations built. This is a direct consequence of forced limited access to the main grid: additional PV plants are needed to cover the SSEES' power demand and storage units are built to mitigate solar production variability. In this way, the system is more autonomous but its management becomes more expensive leading to an increase of the total costs. In all these cases, withdrawal and purchase of electricity represent the net position that the central planner has with respect to the main grid. On the other side, we have a turnaround when parameter $\overline{G}$ is set equal to 1400 kW. This limitation pushes the system to exchange power with the grid generating a negative overall balance, i.e., the system is selling more power to the grid than what is buying. From a practical point of view this is translated into an explosion of investments in PV and storage units, as well as in charging stations. This effect is in line with the value of the binary variable u^{G} associated with uncertainty budget Λ^{G}, which results to be equal to zero only in this specific case. Note that, by fixing $\Lambda^{\mathrm{G}} = 1$, we allow $u^{\mathrm{G}} = 1$, i.e. a long-term increase in the price of electricity exchanged with the main grid. This always represents the worst case scenario for the system, which is mainly draining power from the main grid. On the other side, if the system is overall selling power

to the grid the worst case scenario is represented by the electricity prices remaining constant, i.e., non increasing, in the long run, therefore $u^{\mathrm{G}} = 0$.

3.5.4 Impact of network expansion

The results presented in the above sections are obtained by assuming that the central planner can expand the network, therefore we consider an 8-line SSEES ("8L") with 4 existing and 4 candidate lines. The other considered assumptions are as follows:

- No limits on the power exchange with the main grid is imposed, namely constraint (3.5f) is relaxed.
- The revenues associated with EVs are set both at $C^{\mathrm{E}}_{ot} = 2\tilde{C}^{\mathrm{G}}_{ot}$ and at $C^{\mathrm{E}}_{ot} = 3\tilde{C}^{\mathrm{G}}_{ot}$.
- Uncertainty budgets:
  - $\Lambda^{\mathrm{G}} = 1$, $\Lambda^{\mathrm{L}} = 2$, and $\Lambda^{\mathrm{EV}} = 1$ that identify intermediate SSEES conditions.
  - $\Lambda^{\mathrm{G}} = 1$, $\Lambda^{\mathrm{L}} = 4$, and $\Lambda^{\mathrm{EV}} = 2$ that describe a more extreme situation for the SSEES.

In addition to the above assumptions, we run two sets of simulations:

1. The capacity limits of the existing and candidate lines in the "8L" network are those indicated in Table 3.2. We indicate this case as "8L.F.C.", namely "eight-line network, full line capacity".

2. We assume that the capacity of the candidate lines are as those reported in Table 3.2, but those of the existing lines are reduced by 20%. We indicate this case as "8L.80%F.C.", namely "eight-line network, 80% of the existing line full capacity".

	Candidate lines constructed			
	$\Lambda^{\mathrm{G}} = 1$, $\Lambda^{\mathrm{L}} = 2$, $\Lambda^{\mathrm{EV}} = 1$		$\Lambda^{\mathrm{G}} = 1$ $\Lambda^{\mathrm{L}} = 4$ $\Lambda^{\mathrm{EV}} = 2$	
	8L.F.C.	8L.80%F.C.	8L.F.C.	8L.80%F.C.
$C^{\mathrm{E}}_{ot} = 2\tilde{C}^{\mathrm{G}}_{ot}$	No new lines	Lines 5 and 6	Line 7	Lines 5, 6, and 7
$C^{\mathrm{E}}_{ot} = 3\tilde{C}^{\mathrm{G}}_{ot}$	Line 7	Lines 5 and 6	Line 7	Lines 5, 6, and 7

Table 3.9: Line expansion in the different simulations

Results are summarized in Tables 3.9-3.11. We first concentrate our attention on the column "$\Lambda^{\mathrm{G}} = 1$, $\Lambda^{\mathrm{L}} = 2$, $\Lambda^{\mathrm{EV}} = 1$" of Table 3.9, which shows the network line expansion decisions taken by the central planner under the considered assumptions. There are no investments in candidate lines when the "8L.F.C." case is considered and the condition $C^{\mathrm{E}}_{ot} = 2\tilde{C}^{\mathrm{G}}_{ot}$ applies. This means that the central planner still operates

Uncertainty Budget	# Charging stations		Solar Capacity (kW)		Storage Capacity (kW)		Total Cost ($)	
$\Lambda^{\mathrm{G}}=1$, $\Lambda^{\mathrm{L}}=2$, $\Lambda^{\mathrm{EV}}=1$	8L.F.C.	8L.80%F.C.	8L.F.C.	8L.80%F.C.	8L.F.C.	8L.80%F.C.	8L.F.C.	8L.80%F.C.
$C^{\mathrm{E}}_{ot}=2\tilde{C}^{\mathrm{G}}_{ot}$	59	60	0	0	330	60	403,243	411,171
$C^{\mathrm{E}}_{ot}=3\tilde{C}^{\mathrm{G}}_{ot}$	75	80	0	0	170	60	366,554	375,923

Table 3.10: Impact of network expansion with $\Lambda^{\mathrm{G}}=1$, $\Lambda^{\mathrm{L}}=2$, $\Lambda^{\mathrm{EV}}=1$

with a four-node network and, in fact, the corresponding results reported in Table 3.10 are analogous to those of the related "4L.F.C." scenario where only storage units and charging stations are realized (compare Table 3.10 with Table 3.5). The situation changes if the"8L.F.C." case is combined with the $C^{\mathrm{E}}_{ot}=3\tilde{C}^{\mathrm{G}}_{ot}$ scenario. In this situation, the central planner adopts a strategy that allows it to increase its revenues and, therefore, to reduce its total costs. Since the revenues from selling electricity to the EVs is twice than the value of the electricity exchanged with the main grid, it aims at exploiting this opportunity by expanding the network and building line 7 (see Table 3.9) that connects node 1, the node linked with the main grid, with node 2, where charging stations can be installed (see Figure 3.2). This leads to a reinforcement of the already existing line 1. As a result, it has the possibility to withdrawn more energy from the main grid and increase the amount of power provided to EVs. This trend is also confirmed by the other expansion decisions highlighted in Table 3.10 where one can observe a significant raise of the charging stations built and a contraction of the total costs due to the revenues accruing from EVs in comparison with the "8L.F.C." case associated with and $C^{\mathrm{E}}_{ot}=2\tilde{C}^{\mathrm{G}}_{ot}$ scenario. Moreover, since the access to the main grid is facilitated by the additional line, storage units become less useful and therefore the central planner reduces its investments in these facilities. Note that the network expansion improves the SSEES efficiency since, comparing the outcome of the "8L.F.C." case, combined with the $C^{\mathrm{E}}_{ot}=3\tilde{C}^{\mathrm{G}}_{ot}$ scenario, with the results of the similar "4L.F.C." case reported in Table 3.7, we observe an important reduction of the system total costs.

When considering the "8L.80%F.C." and "$\Lambda^{\mathrm{G}}=1$, $\Lambda^{\mathrm{L}}=2$, $\Lambda^{\mathrm{EV}}=1$" assumptions, the situation changes. Recall that under the "4L.80%F.C." scenarios, the four-line network is congested since the distribution capacity is reduced. Allowing for network expansion in "8L.80%F.C.", congestion is relieved thanks to the investments in new lines 5 and 6 both when C^{E}_{ot} is 100% and 200% higher than $\tilde{C}^{\mathrm{G}}_{ot}$ (see Table 3.9). Line 5 links the main grid with node 4, where consumers' demand is located; line 6 reinforces line 2, connecting the main grid with node 3, where there are both consumers and EVs' electricity demands. Moreover, the strategy adopted by the central planner in terms of investments in charging stations and PV plants is similar to that applied in the corresponding "8L.F.C." cases. A different policy is considered for the charging stations which are much lower than in "8L.F.C." case scenarios and are not affected by

the different revenues deriving from the EVs. This derives from the fact that, since two more lines are built, the SSEES becomes more stable and it is more convenient to withdraw energy from the main grid, when needed, instead of activating storage systems. Indeed, the reduced capacity of the four existing lines represents a disadvantage for the SSEES compared to "8L.F.C." cases, since the central planner is forced to build two candidate lines. This is also reflected in terms of total costs that in the "8L.80%F.C." scenarios are a bit higher than in the corresponding "8L.F.C." conditions.

Uncertainty Budget	# Charging stations		Solar Capacity (kW)		Storage Capacity (kW)		Total Cost ($)	
$\Lambda^{\mathrm{G}}=1,\ \Lambda^{\mathrm{L}}=4,\ \Lambda^{\mathrm{EV}}=2$	8L.F.C.	8L.80%F.C	8L.F.C.	8L.80%F.C.	8L.F.C.	8L.80%F.C.	8L.F.C.	8L.80%F.C.
$C^{\mathrm{E}}_{ot}=2\tilde{C}^{\mathrm{G}}_{ot}$	59	61	0	0	240	0	467,600	475,345
$C^{\mathrm{E}}_{ot}=3\tilde{C}^{\mathrm{G}}_{ot}$	69	71	0	0	240	0	434,427	438,898

Table 3.11: Impact of network expansion with $\Lambda^{\mathrm{G}}=1$, $\Lambda^{\mathrm{L}}=4$, $\Lambda^{\mathrm{EV}}=2$

We now look at the column "$\Lambda^{\mathrm{G}}=1$, $\Lambda^{\mathrm{L}}=4$, $\Lambda^{\mathrm{EV}}=2$" of Table 3.9, namely at the network expansion decisions when the maximum values of the uncertainty budgets are considered. The situation outlined by these extreme long-run uncertainty puts the system under pressure and the four-existing lines alone do not suffice to satisfy the SSEES' needs in any case. When the "8L.F.C." is considered, the central planner decides to support already existing line 1 by building line 7. The network expansion assumes an increasingly important role in the "8L.80%F.C." cases when the capacity of the existing lines is reduced. The combination of higher long-term uncertainty and limited network capacity forces the central planner to construct lines 5, 6, and 7, namely, two additional lines as for the corresponding cases with "$\Lambda^{\mathrm{G}}=1$, $\Lambda^{\mathrm{L}}=2$, $\Lambda^{\mathrm{EV}}=1$" are no longer enough to support the system. These decisions on the grid expansion are complementary with the investment strategies in charging stations and storage units reported in Table 3.11 for the different cases. Due to the significant level of uncertainty in the number of EVs, there is a consequent drop on the number of charging stations constructed compared to related scenarios in Table 3.10. The overall framework makes the system less efficient with respect to the situation with intermediate uncertainty values (compare Tables 3.10 and 3.11), causing an increase of the total costs.

Finally, note that there are no investments in PV units. This holds in all considered cases and this means that it is less expensive to invest in the network and make it adequate to the system requirements instead of building new PV plants.

3.5.5 An ex-post decarbonization analysis

We now analyze whether the adoption of EVs can be environmentally advantageous and can contribute to the achievement of the decarbonization targets imposed by the

European Commission. The penetration of EVs leads to a trade-off: on one side, these are introduced to replace pollutant conventionally fuelled cars. However, on the other side, a progressive integration of EVs would imply an increase of electricity demand. In this case, the main issue is to understand which sources are used for power generation. If EVs are charged using renewable energy only, this would significantly contribute to mitigate CO_2 emissions; otherwise the emissions saved by the replacement of conventionally fuelled cars with EVs are partially or, in the worst case, totally compensated by those emitted when producing the electricity that EVs need. Translating this for our case, the increase of electricity demand due to the penetration of EVs is covered by importing more power from the main grid, or alternatively by installing PV within the SSEES. On the contrary, a system without EVs is importing less power from the main grid, but is emitting CO_2 by using fuel vehicles.

For this decarbonization analysis, we consider the following assumptions:

- No limits on the power exchanged with the main grid is imposed, i.e., constraint (3.5f) is relaxed.
- The revenues associated with EVs are set at $C^{\mathrm{E}}_{ot} = 2\tilde{C}^{\mathrm{G}}_{ot}$.
- All the main cases related to network configuration are analyzed: "4L.F.C.", "4L.80%F.C", "8L.F.C.", and "8L.80%F.C". In all these cases, charging stations are built.
- Uncertainty budgets are fixed to $\Lambda^{\mathrm{G}} = 1$, $\Lambda^{\mathrm{L}} = 2$, and $\Lambda^{\mathrm{EV}} = 1$.

To detect the possible decarbonization achieved with the integration of EVs, we compare two situations: the first corresponds to the formulation discussed in the work where EVs circulate and are charged; in the second, we assume that the charged EVs are replaced by diesel fuelled vehicles. In the following, we denote these two situations as "EVs" and "NO EVs", respectively. We then compute the emissions generated by these two SSEES configurations: in the first one, CO_2 only derives from electricity production; in the second, carbon emissions are a "negative" output of both power generation and car utilization. We start from the amount of CO_2 emitted by electricity production. Solar energy generated by PV units is carbon free. However, emissions could be generated by the electricity withdrawn from the main grid that is used to supply EVs' and consumers' demand. As explained in Section 3.4, our input data mainly refer to Texas. For this reason, we looked for the fuel mix used to generate electricity in that area of the US. According to the Alternative Fuel Data Center,[5] approximately 45% of the electricity production in Texas is generated with natural gas, 29% from coal and the rest from CO_2 free sources, including nuclear power. Taking as reference this fuel mix, we assign to the electricity taken from main grid an emission factor of

[5]See https://www.afdc.energy.gov/vehicles/electric_emissions.php

0.466 Ton CO_2/MWh that is computed as a weighted average of the emission factors associated with the fuels used to produce electricity and their corresponding proportion in the Texan power generation.
To compute the carbon emissions of diesel vehicles, we assume that:

- diesel vehicles replace charging EVs, i.e., the number of cars circulating in the system remains the one resulting from our analysis;
- diesel vehicles replicate exactly the travel path of the EVs;
- a 8.5 km/liter consumption is assumed for diesel vehicles;
- the CO_2 emission rate associated with diesel vehicles is equal to 2.6391 kg CO_2/liter of fuel.[6]

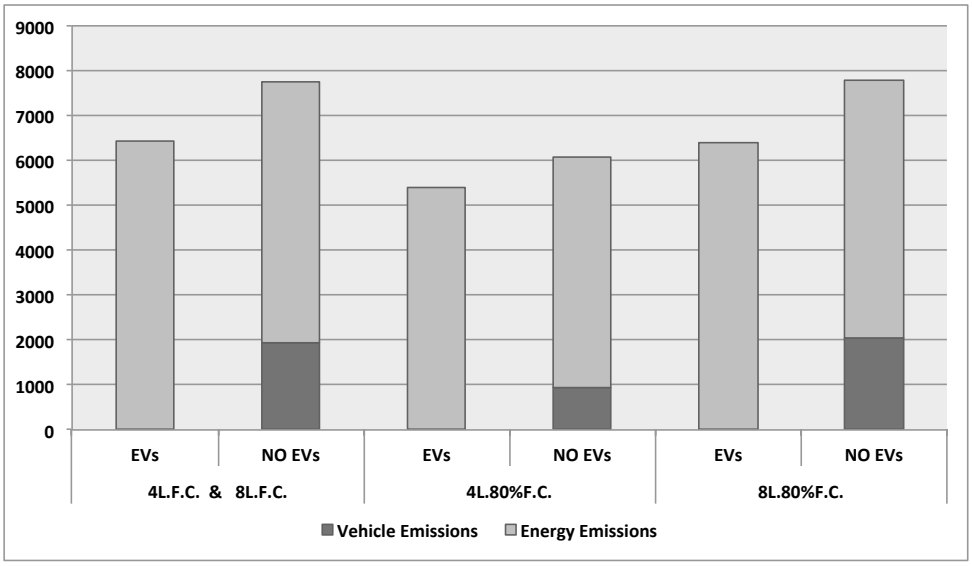

Figure 3.3: Annual ton CO_2 emission in the considered cases

Figure 3.3 shows the annual amount of CO_2 generated in the considered cases. For each market configurations, we compare the CO_2 emissions generated by the whole system in presence and in absence of EVs. Under the "EVs" situation, we consider the emissions generated by the total amount of electricity that supply the SSEES' demand, including the power consumed by EVs and local consumers. In the "NO EVs" situation, we consider the emissions that derive from the electricity required by local consumers only and CO_2 emitted by the diesel fuelled cars. The electricity needed by local consumers is the same in the two situations; what makes the difference is the power used to supply charging stations that is not accounted for in the "NO EVs" situation. Note that, as also indicated in Section 3.5.4, configurations "4L.F.C." and "8L.F.C."

[6]See https://carbonpositivelife.com/co2-per-litre-diesel/

give the same results in terms of expansion choices and total costs and therefore have identical CO_2 emission levels.

From Figure 3.3, we observe that, in all cases, the adoption of EVs allows saving a significant amount of CO_2 compared to the corresponding "NO EVs" situation, notwithstanding the fact that their utilization implies a larger electricity consumption level. These emission cuts are 17%, 11%, and 18% in the "4L.F.C."& "8L.F.C.", "4L.8'0%F.C.", and "8L.80&F.C." scenarios, respectively. This means that the integration of EVs, supported by a parallel penetration of renewable-based power plants and an adequate network development, significantly contribute to climate change mitigation and to the decarbonization targets. Note that, in our analysis, the lowest emission save is achieved in the "4L.8'0%F.C." case, when network is congested and its expansion is not allowed. This is because the congestion reduces the power that is imported from the main grid. Under this framework, PV units are built only to supply residential demand and the number of charging stations installed and, therefore, the electricity used to supply EVs is lower than in the other cases. In this way, the CO_2 reduction is comparatively smaller.

3.6 Conclusions

Considering the adaptive robust optimization approach for the expansion planning of a SSEES carried out in this work, the general conclusions below are in order:

1. Transforming the energy system switching to renewable energy sources and developing alternative fuels are two great opportunities to reach the decarbonization targets of the European Energy Roadmap 2050. The proposed approach considers, in an integrated framework, what is needed to achieve the European decarbonization targets, namely, the planning of a electric energy system with renewable energy sources generation, storage units, network expansion, and charging stations for EVs.

2. Different sources of long-term and short-term uncertainties highly influence generation and network expansion decisions. The proposed approach allows an accurate modeling of these uncertainties.

3. The proposed three-level formulation can be reformulated into a two-level one by merging the second-level problem and the dual of the third-level problem. The resulting problem can be solved efficiently via a column-and-constraint generation algorithm.

Regarding the case study analyzed in this work, we enumerate the following conclusions:

1. The expansion decisions are highly conditioned by the uncertainty budgets: the investment in generation and storage capacity generally increases as we increase the value of the demand uncertainty budget, while the investment in charging stations decreases as we increase the value of the grid uncertainty budget Λ^{G}.

2. Increasing the central planner's revenues from selling electricity to the EVs implies a raise of the number of charging stations built. If these revenues are high enough, they also justify investments in additional storage and PV units, which help satisfying a higher portion of EVs electricity demand.

3. Limiting the power that can be withdrawn from the main grid increases the investments in generation and storage capacity. Above a certain threshold, the system starts selling electricity to the main grid to partially abate total costs.

4. Reducing network capacity creates a congestion that is overcome, whether possible, by expanding the network. Network expansion is also influenced by the values of the uncertainty budgets and by the revenues from selling electricity to the EVs. According to these combinations, building storage units might be better than investing in a prospective line.

5. Adopting EVs increases the electricity demand, which at the time being is still partially satisfied by conventional and pollutant fuels, such as natural gas and coal. Anyway, the adoption of EVs allows important CO_2 savings if compared with an analogous situation with lower electricity demand and diesel vehicles.

Chapter 4

Analysis of long-term natural gas contracts with vine copulas in optimization portfolio problems

This chapter is based on the article:

Allevi E., L. Boffino L., M. E. De Giuli, G. Oggioni.

Analysis of long-term natural gas contracts with vine copulas in optimization portfolio problems

which has been published on Annals of Operations Research,
DOI: 10.1007/s10479-018-2932-x. ISSN: 1572-9338

In this chapter we investigate the dependence risk and the optimal resource allocation of the underlying assets of a gas long-term contract (LTC) through pair-vine copulas and portfolio optimization methods with respect to different risk measures. In Europe gas is sold according to two main methods: long-term contract and hub pricing. Europe is moving towards a mix of long term and spot markets, but the eventual outcome is still unknown. The fall of the European gas demand combined with the increase of the US shale gas exports and the rise of Liquefied Natural Gas availability on international markets have led to a reduction of the European gas hub prices. On the other side, oil-indexed LTCs failed to promptly adjust their positions, implying significant losses for European gas mid-streamers that asked for a re-negotiation of their existing contracts and obtained new contracts linked also to hub spot prices. The debate over the necessity of the oil-indexed pricing is still on-going. The supporters of the gas-indexation state that nowadays the European gas industry is mature enough to adopt hub-based pricing system. With the aim of analyzing this situation and determining whether oil-indexation can still be convenient for the European gas market,

we consider both spot gas prices traded at the hub and oil-based commodities as possible underlyings of the LTCs. Our results show that European LTCs will most likely remain indexed to oil-based commodities, even though a partial dependence on spot hub prices is conceded.

The model developed in this chapter have been implemented and solved in R.

4.1 Introduction

Natural gas can be sold either through long-term contracts (LTCs) or at spot price at market hubs. LTCs have been historically introduced to allow for risk sharing between gas producers and mid-streamers, which respectively face price and volume risks. These contracts have been traditionally concluded over long periods (typically 20 years or more) and are characterized by quantity and price clauses. The Take or Pay (TOP) quantity clause obligates the buyer to take a certain quantity of natural gas or to pay for it. The Price Indexation (PI) clause relates the price at which gas is bought to some index on the market that has been traditionally represented by the price of crude and oil-products. The price clause provides producers with some price stability and reduction of revenue volatility, which are indispensable for ensuring investments in new infrastructures which are very expensive. Moreover, the quantity and price clauses also allow for hedging the mid-streamers' volume risk (see Abada et al. (2017)).

The hub pricing approach was firstly introduced in the nineties in the US and in the UK and it is now developing in Europe. In this system, natural gas is traded, every day, on a spot market that determines prices and volume on the short term. International natural gas market is organized in different ways depending on the considered areas. North America is essentially organized on the basis of Henry Hub spot market. The price on this market is currently very low, at about 3$/MBtu,[1] because of the development of unconventional (shale) gas. The Henry Hub is the best-known of all natural gas trading points. It is both a physical distribution hub for pipeline gas and a pricing point, since it is the basis of spot market trading and of futures trading on the New York Mercantile Exchange (NYMEX).

On the other side, Asia is mainly supplied by Liquefied Natural Gas (LNG) that is traded through expensive LTCs. The Asian LNG long-term contracts has been set on the basis of the average of Japanese customs-cleared crude oil price that is the Japan Crude Cocktail (JCC). After the Fukushima disaster, Japan has significantly increased its imports of LNG, mainly supplied by Australia, Malaysia and Qatar through LTCs (see GIIGNL (2018)).

[1] See http://www.eia.gov/dnav/ng/hist/rngwhhdd.htm

Spot deals exist, but they are bilateral as, up to now, there is no hub in Asia in contrast with America and Europe. Some experts advocate a move from the current system of LTCs to hub-pricing system (e.g IEA (2013)). Singapore has proposed itself as a possible gas hub for Asia as well as Tokyo and Shanghai (see Xunpeng (2016)).

Except for the UK, Europe is still dominated by LTCs, though spot markets are growing and are expected to develop further. In the UK, gas is largely traded at the National Balancing Point (NBP) spot market. NBP is in operation since the late 1990s and is the longest-established spot-traded natural gas market in Europe. It is characterized by high liquidity[2] and the resulting spot price is widely used as an indicator for European wholesale gas market. In continental Europe, Zeebrugge (ZEE) and the Title Transfer Facility (TTF), respectively located in Belgium and in the Netherlands, are the two dominant spot market places and many others are emerging (see Melling (2010)).

The coexistence of LTCs and hub-pricing systems on the European market implies that the natural gas is traded at two different prices on the same market. Depending on the conditions, spot price can be higher or lower than long-term contractual gas, leading to possibly difficult situations for companies loaded with high TOP gas price against the low spot prices. This is what happened in the last years in Europe, where the combined effects of the increase of the US shale gas exports, the reduction of European gas demand due to the economic crisis, and the increased availability of uncommitted LNG from Qatar led to a new supply/demand balance that was reflected into low gas prices at the European hubs. On the other side, oil-indexed LTCs failed to promptly adjust their positions implying significant losses for European gas mid-streamers what were committed by the TOP clause to buy quantities of gas higher than those required at higher prices. As a consequence, European mid-streamers have re-negotiationed the LTCs to make them more flexible and closer to spot gas prices. These re-negotiations have resulted into a decline of oil-indexation and hub-linked pricing has rapidly become the basis for an increasing number of transactions in the UK and in the Northern Western Europe (see Franza (2014); Yafimava (2014)). As indicated by Chyong (2015), leading gas suppliers, such as Statoil, GasTerra, Sonatrach and Gazprom, have been forced to modify their LTC prices and volumes in Europe. However, these gas suppliers have assumed different attitudes: Gazprom and Sonatrach has defended oil indexation and has offered retroactive discounts on existing contracts by introducing either limited degree of spot indexation or reduced minimum TOP provisions. On the other side, GasTerra and Statoil have behaved in a more flexible way, by conceding more spot indexation in their contracts. Notwithstanding this, oil is

[2]The liquidity of a gas hub can be defined as the ratio between the total volume of trade on the hub and the volume of gas consumed in the area served by the hub.

still accounting for the 95% of price formation within the Continental Europe against the 30% of price formation in the UK (see Theisen (2014)). This shows that oil-indexed contract prices still exercise a strong influence over gas prices in Europe. The reliability of prices set on spot markets is one of the main reasons used by the opponents of the spot indexation for LTCs (see Frisch (2010)). Liquidity, transparency, and the ability to attract a significant number of market players are necessary for a hub to become a price maker (see Heather (2012)). For the time being, the NBP and TTF are the only two hubs in Europe with sufficient liquidity (see Heather and Petrovich (2017)). However, some experts advocate a move from the current system of long-term contracts to hub pricing (see Stern and Rogers (2014)). Even though their arguments make sense, these are not supported by numerical analysis.

From these evidences, it turns out that the role of the European spot gas markets and their impacts on LTCs are becoming extremely challenging issues. This work sheds some light on the LTCs re-negotiation, taking into account the mid-streamers' requests. An integrated framework that combines vine copula and optimization techniques traditionally used in the contest of portfolio management. The adopted methodology is well studied in the literature and it is considered mature enough for this task. This allows us to obtain reliable results that can provide usable information and could be easily reproducible by gas market players and practitioners. Our analysis is structured as follows: we estimate, via Pair-Copula Constructions (PCC), the dependence risk structure across the underlyings of LTCs on natural gas. In order to reflect the above mentioned European hybrid pricing system, based on the symbiotic coexistence of oil-indexed contracts and gas-indexed hub prices, we consider the prices of oil-based products and natural gas traded at the hub as component of the gas pricing formula. (see Section 4.3 for more details). We then combine vine copula models and classical portfolio optimization methods to construct the optimal underlying portfolio, applying different performance measures. Copula models represent a suitable tool to this scope. In particular, copula is a function that combines marginal distributions to form multivariate distributions. The application of copulas is very popular in several fields, like finance, insurance, financial economics and econometrics (see e.g. Durante and Sempi (2015); Genest and Bourdeau-Brien (2009); Krzemienowski and Szymczyk (2016); Li and You (2014); Saida and Prigent (2018); Tran et al. (2017)). Nowadays, the modeling of stochastic dependence via copulas has led to an increasing attention also in the commodity market (see e.g. Accioly and Aiube (2008); Aloui et al. (2013); Bassetti et al. (2018); Grégoire et al. (2008); Jäschke (2014); Lu et al. (2014); Reboredo (2011); Wen et al. (2012)).

While there is a wide range of possible alternative copula functions for the bivariate case, in the multivariate setting the use of families different from normal and student-t

is rather scarce, due to computational and theoretical limitations (see e.g. Joe (1997); Nelsen (1999)). For this reason, in order to represent a multivariate copula with suitable sets of bivariate copulas, Joe (1996) introduced the PCC approach, later discussed in detail by Aas et al. (2009); Bedford and Cooke (2001, 2002); Kurowicka and Cooke (2006). A collection of potentially different bivariate copulas is used to construct the joint distribution of interest via PCCs, allowing to represent different types and strengths of dependence in an easy way. PCCs constitute a flexible and very appealing tool for financial analysis, (see Brechmann and Czado (2013); Dalla Valle et al. (2016); Dißmann et al. (2013)). The vine copula models considered for the analysis of the portfolio's dependence risk overcome the restrictive and deterministic features of the bivariate copulas and traditional measures of correlation, due to their suitability in capturing the non-normality, tail dependence and volatility clustering of assets returns. Recently Hernandez (2014) show how the vine copula approach can be appropriately used to investigate the dependence structure among the different components of energy portfolio as well as to derive implications for portfolio risk management. In this work, we investigate via PCC, the dependence risk structure across the underlying assets of LTCs on natural gas. We define the optimal portfolio composition under different performance measures.

To the best of our knowledge the optimal composition of the assets, commonly used to price the gas LTCs, has not been investigated using the aforementioned approach. In doing this, we consider both the traditional oil-based commodities and spot gas prices to address the debate over oil/spot indexation related to the re-negotiation of European LTCs. Our results confirm the effectiveness of the hybrid pricing system currently existing in the continent, but indicates that oil should still play an important role in the definition of the price of the LTCs.
The remainder of this work is organized as follows: Section 4.2 briefly presents the PCC and the vine copulas; Section 4.3 provides the data analysis and introduces the pair vine copula that we use in our study; Section 4.4 overviews the optimization portfolio problems that we solve to estimate the risk of the optimal portfolio of the underlying assets of LTCs, and illustrates the results of our analysis. Finally, concluding remarks are given in Section 4.5.

4.2 PCC approach and vine copulas

PCC is a multivariate copula constructed by using only bivariate copula or pair-copulas as building blocks. All copulas involved in the decomposition may be selected freely among the wide range of bivariate copula family that are capable of modeling joint distribution with different characteristics. Hence, PCC allows high flexibility in repre-

senting complex structures of dependence among multivariate data. It is based on the decomposition of a d-dimensional joint density function $f(x_1, \ldots, x_d)$ of the random vector $X = (X_1, \ldots X_d)$, as a product of conditional densities:

$$f(x_1, \ldots, x_d) = f_d(x_d) \times f_{d-1|d}(x_{d-1} \,|x_d\,) \times \cdots \times f_{1|2\cdots d}(x_1 \,|x_2 \cdots, x_d)\,. \tag{4.1}$$

Each term in (4.1) can be decomposed using Sklar theorem (see Sklar (1959)) to express the conditional density for a generic element x_j conditioned on the d-dimensional vector $\mathbf{v}$ as in (4.2):

$$f_{x_j|\mathbf{v}}(x_j \,|\mathbf{v}\,) = c_{x_j,v_l|\mathbf{v}_{-l}}(F_{x_j|\mathbf{v}_{-l}}(x_j \,|\mathbf{v}_{-l}\,), F_{v_l|\mathbf{v}_{-l}}(v_l \,|\mathbf{v}_{-l}\,) \times f_{x_j|v_{-l}}(x_j \,|\mathbf{v}_{-l}\,), \tag{4.2}$$

where v_l is an arbitrary component of $\mathbf{v}$, $\mathbf{v}_{-l}$ denotes the $(d-1)$ dimensional vector without v_l, $c_{x_j,v_l}\,|\mathbf{v}_{-l}\,(\cdot,\cdot)$ is the conditional pair copula density and $F_{x_j|\mathbf{v}_{-l}}(\cdot\,|\cdot)$ is the conditional distribution of x_j given $\mathbf{v}_{-l}$. More precisely, for every j, Joe (1996) proves that:

$$F_{x_j|\mathbf{v}}(x_j \,|\mathbf{v}\,) = \frac{\partial C_{x_j,v_l|v_{-l}}(F_{x_j|\mathbf{v}_{-l}}(x_j \,|\mathbf{v}_{-l}\,), F_{v_l|\mathbf{v}_{-l}}(v_l \,|\mathbf{v}_{-l}\,)\,|\theta\,)}{\partial F_{v_l|\mathbf{v}_{-l}}(v_l \,|\mathbf{v}_{-l}\,)}, \tag{4.3}$$

where the bivariate copula function is specified by $C_{x_j,v_l|v_{-l}}$, with parameters θ. In working with copula models a function $h(x, v, \Theta)$ can be defined in order to represent the conditional distribution function when x and v are uniform, i.e. $f(x) = f(v) = 1$, $F(x) = x$ and $F(v) = v$. The h-function can be calculated as follows:

$$h(x, v, \Theta) = F(x|v) = \frac{\partial C_{x,v}(x, v, \Theta)}{\partial v}, \tag{4.4}$$

where the second parameter of $h(x, v, \Theta)$ always corresponds to the conditioning variable and Θ denotes the set of parameters for the copula of the joint distribution function of x and v. For high-dimensional distributions the number of possible pair-copulas constructions is manifold. In order to organize them, Bedford and Cooke (2001, 2002) have introduced a graphical model denoted regular vines that depict multivariate copulas built up using a cascade of bivariate copulas (or pair-copulas). This allows to understand which conditional specifications are used to describe the joint distribution. A regular vine $V(d)$ on d variables is a nested set of trees T_i where $i = 1, ..., d-1$. In particular the first tree has d nodes and $d-1$ edges that represents the pair-copula densities between the nodes. While, the j trees have $d+1-j$ nodes deriving from the edges of tree $j-1$ and $d-j$ edges that are the conditional pair-copula densities. Moreover the proximity condition states that if the nodes of tree $j+1$ are connected by an edge, than the corresponding edges in tree j share a common node. According to Kurowicka and Cooke (2006) the joint of a random vector $X = (X_1, \ldots X_d)$ following

an R-vine distribution can be written as:

$$f(x_1,\dots,x_d) = \left[\prod_{k=1}^{d} f_k(x_k)\right] \cdot \left[\prod_{i=1}^{d-1}\prod_{e\in E_i} c_{j(e),k(e)|D(e)}(F(x_{j(e)}|x_{D(e)}), F(x_{k(e)}|x_{D(e)}))\right]. \tag{4.5}$$

with node set $\mathcal{N} := \{N_1,\dots,N_{d-1}\}$ and edge set $\mathcal{E} := \{E_1,\dots,E_{d-1}\}$. Each parameter $e = j(e),k(e)|D(e)$ is an edge, while $c_{j(e),k(e)|D(e)}$ represents a bivariate conditional density copula. $j(e)$ and $k(e)$ are the conditioned nodes and $D(e)$ is the conditioning set. The union $\{j(e),k(e),D(e)\}$ is called constraint set. The right term of equation (4.5) which involves $d(d-1)/2$ bivariate copula densities, is called an R-vine copula. Special classes of R-vines are Canonical vines (C-vines) and Drawable vines (D-vines). A C-vine is a regular vine where each tree T_i has a unique node that is connected to $d-i$ edges; while a D-vine is a regular vine where each node is connected to no more than two other nodes. Each tree in a C-vine is a star with one unique node that connects to all other nodes, whereas a D-vine is represented by line trees. In a C-vine, at the first root node at level 1 of the nested set of trees, the key variable presents the highest correlation value in regard to the other variables and governs the dependence structure among the others. Intuitively, we use a C-vine to describe a scenario where one variable dominates the others, whereas in the D-vines we do not assume the existence of a particular node dominating the dependencies.
More precisely, the joint density function $f(x_1,\cdots,x_n)$ of a C-vine of dimension d takes the following form:

$$\begin{aligned} &f(x_1,\dots,x_d) = \\ &= \prod_{k=1}^{d} f_k(x_k) \cdot \prod_{i=1}^{d-1}\prod_{j=1}^{d-i} c_{i,i+j|1,\dots,i-1}(F(x_i|x_1,\dots,x_{i-1}), F(x_{i+j}|x_1,\dots,x_{i-1})|\theta_{i,i+j|1,\dots,i-1}). \end{aligned} \tag{4.6}$$

In a similar way, the joint density function of a D-vine is given by:

$$\begin{aligned} &f(x_1,\dots,x_d) = \\ &= \prod_{k=1}^{d} f_k(x_k) \cdot \prod_{i=1}^{d-1}\prod_{j=1}^{d-i} c_{j,j+i|j+1,\dots,j+i-1}(F(x_j|x_{j+1},\dots,x_{j+i-1}), F(x_{j+i}|x_{j+1},\dots,x_{j+i-1})|\theta_{j,j+i|j+1,\dots,j+i-1}). \end{aligned} \tag{4.7}$$

Differently from C-vines and D-vine the joint density function of the R-vine can vary significantly according to the statistical feature of the multivariate distribution being modeled. For this reason, Morales-Napoles (2010); Dißmann et al. (2013) proposed an efficient method for storing the indices of the pair-copula. It relies on the

specification of a lower triangular matrix $M = (m_{i,j}|i, j = 1, ..., d) \in \{0, ..., d\}^{dxd}$, whose diagonal entries $m_{i,i}$ are the nodes $1, ..., d$ of the first tree. Each row from the bottom up represents a tree. The conditioned sets of a node are determined by a diagonal entry and the corresponding column entry of the row under consideration, while the the column entries below this row provides the conditioning set. Corresponding copula types can also be stored in matrices similar to M (see Section 4.3.2 for more details).

4.3 Data and dependence structure

4.3.1 Data analysis

With the aim of analyzing the re-negotiation of the European LTCs, we consider both the oil-based commodities traditionally used to determine the LTCs price and the main spot gas prices traded at the hub.

In particular the historical daily prices of the following assets have been taken into account: Crude Ice Brent DTD, Gasoil NWECIF, Jet Fuel NWECIF, Naphtha NWECIF, Lsfo 1% NWECIF, Gas NBP 1stMonth, Gas HenryHub 1stMonth. The label "NWE" stands for the reference market "North West Europe", while "CIF" indicates the "Cost, Insurance and Freight" that are the costs included in the prices. For the sake of simplicity, in the rest of the work, we denote the seven time series as follows: "Brent", "Gasoil", "JetF", "Naphtha", "Lsfo", "Gas NBP" and "Gas HenryHub".

We analyze the period from the 4th of January 2012 to the 24th of July 2014 for a total of 647 observations. The first five time series, referred to oil and its by-products, are spot prices. The last two series, respectively referred to the natural gas traded at the NBP and Henry Hub spot markets, are the first month future prices that can be considered as good proxy of the gas spot prices. Data are provided by Datastream Thomson Reuters and all the numerical computations are run in R 3.3.2.

For each historical daily price time series, we construct the log returns and we report their basic statistics in Table 4.1. There is evidence of negative skewness and significant excess kurtosis.

Fig 4.1 shows the log returns, the 30-days horizon rolling standard deviation on log returns, and the volatility associated with the Gas NBP time series. In particular, figure 4.1b shows the volatility clustering, namely "*large changes tend to be followed by large changes, of either sign, and small changes tend to be followed by small changes*", as observed by Mandelbrot (1963) (for the other series, see Fig. 4.A.1-4.A.6 in Appendix 4.5).

The volatility clustering is confirmed also by the sample autocorrelation function (ACF) of the squared mean adjusted log returns (see left hand side of Fig. 4.2 for the

Table 4.1: Basic statistics of log return time series referred to the period January 4, 2012 - July 24, 2014

	Mean	Max	Min	Std. Dev	Skewness	Kurtosis
Brent	-0.01%	6.57%	-5.67%	1.26%	-0.068	2.063
Gasoil	-0.01%	5.08%	-3.11%	1.06%	0.049	1.077
JetF	-0.01%	5.05%	-3.98%	1.03%	0.075	1.599
Naphtha	0.00%	5.27%	-7.72%	1.30%	-0.440	3.654
Lsfo	-0.02%	3.54%	-6.80%	1.13%	-0.758	4.551
Gas NBP	-0.04%	9.10%	-7.69%	1.59%	0.294	3.620
Gas HenryHub	0.04%	13.27%	-11.93%	2.78%	0.290	2.342

GAS NBP series and Fig. 4.A.7-4.A.8 in Appendix 4.5 for other series).

In addition, we observe that all log return series are stationary with respect to the ADF (Dickey and Fuller (1981)) and the PP tests (Phillips and Perron (1988)). The series are also stationary compared to the KPSS test (Kwiatkowski et al. (1992)) with the exception of the Gas NBP log return series. The KPSS is negligible for the latter since only the ACF plot of the differentiated series shows the presence of unit root.

Table 4.2: Unit root test results for the considered series

P-Value	Brent	Gasoil	JetF	Naphtha	Lsfo	Gas NBP	Gas HenryHub
ADF	< 0.01	< 0.01	< 0.01	< 0.01	< 0.01	< 0.01	< 0.01
PP	< 0.01	< 0.01	< 0.01	< 0.01	< 0.01	< 0.01	< 0.01
KPSS	> 0.1	> 0.1	> 0.1	> 0.1	> 0.1	0.013	> 0.1

For modeling the volatility of the series, we test several GARCH models and, for each one, we select the best model according to the significance of parameters, the log-likelihood value and the information criteria. In the case of extreme market events, dummy variables associated with these events have been used to model volatility spikes. Every series is filtered using a TGARCH model with a skewed-t distribution for innovations that allows to capture the asymmetry in volatility (i.e. the leverage effect). ARMA models have been used to compensate for autocorrelation, modeling the conditional mean where needed. Table 4.3 reports the results of the ARMA-GARCH fitting procedure. The application of the Ljung-Box test on both standardized residuals standardized squared residuals shows the absence of series correlation and the ARCH-LM test (see Fisher and O. Gallagher (2012)) confirms the adequacy of the ARCH processes. The ACF and the Partial ACF (PACF) of both the log return series and the corresponding residuals are reported in Fig 4.3-4.4 for the GAS NBP series and Fig. 4.A.9-4.A.12 in Appendix 4.5 for other series. This indicates that there is no evidence of autocorrelation at any lag.

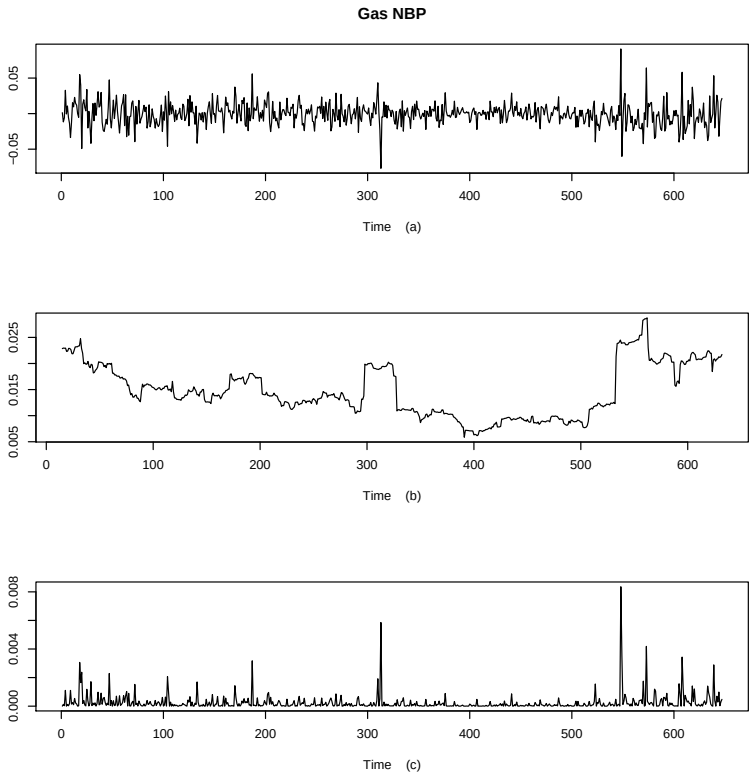

Figure 4.1: Log returns (a), 30-days horizon rolling standard deviation on log returns (b), and volatility (c) associated with the Gas NBP time series

The reduction of the volatility after fitting the ARMA-GARCH models is confirmed by the ACF of the squared mean adjusted residuals reported in the right hand side of Fig. 4.2 for the GAS NBP series and Fig. 4.A.7-4.A.8 in Appendix 4.5 for other series.

4.3.2 Pair-Copula Constructions

Using the probability integral transformation on the standardized residuals we obtain copula u-data. In order to avoid the misspecification of the margins that may lead to the bias of the copula parameter estimates, we perform the Berkowitz test on the u-data. The outcome of this test does not indicate evidence against the uniform (0,1).

Table 4.4 reports the pair-wise Kendall's τ correlation between the series. This allow us to construct the vine copula models using the maximum spanning tree algorithm proposed by Czado et al. (2012). We can note that if the strength of dependence is rather small, a good start of a bivariate data analysis is an independent test based on Kendall's τ correlation measure (see Genest and Favre (2007)). In the following, we estimate and analyze three different vine structures, namely C-vine, D-vine, R-

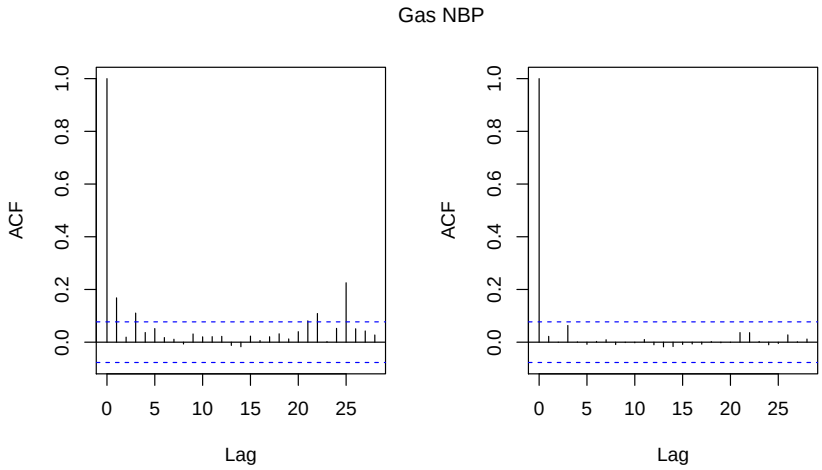

Figure 4.2: ACF of the squared mean adjusted log return series and ACF of the squared mean adjusted residuals of Gas NBP log return series.

vine together with the multivariate Student's t and the multivariate Gaussian copulas. Note that the multivariate Gaussian and multivariate Student's t copulas are both simplified PCCs and can be represented as an R-vine copula. In particular, the former is an R-vine with Gaussian pair-copulas, where the parameters are determined by the associated partial correlation; whereas the multivariate Student's t copula can be represented through an R-vine with bivariate t-copulas as building blocks under specific assumptions on the parameters (see Czado et al. (2009)). The R packages by Hofert et al. (2017); Schepsmeier et al. (2018) have been used for the analysis conducted in this section.

We first apply the C-vine copula model to account for the dependence structure. The application of the Kendall's τ independence test, with a confidence level of 5%, underlines the independence of the pair Gasoil-Gas HenryHub series as shown in the first C-vine tree of Figure 2. Akaike Information Criterion (AIC) and Bayesian Information Criterion (BIC) tests are used to select copulas. First, all available copulas are fitted with Maximum Likelihood Estimation (MLE). Then, the criteria are computed for all available copula families and the family with the minimum value is chosen.

The parameters of the PCC can be evaluated using any multivariate copula estimator such as the maximum pseudo likelihood (MPL) estimator or the inference function for margins (IFM). However the computational effort increases exponentially with the dimension. Therefore the sequential method proposed by Aas et al. (2009), is used to estimate the parameters level by level. The selected copulas in the first tree are estimated using the MLE method. To calculate the observations (i.e conditional distributions functions) of the second C-vine tree we use the h-functions (see (4.4) in

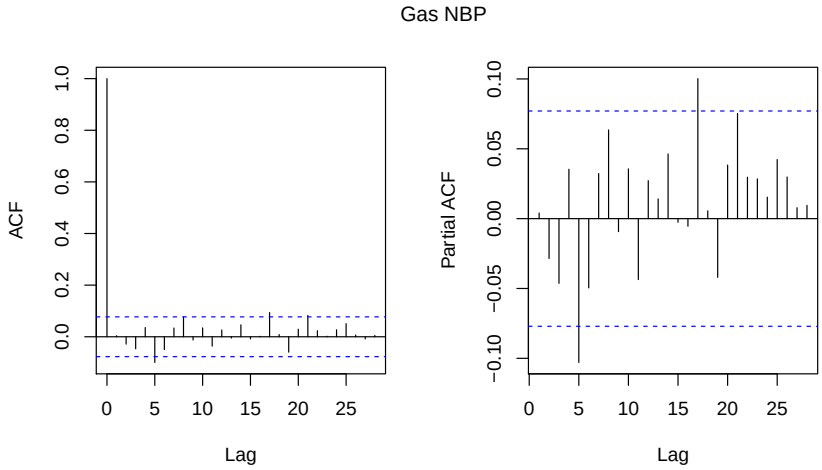

Figure 4.3: ACF and PACF of Gas NBP log return series

Table 4.3: p-values of ARMA GARCH models. The corresponding statistics are reported in parentheses. WLB=Weighted Ljung-Box Test, WALM= Weighted Arch LM Test. S.R= Standardized Residuals. S.S.R= Standardized Squared Residuals

	Series	**Brent**	**Gasoil**	**JetF**	**Naphtha**	**Lsfo**	**Gas NBP**	**Gas HenryHub**
	GARCH Model	TGARCH(1,2)	TGARCH(1,1)	TGARCH(2,0)	TGARCH(1,2)	TGARCH(1,2)	TGARCH(1,1)	TGARCH(1,1)
	ARMA Model	ARFIMA(1,0,1)	ARFIMA(0,0,0)	ARFIMA (0,0,0)	ARFIMA(9,0,0)	ARFIMA(14,0,0)	ARFIMA(17,0,0)	ARFIMA(13,0,0)
WLB Test on S.R.	Lag[1]	0.9995 (4.364e-07)	0.9401 (0.005655)	0.7433 (0.1073)	0.9692 (0.001495)	0.8531 (0.03427)	0.8179 (0.05303)	0.7959 (0.0669)
	Lag[2*(p+q)+(p+q)-1]	1 (1.093)	0.9908 (0.008741)	0.9089 (0.1175)	1 (6.642716)	1 (10.24734)	1 (18.76113)	1 (7.8402)
	Lag[4*(p+q)+(p+q)-1]	0.6123 (4.330)	0.83 (1.1283)	0.533 (2.3745)	0.9993 (12.9167)	0.9974 (24.0307)	0.7594 (39.0382)	1 (16.8326)
WLB Test on S.S.R.	Lag[1]	0.2416 (1.371)	0.5683 (0.3256)	0.8934 (0.01796)	0.8808 (0.02248)	0.6537 (0.2013)	0.2902 (1.119)	0.3185 (0.995)
	Lag[2*(p+q)+(p+q)-1]	0.1808 (6.604)	0.9592 (0.4904)	0.9904 (0.22823)	0.6261 (3.32382)	0.286 (5.5291)	0.5591 (2.257)	0.225 (4.245)
	Lag[4*(p+q)+(p+q)-1]	0.2619 (9.213)	0.9871 (0.9792)	0.8128 (2.66476)	0.4987 (7.05544)	0.3085 (8.7125)	0.7089 (3.298)	0.3887 (5.285)
WALM Tests	ARCH Lag[4]	0.1355 (2.228)	0.8308 (0.04564)	0.7293 (0.1198)	0.3062 (1.047)	0.1477 (2.096)	0.1866 (1.745)	0.5247 (0.4047)
	ARCH Lag[6]	0.3469 (2.750)	0.9045 (0.42836)	0.9347 (0.3207)	0.5359 (1.802)	0.1811 (4.078)	0.5012 (1.868)	0.8632 (0.5685)
	ARCH Lag[8]	0.4318 (3.637)	0.9521 (0.73775)	0.856 (1.3236)	0.6851 (2.279)	0.2384 (5.100)	0.7118 (2.026)	0.9105 (1.0185)

Section 4.2). This procedure is iterated tree by tree. After having fitted all the trees, a joint MLE is provided in order to improve the estimation. This procedure requires the observations to be independent over time, in fact the PCC has been fitted on the standardized residuals obtained by filtering the original series with the ARMA-TGARCH models previously described.

In a straightforward way, we can represent the C-vine copula density factorization using the specification matrix M, while the T matrix is the copula type matrix where each row corresponds to a specific tree and each number denotes the type of pair-copula

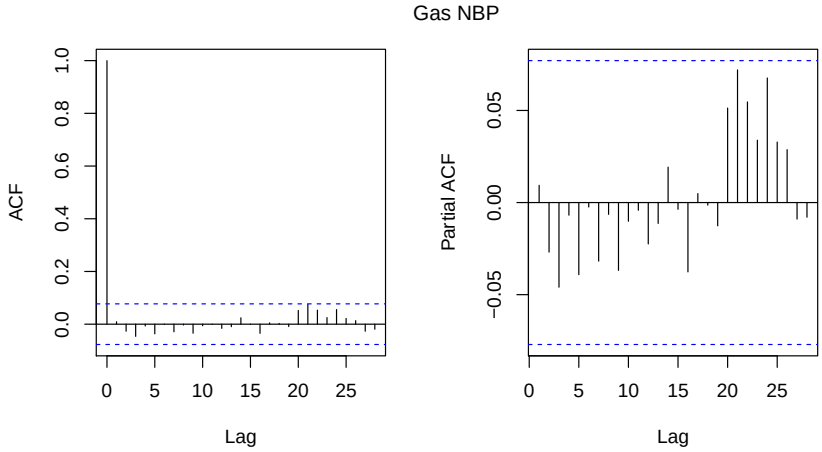

Figure 4.4: ACF and PACF of Gas NBP residuals

Table 4.4: Kendall's τ correlation between u-data

	Brent.u	**Gasoil.u**	**JetF.u**	**Naphtha.u**	**Lsfo.u**	**Gas NBP.u**	**Gas HenryHub.u**
Brent.u	1.0000	0.6037	0.6002	0.3143	0.2750	0.0851	0.0213
Gasoil.u	0.6037	1.0000	0.7805	0.2887	0.2608	0.0847	0.0341
JetF.u	0.6002	0.7805	1.0000	0.2797	0.2524	0.0863	0.0408
Naphtha.u	0.3143	0.2887	0.2797	1.0000	0.2976	0.1004	-0.0428
Lsfo.u	0.2750	0.2608	0.2524	0.2976	1.0000	0.0990	-0.0025
Gas NBP.u	0.0851	0.0847	0.0863	0.1004	0.0990	1.0000	0.0111
Gas HenryHub.u	0.0213	0.0341	0.0408	-0.0428	-0.0025	0.0111	1.0000

family.[3]

$$M = \begin{pmatrix} 7 & & & & & & \\ 6 & 6 & & & & & \\ 5 & 5 & 5 & & & & \\ 4 & 4 & 4 & 4 & & & \\ 3 & 3 & 3 & 3 & 3 & & \\ 2 & 2 & 2 & 2 & 2 & 2 & \\ 1 & 1 & 1 & 1 & 1 & 1 & 1 \end{pmatrix}$$

[3]Copula family type: 0 = Independence copula; 1 = Gaussian copula; 2 = Student-t copula (t-copula); 3 = Clayton copula; 5 = Frank copula; 13 = rotated Clayton copula (180 degrees); 14 = rotated Gumbel copula (180 degrees); 16= Rotated Joe copula (180 degrees);

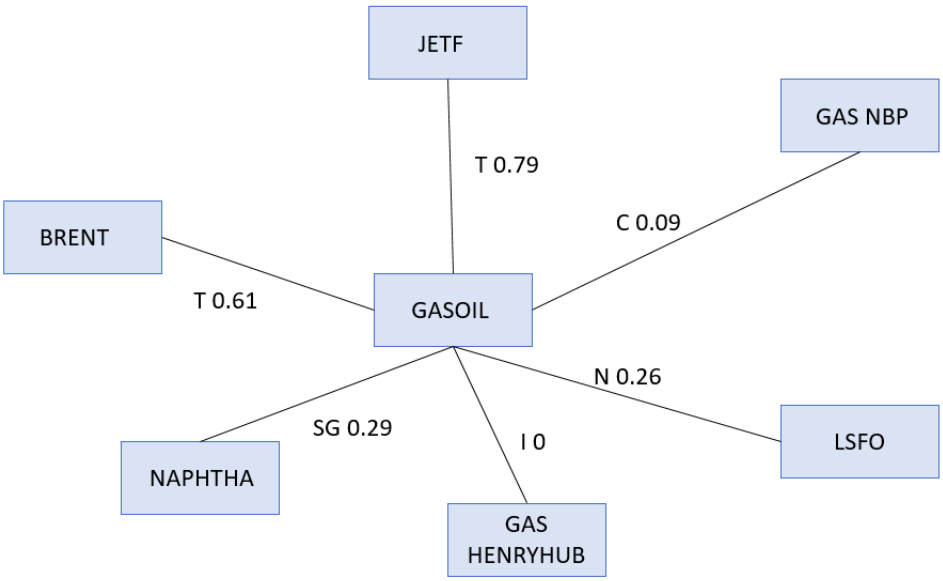

Figure 4.5: First tree of the C-vine with a 5% confidence level. The letters reported between the root nodes indicate the type of the bivariate copulas used to model the dependence, while the numbers refer to the corresponding Kendall's τ correlation.

$$T = \begin{pmatrix} 0 & & & & & \\ 0 & 5 & & & & \\ 5 & 5 & 2 & & & \\ 0 & 0 & 1 & 1 & & \\ 0 & 0 & 13 & 2 & 2 & \\ 0 & 3 & 1 & 14 & 2 & 2 \end{pmatrix}$$

We recall that Gaussian and Student-t copulas accounts for a symmetric tail dependence. In particular, Gaussian copula is designed to model the dependence in the center of the joint distributions, while the Student-t copula is both lower and upper-tail dependent. Student-t copula allows for joint extreme events either in both bivariate tails or none of them. Moreover, Frank copula models the dependence in the centre of distribution, i.e. strong dependence in non-extreme scenarios. With respect to the bivariate Gaussian, Frank copula can account for the non linearity in the center of the joint distribution, while the first one only focuses on linear dependence relationship. Finally, Clayton copula is only lower-tail dependent and is characterized by the asymmetric correlation. Together with the 180° rotated Joe and Gumbel is adequate to model greater dependence in the negative tail. The 180° rotated Clayton is suitable to model dependence in the positive tail.

The D-vine structure is reported in Fig. 4.6. The results of the independence test

based on the Kendall's τ correlation measure with a 5% confidence level points out the independence of the pair Gas NPB-Gas HenryHub as shown in the first tree of the D-vine structure in figure 3. In the following the specification matrix M and copula type matrix T are reported for the D-vine structure.

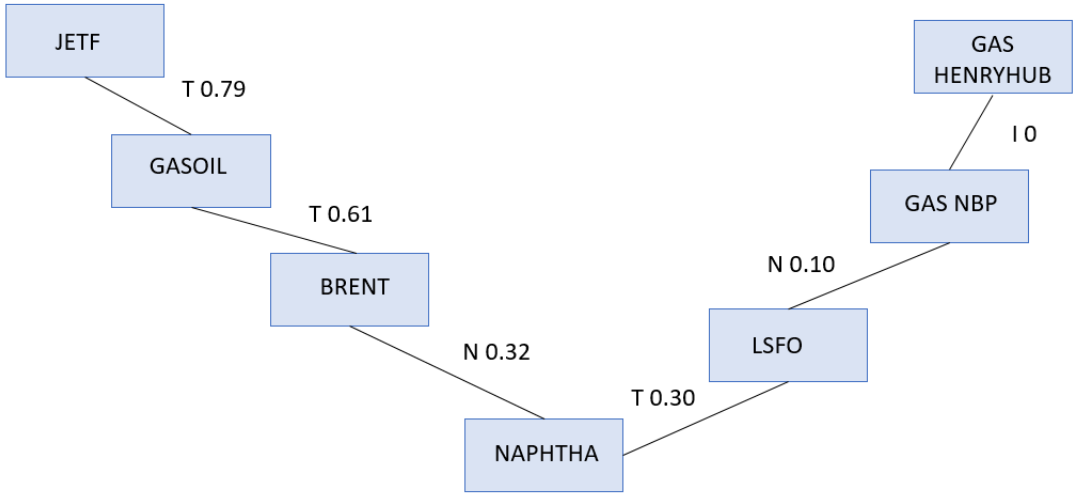

Figure 4.6: First tree of the D-vine with a 5% confidence level. The letters reported between the root nodes indicate the type of the bivariate copulas used to model the dependence, while the numbers refer to the corresponding Kendall's τ correlation.

$$M = \begin{pmatrix} 7 & & & & & & \\ 1 & 6 & & & & & \\ 2 & 1 & 5 & & & & \\ 3 & 2 & 1 & 4 & & & \\ 4 & 3 & 2 & 1 & 3 & & \\ 5 & 4 & 3 & 2 & 1 & 2 & \\ 6 & 5 & 4 & 3 & 2 & 1 & 1 \end{pmatrix}$$

$$T = \begin{pmatrix} 3 & & & & & & \\ 0 & 5 & & & & & \\ 0 & 0 & 1 & & & & \\ 0 & 0 & 2 & 0 & & & \\ 0 & 0 & 5 & 5 & 2 & & \\ 0 & 1 & 2 & 1 & 2 & 2 & \end{pmatrix}$$

The R-vine structure is reported in Fig. 4.7 and the respective specification matrix M and copula type matrix T are as follows.

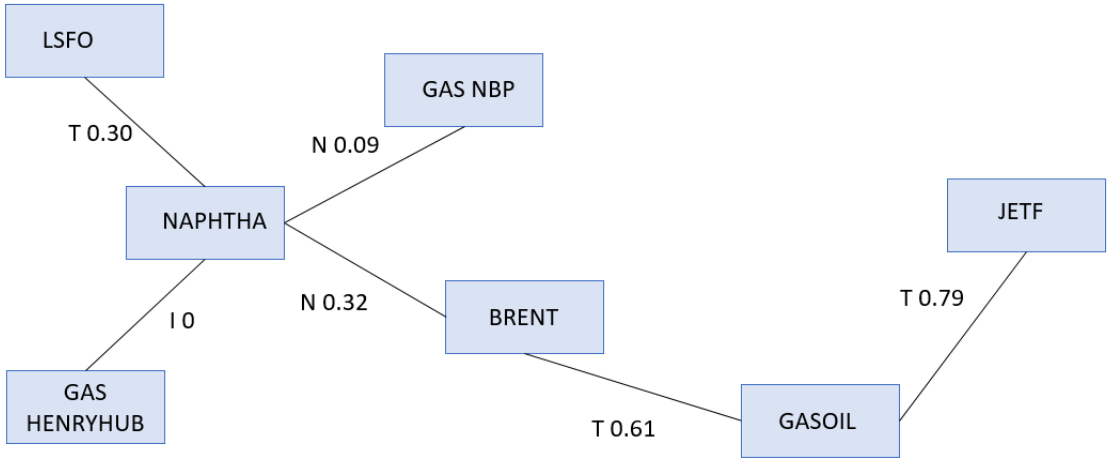

Figure 4.7: First tree of the R-vine with a 5% confidence level. The letters reported between the root nodes indicate the type of the bivariate copulas used to model the dependence, while the numbers refer to the corresponding Kendall's τ correlation.

$$M = \begin{pmatrix} 7 & & & & & & \\ 6 & 1 & & & & & \\ 5 & 6 & 2 & & & & \\ 1 & 5 & 6 & 3 & & & \\ 2 & 4 & 5 & 6 & 5 & & \\ 3 & 3 & 4 & 5 & 6 & 4 & \\ 4 & 2 & 3 & 4 & 4 & 6 & 6 \end{pmatrix}$$

$$T = \begin{pmatrix} 0 & & & & & & \\ 0 & 0 & & & & & \\ 0 & 0 & 0 & & & & \\ 0 & 1 & 0 & 0 & & & \\ 1 & 1 & 16 & 2 & 0 & & \\ 1 & 2 & 1 & 2 & 2 & 0 & \end{pmatrix}$$

The multivariate Gaussian copula is often used for modeling multivariate data, assuming linear dependence structure and no tail dependencies. The multivariate Student's t copula also assumes linear dependence, but accounts for tail dependence with the restriction of same tail heaviness within the distribution. We fit different multivariate Student's t copula by fixing 5, 10, 15 and 20 degrees of freedom (df). T-copulas families with 10, 15, and 20 df are not rejected at a 5% significance level. In the following, we consider the statistics of the 10 df Student's t copula whose p-value resulting from the multiplier goodness-of-fit (gof) test is equal to 28%.

Log-likelihood, AIC and BIC are statistics commonly used in the literature to compare different copula structures and determine their relative ranking (see, e.g., Schepsmeier (2016); Schepsmeier and Czado (2016)). The value of the log-likelihood of the estimated copula models is a gof measure, while AIC and BIC criteria are other comparison measures that take into account model complexity. The computation of these statistics for our models allows us to establish a preference for vine structures with respect to multivariate Gaussian and Student's t copulas (see Table 4.5). In particular among the vines, *C*-vine has the highest AIC, while *R*-vine is preferred in terms of BIC due to its lower number of parameters.

Table 4.5: Log-likelihood, AIC and BIC for the estimated copula models

	***C*-vine**	***D*-vine**	***R*-vine**	**Student's t**	**Gaussian**
Log-likelihood	1336	1321	1328	1218	1158
AIC	-2632	-2607	-2626	-2394	-2300
BIC	-2547	-2531	-2563	-2300	-2265

The comparison of the three T matrices of the considered vine structures provides additional information on tail dependence. More specifically, about 5-30% of the selected pair-copulas have either lower or upper tail dependence, i.e Clayton, Gumbel and Joe, while 20-25% have both upper and lower tail dependence modeled with a Student's t copula. Furthermore, tail dependence is non-negligible since the tail dependence coefficient calculated from the estimated pair-copula is on average greater than 0.2.
In conclusion, vine-copula structures are preferred according to the results of Table 4.5. Moreover, thanks to their flexibility, vine-copula structures can account for asymmetric estimated tail dependence. For all these reasons, we exclude the multivariate Gaussian and Student's t copulas from further analysis. As an additional step, we run the ECP and ECP2 gof tests on the three selected vine structures. These are non-parametric tests based on the Cramer-von Mises (CvM) and Kolmogorov-Smirnov (KS) test statistics (see Schepsmeier (2016) for more details on the tests).

The resulting p-values are reported in Table 4.6. None of the structures can be rejected at a 5% significance level, i.e all of them fit the data quite well. As suggested by Gaupp et al. (2017), future developments of improved goodness-of-fit tests are needed to help distinguishing between alternative structuring approaches. We also perform the likelihood ratio tests by Vuong (1989) and Clarke (2007) to select the structure that better accounts for the dependence among the assets. The results for each possible couple of vine structures are reported in Table 4.7 and Table 4.8, respectively. These show that, in almost all cases, no decision among the models is possible, i.e the null hypothesis that both models are statistically equivalent cannot be rejected. The only

Table 4.6: Goodness-of-fit test on C-vine, D-vine and R-vine with bootstrap repetition rate $x = 200$.

	ECP (CvM)	**ECP (KS)**	**ECP2 (CvM)**	**ECP2 (KS)**
***D*-vine**	p=0.49 ts=1.43	p=0.93 ts=0.61	p=1 ts=0.01	p=0.94 ts=0.61
***C*-vine**	p=0.42 ts=1.47	p=0.78 ts=0.68	p=1 ts=0.01	p=0.84 ts=0.68
***R*-vine**	p=0.33 ts=1.53	p=0.38 ts=4.91	p=1 ts=0.01	p=0.97 ts=0.50

Table 4.7: Vuong test results at level $\alpha = 5\%$

	Statistic	**Statistic Akaike**	**Statistic Schwarz**	**p-value**	**p-value Akaike**	**p-value Schwarz**
***D*-vine VS *C*-vine**	1.121	1.637	2.791	0.262	0.201	0.005
***R*-vine VS *C*-vine**	-1.094	-0.413	1.107	0.273	0.679	0.267
***R*-vine VS *D*-vine**	-1.641	-1.416	-0.911	0.100	0.156	0.361

exception is represented by the result of the Clark test where the R-vine is preferred to the C-vine.

4.4 The optimal composition of long-term natural gas contract

4.4.1 Optimization portfolio problems

In the following, we summarize the optimization portfolio problems that we solve to compute the optimal weights of each underlying asset of a LTC under the minimum portfolio risk. We consider five well-known risk measures that are represented by Variance, Mean Absolute Deviation (MAD), MiniMax, Conditional Value-at-Risk (CVaR), and Conditional Drawdown at Risk (CDaR). We simulate the portfolio returns based on the dependence structures specified in the C-vine, D-vine and R-vine models described above and estimate the risk of the seven-dimensional long-term natural gas contract.

Table 4.8: Clark test results

	Statistic	**Statistic Akaike**	**Statistic Schwarz**	**p-value**	**p-value Akaike**	**p-value Schwarz**
***D*-vine VS *C*-vine**	306	311	320	0.181	0.345	0.813
***R*-vine VS *C*-vine**	293	302	329	0.018	0.098	0.694
***R*-vine VS *D*-vine**	312	317	338	0.387	0.637	0.270

We assume to have M assets ($m = 1, ..., M$) and T time periods ($t = 1, ..., T$). Recall that, in our analysis, the assets are represented by the seven time series indicated in Section 4.3.1. More precisely, we denote with w_m the weights associated with each asset m of the portfolio; $r_{t,m}$ the return of each asset m in time period t; μ_m the average return of asset m that is $\mu_m = \frac{1}{T}\sum_{t=1}^{T} r_{t,m}$ and μ_p the portfolio target return. The mean variance (EV) nonlinear optimization problem (see Markowitz (1952)) is the following:

$$\min_{w} \frac{1}{T}\sum_{t=1}^{T}\left(\sum_{m=1}^{M} w_m(r_{t,m} - \mu_m)\right)^2 \tag{4.8a}$$

$$s.t. \tag{4.8b}$$

$$\sum_{m=1}^{M} w_m\mu_m = \mu_p \tag{4.8c}$$

$$\sum_{m=1}^{M} w_m = 1 \tag{4.8d}$$

$$w_m \geq 0 \quad \forall j = 1, \cdots, M. \tag{4.8e}$$

This optimization problem aims at minimizing portfolio variance (4.8a) under the portfolio target return (4.8c), assuming that the sum of the asset weights has to be equal to one (4.8d) and the non-negativity of weights w_m (4.8e).

We then consider the portfolio optimization model that is based on the MAD risk measure (see Konno et al. (1993)):

$$\min_{w} \frac{1}{T}\sum_{t=1}^{T}\left|\sum_{m=1}^{M}(r_{t,m} - \mu_m)w_m\right| \tag{4.9a}$$

$$s.t. \tag{4.9b}$$

$$\sum_{m=1}^{M} w_m\mu_m = \mu_p \tag{4.9c}$$

$$\sum_{m=1}^{M} w_m = 1 \tag{4.9d}$$

$$w_m \geq 0 \quad \forall m = 1, \cdots, M. \tag{4.9e}$$

Problem (4.9a)-(4.9e) can be transformed in the following linear optimization problem:

$$min_{w,y}\frac{1}{T}\sum_{t=1}^{T} y_t \tag{4.10a}$$

$$s.t. \tag{4.10b}$$

$$\left|\sum_{m=1}^{M}(r_{t,m}-\mu_m)w_m\right| \leq y_t \tag{4.10c}$$

$$\sum_{m=1}^{M} w_m\mu_m = \mu_p \tag{4.10d}$$

$$\sum_{m=1}^{M} w_m = 1 \tag{4.10e}$$

$$w_m \geq 0 \quad \forall m = 1, \cdots, M. \tag{4.10f}$$

The MiniMax model proposed by Young (1998) aims at maximizing the minimum return L_p, namely minimizing the maximum loss, defined as:

$$L_p = \min_t \left(\sum_{m=1}^{M} w_m r_{t,m}\right) \quad \forall t = 1, .., T.$$

On the basis of this assumption, the model is formulated as follows:

$$\max_{L_p,w} L_p \tag{4.11a}$$

$$s.t. \tag{4.11b}$$

$$\sum_{m=1}^{M} w_m r_{t,m} - L_p \geq 0 \quad \forall t = 1, .., T \tag{4.11c}$$

$$\sum_{m=1}^{M} w_m\mu_m = \mu_p \tag{4.11d}$$

$$\sum_{m=1}^{M} w_m = 1 \tag{4.11e}$$

$$w_m \geq 0 \quad \forall m = 1, \cdots, M. \tag{4.11f}$$

Following Rockafellar and Uryasev (2000), the portfolio optimization problem with respect to the CVaR measure can defined as follows:

$$\min_{w,d,v} \frac{1}{(1-\alpha)T}\sum_{t=1}^{T} d_t + v \tag{4.12a}$$

$$s.t. \tag{4.12b}$$

$$\sum_{m=1}^{M} w_m r_{t,m} + v \geq -d_t \quad \forall t = 1, .., T \tag{4.12c}$$

$$\sum_{m=1}^{M} w_m\mu_m = \mu_p \tag{4.12d}$$

$$\sum_{m=1}^{M} w_m = 1 \tag{4.12e}$$

$$w_m \geq 0 \quad \forall m = 1, \cdots, M \tag{4.12f}$$

$$d_t \geq 0 \quad \forall t = 1, \cdots, T. \tag{4.12g}$$

where v represents the VaR, $(1-\alpha)$ is the coverage rate and d_t is the deviation value below the VaR.

Following Chekhlov et al. (2005), the CDaR optimization problem is as follows:

$$\min_{w,u,v,z} \frac{1}{(1-\alpha)T} \sum_{t=1}^{T} z_t + v \tag{4.13a}$$

$$s.t. \tag{4.13b}$$

$$\sum_{m=1}^{M} w_m r_{t,m} + u_t - u_{t-1} \geq 0, \quad u_0 = 0 \quad \forall t = 1, .., T \tag{4.13c}$$

$$z_t - u_t + v \geq 0 \quad \forall t = 1, .., T \tag{4.13d}$$

$$\sum_{m=1}^{M} w_m \mu_m = \mu_p \tag{4.13e}$$

$$\sum_{m=1}^{M} w_m = 1 \cdots, M \tag{4.13f}$$

$$w_m \geq 0 \quad \forall m = 1, \cdots, M \tag{4.13g}$$

$$z_t \geq 0 \quad \forall t = 1, \cdots, T \tag{4.13h}$$

$$u_t \geq 0 \quad \forall t = 1, \cdots, T \tag{4.13i}$$

$$\tag{4.13j}$$

where z is an auxiliary vector of variables of the conditional drawdowns, u is the auxiliary vector of variables used to model the cumulative returns and v represents the Drawdown Risk at the quantile $(1-\alpha)$.

4.4.2 Results

In our analysis we combine pair-vine copula models and portfolio optimization methods to define the optimal allocation of the underlying assets of a LTC. The integration of the PCC into the portfolio optimization allows to capture the complete multivariate dependence risk structure across the considered assets. As mentioned in Section 4.3.2, the PCC exploits the relationship between the pair-copula family and the corresponding Kendall's τ to compute the correlations coefficients among the assets. This methodology does not constraint the returns to be normal, but it captures the asymme-

try and nonlinear dependence among the commodities. For each of five risk measures (EV, MAD, MiniMax, CVaR, and CDaR) we minimize the portfolio risk by fixing the same target return μ_p for the three structures. Tables 4.9, 4.10 and 4.11 report the optimal assets allocation for C-vine, D-vine and R-vine structures, respectively. These weights can be interpreted as the proportions to attribute to the different underlyings of LTC, according to the minimum risk optimal portfolio.

Table 4.9: Optimal weights for long-term natural gas portfolio C-vine

	EV	**MAD**	**MiniMax**	**CVaR**	**CDaR**
Brent	0.13	0.14	0.26	0.13	0.38
Gasoil	0.06		0.06		
JetF	0.11	0.17	0.07	0.17	0.62
Naphtha	0.17	0.16	0.12	0.18	
Lsfo	0.31	0.31	0.27	0.30	
Gas NBP	0.12	0.13	0.18	0.13	
Gas HenryHub	0.09	0.09	0.04	0.09	
Min Risk	0.01%	0.03%	0.12%	0.07%	5.32%

Table 4.10: Optimal weights for long-term natural gas portfolio D-vine

	EV	**MAD**	**MiniMax**	**CVaR**	**CDaR**
Brent	0.16	0.17	0.26	0.17	0.14
Gasoil	0.06				
JetF	0.11	0.17		0.18	
Naphtha	0.16	0.16		0.16	0.19
Lsfo	0.29	0.28	0.58	0.28	0.41
Gas NBP	0.13	0.14	0.16	0.13	0.19
Gas HenryHub	0.09	0.08		0.09	0.07
Min Risk	0.01%	0.03%	0.14%	0.07%	3.67%

The analysis of the optimal asset allocation shows that, in general, there is a convergence in the weight of the same asset within the same risk measure among the three structures. This is in line with the findings of Section 4.3.2, where it is shown that all the three structures are appropriate for modeling the considered series.
The combination of vine copula models with optimization methods leads to optimal portfolios with total risk close to zero.

By focusing on each risk measure, we analyze the optimal asset allocation in the three structures. We first observe that the optimal asset allocation in the three vine copula models is very similar when applying the EV, MAD, and CVaR risk measures (compare Tables 4.9-4.11). In addition, these three risk measures lead to optimal portfolios with equal risk when analyzing the same risk measure. There is also a

Table 4.11: Optimal weights for long-term natural gas portfolio R-vine

	EV	**MAD**	**MiniMax**	**CVaR**	**CDaR**
Brent	0.16	0.16	0.03	0.17	0.27
Gasoil	0.06				0.59
JetF	0.12	0.19		0.31	0.17
Naphtha	0.14	0.14	0.24	0.14	
Lsfo	0.31	0.29	0.26	0.29	
Gas NBP	0.13	0.13	0.04	0.14	0.01
Gas HenryHub	0.09	0.09	0.11	0.09	0.14
Min Risk	0.01%	0.03%	0.13%	0.07%	4.59%

similar portfolio composition when comparing the aforementioned three risk measures within the same vine structure. Starting from the EV, the resulting portfolio is the one with the minimum risk. All assets are considered with Lsfo constituting approximately 30% of the portfolio, followed by Naphtha, Brent and Gas NBP. Gasoil plays instead a marginal role. This is registered in all the three vine copula models considered. A similar composition results by applying MAD and CVaR risk measures to the three structures. Lsfo is still the asset with the highest weight followed by Jetf, Naphtha and Brent; Gasoil is not included among the optimal underlyings.

The application of MiniMax and CDaR risk measures generates divergences in the components of the optimal portfolio compared to what obtained with the EV, MAD, and CVaR risk measures. A similar behavior for these risk measures is also observed in Bekiros et al. (2015).

We recall that MiniMax considers the maximum loss in the portfolio, while CDaR takes into account a number of draw down events in the historical return distribution. Both measures are sensible to large losses occurring with low probability, which may differ in the simulated distributions of the three structures. The MiniMax portfolio includes Lsfo, Brent and Gas NBP with different weights in the three structures. In the CDaR portfolio, Brent is the only common underlying among the three structures that show also a significance difference in the total risk. Table 4.12 quantifies the impact of oil-based commodities and spot gases within the optimal portfolios using the information provided by Tables 4.9-4.11. In particular, the values denoted as "Oil-based commodities" are determined by summing up the optimal weights assigned to Brent, Gasoil, JetF, Naphtha, and Lsfo, while the terms "Spot Gases" results from the sum of the optimal weights of Gas NBP and Gas HenryHub.

It is worth noting that, when the EV, MAD and CVaR measures are applied, there is a perfect convergence in the composition of the optimal portfolios resulting from the three structures: 78% is constituted by oil-based commodities and the remaining 22% is represented by gas traded on spot markets. On the contrary, the MiniMax and CDaR

Table 4.12: Oil and gas composition of the optimal portfolios

Copula	Asset	EV	MAD	MiniMax	CVaR	CDaR
C-vine	Oil-based commodities	0.78	0.78	0.78	0.78	1.00
	Spot Gases	0.22	0.22	0.22	0.22	0.00
D-vine	Oil-based commodities	0.78	0.78	0.84	0.78	0.74
	Spot Gases	0.22	0.22	0.16	0.22	0.26
R-vine	Oil-based commodities	0.78	0.78	0.85	0.78	0.85
	Spot Gases	0.22	0.22	0.15	0.22	0.15

risk measures lead to optimal portfolios that differ in the three vine copula models, even though the oil-based underlyings still cover the larger share. This confirms the results discussed above.

A synthesis of the portfolio optimization indicates that oil-based commodities, such as Lsfo, Brent, Jetf, and Naphtha, appear to be fundamental picks in our asset allocation, together with the Gas NBP. This is an evidence of the important role still played by the oil-indexation in the LTCs. The influence of oil-based commodities in gas contracts is measured and included in our analysis through the pair-copulas. However, the choice of Gas NBP and Gas HenryHub gases, that together, on average, account for more that 20% of the optimal portfolio, reflects the fact that the re-negotiation policy advocated by mid-streamers in Europe is possible (see Franza (2014)).

4.5 Conclusions

This analysis takes inspiration from the current situation of the European natural gas market where both long-term contracts and hub spot price systems are applied. The fall of the European gas demand combined with the increase of the US shale gas exports and the rise of LNG availability on international markets have led to a reduction of the gas-hub prices in Europe. On the other side, oil-indexed LTCs failed to promptly adjust their positions implying significant losses for European gas mid-streamers that asked for a re-negotiation of their existing contracts and obtained new contracts linked also to hub spot prices. The debate over the necessity of the oil-indexed pricing is still on-going and the main issue is that in the early days of the European gas industry this was the only option to mitigate the risk of launching such a highly capital expensive industry. The supporters of the gas-indexation state that nowadays the gas industry is mature enough and for this reason hub-based pricing reflects the true supply and demand dynamics in natural gas market. This work investigates the risk dependence and the optimal resource allocation of the underlying assets of a LTC through pair-vine copulas and portfolio optimization methods with respect to five risk measures (EV,

MAD, MiniMax, CVaR, and CDaR). In order to address the above mentioned debate both spot gas and oil commodities are included as underlyings. The usage of the PCC allows modeling the conditional dependence structure, overcoming the drawbacks of the mean-variance Markowitz optimization, including normally distributed returns and linear correlation among the assets of the same portfolio. The results of our simulations suggest that the weight allocation across portfolios obtained by implementing different vine structures, in almost all cases, converge within the same risk measure. A general finding is that oil commodities still cover the largest share of the optimal portfolios, but spot gas are also included. This suggests that European LTCs will most likely remain indexed to oil-based commodities. In other words, both spot gas and oil-based commodities can be included among the underlyings of long-term gas contract, but the latter will still exercise a major impact. This is a crucial point because increasing the share of spot gas in LTCs would artificially make long-term prices closer to hub price levels. From an economic perspective, this can leave room to a spiral mechanism of downward price adjustment to hub prices that are, in turns, influenced by long-term contract prices.

Appendix

4.A Additional Figures

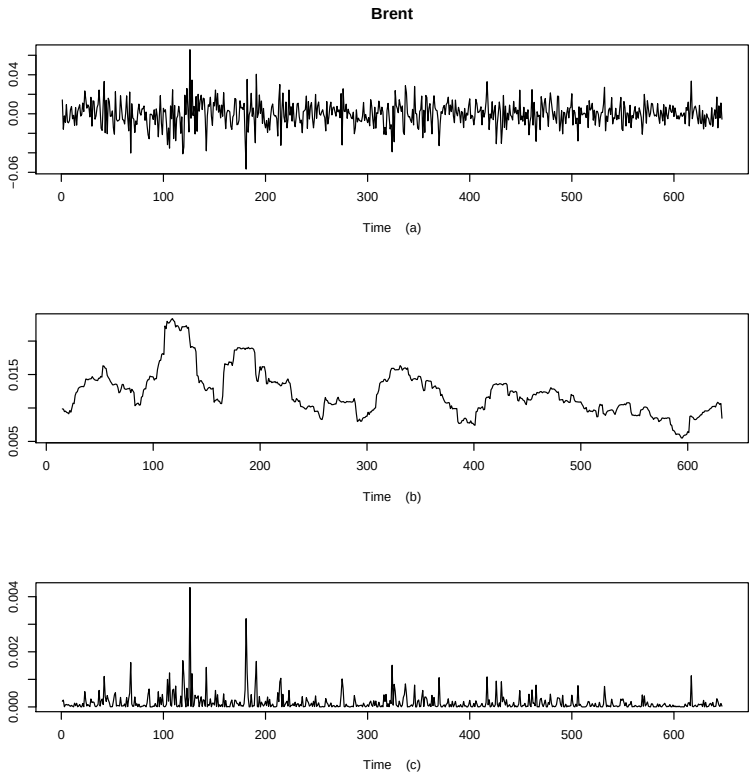

Figure 4.A.1: Log returns (a), 30-days horizon rolling standard deviation on log returns (b), and volatility (c) associated with the Brent series

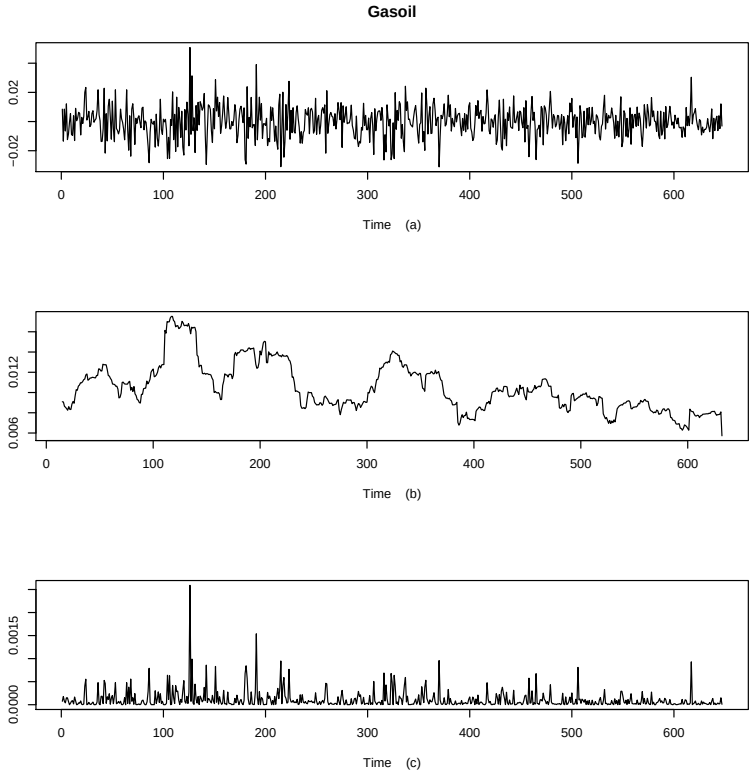

Figure 4.A.2: Log returns (a), 30-days horizon rolling standard deviation on log returns (b), and volatility (c) associated with the Gasoil series.

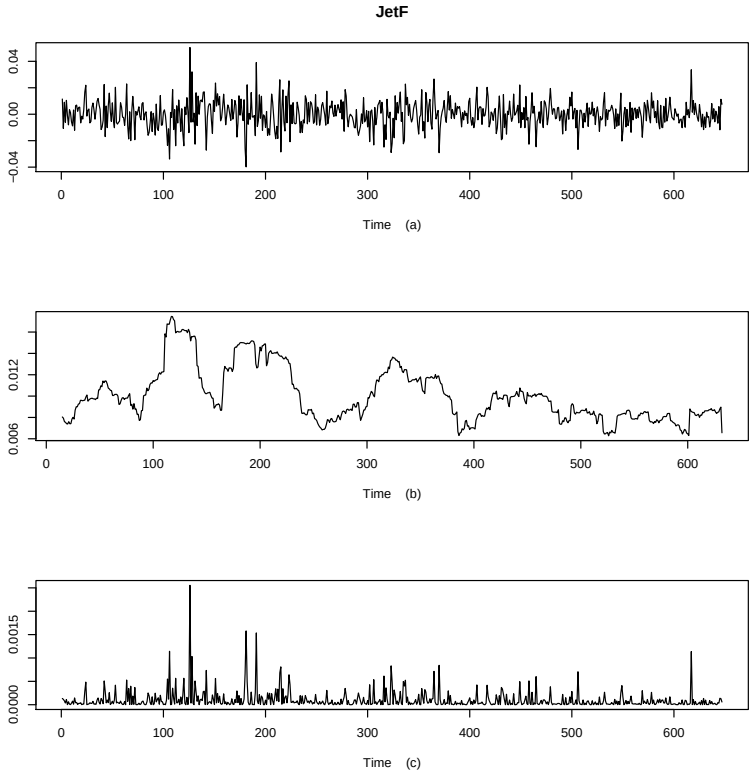

Figure 4.A.3: Log returns (a), 30-days horizon rolling standard deviation on log returns (b), and volatility (c) associated with the JetF series.

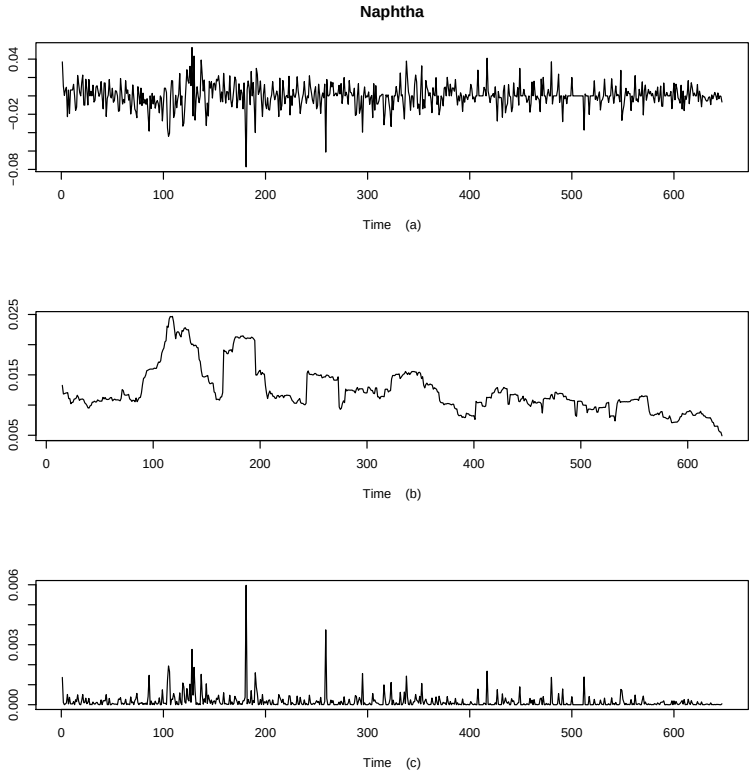

Figure 4.A.4: Log returns (a), 30-days horizon rolling standard deviation on log returns (b), and volatility (c) associated with the Naphtha series.

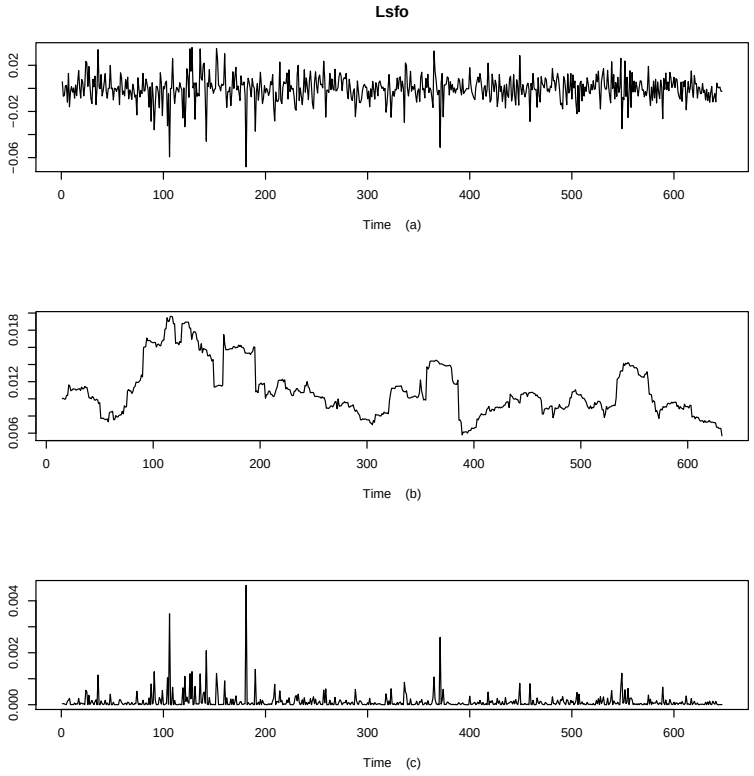

Figure 4.A.5: Log returns (a), 30-days horizon rolling standard deviation on log returns (b), and volatility (c) associated with the Lsfo series.

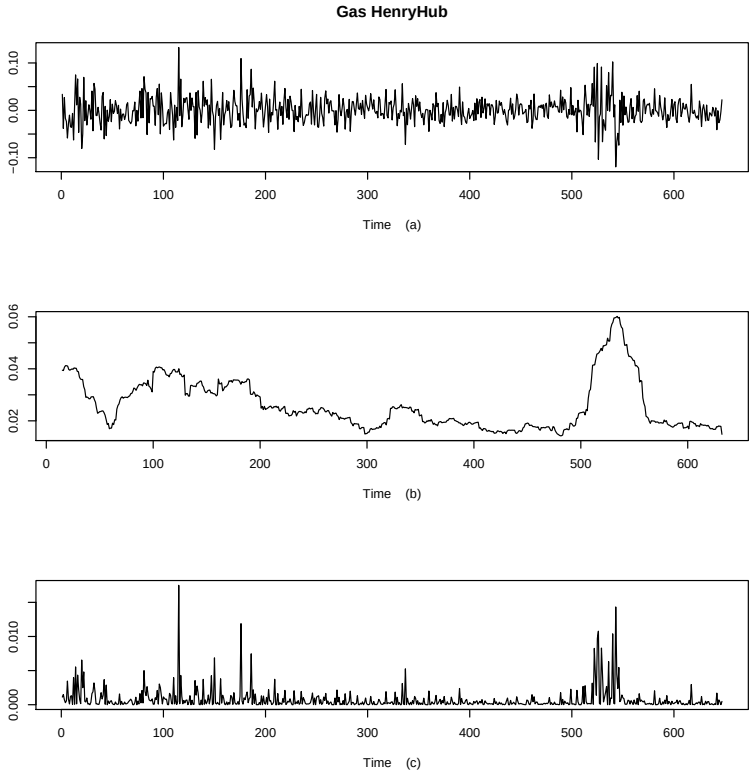

Figure 4.A.6: Log returns (a), 30-days horizon rolling standard deviation on log returns (b), and volatility (c) associated with the Gas HenryHub series.

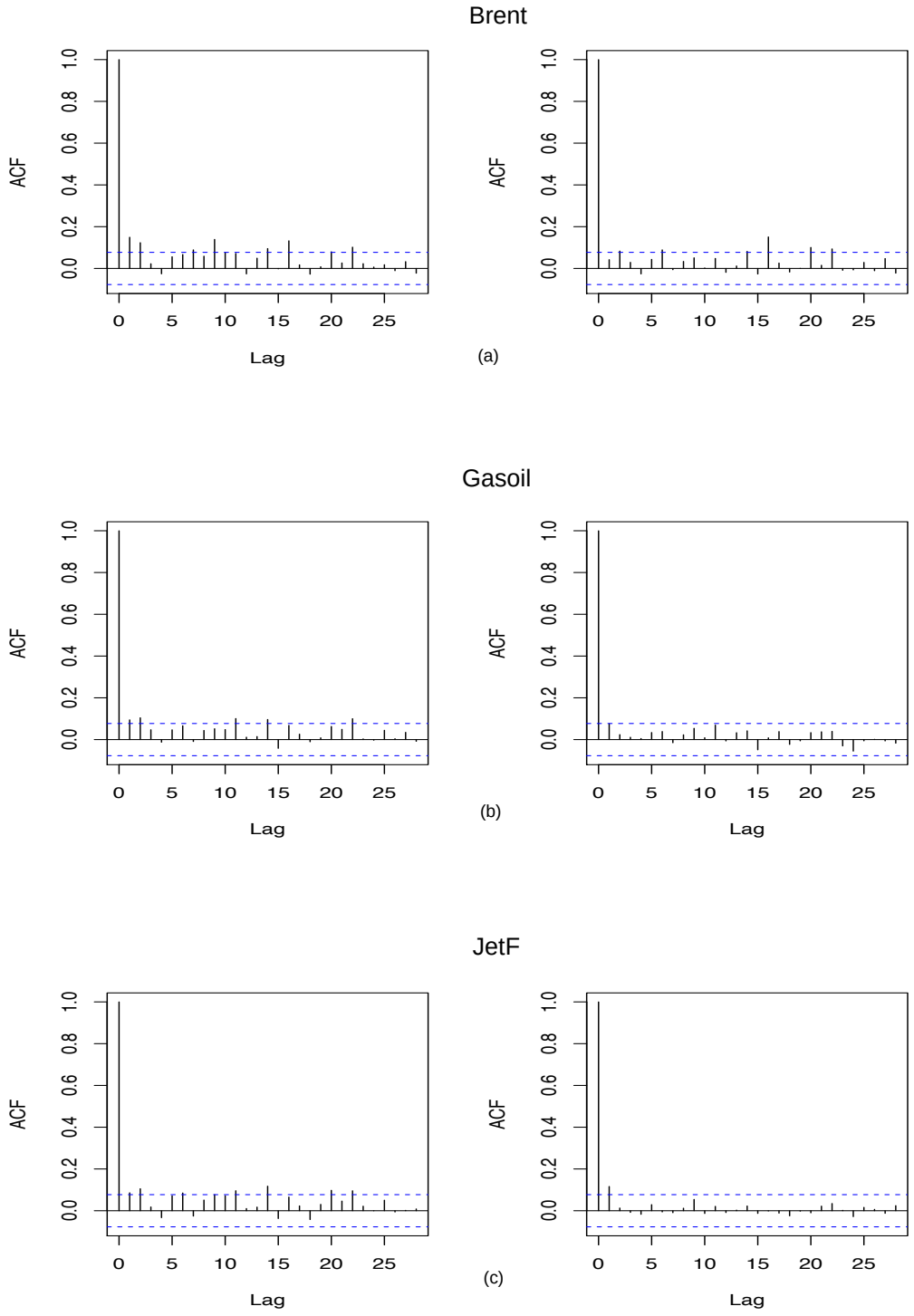

Figure 4.A.7: ACF of the squared mean adjusted log return series and ACF of the squared mean adjusted residuals of Brent (a), Gasoil (b), and JetF (c) log return series.

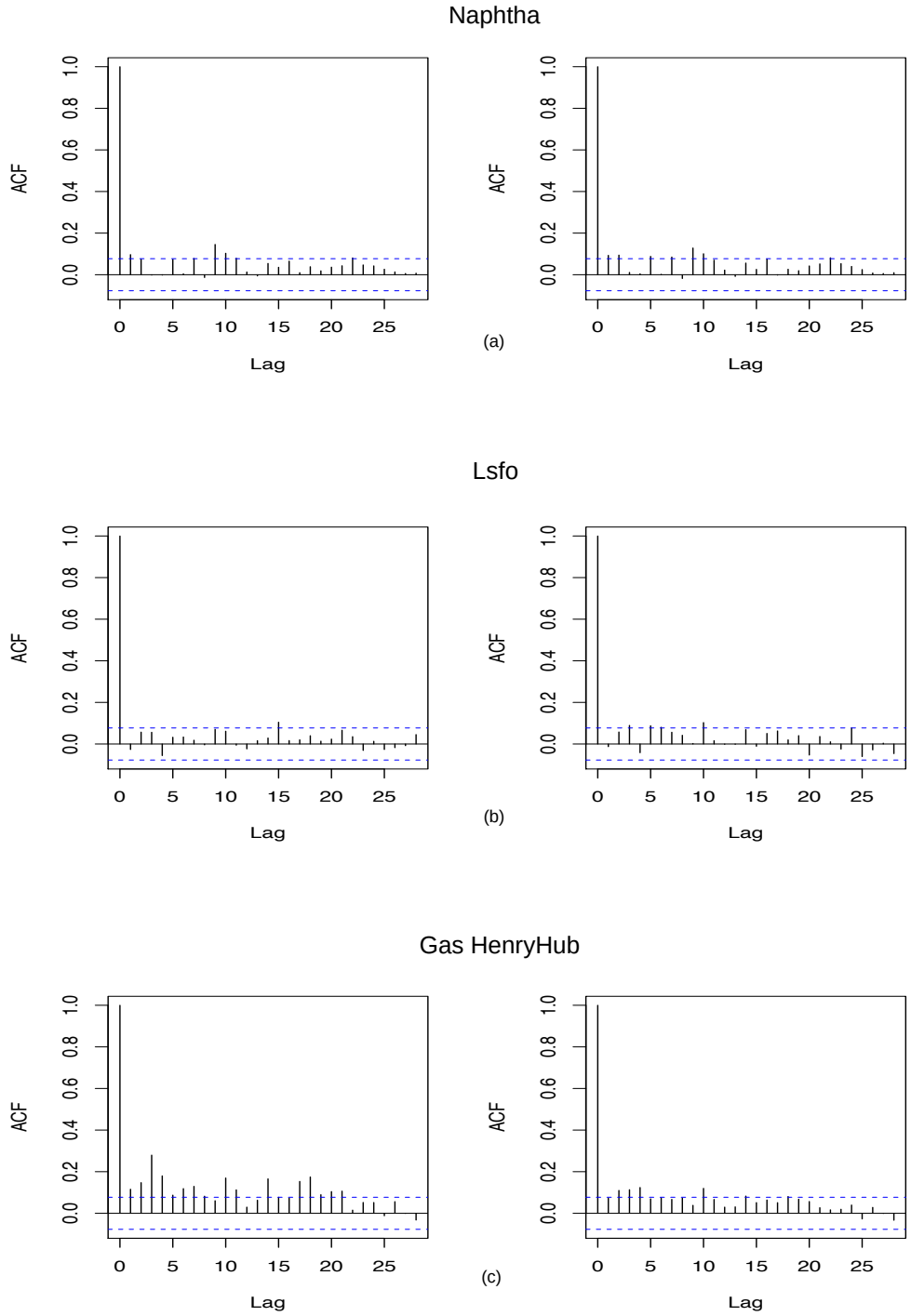

Figure 4.A.8: ACF of the squared mean adjusted log return series and ACF of the squared mean adjusted residuals of Naphtha (a), Lsfo (b), and Gas HenryHub (c) log return series.

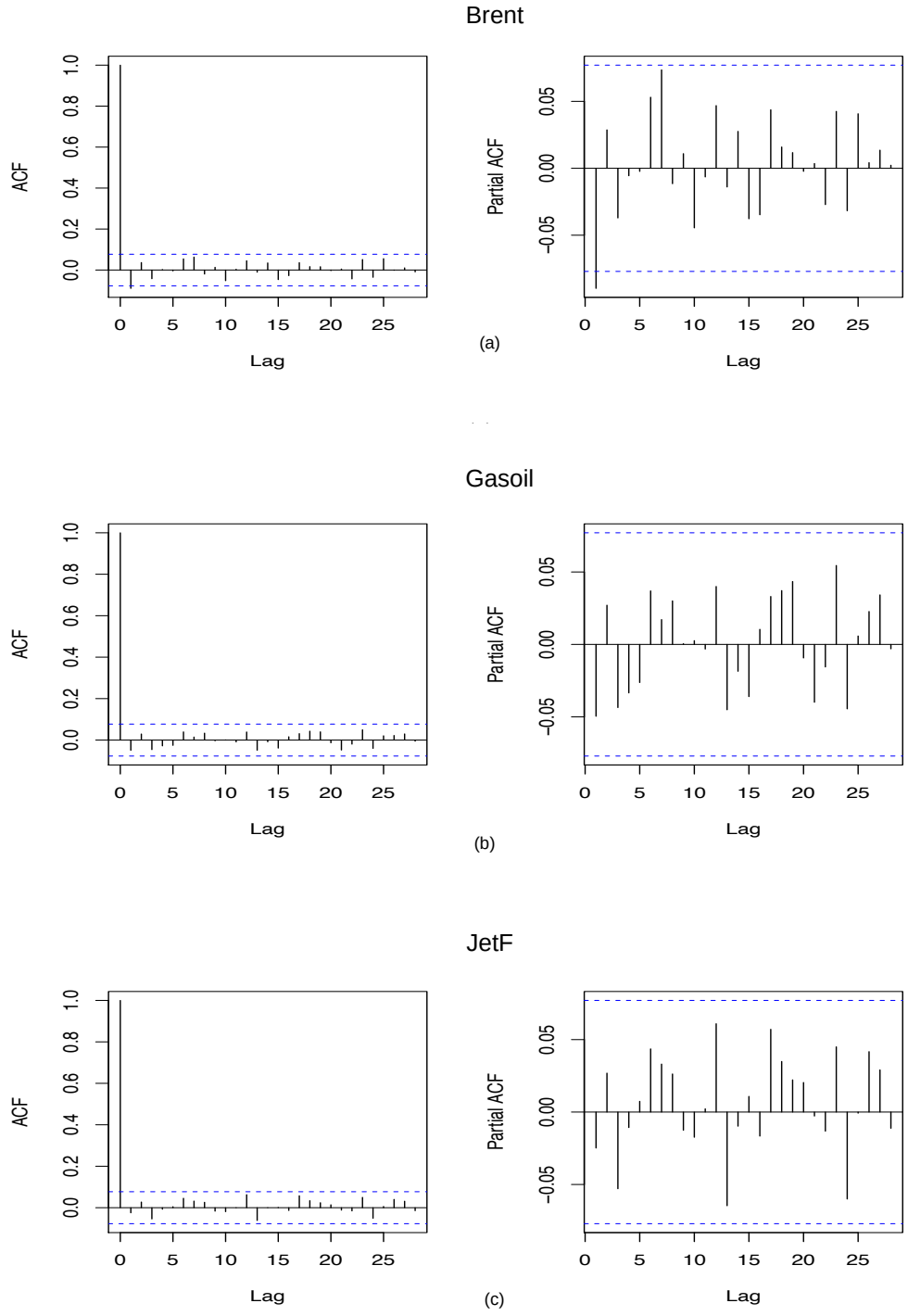

Figure 4.A.9: ACF and PACF of Brent (a), Gasoil (b), and JetF (c) log return series

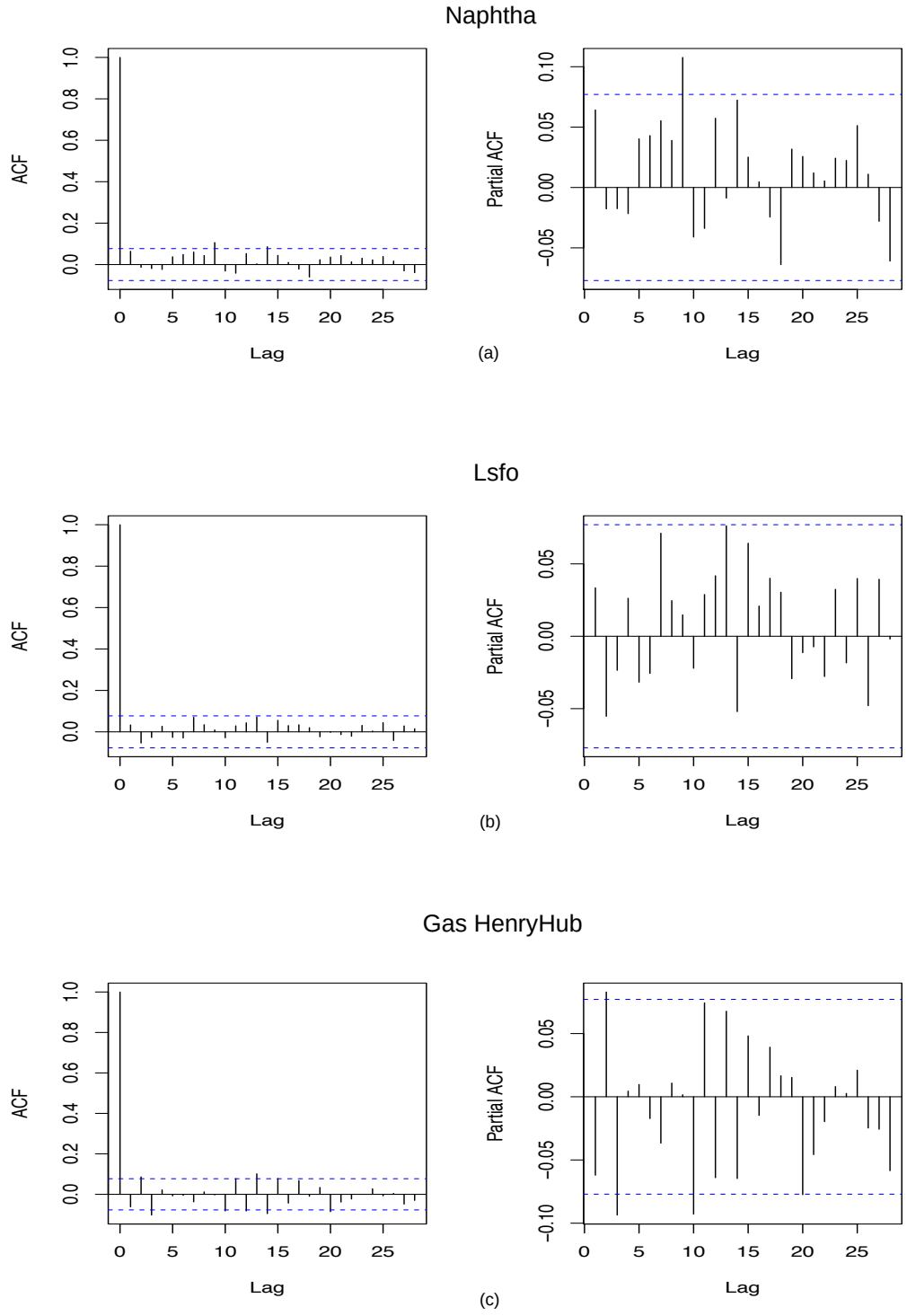

Figure 4.A.10: ACF and PACF of Naphtha (a), Lsfo (b), and Gas HenryHub (c) log return series.

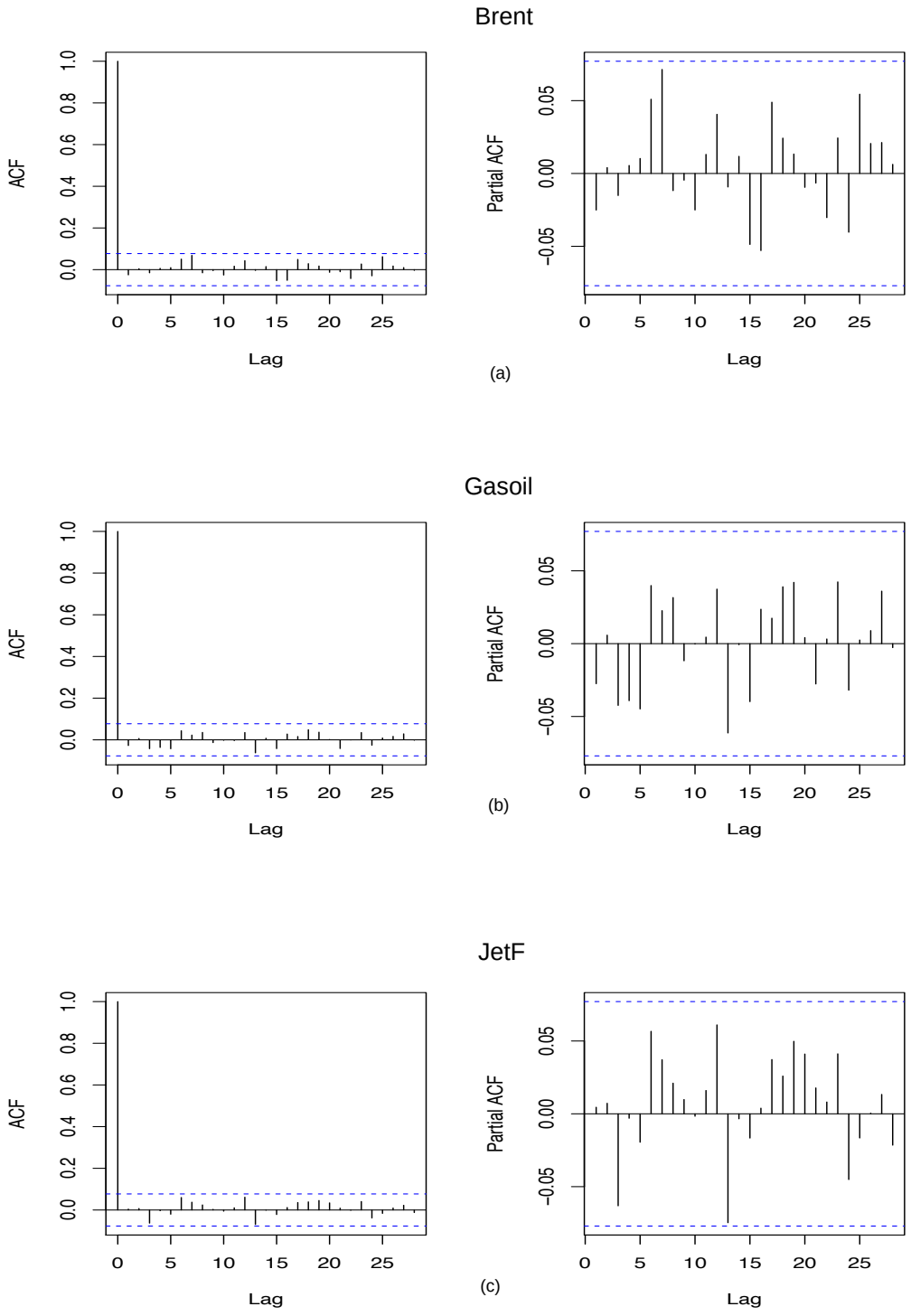

Figure 4.A.11: ACF and PACF of Brent (a), Gasoil (b), and JetF (c) residuals.

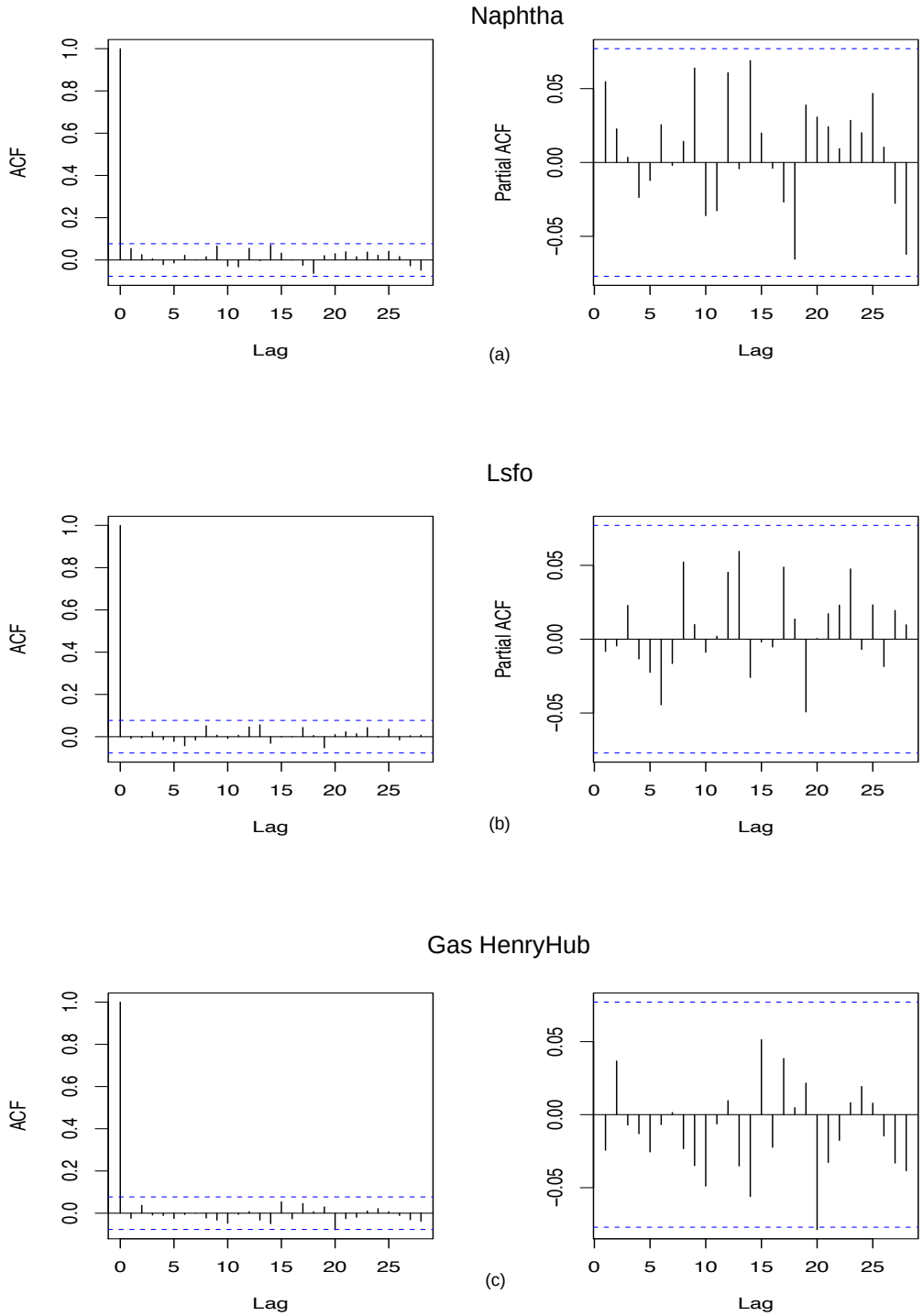

Figure 4.A.12: ACF and PACF of Naphtha (a), Lsfo (b), and Gas HenryHub (c) residuals.

Chapter 5

Evaluating the impacts of the external supply risk in a natural gas supply chain: the case of the Italian market

This chapter is based on the article:

Allevi E., L. Boffino L., M. E. De Giuli, G. Oggioni.
Evaluating the impacts of the external supply risk in a natural gas supply chain: the case of the Italian market

which has been published on the Journal of Global Optimization,
vol. 70, pp. 347-384. ISSN: 1573-2916.

A large part of the European natural gas imports originates from unstable regions exposed to the risk of supply failure due to economical and political reasons. This has increased the concerns on the security of supply in the European natural gas market.

In this chapter, we analyze the security of external supply of the Italian gas market that mainly relies on natural gas imports to cover its internal demand. To this aim, we develop an optimization problem that describes the equilibrium state of a gas supply chain where producers, mid-streamers, and final consumers exchange natural gas and Liquefied Natural Gas. Both long-term contracts (LTCs) and spot pricing systems are considered. Mid-streamers are assumed to be exposed to the external supply risk, which is estimated with indicators that we develop starting from those already existing in the literature. In addition, we investigate different degrees of mid-streamers' flexibility by comparing a situation where mid-streamers fully satisfy the LTC volume clause ("No FLEX" assumption) to a case where the fulfillment of this volume clause is not

compulsory ("FLEX" assumption).

Our analysis shows that, in the "No FLEX" case, mid-streamers do not significantly change their supplying choices even when the external supply risk is considered. Under this assumption, they face significant profit losses that, instead, disappear in the "FLEX" case when mid-streamers are more flexible and can modify their supply mix. However, the "FLEX" strategy limits the gas availability in the supply chain leading to a curtailment of the social welfare.

The model developed in this chapter have been implemented in GAMS and solved with PATH.

5.1 Introduction

Natural gas covers a significant quota of the energy mix of many of the European countries with a share of 24% in the Total Primary Energy Supply (see Holz et al. (2014)). Many of the European natural gas imports originate from unstable regions and suppliers exposed to the risk of supply failure due to political and economical instability. The political instabilities of Northern Mediterranean area and the disturbances between the European-Russian relationship in the last years have increased the concerns on security of supply in the European natural gas market. Italy is one of the three largest gas consumers in Europe after Germany and the United Kingdom,[1] but it mainly relies on natural gas imports to cover its internal demand since its national production is very low. In particular, the 90.6% of the Italian gas demand in 2015 was satisfied with imports from Russia, Algeria, Libya, the Netherlands, Qatar, and Norway (see AEEGSI (2016)).

Considering this framework, in this work we aim at analyzing the security of the external natural gas and Liquefied Natural Gas (LNG) supply (imports) of the Italian gas market. For this reason, we develop an optimization model that describes the equilibrium state of the natural gas supply chain where natural gas producers (suppliers), mid-streamers, and consumers can sell and buy both natural gas and LNG through long-term contracts (LTCs) or/and on spot market. Mid-streamers take on the role of intermediates in this supply chain network: on one side they exchange natural gas and LNG with supplying countries; on the other side they sell gas to final consumers. Since they are in charge of selecting the origin of natural gas and LNG imports, we assume that mid-streamers are the agent group exposed to the external supply risk associated with the imports from foreign countries. In other words, mid-streamers define the amount of gas and LNG to be imported not only on the basis of the relative pro-

[1] See Eurostat at http://ec.europa.eu/eurostat/statistics-explained/index.php/Natural_gas_consumption_statistics

duction and transportation costs, but also taking into account the external supply risk related to the countries from which the gas originates. This risk is evaluated through indicators that we develop starting from those already existing in the literature (see Section 5.3.2 for a literature review on these indicators). These risk indicators are then inserted in the optimization problem as a weight assigned to the Italian natural gas and LNG imports operated by mid-streamers.

Several works in the literature studies different aspects of the natural gas market. For instance, Egging and Gabriel (2006) develop a mixed complementarity model for the European natural gas market where producers can behave either in a perfectly competitive or in a Cournot strategic way, while the other players in storage and transmission services operate in perfect competition only. This model investigates the impacts of producers' market power and the importance of pipeline and storage capacity. Egging et al. (2008) propose a detailed complementarity model for defining the equilibrium of the European natural gas market under a set of scenarios, including the disruption of Ukrainian pipelines, the disruption of Algerian supplies, and the increased transportation costs. Market players are represented by producers, pipeline and storage operators, marketers, liquefiers and regasifiers, LNG tankers, and final consumers. Egging et al. (2010) present an extensive model of the global natural gas market that allows for the description of the flows and endogenous investment decisions in infrastructures and the evaluation of the market power in the pipeline and LNG markets. Holz et al. (2016) analyze the infrastructure needs of the European natural gas market to adequate it to the decarbonization targets of the European energy system. Their results show that the current import infrastructures and intra-European transit capacity are sufficient to accommodate future import needs under the scenarios of increasing and decreasing consumption. The authors conclude that the supply security would benefit from relaxing the political and technical constraints on investments. Egging and Holz (2016) develop a stochastic global gas market model to study the infrastructure investments and the trade in an imperfect market structure taking into account the possible disruption of the Russian gas transit via Ukraine from 2020; the variation of the electricity intensity generation in the OECD countries after 2025; the availability of the US shale gas after 2030.

All these papers analyze the possible supply disruption with a set of scenarios, operating a sensitivity analysis. In our work, we depart from this approach and we study the risk of external supply by directly integrating new risk indicators in our model. Our goal is to detect whether this risk affects the import choices of mid-streamers that can change not only their supplying country mix but also the type of gas purchased (i.e. they can favor gas to LNG or viceversa) and the payment method (i.e. LTCs vs. spot). To the best of our knowledge, it is the first time that such an

approach is considered and this represents one of the contributions of our work.

A second contribution of this is work is represented by the investigation of two different degrees of mid-streamers' flexibility. In particular, we compare a situation where the mid-streamers fully accomplish the LTC volume requirements with a case where the mid-streamers behave in a more flexible way and they are not obliged to purchase all the quantity of gas and LNG contracted with LTCs. We assume that this flexibility regards both the gas and the LNG bought through LTCs, with and without external supply risk. This analysis aims at describing the current configuration of the European gas market where the co-existence of LTCs and hub-pricing systems implies that the natural gas is traded at two different prices on the same market. Depending on the conditions, spot price can be higher or lower than long-term contractual gas, implying possibly difficult situations for companies loaded with high price TOP gas against the low spot prices. This is what happened in the last years, where an excess of gas availability on the market has been reflected into prices at the European hubs lower than those fixed in the LTCs. As a reaction, mid-streamers have asked for an increase of the LTCs flexibility (see Sections 5.2 and 3.5 for more details).

For our analysis, we consider a single optimization problem that is then transformed in complementarity form through the corresponding Karush-Kuhn-Tucker conditions (see Facchinei and Pang (2007); Gabriel et al. (2013); Nagurney (1999)). Complementarity-based models facilitate the formulation of equilibrium problems that describe the interactions of several agents whose choices are subject to technical and economic constraints, as it happens in our model.

The remainder of the chapter is organized as follows. Section 5.2 illustrates the natural gas supply chain that we consider in our analysis and we provide some insights related to mid-streamers' behaviour in the European gas market. Section 5.3 describes the new external supply risk indicators that we construct and the optimization models that we develop. The case study is presented in Section 5.4, while Section 5.5 presents the results of our analysis. Section 5.6 concludes with the final remarks.

5.2 The natural gas market

In this work, we aim at analyzing the interactions of the main players of a natural gas supply chain taking into account the external supply risk. The considered players are N supplying countries (producers), M mid-streamers, and S consumers. The latest two agents' groups are both located in the destination country that, in our case, is represented Italy (see 5.1).

We assume that gas can be sold/purchased either through long-term contracts

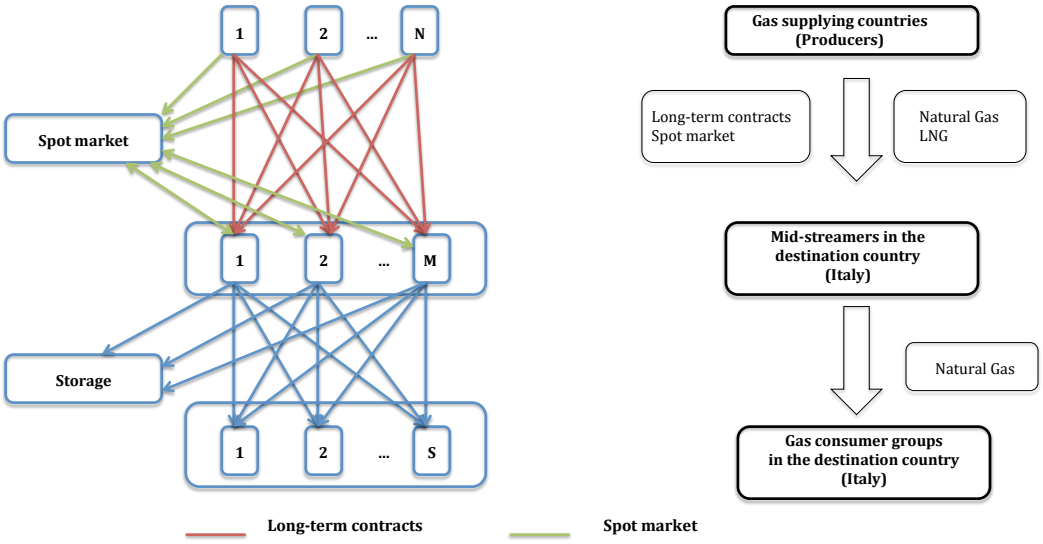

Figure 5.1: Natural gas supply chain

(LTCs) or on spot markets (hub pricing). This assumption aims at representing the current situation of the European gas market where LTCs and the hub pricing systems co-exist, even though it is still dominated by long-term contracts. The LTCs have been traditionally concluded over long periods (typically 20 years or more) and are characterized by quantity and price clauses that have been historically introduced to allow for risk sharing between gas producers and mid-streamers that respectively face price and volume risks (Abada et al. (2017)). The Take or Pay (TOP) quantity clause obligates the buyer to take a certain quantity of natural gas or to pay for it. The Price Indexation clause relates the price at which gas is bought to some index on the market that has been traditionally represented by the price of crude and oil-products. The hub pricing approach developed in the nineties in the US and UK and is now developing in Europe. In this system, natural gas is traded, every day, on a spot market that determines prices and volume on the short term. International natural gas market is organized in different ways depending on the considered areas. North America is essentially organized on the basis of Henry Hub spot market; Asia is mainly supplied through long-term contracts; Europe is still dominated by long-term contracts, even though spot markets are growing and are expected to develop further. The main exception in Europe is represented by the UK where gas is largely traded at the National Balancing Point (NBP) spot market. In continental Europe, Zeebrugge (ZEE) and the Title Transfer Facility (TTF), respectively located in Belgium and in the Netherlands, are the two dominant spot market places and many others are emerging such as the Punto di Scambio Virtuale (PSV) in Italy (see Melling (2010)).

The co-existence of two pricing systems in Europe implies that the natural gas is

traded at two different prices on the same market, causing possibly difficult situations for companies (mid-streamers) that are charged with high LTC prices against the low spot prices. This is what happened in the last years, where the combined effects of the increase of the US shale gas exports, the reduction of European gas demand due to the economic crisis, and the increased availability of uncommitted LNG from Qatar led to an excess of gas availability on the market that was reflected into low gas prices at the European hubs. On the other side, oil-indexed long-term gas contracts failed to promptly adjust their positions implying significant losses for European gas mid-streamers that were stuck with their LTCs and could only dump the excess of gas on the spot market. As a consequence of this short-term but dramatic issue, European mid-streamers have asked for a re-negotiation of their long-term gas contracts to make them more flexible and closer to spot gas prices. These re-negotiations have resulted into a decline of oil-indexation and hub-linked pricing has rapidly become the basis for an increasing number of transactions in the European gas market. In addition, with regard to newly signed contracts for pipeline sales to Europe, there is a clear trend towards shorter commitments (see Franza (2014)).

In addition to the external supply risk, this work aims at analyzing this structural problem of the gas industry by focusing on the short term and considering different degrees of flexibility of mid-streamers' behaviour. In particular, we compare the following two cases:

- **No flexibility**: In this case, we assume that the mid-streamer has to comply with all the LTCs that it already has. This corresponds to the situation where the mid-streamer has to buy at least the amount of natural gas and LNG already contracted. Under this assumption, they are also allowed to conclude new LTCs.

- **Flexibility**: This case aims at representing the current situation of the European gas market where LTCs and the hub pricing systems co-exist. In particular, we assume that the mid-streamer has the possibility to decide whether or not buying gas or LNG via LTCs. In other words, the mid-streamers is allowed to not respect the TOP clause for a short period (as the time framework that we consider).

As depicted in Fig. 5.1, in our model, we assume that supply countries produce gas and LNG that they directly sell to mid-streamer with LTCs or on the spot market. On the other side, mid-streamers can decide to buy gas and/or LNG from supplying countries through LTCs. They can also operate on the spot market by either buying and selling gas. On the other side, we assume that mid-streamers can only buy LNG on spot because according to GIIGNL (2018), Italy does not re-export the imported LNG. Mid-streamers are also in charge of managing the storage site in the destination

country. Finally, we consider three groups of consumers represented by industry, power generation, and residential/commercial.

5.3 Modeling the gas supply chain with external supply risk

In this section, we develop the optimization model used to describe the gas supply chain with producing countries, mid-streamers operating, and consumers located in the destination country. We consider a time span of one year, sub-divided into two time segments corresponding to a low-demand and high-demand periods. We start from the notation used in the mathematical formulation, we then describe the external supply risk indicators, and finally we present the optimization model.

5.3.1 Notation

Indices

- N: number of countries producing and supplying natural gas (producers/supplying countries), $n = 1, ..., N$;
- M: number of mid-streamers located in the destination country, $m = 1, ..., M$. In our model, we assume one destination country;
- F: number of natural gas entry points located in the destination country, $f = 1, ..., F$;
- S: number of consumption sectors in the destination country (industry, power generation, and residential/commercial) $s = 1, ..., S$;
- T: number of time periods, $t = 1, ..., T$. More precisely, we consider $T = 2$, where $t = 1$ is low-demand period and $t = 2$ is high-demand period.

Parameters:

- θ_t: duration in days of time periods t;
- $\bar{X}_n$: gas production capacity of producer n;
- $\bar{GP}_n$: capacity of gas pipeline connecting producing country n with the destination market where mid-streamers are located;
- $\bar{L}_n$: liquefaction capacity of producer n;
- $\bar{R}_m$: regasification capacity of mid-streamer m;

- $\bar{I}_m$: injection limit of storage site managed by mid-streamer m;
- $\bar{W}_m$: withdrawal limit of storage site managed by mid-streamer m;
- WG_m: working gas volume available at storage site managed by mid-streamer m;
- α_n: rate of liquefaction loss faced by producer n;
- β_m: rate of regasification loss faced by mid-streamer m;
- stc_{nm}^{LNG}: transportation costs of LNG through ship from the producing country n to the destination market where mid-streamers m are located;
- ptc_{nm}^{G}: transportation costs of gas through pipelines from the producing country n to the destination market where mid-streamers m are located;
- ptc_{n}^{SpotG}: pipeline transportation costs of gas sold on spot faced by the producing country n;
- dc_{ms}: gas distribution costs through pipelines faced by mid-streamer m to supply consumer s;
- τ_{nm}: (minimum) annual amount of gas that producer n supplies to mid-streamer m through long-term contracts;
- ξ_{nm}: (minimum) annual amount of LNG that producer n supplies to mid-streamer m through long-term contracts;
- Υ_{ft}: limit of the pipeline entry point f in the destination country in time period t;
- Γ_{fn}: limit of the pipeline entry point f that receives gas from producing country n in time period t.

Variables

- X_{nt}^{G}: total amount of natural gas produced by supplying country n in one day of time period t (mcm/d).
- x_{nmt}^{G}: amount of natural gas supplied by producer n through long-term contracts (LTCs) to mid-streamer m in one day of time period t (mcm/d).
- X_{nt}^{LNG}: total amount of natural gas transformed in LNG by supplying country n in one day of time period t (mcm/d).
- x_{nmt}^{LNG}: amount of LNG supplied by producer n through long-term contracts (LTCs) to mid-streamer m in one day of time period t (mcm/d).
- x_{nt}^{SpotG}: amount of natural gas sold by producer n on spot market in one day of time period t (mcm/d).

- $x_{nmt}^{SpotLNG}$: amount of LNG sold by producer n to mid-streamer m on spot basis in one day of time period t (mcm/d).
- Y_{mt}^{LNG}: total amount of natural gas re-gasified by mid-streamer m in one day of time period t (mcm/d).
- y_{nmt}^{LNG}: amount of LNG purchased by mid-streamer m through LTC from producer n in one day of time period t (mcm/d).
- y_{mt}^{SpotG}: amount of natural gas purchased by mid-streamer m on spot market in one day of time period t (mcm/d).
- $y_{nmt}^{SpotLNG}$: amount of LNG purchased by mid-streamer m from producer n on spot basis in one day of time period t (mcm/d).
- q_{mt}^{SpotG}: amount of natural gas sold by mid-streamer m on spot market in one day of time period t (mcm/d).
- z_{mst}: nonnegative amount of natural gas that mid-streamer m sells to consumer sector s in one day of time period t in Bcm.
- i_{mt}: nonnegative amount of natural gas injected by mid-streamer m in the storage site in one day of time period $t = 1$ in Bcm.
- w_{mt}: nonnegative amount of natural gas withdrawn by mid-streamer m from the storage site in one day of time period $t = 2$ in Bcm.
- d_{st}: nonnegative amount of natural gas demanded by consumer s in one day of time period t in Bcm.
- $P_{st}(d_{st})$: Inverse demand function of consumer s in one day of time period t in Bcm. This function can be stated as $P_{st}(d_{st}) = a_{st} - b_{st} \cdot d_{st}$ where a_{st} is the intercept of consumers' (affine) demand functions in time period t (€/Bcm) and b_{st} is the slope of consumers' (affine) demand functions in time period t (€/Bcm^2).

All these variables are assumed to be nonnegative. As already indicated, we consider a time span of one year subdivided into low-demand and high-demand periods with a duration in days θ_t, respectively. For each of these two periods, we consider a representative day and, therefore, variables and parameters have to be weighted by the duration θ_t in order to get annual values. Finally, we do not list here the dual variables associated with the constraints appearing in our model formulation. These are directly indicated next to the constraints to which they refer.

5.3.2 External supply risk indicators

Energy security is defined as the availability of a regular supply of energy at an affordable price (see IEA/OECD (2001)). Security of gas supply in energy systems has always been an important issue due to the high dependence on energy. This is particularly true for Europe where about one quarter of all the energy used is natural gas, and many European countries import nearly all their supplies, as it happens for Italy. Supply disruptions caused by infrastructure failure or political disputes are real phenomena. As an example, we recall the the severe shortfall of gas in Western Europe due to Russia's decision to suspend gas deliveries to Ukraine in January 2009. A way to deal with energy security is a process of managing the associated risk. For this reason, in our analysis, we concentrate on short-term indices to assess the risk associated with external energy supply and possible insecurity of supply. The Herfindahl-Hirschman Index (HHI), the Shannon-Wiener Index (SWI), and the variations of it, such as the Shannon-Wiener-Neumann indeces (SWNIs) are amongst the most commonly used aggregate indicators for energy security applied to evaluate the diversification of the market (see Neumann (2004)).

The HHI is adopted as a measure of market concentration, namely the total number of companies operating. In a similar way, the diversity of energy suppliers is given by the sum of the squares of each supplier market share q_n:

$$HHI = \sum_{n=1}^{N} q_n^2 \tag{5.1}$$

where q_n represents the share of imports from a particular country n into the country considered. Thus, the higher the value of the index, the more concentrated the market is; the maximum value of the index is achieved when there is only one supplier. Consequently, the HHI is only used to investigate markets with a lack of diversity of suppliers, or to give greater weight to the larger suppliers (see e.g. Blyth and Lefevre (2004); Cohen et al. (2011); Grubb et al. (2006); Gupta (2008); Kruyt et al. (2009); Frondel and Schmidt (2008)).

The Shannon-Wiener concentration Index is an alternative approach to measure the diversity of energy suppliers. This index is computed as follows:

$$SWI = -\sum_{n=1}^{N} q_n \ln q_n \tag{5.2}$$

where q_n is the supplier's market share as in the HHI. The higher the value of the index, the more diverse the market is. Moreover, differently from the HHI, it puts more weights on the impact of smaller suppliers (see Kruyt et al. (2009), footnote 13,

for more details on the mathematical properties of the SWI).

However, the security of external energy supply may be affected by the political situation in the exporting country. Starting from the SWI, Neumann (2004) takes this into account by using a measure of the political stability of the supplier n that we denote with r_n. In particular, Neumann (2004) proposes two additional indicators SWNI_1 and SWNI_2 that are defined as follows:

$$SWNI_1 = -\sum_{n=1}^{N}(r_n q_n \ln q_n), \tag{5.3}$$

and:

$$SWNI_2 = -\sum_{n=1}^{N}(r_n q_n \ln q_n)(1+g_n), \tag{5.4}$$

where r_n identifies the political risk rating associated with the supplying country n and g_n in the SWNI_2 represents the indigenous production of the resource in the supplying country n.

On the other side, Quemada et al. (2012) propose the Geopolitical Energy Security (GES) indicator that is computed as:

$$GES = \sum_{f=1}^{F}\left[\left(\sum_{n=1}^{N} r_n q_{nf}^2\right)\cdot e^{\frac{1}{P_f}}\right]\cdot\frac{C_f}{TPES} \tag{5.5}$$

where the index f represents the fuel type, and the ratio $\frac{\text{C}_\text{f}}{\text{TPES}}$ denotes the share of total consumption of fuel f in the Total Primary Energy Supply (TPES). The GES indicator combines a country exposure measure of market concentration q_{nf}^2, similarly to the HHI, with the market liquidity, involving as a key role the exponential function e^{1/P_f} where P_f represents the ratio between the offer of the resource f and its consumption. The GES indicator is an expansion of the $\text{ESI}_{\text{price}}$ index that does not consider the market liquidity, i.e. the exponential function (see IEA (2007)).

Le Coq and Paltseva (2009) develops the Risky External Energy Supply (REES) for each destination country a that is defined as follows:

$$REES_a^f = \left[\sum_{n=1}^{N}\left(\frac{NPI_{na}^f}{NPI_a^f}\right)^2 F_{na}^f r_n d_{na}\right]\cdot NID_a^f \cdot SF_a^f \tag{5.6}$$

where NPI_{na}^f is the net positive imports of fuel f from supplying country n to the destination country a, NPI_a^f is the sum of the net positive imports over all suppliers of country a, F_{na}^f is the fungibility of fuels f imported from n to a, r_n is the political risk index of the supplier country, d_{na} is a measure of a distance between countries n and a,

NID_a^f is the net import dependency of country a for fuel f and SF_a^f is a share of fuel f in country a (see Le Coq and Paltseva (2009)).[2] The REES is the most comprenhesive among the indicators here illustrated, since it accounts for the diversification of the energy sources f, the political risk r_n, the distance between supplying and destination country d_{na}, and the fungibility F_{na}^f of imported fuels, in addition to the diversification of suppliers and the energy dependence. Note that the distance d_{na} represents a proxy for the risk involved in the transportation phase. On the other side, the market liquidity is a feature of the GES indicator.

Our analysis aims at measuring the effects of the external supply risk on the natural gas and LNG exchanges between producing and supplying countries n and mid-streamers m all operating in same destination country. In this framework, we assume that mid-streamer selects the supply countries from which importing natural gas and LNG on the basis of external supply risk of these producing countries. Our idea is to consider the external supply risk as an additional cost that the mid-streamers face when buy both natural gas LNG from the different supplying countries. This cost is indeed proportional to the amount of gas bought and therefore, in our model formulation, we weight each exchange of natural gas and LNG between the producers and the mid-streamers by the associated external supply risk that varies according to the considered supplying country. We are therefore interested in evaluating a risk per each type of natural gas imported and per each supplying country. The indicators presented above aggregated all this information that we, instead, need in a disaggregated form.

For this reason, we consider the HHI, the SWNI_2, the GES, and the REES presented above and we modify them in order to make them suitable for our scope. In this way, we develop new indicators that are all denoted as "Π". For their construction, we account for two fuels, natural gas (G) and LNG ($f = G, LNG$ considering the GES and the REES indicators) and one destination country (this means that, using the REES notation, $a = 1$). This latter assumption implies that mid-streamers face an identical external supply risk when importing the same type of gas from the same country.

The new indicators that we introduce are:

1.
$$\Pi_{nm}^{HHI,G} = (q_{nm}^G)^2 \quad \text{and} \quad \Pi_{nm}^{HHI,LNG} = (q_{nm}^{LNG})^2, \tag{5.7}$$

These are a transformation of the HHI where q_{nm}^G and q_{nm}^{LNG} represents the share of imports of mid-streamer m from a particular country n respectively for natural gas and LNG. For the reasons explained above, we do not consider the sum over all supplying countries.

[2]Note that all the other indicators presented above are computed per each destination country even though not explicitly indicated.

2.

$$\Pi_{nm}^{SWNI_2,G} = -(r_n q_{nm}^G \ln q_{nm}^G)(1+g_n), \tag{5.8}$$

$$\Pi_{nm}^{SWNI_2,LNG} = -(r_n q_{nm}^{LNG} \ln q_{nm}^{LNG})(1+g_n), \tag{5.9}$$

These are similar to the SWNI_2, but, as in the $\Pi_{nm}^{HHI,\,G}$ and $\Pi_{nm}^{HHI,\,LNG}$, are computed taking into account the share of natural gas and LNG that country n supplies to mid-streamer m, without considering the sum over all supplying countries. The other terms r_n and g_n are as in the $SWNI_2$ indicator.

3.

$$\Pi_{nm}^{GES,G} = \left[\left(r_n (q_{nm}^G)^2\right) \cdot e^{\frac{1}{P_G}}\right] \cdot \frac{C_G}{TPES}, \tag{5.10}$$

$$\Pi_{nm}^{GES,LNG} = \left[\left(r_n (q_{nm}^{LNG})^2\right) \cdot e^{\frac{1}{P_{LNG}}}\right] \cdot \frac{C_{LNG}}{TPES}, \tag{5.11}$$

These result from the modification of the GES indicator, where we consider the share of natural gas and LNG imported by the mid-streamer m from country n, without operating the sum overall supplying countries. In addition, we maintain separate the two fuels supplied. The other terms are as in the GES indicator.

4.

$$\Pi_{nm}^{REES,G} = \pi_{nm}^G \cdot r_n \cdot d_{nm} \cdot F_{nm}^G, \tag{5.12}$$

$$\Pi_{nm}^{REES,LNG} = \pi_{nm}^{LNG} \cdot r_n \cdot d_{nm} \cdot F_{nm}^{LNG} \tag{5.13}$$

where, as in the REES indicator, r_n is the measure of political risk, d_{nm} is a factor that accounts for the distance between the capitals of the producing country and the location of mid-streamers, F_{nm}^G and F_{nm}^{LNG} are the fungibility respectively of natural gas and LNG, and π_{nm}^G and π_{nm}^{LNG} are the shares of natural gas and LNG that mid-streamer m in the destination country imports from supplying country n. These shares are computed as indicated below:

$$\pi_{nm}^{G} = \left(\frac{\tilde{q}_{nm}^{G}}{\sum_{n=1}^{N} \tilde{q}_{nm}^{G}} \right)^2$$

$$\pi_{nm}^{LNG} = \left(\frac{\tilde{q}_{nm}^{LNG}}{\sum_{n=1}^{N} \tilde{q}_{nm}^{LNG}} \right)^2$$

where $\tilde{q}_{nm}^{G}$ and $\tilde{q}_{nm}^{LNG}$ are parameters defining the *net* gas and LNG imports of mid-streamer m from the supplying country n.

Table 5.1 summarizes the indicators already existing in the literature, which we have present above, and the new indicators that we introduce starting from them.

Table 5.1: Summary of the new indicators proposed

Indicators existing in the literature	**New indicators proposed**	
HHI	$\Pi_{nm}^{HHI,G}$	$\Pi_{nm}^{HHI,LNG}$
$SWNI_2$	$\Pi_{nm}^{SWNI_2,G}$	$\Pi_{nm}^{SWNI_2,LNG}$
GES	$\Pi_{nm}^{GES,G}$	$\Pi_{nm}^{GES,LNG}$
REES	$\Pi_{nm}^{REES,G}$	$\Pi_{nm}^{REES,LNG}$

Finally, note that in Section 5.3.4, we generally refer to these new indicators with the symbols Π_{nm}^{G} and Π_{nm}^{LNG}. In Section 5.5, we show the effects of the application of all these indicators that we have constructed.

5.3.3 Model assumptions

In this section, we illustrate the main assumptions that characterize our model formulation.

- **Producing/supplying countries**. In the considered gas supply chain, supplying countries produce natural gas and/or LNG and can decide to sell them directly to mid-streamers with LTCs or on the spot market. We assume that gas is extracted from sites directly owned by producers. The extraction process is supposed to be lossless. Therefore, the amount of gas extracted corresponds to the one produced. As indicated in the nomenclature, the variables x_{nmt}^{G} and x_{nmt}^{LNG} identify the amount of natural gas x_{nmt}^{G} and LNG x_{nmt}^{LNG} that the production country n sells to mid-streamer m in the low- and in the high-demand periods, respectively. We assume that these quantities as well as their relative prices depend on time to account for possible renegotiation or updates of the contract price in short term (see Franza (2014)). The quantity of natural gas sold on

the spot market x_{nt}^{SpotG} depends on the production country n and on the time period t only. This assumption reflects the fact that the producer participates to the spot market by submitting bids but without knowing who will be the buyer. Finally, the quantity of LNG sold on spot basis $x_{nmt}^{SpotLNG}$ refers to uncommitted ships that are already arrived in the destination country and can be traded in the short term between the supplying country n and the mid-streamer m.

- **Destination country**. It is assumed that there is just one destination country that corresponds to Italy (see Section 5.4).

- **Mid-streamers**. We assume that all mid-streamers operate in the considered destination country and are located in one citygate. As already indicated, mid-streamers can decide to either enter in gas/LNG LTCs with supply countries or exchange gas/buy LNG on the corresponding spot markets. They select the supply countries from which importing natural gas and LNG on the basis of their external supply risks. As final step, they sell gas to the consumption sectors that we classify into power generation, industrial sector, and residential/commercial. In addition, we assume that mid-streamers operate the storage sites and can take advantage of seasonal arbitrage by buying and injecting gas into storage in the low-demand season (summer) and then selling it to consumers in the high-demand season (winter). Parallel to the modeling of the producers' variables, we assume that the variables y_{nmt}^{G} and y_{nmt}^{LNG} respectively identify the amount of natural gas y_{nmt}^{G} and LNG y_{nmt}^{LNG} that the mid-streamer m buy from producing country n with LTCs in the two time periods. We further assume that mid-streamer can both buy and sell natural gas on the spot market. These mid-streamer's actions are identified by the variables y_{mt}^{SpotG} and q_{mt}^{SpotG}, respectively. Note that these variables depend on the mid-streamer m on the time period t only. This assumption reflects the fact that the mid-streamer participates with bids/offers to the spot market without knowing who will be the counterparts. Finally, the quantity of LNG purchased on spot basis $y_{nmt}^{SpotLNG}$ refers to uncommitted ships that can be traded in the short term between the n supplying and the m importing countries. As already explained, we do not model the mid-streamer's opportunity to re-sell the LNG acquired on the spot basis.

- **Consumers**. We assume that the gas demands of three consumer groups (industry, power generation, and residential/commercial) are endogenously determined through inverse demand functions. The variable d_{st} denotes the quantity of natural gas required by consumer s in time t.

- **Time framework and LTCs**. We consider a time framework of one year. Since LTCs have a duration of 20-25 years, we take a different approach to study the aforementioned "no flexibility" and the "flexibility" cases. In particular, in the case of "no flexibility", we assume that, in the considered year, mid-streamers have to respect all the LTCs that they have already stipulated, but they can also decide to sign new LTCs. On the contrary, in the "flexibility" case, mid-streamers can ask for a re-negotiation of the existing contracts and therefore are not obliged to buy all the quantity of gas or LNG defined by the existing contracts.

- **Gas/LNG volumes and prices and degrees of mid-streamers' flexibility**. All gas/LNG volumes and prices are endogenously determined in the model. The volumes are defined through the supplying countries and mid-streamers' variables indicated above, while the LTCs and the spot prices correspond to the values of the dual variables associated with the relative gas and LNG balance constraints. Note that we impose some limits on the gas and LNG volumes contracted with LTCs. These limits vary according to the flexibility assumptions considered for mid-streamers. More precisely, we take as reference the annual volumes of gas and LNG that mid-streamers have contracted with already existing LTCs (these annual volumes are input data) and in the "no flexibility" case we assume that these amounts establish lower bounds on the total quantities of gas and LNG that mid-streamers have to buy with LTCs in the year. This reflects the idea that mid-streamers have to respect all the LTCs that they have already stipulated, but they can also decide to sign new LTCs in the considered year. In contrast, to respect the re-negotiation assumption that characterizes the "flexibility" case, the amounts of already stipulated gas and LNG LTCs are used as upper bounds on the volumes of gas and LNG that mid-streamers can purchase.

- **Pipeline and tanker transportation limits**. For sake of simplicity, we assume that the tanker used to transfer LNG have no capacity limits. A similar assumption has been adopted for the gas pipelines. Pipeline gas and LNG transportation costs are included as exogenous charges in the model. Moreover, we assume that in the destination country there are some entry points for pipeline gas. Each of this entry point has a specific location in the destination country and collects the gas coming from a subset of supplying countries. We use the incidence matrix Γ_{fn} to define the link between supplying country and entry point. These entry points are characterized by a limited capacity that we model though a constraint.

- **External supply risk**. The external supply risk is considered as an externality that we internalize in our optimization problem. In general, the insecurity of

supply could intervene at the time the prices are negotiated. As explained above, LTCs and spot prices for both gas and LNG are endogenously determined in our model. However, we assume that only gas and LNG traded with LTCs are exposed to the external supply risk. This is due to the fact that spot LNG refers to gas that is already landed in the destination country and therefore it is not risky. Similarly, the spot gas is freely traded on a short notice at the hub and therefore we suppose the external supply risk does not apply to its exchange. The inclusion of the risk indicators in our model is conducted as follows: we first construct and compute the values of the indicators presented in Section 5.3.2 on the basis of the ex-ante structure external supply of the considered destination country (Italy). We then use these indicators to weight the quantities of gas y^G_{nmt} and LNG y^{LNG}_{nmt} that appear in the respective LTC balance constraints (see model formulation in Section 5.3.4). We introduce the external supply risk indicators in the balances of the gas and LNG LTCs because these constraints not only represent the agreement between supplying countries and mid-streamers on the exchanged volumes but also are those that affect the prices of these LTCs. In this way, we can evaluate whether the external supply risk can modify the gas/LNG contract prices and volumes.

5.3.4 Optimization model for a natural gas supply chain with external supply risk

Finding the equilibrium state of the described natural gas chain with endogenous final consumers' demand consists in solving a social welfare optimization problem subject to some technical constraints. We first describe the cost functions that are included in our model formulation.

Supplying countries gain from selling gas but they face some costs in the gas production process. Let C_{nt} denote the production costs incurred by producer n. This is a continuous and convex function that depends on the total quantity of natural gas X^G_{nt} that supplying country n extracts in time period t. In particular, one has:

$$C_{nt} = C_{nt}\left(X^G_{nt}\right) \quad \forall n,\ \forall t \tag{5.14}$$

It could happen that a part of the produced gas is then sold as LNG by some of the supplying countries n. These countries face additional liquefaction costs that are denoted with the function LC_{nt}. This function is assumed to be continuous and convex and depends on the total amount of LNG X^{LNG}_{nt} that country n supplies in time period t:

$$LC_{nt} = LC_{nt}\left(X_{nt}^{LNG}\right) \quad \forall n,\ \forall t \tag{5.15}$$

On the other side, mid-streamers who import LNG in the destination (importing) country face the related regasification costs. These costs are represented by a continuous and convex function, denoted as RC_{mt}, that depends on the total quantity of LNG Y_{mt}^{LNG} that mid-streamer m regasifies in time period t. In particular, one has:

$$RC_{mt} = RC_{mt}\left(Y_{mt}^{LNG}\right) \quad \forall m,\ \forall t \tag{5.16}$$

In our gas supply chain, we further assume that mid-streamers manage the storage systems. They withdraw gas in the high-demand period $t = 2$ at zero cost,[3] while the gas injection is operated in the low-demand period $t = 1$ with a cost that we denote with I_{m1}. This is assumed to be a continuous and convex function that depends on the quantity of natural gas i_{m1} that mid-streamer m injects in the storage site in $t = 1$. In particular, one has:

$$I_{m1} = I_{m1}\left(i_{m1}\right) \quad \forall m \tag{5.17}$$

In the following, we first describe the optimization model for the "no flexibility" case (Section 5.3.4) and we then illustrate the modifications that are introduced for modeling the "flexibility" assumption (Section 5.3.4).

"No flexibility" case

Finding the equilibrium state of the described natural gas chain with endogenous final consumers' demand consists in solving the social welfare optimization problem (5.18)-(5.38) presented below. The objective function (5.18) corresponds to the (annual) social welfare that is given by the difference between the final consumers' willingness to pay $\int_0^{d_{st}} P_{st}(\xi)d\xi$ and all the costs respectively faced by supplying countries and mid-streamers. In particular, supplying countries pay the production, the LNG liquefaction, the pipeline and the cargo transportation costs; on the other side mid-streamers bear the regasification, the storage injection, and the distribution charges. The objective function (5.18) is subject to several constraints as detailed in the following.

$$\textbf{Max} \quad \sum_{s=1}^{S}\sum_{t=1}^{T}\theta_t \int_0^{d_{st}} P_{st}(\xi)d\xi - \sum_{n=1}^{N}\sum_{t=1}^{T}\theta_t \cdot \left[C_{nt}\left(X_{nt}^{G}\right) + LC_{nt}\left(X_{nt}^{LNG}\right)\right] \tag{5.18}$$
$$- \sum_{n=1}^{N}\sum_{t=1}^{T}\theta_t \cdot \left[\sum_{m=1}^{M} ptc_{nm}^{G} \cdot x_{nmt}^{G} + \sum_{m=1}^{M} stc_{nm}^{LNG} \cdot x_{nmt}^{LNG}\right] +$$

[3] This assumption is taken from Egging et al. (2008).

$$- \sum_{n=1}^{N} \sum_{t=1}^{T} \theta_t \cdot \left[ptc_n^{SpotG} \cdot x_{nt}^{SpotG} + \sum_{m=1}^{M} stc_{nm}^{LNG} \cdot x_{nmt}^{SpotLNG} \right] +$$
$$- \sum_{m=1}^{M} \sum_{t=1}^{T} \theta_t \cdot \left[RC_{mt} \left(Y_{mt}^{LNG} \right) \right] - \sum_{m=1}^{M} \theta_1 \cdot I_{m1}(i_{m1}) - \sum_{s=1}^{S} \sum_{t=1}^{T} \theta_t \cdot [dc_{ms} \cdot z_{mst}]$$

subject to

$$\bar{X}_n - X_{nt}^G \geq 0 \quad \forall n, \forall t \qquad (\overline{\gamma}_{nt}) \tag{5.19}$$

$$X_{nt}^G - \left(\sum_{m=1}^{M} x_{nmt}^G + x_{nt}^{SpotG} + X_{nt}^{LNG} \right) = 0 \quad \forall n, \forall t \qquad (\gamma_{nt}) \tag{5.20}$$

$$(1 - \alpha_n) \cdot X_{nt}^{LNG} - \left(\sum_{m=1}^{M} x_{nmt}^{LNG} + \sum_{m=1}^{M} x_{nmt}^{SpotLNG} \right) = 0 \quad \forall n, \forall t \qquad (\delta_{nt}) \tag{5.21}$$

$$\bar{L}_n - (1 - \alpha_n) \cdot X_{nt}^{LNG} \geq 0 \quad \forall n, \forall t \qquad (\overline{\delta}_{nt}) \tag{5.22}$$

$$\bar{R}_m - (1 - \beta_m) \cdot Y_{mt}^{LNG} \geq 0 \quad \forall m, \forall t \qquad (\overline{\eta}_{mt}) \tag{5.23}$$

$$(1 - \beta_m) \cdot Y_{mt}^{LNG} - \left(\sum_{n=1}^{N} y_{nmt}^{LNG} + \sum_{n=1}^{N} y_{nmt}^{SpotLNG} \right) = 0 \quad \forall m, \forall t \qquad (\eta_{mt}) \tag{5.24}$$

$$\sum_{n=1}^{N} y_{nmt}^G + \sum_{n=1}^{N} y_{nmt}^{LNG} + y_{mt}^{SpotG} + \sum_{n=1}^{N} y_{nmt}^{SpotLNG} +$$
$$- i_{mt} \geq \sum_{s=1}^{S} z_{mst} + q_{mt}^{SpotG} \quad \forall m,\ t = 1 \quad (\lambda_{mt}) \tag{5.25}$$

$$\sum_{n=1}^{N} y_{nmt}^G + \sum_{n=1}^{N} y_{nmt}^{LNG} + y_{mt}^{SpotG} + \sum_{n=1}^{N} y_{nmt}^{SpotLNG} +$$
$$+ w_{mt} \geq \sum_{s=1}^{S} z_{mst} + q_{mt}^{SpotG} \quad \forall m,\ t = 2 \quad (\lambda_{mt}) \tag{5.26}$$

$$i_{m1} \cdot \theta_1 - w_{m2} \cdot \theta_2 \geq 0 \quad \forall m \qquad (\mu_m) \tag{5.27}$$

$$\bar{I}_m - i_{m1} \geq 0 \quad \forall m \qquad (\nu_m) \tag{5.28}$$

$$\bar{W}_m - w_{m2} \geq 0 \quad \forall m \qquad (\sigma_m) \tag{5.29}$$

$$WG_m - \theta_2 \cdot w_{m2} \geq 0 \quad \forall m \qquad (\phi_m) \tag{5.30}$$

$$\sum_t \theta_t \cdot y^G_{nmt} - \tau_{nm} \geq 0 \quad \forall n, \forall m \qquad (\psi^G_{mn}) \tag{5.31}$$

$$\sum_t \theta_t \cdot y^{LNG}_{nmt} - \xi_{nm} \geq 0 \quad \forall n, \forall m \qquad (\psi^{LNG}_{mn}) \tag{5.32}$$

$$\Upsilon_{ft} - \left(\sum_{n=1}^{N} \sum_{m=1}^{M} \Gamma_{fn} \cdot y^G_{nmt} + \sum_{n=1}^{N} \Gamma_{fn} \cdot x^{SpotG}_{nt} \right) \geq 0 \quad \forall f, \forall t \qquad (\kappa_{ft}) \tag{5.33}$$

$$x^G_{nmt} - \Pi^G_{nm} \cdot y^G_{nmt} = 0 \quad \forall n, \forall m, \forall t \quad (p^G_{nmt}) \tag{5.34}$$

$$x^{LNG}_{mnt} - \Pi^{LNG}_{nm} \cdot y^{LNG}_{mnt} = 0 \quad \forall n, \forall m, \forall t \qquad (p^{LNG}_{mnt}) \tag{5.35}$$

$$\sum_{n=1}^{N} x^{SpotG}_{nt} + q^{SpotG}_{mt} - \sum_{m=1}^{M} y^{SpotG}_{mt} = 0 \quad \forall t \quad (p^{SpotG}_t) \tag{5.36}$$

$$x^{SpotLNG}_{nmt} - y^{SpotLNG}_{nmt} = 0 \quad \forall n, \forall m, \forall t \quad (p^{SpotLNG}_{nmt}) \tag{5.37}$$

$$\sum_m z_{mst} - d_{st} = 0 \quad \forall s, \forall t \qquad (p_{st}) \tag{5.38}$$

Constraints (5.19)-(5.22) identify the supply countries' activities. In particular, constraint (5.19) imposes an upper bound on the total quantity of gas that producers can extract (X^G_{nt}). As stated by the constraint (5.20), the gas produced by supplying countries can can be left in the gaseous form, and then sold either with LTCs (see variable x^G_{nmt}) or on the spot market (see variable x^{SpotG}_{nt}), or can be transformed in LNG (see variable X^{LNG}_{nt}). The variable X^{LNG}_{nt} represents the total amount of LNG produced by the supply country n that is then sold either with LTCs (x^{LNG}_{nmt}) or on spot ($x^{SpotLNG}_{nmt}$), as indicated by constraint (5.21). On the other side, constraint (5.22) imposes capacity limits on the liquefaction process. Note that the variable X^{LNG}_{nt} in

constraints (5.21) and (5.22) is multiplied by the factor $(1-\alpha_n)$ to account for the gas loss α_n that accrues during the liquefaction phase.

Constraints (5.23)-(5.32) refer to mid-streamers. In particular, mid-streamers buy gas and LNG from supplying countries with LTCs, or buy/sell gas on the spot market, or buy spot LNG. Mid-streamers regasify the total amount of LNG purchased (Y_{mt}^{LNG}) taking into account the capacity of their technologies as indicated in constraint (5.23). On the other side, constraint (5.24) explains that Y_{mt}^{LNG} accounts for the LNG that mid-streamers purchase both with LTCs (y_{nmt}^{LNG}) and on spot ($y_{nmt}^{SpotLNG}$). Note that both in (5.23) and (5.24) the variable Y_{mt}^{LNG} is multiplied by the factor $(1-\beta_m)$ to consider the losses of the regasification process. Constraints (5.25) and (5.26) define the balances among the quantities of gas managed by mid-streamer in the low ($t=1$) and in the high-demand ($t=2$) periods, respectively. More precisely, constraint (5.25) enforces that the total amount of gas purchased by the mid-streamer minus the gas injected in the storage site has to be greater or equal to the amount of gas sold to final consumers (z_{mst}) and on the spot market. In contrast, constraint (5.26) imposes that total amount of gas purchased by the mid-streamer plus the gas withdrawn from the storage site has to be greater or equal to the quantity of gas sold to final consumers (z_{mst}) and on the spot market. Constraints (5.27)-(5.30) regulate the storage process. In particular, (5.27) enforces that amount of gas injected in the storage site has to greater than the quantity withdrawn. Constraints (5.28) and (5.29) respectively define the injection and the withdrawal capacity limits, and, finally, (5.30) imposes the working gas limit throughout all withdrawal periods. On the other side, constraints (5.31) and (5.32) are used to model the "no flexibility" assumption described above. In particular, they respectively impose that the yearly amounts of gas and LNG that mid-streamers have to buy through LTCs have to be greater or equal to the volumes established (for that year) in already existing contracts. Such a constraint formulation allows mid-streamers not only to accomplish the volume TOP clause of the LTCs into which they have already enter, but also to possible negotiate new contracts. We explain in Section 5.3.4 how these constraints are modified to model the mid-streamers' flexible behaviour.

Constraint (5.33) enforces the capacity limit of the entry points located in the destination country, while constraints (5.34), (5.35), (5.36) and (5.37) are the balances for gas and LNG respectively traded with LTCs and exchanged on a spot basis. Note that, as mentioned above, constraints (5.34) and (5.35) also include the external supply risk indicator as a weight of the quantities of gas and LNG purchased by the mid-streamers. Constraint (5.38) imposes the balance between the total quantity of gas sold by mid-streamers (z_{mst}) and demanded by consumers (d_{st}).

Finally, In order to detect the behaviur of the different players involved in the natural gas supply chain we consider complementarity formulation of this optimization

problem:

$$0 \leq -\gamma_{nt} + \frac{\partial C_{nt}\left(X_{nt}^{G}\right)}{\partial X_{nt}^{G}} + \overline{\gamma}_{nt} \perp X_{nt}^{G} \geq 0 \quad \forall n, \forall t \tag{5.39}$$

$$0 \leq -(1-\alpha_n)\cdot\delta_{nt} + (1-\alpha_n)\cdot\overline{\delta}_{nt} + \gamma_{nt} + \frac{\partial LC_{nt}\left(X_{nt}^{LNG}\right)}{\partial X_{nt}^{LNG}} \perp X_{nt}^{LNG} \geq 0 \; \forall n, \forall t \tag{5.40}$$

$$0 \leq -p_{nmt}^{G} + ptc_{nm}^{G} + \gamma_{nt} \perp x_{nmt}^{G} \geq 0 \quad \forall n, \forall m, \forall t \tag{5.41}$$

$$0 \leq -p_{t}^{SpotG} + \gamma_{nt} + ptc_{n}^{SpotG} + \sum_{f=1}^{F} \Gamma_{fn}\cdot\kappa_{ft} \perp x_{nt}^{SpotG} \geq 0 \quad \forall n, \forall t \tag{5.42}$$

$$0 \leq -p_{nmt}^{LNG} + stc_{nm}^{LNG} + \delta_{nt} \perp x_{nmt}^{LNG} \geq 0 \quad \forall n, \forall m, \forall t \tag{5.43}$$

$$0 \leq -p_{nmt}^{SpotLNG} + stc_{nm}^{LNG} + \delta_{nt} \perp x_{nmt}^{SpotLNG} \geq 0 \quad \forall n, \forall m, \forall t \tag{5.44}$$

$$0 \leq -p_{st} + dc_{ms} + \lambda_{mt} \perp z_{mst} \geq 0 \quad \forall m, \forall s, \forall t \tag{5.45}$$

$$0 \leq -(1-\beta_m)\cdot\eta_{mt} + \frac{\partial RC_{m}\left(Y_{mt}^{LNG}\right)}{\partial Y_{mt}^{LNG}} + (1-\beta_m)\cdot\overline{\eta}_{mt} \perp Y_{mt}^{LNG} \geq 0 \quad \forall m, \forall t \tag{5.46}$$

$$0 \leq -\lambda_{mt} - \psi_{nm}^{G} + \Pi_{nm}^{G}\cdot p_{nmt}^{G} + \sum_{f=1}^{F} \Gamma_{fn}\cdot\kappa_{ft} \perp y_{nmt}^{G} \geq 0 \quad \forall n, \forall m, \forall t \tag{5.47}$$

$$0 \leq -\lambda_{mt} + p_{t}^{SpotG} \perp y_{mt}^{SpotG} \geq 0 \quad \forall m, \forall t \tag{5.48}$$

$$0 \leq -\lambda_{mt} - \psi_{nm}^{LNG} + \Pi_{nm}^{LNG}\cdot p_{nmt}^{LNG} + \eta_m \perp y_{nmt}^{LNG} \geq 0 \quad \forall n, \forall m, \forall t \tag{5.49}$$

$$0 \leq -\lambda_{mt} + p_{nmt}^{LNG} + \eta_m \perp y_{nmt}^{SpotLNG} \geq 0 \quad \forall m, \forall t \tag{5.50}$$

$$0 \leq -p_{t}^{SpotG} + \lambda_{mt} \perp q_{mt}^{SpotG} \geq 0 \quad \forall m, \forall t \tag{5.51}$$

$$0 \leq -\mu_m + \frac{\partial I_{m1}\left(i_{m1}\right)}{\partial i_{m1}} + \nu_m + \lambda_{m1} \perp i_{m1} \geq 0 \quad \forall m, t = 1 \tag{5.52}$$

$$0 \leq -\lambda_{m2} + \mu_m + \sigma_m + \phi_m \perp w_{m2} \geq 0 \quad \forall m, \forall t = 2 \tag{5.53}$$

$$0 \leq \bar{X}_n - X_{nt}^{G} \perp \overline{\gamma}_{nt} \geq 0 \quad \forall n, \forall t \tag{5.54}$$

$$0 \leq \bar{L}_n - (1-\alpha_n)\cdot X_{nt}^{LNG} \perp \overline{\delta}_{nt} \geq 0 \quad \forall n, \forall t \tag{5.55}$$

$$0 \leq \bar{R}_m - (1-\beta_m)\cdot Y_{mt}^{LNG} \perp \overline{\eta}_{mt} \geq 0 \quad \forall m, \forall t \tag{5.56}$$

$$0 \leq \sum_{n=1}^{N} y_{nmt}^{G} + \sum_{n=1}^{N} y_{nmt}^{LNG} + y_{mt}^{SpotG} + \sum_{n=1}^{N} y_{nmt}^{SpotLNG} +$$
$$-i_{mt} - \sum_{s=1}^{S} z_{mst} - q_{mt}^{SpotG} \perp \lambda_{mt} \geq 0 \quad \forall m,\ t = 1 \tag{5.57}$$

$$0 \leq \sum_{n=1}^{N} y_{nmt}^{G} + \sum_{n=1}^{N} y_{nmt}^{LNG} + y_{mt}^{SpotG} + \sum_{n=1}^{N} y_{nmt}^{SpotLNG} + w_{mt} +$$

$$-\sum_{s=1}^{S} z_{mst} - q_{mt}^{SpotG} \perp \lambda_{mt} \geq 0 \quad \forall m,\ t = 2 \tag{5.58}$$

$$0 \leq i_{m1} - w_{m2} \perp \mu_m \geq 0 \quad \forall m \tag{5.59}$$

$$0 \leq \bar{I}_m - i_{m1} \perp \nu_m \geq 0 \quad \forall m \tag{5.60}$$

$$0 \leq \bar{W}_m - w_{m2} \perp \sigma_m \geq 0 \quad \forall m \tag{5.61}$$

$$0 \leq WG_m - \theta_2 \cdot w_{m2} \perp \phi_m \geq 0 \quad \forall m \tag{5.62}$$

$$0 \leq \sum_t \theta_t \cdot y_{nmt}^{G} - \tau_{nm} \perp \psi_{mn}^{G} \geq 0 \quad \forall n, \forall m \tag{5.63}$$

$$0 \leq \sum_t \theta_t \cdot y_{nmt}^{LNG} - \xi_{nm} \perp \psi_{mn}^{LNG} \geq 0 \quad \forall n, \forall m \tag{5.64}$$

$$0 \leq \Upsilon_{ft} - \left(\sum_{n=1}^{N} \sum_{m=1}^{M} \Gamma_{fn} \cdot y_{nmt}^{G} + \sum_{n=1}^{N} \Gamma_{fn} \cdot x_{nt}^{SpotG} \right) \perp \kappa_{ft} \geq 0 \quad \forall t \tag{5.65}$$

$$0 \leq p_{st} - a_{st} + b_{st} \cdot d_{st} \perp d_{st} \geq 0 \quad \forall s, \forall t \tag{5.66}$$

$$X_{nt}^{G} - \left(\sum_{m=1}^{M} x_{nmt}^{G} + x_{nt}^{SpotG} + X_{nt}^{LNG} \right) = 0 \quad \forall n, \forall t \qquad (\gamma_{nt} : \text{free}) \tag{5.67}$$

$$(1 - \alpha_n) \cdot X_{nt}^{LNG} - \left(\sum_{m=1}^{M} x_{nmt}^{LNG} + \sum_{m=1}^{M} x_{nmt}^{SpotLNG} \right) = 0 \quad \forall n, \forall t \qquad (\delta_{nt} : \text{free}) \tag{5.68}$$

$$(1 - \beta_m) \cdot Y_{mt}^{LNG} - \left(\sum_{n=1}^{N} y_{nmt}^{LNG} + \sum_{n=1}^{N} y_{nmt}^{SpotLNG} \right) = 0 \ \forall m, \forall t \ (\eta_{mt} : \text{free}) \tag{5.69}$$

$$x_{nmt}^{G} - \Pi_{nm}^{G} \cdot y_{nmt}^{G} = 0 \quad \forall n, \forall m, \forall t \ (p_{nmt}^{G} : \text{free}) \tag{5.70}$$

$$\sum_{n=1}^{N} x_{nt}^{SpotG} + q_{mt}^{SpotG} - \sum_{m=1}^{M} y_{mt}^{SpotG} = 0 \quad \forall t \quad (p_t^{SpotG} : \text{free}) \tag{5.71}$$

$$x_{mnt}^{LNG} - \Pi_{nm}^{LNG} \cdot y_{mnt}^{LNG} = 0 \quad \forall n, \forall m, \forall t \qquad (p_{mnt}^{LNG} : \text{free}) \tag{5.72}$$

$$x_{nmt}^{SpotLNG} - y_{nmt}^{SpotLNG} = 0 \quad \forall n, \forall m, \forall t \quad (p_{nmt}^{SpotLNG} : \text{free}) \tag{5.73}$$

$$\sum_m z_{mst} - d_{st} = 0 \quad \forall s, \forall t \qquad (p_{st} : \text{free}) \tag{5.74}$$

"Flexibility" case

The formulation of the welfare optimization problem under the "flexibility" assumption is identical to that presented in Section 5.3.4 with the exception of the constraints regulating the volumes of gas and LNG volumes that mid-streamers have to buy with LTCs. In particular, this change change regards constraints (5.31) and (5.32) that from lower bounds on the gas and LNG volumes purchased with LTCs become upper bounds. These are expressed as follows:

$$\tau_{nm} - \sum_t \theta_t \cdot y^G_{nmt} \geq 0 \quad \forall n, \forall m \qquad (\psi^G_{mn}) \tag{5.75}$$

$$\xi_{nm} - \sum_t \theta_t \cdot y^{LNG}_{nmt} \geq 0 \quad \forall n, \forall m \qquad (\psi^{LNG}_{mn}) \tag{5.76}$$

From a mathematical point of view, this constraint modification implies some small changes in the KKT formulation of the optimization problem. In particular, conditions (5.47), (5.49), (5.63), and (5.64) are respectively substituted with the following ones:

$$0 \leq -\lambda_{mt} + \psi^G_{nm} + \Pi^G_{nm} \cdot p^G_{nmt} + \sum_{f=1}^{F} \Gamma_{fn} \cdot \kappa_{ft} \perp y^G_{nmt} \geq 0 \quad \forall n, \forall m, \forall t \tag{5.77}$$

$$0 \leq -\lambda_{mt} + \psi^{LNG}_{nm} + \Pi^{LNG}_{nm} \cdot p^{LNG}_{nmt} + \eta_m \perp y^{LNG}_{nmt} \geq 0 \quad \forall n, \forall m, \forall t \tag{5.78}$$

$$0 \leq \tau_{nm} - \sum_t \theta_t \cdot y^G_{nmt} \perp \psi^G_{mn} \geq 0 \quad \forall n, \forall m \tag{5.79}$$

$$0 \leq \xi_{nm} - \sum_t \theta_t \cdot y^{LNG}_{nmt} \perp \psi^{LNG}_{mn} \geq 0 \quad \forall n, \forall m \tag{5.80}$$

More precisely, since constraints (5.75) and (5.76) impose upper bounds on the primal variables y^G_{nmt} and y^{LNG}_{nmt}, the associated dual variables ψ^G_{mn} and ψ^{LNG}_{mn} enter with a positive sign in the KKT conditions (5.77) and (5.78) of these primal variables. The reverse happens in the complementarity formulation of the optimization problem under the "no flexibility" assumption. Since constraints (5.31) and (5.32) define lower bounds on variables y^G_{nmt} and y^{LNG}_{nmt} the associated dual variables ψ^G_{mn} and ψ^{LNG}_{mn} enter with a negative sign in the KKT conditions (5.47) and (5.49) of these primal variables. Finally, all the other KKT conditions are as indicated in Section 5.3.4. From an economical point of view, the illustrated constraint modification allows us to describe a more flexible behaviur of the mid-streamers which, in this case, have the possibility to ask for a LTC re-negotiation or to avoid the respect of the contract TOP clause for a short period.

5.4 Case study

Our case study is based on the Italian gas market that we consider as the gas destination area where mid-streamers operate. We select this market for two reasons: first, it is one of the three largest gas markets in Europe together with the UK and Germany; second, it mainly relies on natural gas imports to cover its demand since the national production is very low. According to the annual report of the Italian Authority (see

AEEGSI (2016)[4]) the 90.6% of the national gas demand in 2015 was satisfied with imports from Russia, Algeria, Libya, the Netherlands, Qatar, and Norway. The main companies (mid-streamers) operating in Italy are ENI, Edison, and Enel with a market share of respectively 53.8%, 21.2%, and 11.2% (see AEEGSI (2016)). In 2015, these companies bought natural gas from Russia, Algeria, Libya, the Netherlands, and Norway; while LNG was imported by Qatar and Algeria (see AEEGSI (2016)). In general, residential/commercial is the gas consumers' sector with the highest demand, followed by power generation, and industrial sector (see also AEEGSI (2016)). The Italian natural gas and LNG imports are mainly delivered via long-term contracts, even though gas can also be traded on the Italian spot market "Punto di Scambio Virtuale (PSV)" that was created in 2003 (see Honoré (2013) for a description of the liberalization process of the Italian gas market and the establishment of the PSV).

Considering this framework, our analysis refers to 2015 data and it is based on the following assumptions:

- **Destination country**: Italy.
- **Supplying countries**: Russia (RU), Algeria (AL), Libya (LIB), the Netherlands (NL), Qatar (QT), and Norway (NW). Since in the last years the Italian gas production is progressively reducing (see AEEGSI (2016)), we do not account for Italy among the producing and supplying countries.
- **Natural gas origin**: Russia, Algeria, Libya, the Netherlands, and Norway. For modeling the mid-streamers' flexibility assumptions, we consider the LTCs that Italy has established with these countries in the last years and are still active in 2015.
- **LNG origin**: Algeria and Qatar (see BP (2016); GIIGNL (2018)). Similarly to gas, we consider the LNG LTCs that Italy has established with these two countries in the last years and are still active in 2015 to model the mid-streamers' flexibility assumptions.
- **Mid-streamers**: We assume that there is just one mid-streamer, since we do not dispose of detailed data for all the companies operating in the Italian gas market. This representative mid-streamer can buy both natural gas and LNG through LTCs or can trade them on the respective spot markets.

As already explained, we account for a time span of one year subdivided into two time periods with different demand levels. The high-demand period is assumed to have

[4]This annual report is in Italian and refer to 2015 data. An English version is available at http://www.autorita.energia.it/allegati/relaz_ann/15/annual_report2015.pdf but refers to 2014 data.

a duration of 151 days and comprehends the months from November to March included; the low-demand period lasts 214 days and covers the remaining months. Since, in our analysis, we consider a representative day per each period, all quantities are expressed in mcm/day while prices and costs are in €/cm.

The production (extraction) capacity data of the aforementioned supplying countries are taken from Egging et al. (2008) .[5] These data are not recent but considering that the gas reserve to production (R/P) ratio computed at worldwide level has been almost unchanged in the last twenty years,[6] we consider these capacity data as a reasonable proxy. The liquefaction capacity data related to the supplying countries are taken from GIIGNL (2018) and refer to 2015.

No capacity limits are imposed on the natural gas transports via pipelines between supplying countries and Italy or on the LNG cargos. However, we consider the capacity of the entry points located at the borders of the Italian network that enforces restrictions on the amount of natural gas imported via pipelines. Italy has five entry points for pipelines that are Mazara del Vallo, Gela, Tarvisio, Passo Gries, and Gorizia. In Mazara del Vallo, natural gas is imported from Algeria thanks to the connection with the pipeline Transmed/Enrico Mattei; the natural gas from Libya enters in Gela though the connection with the pipeline Greenstream; Gorizia and Tarvisio receive gas from Russia thought the TAG pipeline, and, finally, Pass Gries gets gas from the Netherlands and Norway respectively via the Trans-European pipeline and the Transitgas. Considering this information about the gas provenience at the different entry points, we are able to limits the imports between Italy and the supplying countries (see constraint (5.33) in our formulation). The 2015 capacity data of these entry points are provided by Snam (2016). For what concerns LNG, the capacity of the regasification plants implicitly limits the Italian LNG imports. There are three regasification plants in Italy that are located in Rovigo, Livorno, and Panigaglia. In our case study, we consider just one regasification plant whose capacity is obtained by aggregating those of these two plants. The respective data are taken from GIIGNL (2018) and refer to 2015.

The natural gas production costs faced by supplying countries are defined as linear function of the following type:

$$C_{nt} = c_n^G \cdot X_{nt}^G \quad \forall n,\ \forall t$$

where the parameter c_n^g has been estimated taking as reference Egging et al. (2008). In particular, the value of c_n^g for the considered supplying countries is obtained by

[5] See Table 14 at page 2410 of Egging et al. (2008).

[6] See BP at http://www.bp.com/en/global/corporate/energy-economics/statistical-review-of-world-energy/natural-gas/natural-gas-reserves.html

multiplying the marginal production costs reported in the column "Max mag" of Table 14 in Egging et al. (2008) by 1.9 that is the average for 2015 of the "Euro Area Gross Domestic Product Chained 2010 Prices YoY".[7]

The liquefaction costs incurred by supplying countries are determined by the following quadratic function:

$$LC_{nt} = lc1_n^{LNG} \cdot X_{nt}^{LNG} + lc2_n^{LNG} \cdot (X_{nt}^{LNG})^2 \quad \forall n, \ \forall t$$

where the terms $lc1_n^{LNG}$ and $lc2_n^{LNG}$, as for the production costs, have been estimated taking as reference the data and the approach proposed by Egging et al. (2008). More precisely, the values of $lc1_n^{LNG}$ and $lc2_n^{LNG}$ respectively correspond to the α and β parameters reported in Table 15 of in Egging et al. (2008) multiplied by 1.9. i.e. the 2015 GDP.

For the Italian mid-streamer's regasification costs, we consider the following quadratic function:

$$RC_t = rc1^{LNG} \left(\sum_{n=1}^{N} Y_{nt}^{LNG} \right) + rc2^{LNG} \left(\sum_{n=1}^{N} Y_{nt}^{LNG} \right)^2 \quad \forall t$$

where the terms $rc1_n^{LNG}$ and $rc2_n^{LNG}$ have been evaluated using the data available in Egging et al. (2008). More precisely, the values of $rc1_n^{LNG}$ and $rc2_n^{LNG}$ respectively correspond to the α and β parameters reported in Table 16 of in Egging et al. (2008) multiplied by 1.9. i.e. the 2015 GDP.

The mid-streamer also controls and manages the storage site. We suppose that there is just one storage site whose capacity and injection rate are obtained by aggregating the capacities and injection rates of all the storage sites available in Italy. As in Egging and Gabriel (2006), we impose that the injection rate is equal to the peak output rates, while the extraction capacity is assumed to be twice the injection capacity. The data related to working gas and storage rates refer to 2015 and are taken from IEA (2016a) and from the Stogit website.[8] Injection costs are defined through the following linear function:

$$I_1 = ic \cdot i_1$$

where the parameter ic is the unitary injection cost whose value has been taken

[7] Gross domestic product (GDP) measures the final market value of all goods and services produced within a country. It is the most frequently used indicator of economic activity. The GDP by expenditure approach measures total final expenditures (at purchasers' prices), including exports less imports. This concept is adjusted for inflation. For our simulation, we GDP data from Bloomberg (ticker: EUGDEMU). See https://www.bloomberg.com/quote/EUGNEMUY:IND

[8] See http://www.stogit.it/en/about-us/where-you-can-find-us/storage-sites.html

from AEEGSI (2016).

Supplying countries also face the natural gas and LNG transportation costs. The costs of transfer natural gas though pipelines are taken from NERA (2014). In particular, we have taken the 2018 data in Figure 77 at page 132 of Appendix A and we have adjusted them with the pipeline cost adders provided in Figure 87 at page 139 of Appendix A for 2018. We have finally transformed all cost data from \$/Mcf to €/cm. On the other side, for evaluating the LNG transportation costs we follow the same approach adopted for production, liquefaction, and regasification costs. We consider a cost of 0.005€/cm/1000 sea miles that we have taken from Egging et al. (2008) and we have then multiplied it by 1.9. The sea miles are deduced from GIIGNL (2018). On the other side, the distribution costs faced by the mid-streamer are taken from AEEGSI (2016).

The data needed for the computation of the external supply risk indicators refer to 2015 and are taken from BP (2016); GIIGNL (2018); AEEGSI (2016). As in Le Coq and Paltseva (2009), we consider the political risk rating for 2015 published by the PRS Group.[9] This political risk measure assigns countries a rate whose values are between 1 and 100 with the following reasoning: the highest the rate, the lowest the political risk associated. In all indicators that we construct, we consider the complementary of this PRS risk, namely r_n is set in the following way:

$$r_n = 100 - \text{PRS}_{\text{Risk}}$$

Recall that the indicators $\Pi_{nm}^{REES,G}$ and $\Pi_{nm}^{REES,LNG}$ also account for the distance (d_{nm}) between the supplying and the destination countries and the fungibility of natural gas (F_{nm}^{G}) and the LNG (F_{nm}^{LNG}). Following Le Coq and Paltseva (2009), we set $F_{nm}^{G} = 1$ and $F_{nm}^{LNG} = 2$, and the transport risk is identified by the following parameter d_{nm}:

$$d_{nm} = \begin{cases} 1, & \text{distance between capitals } < \text{ 1700 Km} \\ 2, & \text{1700 Km} \leq \text{distance between capitals } < \text{ 2500 Km} \\ 3, & \text{2500 Km} \leq \text{distance between capitals } < \text{ 3300 Km} \\ 4, & \text{distance between capitals } \geq \text{3300 Km} \end{cases} \tag{5.81}$$

The external risk indicators that we obtain from our computations are reported in Table 5.2.

In order to model the different degrees of mid-streamer's flexibility, we need the data of the annual volumes of gas and LNG that have been regulated by LTCs in 2015. We recall that Italy has natural gas LTCs with Russia, Algeria, the Netherlands,

[9] See https://www.prsgroup.com/category/risk-index

Table 5.2: External supply risk indicators

	$\Pi_{nm}^{HHI,G}$	$\Pi_{nm}^{SWN2,G}$	$\Pi_{nm}^{GES,G}$	$\Pi_{nm}^{REES,G}$
NW	1.598	2.877	0.102	0.115
NL	1.174	3.974	0.113	0.126
RU	18.779	19.140	11.564	6.464
AL	1.508	8.784	0.300	0.335
LIB	1.377	15.494	0.495	0.553
	$\Pi_{nm}^{HHI,LNG}$	$\Pi_{nm}^{SWN2,LNG}$	$\Pi_{nm}^{GES,LNG}$	$\Pi_{nm}^{REES,LNG}$
AL	0.111	3.515	0.001	0.003
QT	93.444	0.360	0.973	0.799

Norway, and Libya; while LNG LTCs are with Algeria and Qatar. The considered annual data are reported in Table 5.3 and are taken from Cedigaz[10]

We consider the following inverse demand functions to model the final consumers' gas demand:

$$p_{st} = a_{st} - b_{st} \cdot d_{st} \quad \forall s, \forall t$$

Parameters a_{st} and b_{st} have been estimated using an elasticity value of -0.1 for all consumer groups, the amount of gas demanded by Italian industry, power sector, and residential/commercial and the average prices that they paid for purchasing gas in 2015. These data are taken from AEEGSI (2016).

Table 5.3: Volumes of gas and LNG regulated by LTCs between Italy and supplying countries in 2015 (annual value)

	Gas	**LNG**
NW	5,450	-
NL	9,200	-
RU	35,000	-
AL	27,380	1,840
LIB	5,610	-
QT	-	6,400
Tot	82,640	8,240

Finally, we recall that the solution of the optimization problems presented in Sections 5.3.4 and 5.3.4 is found by implementing their complementarity conditions. These

[10]See http://www.cedigaz.org/products/natural-gas-database.aspx

KKT conditions are run in the GAMS modeling environment, using PATH as solver (see Dirkse and Ferris (1995)).

5.5 Results

To analyze the impacts of external supply risk on the mid-streamer imports' choices and we consider the following assumptions

1. **Mid-streamer's behaviour:**
    - The mid-streamer has *at least* to buy an amount of gas and LNG as defined in already existing LTCs ("No FLEX" case in the following);
    - The mid-streamer has *at most* to buy an amount of gas and LNG as defined in already existing LTCs ("FLEX" case in the following).
2. **External supply risk:**
    - No external supply risk is considered in model ("NO Risk" case in the following);
    - All external supply risk indicators that we constructed are considered in the model as explained in the previous sections ("Risk" case in the following).

In the following we first analyze the impacts of the application of different degrees of mid-streamers' flexibility by comparing the "No FLEX" and "FLEX" without considering any of the external supply risk indicators (see Section 5.5.1). The effects of gas/LNG volumes and prices with risk are then presented in Section 5.5.2. Note that in this section we consider the risk indicators imposed in both the "No FLEX" and the "FLEX" cases. Note that, in any of the simulations that we have implemented, the mid-streamer re-sells gas on the spot market. Finally, we assume that the risk regards both the supply of gas and LNG with LTCs at the same time.

5.5.1 No external supply risk

We first consider the effects of the mid-streamer's flexibility on the annual amount of gas purchased. Fig. 5.2a illustrate the yearly volume of natural gas, both in gaseous and liquefied forms, that the mid-streamer exchanges in the "No FLEX" and the"FLEX") cases, assuming that the external supply risk is not considered ("NO Risk").

The mid-streamer accomplishes all gas and LNG LTCs that it has with all the supplying countries (compare the values reported in Figure 2a with those reported in

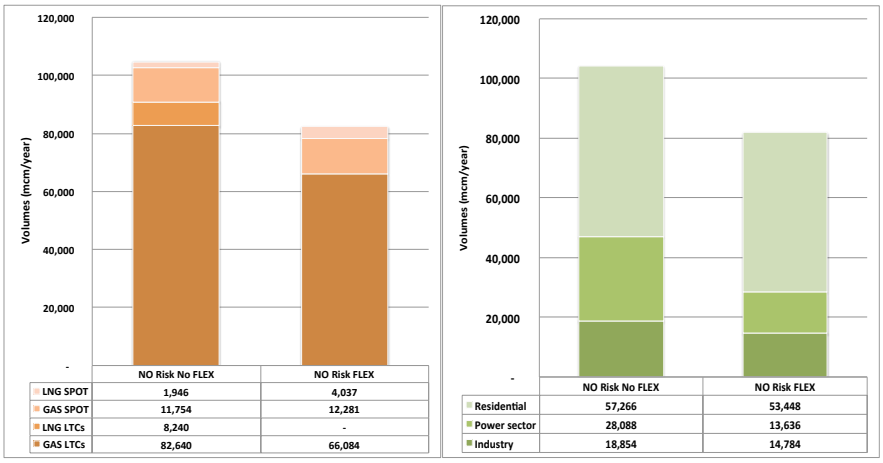

(a) (b)

Figure 5.2: Yearly volume of gas exchanged per type and yearly demand per consumer group (mcm/year)

Table 5.3), while this does not happen under the "FLEX" assumption leading to a gas volume drop of 21%. In particular, the mid-streamer reduces by 20% the annual volume of gas purchased with LTCs and does no longer buy LNG with LTCs. Even though it increases respectively by 4% and 107% the amount of gas and LNG acquired on spot markets at yearly basis, these spot purchases do not suffice to compensate the reduction in the LTC volumes. This has a negative impact on final consumers that see their gas availability reduced in the "FLEX" case. In particular, the mid-streamer still guarantee almost the entire gas supply to the residential/commercial sector (the drop is "only" by 7%), but it decreases the supply to the power companies and industry respectively by 51% and 22% with respect to the "No FLEX" case (see Fig. 5.2b).

Fig. 5.3 and 5.4 provide more details on the daily amount of gas and LNG exchanged between supplying countries and mid-streamers in the low- and in the high-demand periods under the "No FLEX" and "FLEX" assumptions. In general, we observe that between the flexibility and not flexibility cases, there is no a drastic variation of the mix of supplying countries. What the mid-streamer significantly modifies is the amount of gas/LNG purchased in the two time periods (shift of volumes exchanged in low- and high-demand periods) and the selection of the physical status of the gas traded (shift between the quantities of gas and LNG purchased, especially for the supply from Algeria). The set of supplying countries from which the mid-streamer receives gas/LNG is not subject to many modifications. Considering LTCs (Fig 5.3), the main changes in the gas supply mix between the "No FLEX" and "FLEX" cases are as follows: under the flexibility assumption, Norway does no longer provide gas to Italy in any period; Libya still procures Italy with gas but only in the low-demand period; and, finally, the

total amount of gas provided by Algeria reduces, especially in the low-demand period. Note that this unsold Algerian gas is then transformed in LNG and sold on the spot market (see Fig. 5.4. For what concerns LNG, as already indicated above, the difference between the "No FLEX" and "FLEX" cases is that the volume TOP clause of the Algerian and Qatari LTCs is not respected under the flexibility assumption because the mid-streamer prefers to buy spot LNG. On the other side, both in the "No FLEX" and "FLEX" cases, Libya and the Netherlands supply spot gas to Italy, even though in different quantities. Moreover, in the high-demand period of the "FLEX" case Russia appears as an additional supplier.

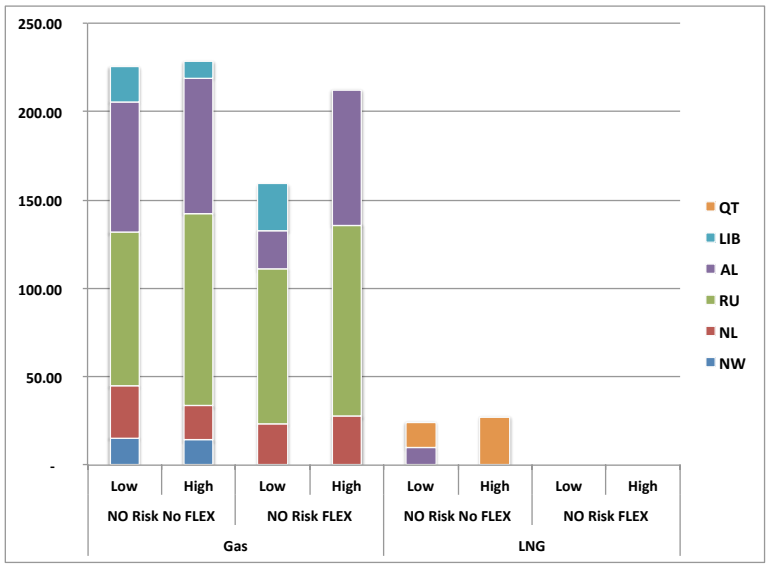

Figure 5.3: Natural gas and LNG bought through LTCs (mcm/day)

The comparison of the "No FLEX" and "FLEX" results under the assumption of absence of external supply risk shows that the mid-streamer changes its supply choices when it has the possibility to do that. The profit analysis can help understanding this change of strategies in the mid-streamer's behaviur. Table 5.4 reports supplying countries and the mid-streamer's profits, the final gas consumers' surplus, and the social welfare in the "No FLEX" and "FLEX" cases. In the "No FLEX" case, the mid-streamer is forced to satisfy the LTCs that it has already contracted. This guarantees the remuneration of the supplying countries which gain from their activities, but it causes a significant loss for the mid-streamer because its cost of purchasing gas and LNG ("Purchase costs") is higher than the revenues it obtains from selling gas to final consumers (compare Tables 5.5, 5.6, and 5.7 that report the LTC prices, the

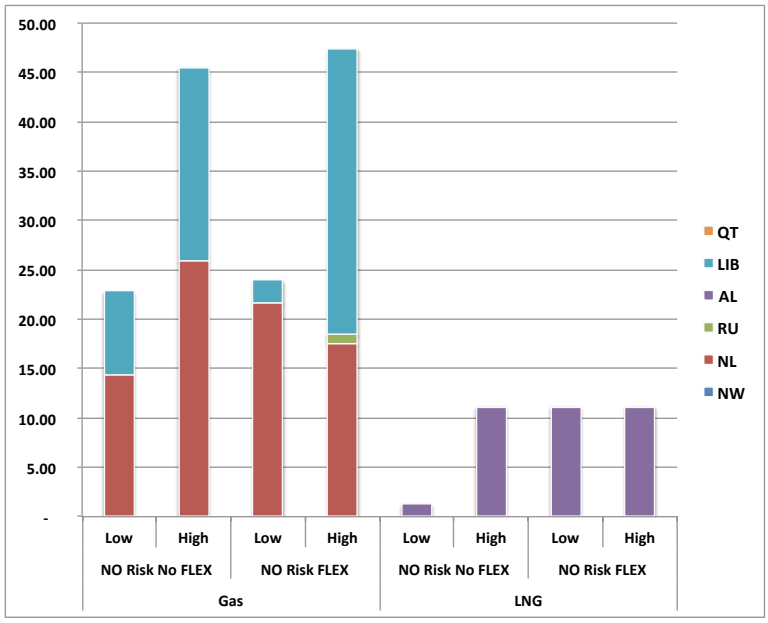

Figure 5.4: Natural gas and LNG bought on the spot market (mcm/day)

Table 5.4: Supplying countries and mid-streamer's profits, final consumers' surplus, and social welfare under the "NO Risk" assumption (€/year)

€/cm		NO Risk No FLEX	NO Risk FLEX
Supplying countries	Revenues	51,021	38,342
	Production costs	14,745	11,171
	Transport costs	36,057	27,188
	Net profits	**218**	**-17**
Mid-streamer	Revenues	50,247	52,550
	Distribution costs	11,326	9,895
	Purchase costs	51,021	38,342
	Regasification costs	149	53
	Injection costs	161	150
	Net profits	**-12,410**	**4,110**
Final consumers	Industry's surplus	21,820	13,962
	Power Sector 's surplus	14,454	4,899
	Residenatial's surplus	182,618	159,711
	Total surplus	**218,892**	**178,572**
Social welfare		**206,700**	**182,664**

spot prices, and the prices charged to final consumers, respectively).[11] The situation changes in the "FLEX" case where the mid-streamer is not obliged to fully satisfy all

[11]Note that, in the "No FLEX" case, the weighted average gas and LNG prices computed over the involved supplying countries and paid by the mid-streamer are: 0.50 €/cm (gas LTCs), 0.66 €/cm (LNG LTCs), 0.32 €/cm (gas spot), and 0.50 €/cm (LNG spot). In contrast, the weighted average price that the mid-streamer applies to final consumers is 0.48 €/cm).

the contracts. The outcome is that the mid-streamer modifies its supply mix in such a way it avoids negative profits. However, the mid-streamer's strategy of reducing its purchase of gas and LNG with LTCs compared to the "No FLEX" case is not beneficial for the whole gas supply chain because it implies not only a reduction of gas availability for final consumers with a consequent decrease of their surplus, but also a drop of supplying countries' profits that become negative (see Table 5.4). The final result is a 12% reduction of the social welfare. We recall that the remuneration of supplying countries is important because these guarantee the maintenance of the existing infrastructures and the investments in new ones, whose costs are, in general, very high. Considering these results, we can say that LTCs are necessary to maintain the stability and to guarantee the security of supply, even though this may incur in losses for the mid-streamers.

We finally reports in Tables 5.5 and 5.6 the prices for natural gas and LNG respectively sold with LTCs and on the spot market obtained in the "No FLEX" and the "FLEX" cases. Note that the label "n.s." in Tables 5.5 and 5.6 stands for "not sold". We recall that the gas spot price is not differentiated per supplier because we assume that there is just one market where all participants submit their offers and bids. This market sets the price for spot gas on a daily basis. The prices of LTCs for gas and LNG are higher than those defined on the spot market both under the "No FLEX" and the "FLEX" assumptions. This reflects the differences between these two pricing systems and explains the reason why mid-streamers have asked for the re-negotiation of the LTCs. Indeed, higher LTCs prices guarantee returns to supplying countries, but also they may lead to possible losses for mid-streamers. Moreover, as expected, the spot prices in the low-demand period are lower than in those in high-demand period because of the different consumption levels in the two time frameworks.

Table 5.5: Prices of gas and LNG LTCs under the "NO Risk" assumption (€/cm)

		NW	NL	RU	AL	LIB	QT
Gas LTCs	**No FLEX**	0.54	0.38	0.51	0.54	0.41	
	FLEX	n.s.	0.38	0.51	0.55	0.41	
LNG LTCs	**No FLEX**				0.51		0.72
	FLEX				n.s.		n.s.

Looking at Table 5.5, one can see that the gas prices of the LTCs with the Netherlands, Russia, and Libya are identical in the "No FLEX" and "FLEX" cases. In fact, the quantities of gas LTCs exchanged between these countries and Italy are the same under the two flexibility assumptions. This explains the effects on the volume re-shuffle between low- and high-demand periods to which we assist in the "FLEX" case, as explained above. The unique exception is Algeria where the LTCs price in the "FLEX"

Table 5.6: Prices spot of gas and LNG under the "NO Risk" assumption (€/cm)

			Low	High
Gas Spot	**No FLEX**		0.31	0.33
	FLEX		0.25	0.32
LNG Spot	**No FLEX**	**AL**	0.49	0.50
		QT	n.s.	n.s.
	FLEX	**AL**	0.31	0.38
		QT	n.s.	n.s.

case is higher than under the "No FLEX" assumption. This is the reason why, in the "FLEX" case, the mid-streamer decides to reduce the amount of gas purchased with LTCs from Algeria and buy this gas on the spot basis at lower prices (compare Algerian prices in Tables 5.5 and 5.6).

Considering Table 5.6, one can notice that the prices of the gas and LNG traded on the spot markets are lower in the "FLEX" case than in the "No FLEX" instance. This is the reason why the mid-streamer increase its purchases on spot.

Finally Table 5.7 reports the prices applied in the two time periods to final consumers in the "no FLEX" and the "FLEX" cases. Note that the prices that the mid-streamer is able to apply to final consumers under the "FLEX" assumption are higher than those imposed in the "no FLEX" case. This indeed allows mid-streamer to increase its revenues and compensate its costs in such a way it does not incur in a profit loss (see Table 5.4).

Table 5.7: Final consumers' prices under the "NO Risk" assumption (€/cm)

	NO Risk No FLEX		**NO Risk FLEX**	
	Low	**High**	**Low**	**High**
Industry	0.39	0.48	0.57	0.60
Power sector	0.37	0.45	0.55	0.58
Residential/commercial	0.47	0.56	0.65	0.68

5.5.2 External supply risk

In this section, we analyze the effects of the application of the external supply risk in the "No FLEX" and "FLEX" cases. We recall that the risk is applied only on gas and LNG LTCs.

The main outcomes are as follows. The external supply risk does not affect the mid-streamer's behaviur in the "No FLEX" case since the total volume of exchanged gas and LNG both via LTCs and on spot are as under the "NO Risk No FLEX"

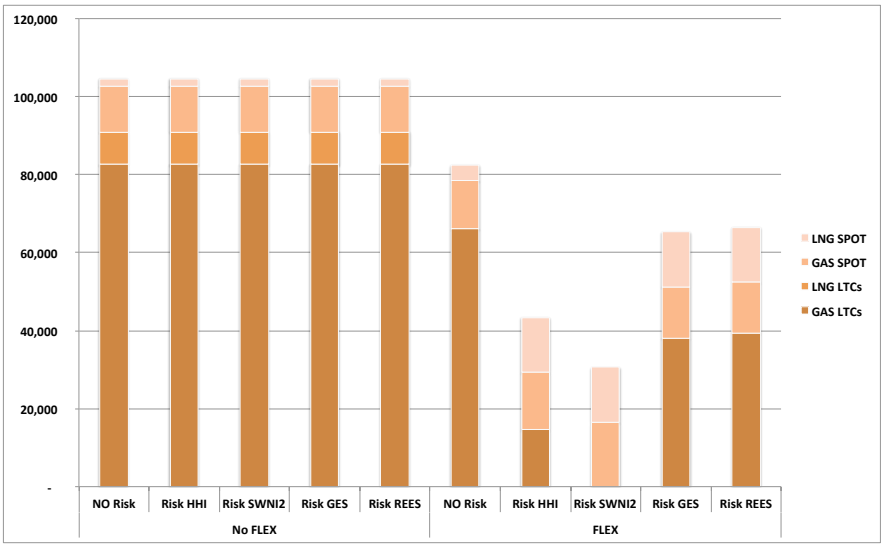

Figure 5.5: Yearly volume of gas exchanged per type (mcm/year)

assumption (see Fig. 5.5) with the consequence that the total quantity of gas offered to final consumers remains unchanged (see Fig. 5.13). Moreover, no changes in the supplying country mix is encountered with respect to the not-flexible risk without risk. As in the "NO Risk No FLEX" case, the mid-streamer accomplishes the natural gas and LNG LTCs independently of the risk measure considered (see Fig. 5.6 and 5.7).

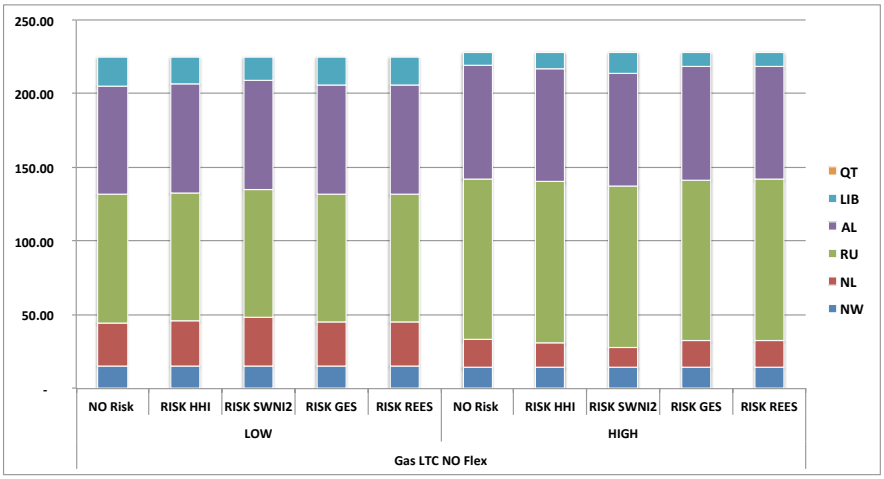

Figure 5.6: Volumes of gas exchanged via LTCs under the "Risk" and "No FLEX" assumptions (mcm/day)

This depends on the fact that the mid-streamer must satisfy the LTC volume clause and it has, at least, to buy the volumes of gas and LNG that it has already contracted. The risk does not either affect the spot supply, even though the mid-streamer does not have any constraints on the amount of gas and LNG that it has to buy on the spot

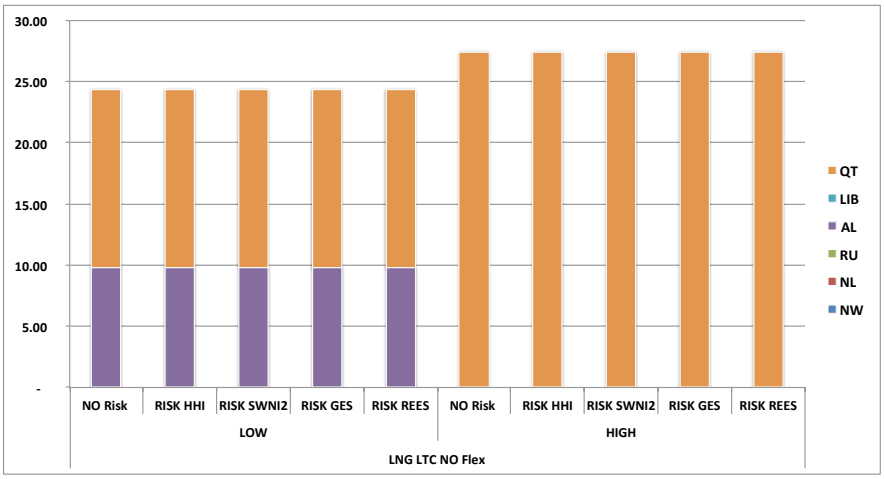

Figure 5.7: Volumes of LNG exchanged via LTCs under the "Risk" and "No FLEX" assumptions (mcm/day)

markets (see Fig. 5.8 and 5.9).

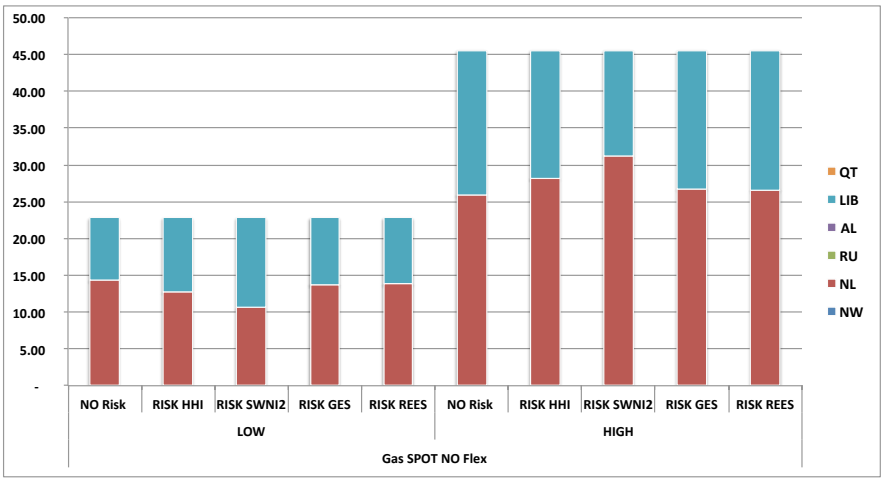

Figure 5.8: Volumes of spot gas exchanged under the "Risk" and "No FLEX" assumptions (mcm/day)

In other words, the external supply risk does not have significant impacts on the mid-streamer's strategies when no flexibility is allowed. We register only some shifts between the quantities of the LTCs and spot gas purchased in the low- and in the high-demand period (see Fig. 5.6 and 5.8, respectively). This implies that the gas and LNG prices as well as those paid by the final consumers in all "Risk No Flex" cases are identical to those reported in Tables (5.5)-(5.7) for the corresponding "NO Risk No Flex" case, independently of the considered external supply risk indicator. The same holds for the social welfare of the gas supply chain and the profits/surplus of its player groups.

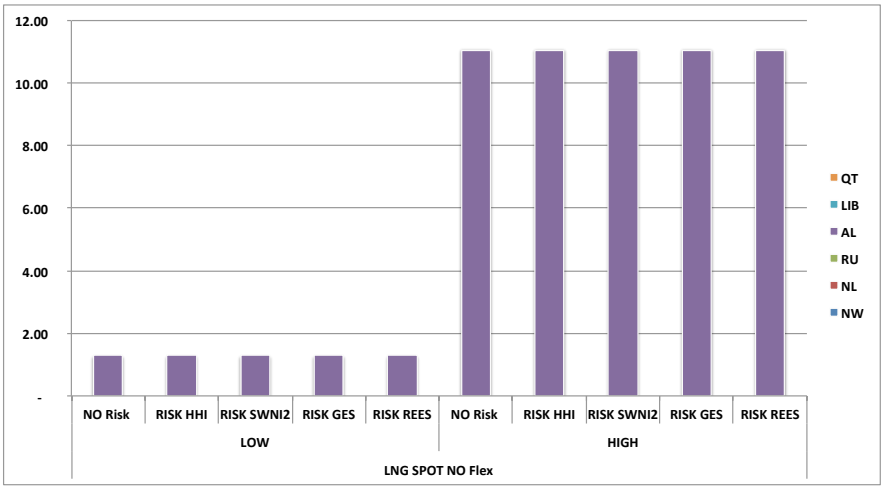

Figure 5.9: Volumes of natural gas exchanged via LTCs under the "Risk" and "No FLEX" assumptions (mcm/day)

The situation in the "Risk FLEX" cases remains in line with that described under the "NO Risk FLEX" assumption and, depending on the considered supply risk indicator, it is even more exacerbated. The mid-streamer's actions in the "Risk FLEX" cases can be summarized with the following items (see Fig. 5.5 and Fig. 5.10-5.12):

1. The total amount of natural gas that is traded in the "Risk FLEX" cases is lower than under the "NO Risk FLEX" assumption. This is particular evident when the Π_{nm}^{HHI} and $\Pi_{nm}^{SWNI_2}$ indicators are applied. Globally, we register a significant drop of gas imports compared to the "No FLEX" cases;

2. In the "Risk FLEX" cases, the mid-streamer modifies the mix of supplying countries depending on the applied risk indicator;

3. The amount of gas that the mid-streamer exchanges with LTCs in the "Risk FLEX" cases is lower than the corresponding one in the "NO Risk FLEX" because the risk induces the mid-streamer to buy cheaper gas and LNG on the respective spot markets;

4. The volumes of gas and LNG that are exchanged on the spot markets increases under the "Risk FLEX" assumptions compared to the "NO Risk FLEX" (and also "NO Risk No FLEX") cases, but this increase does not suffice to recover the amount of gas that is not bought with LTCs;

5. As in the "NO Risk FLEX" case, also under all "Risk FLEX" assumptions, the mid-streamer does not respect the volume TOP clause of the LNG LTCs; i.e. no LNG is exchanged with contracts.

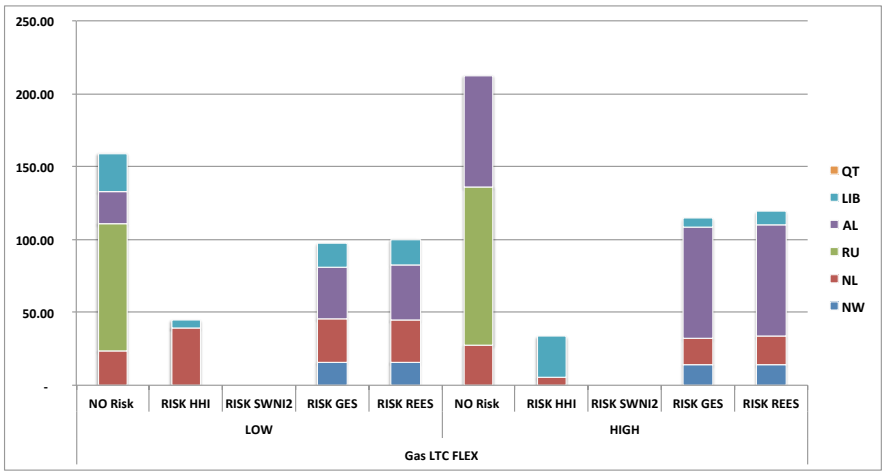

Figure 5.10: Volumes of natural gas exchanged via LTCs under the "Risk" and "FLEX" assumptions (mcm/day)

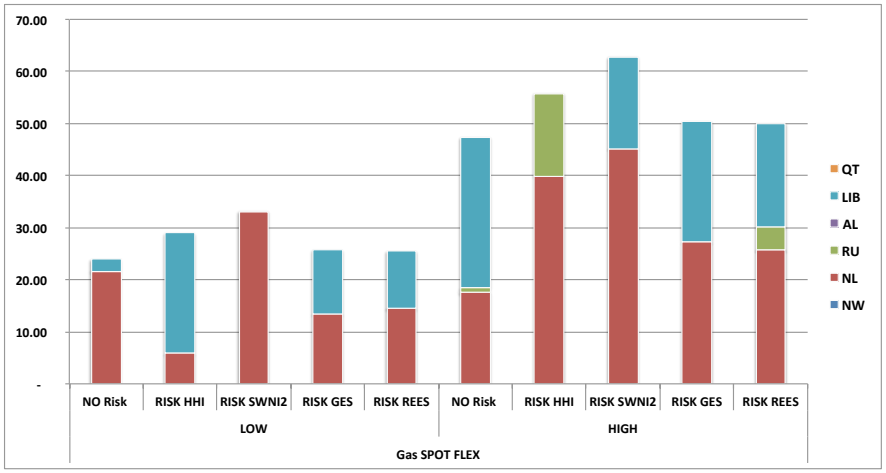

Figure 5.11: Volumes of spot gas exchanged under the "Risk" and "FLEX" assumptions (mcm/day)

Table 5.8 provides a summary of the supplying countries that exchanges the different types of gas with Italy under the risk and flexibility assumptions. These are compared to the results obtained in the "NO Risk FLEX" case. For each case analyzed, "Yes" in the table cells indicates that there is a trade and the subsequent percentage reported in brackets corresponds to the weight in terms of volumes that the considered country has in the Italian supply mix. The symbol "-" means that no exchanges of gas or LNG are allowed between Italy and the producer, while "-No" means that Italy does not import from the specific country even though it has the possibility to do it. The provenience of spot gas and LNG is not affected by risk since the relative indicators are applied only on LTCs. As we already observed, there is an increase of the total volume of spot gas and LNG that is imported both from Algeria and Qatar, but this

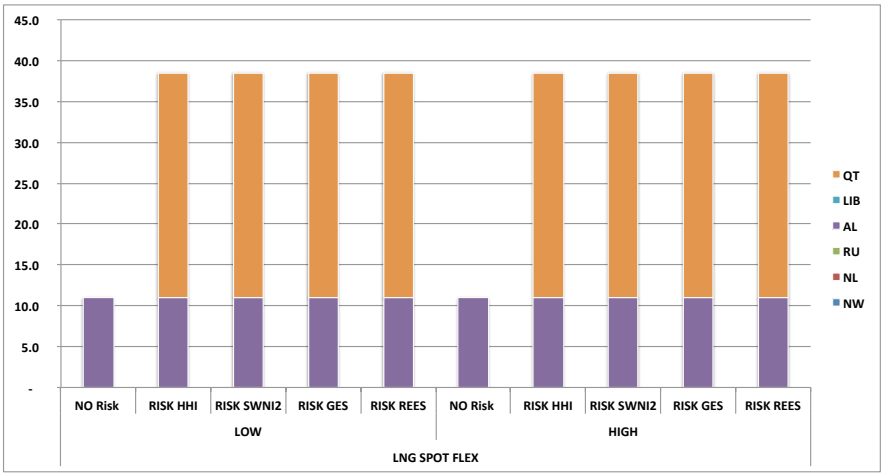

Figure 5.12: Volumes of spot LNG exchanged under the "Risk" and "FLEX" assumptions (mcm/day)

increase is not enough to restore the gas volume availability guaranteed by the respect of LTCs. The inclusion of risk has a significant impact on the external supply of gas with LTCs because the mid-streamer changes the provenience and the proportion of gas imported depending on the indicator. The principle driving the mid-streamer's choice is considering not risky countries. For instance, under the Π_{nm}^{HHI}, the mid-streamer decides to fully respect the gas LTCs with the Netherlands and Libya because these are the two countries with the lowest risk level (see $\Pi_{nm}^{HHI,G}$ in Table 5.2). The same happens when applying the other risk indicators. Note that the gas contracts with Russia are not honored because this is the producer with the highest risk in all considered indicators and, moreover, the mid-streamer does not accomplish to any gas LTCs under the $\Pi_{nm}^{SWNI_2}$ since the risk values associated with the different countries in this indicator are extremely high, much higher than those of the other indicators (see Table 5.2). On the other side, the mid-streamers does not buy LNG with contracts but prefers to resort to its purchase on spot, as it happens in the "NO Risk FLEX" case. This drop of natural gas import with LTCs has been already observed in Section 5.5.1 when describing the effect of the "NO Risk FLEX" case. The combination of the flexibility with the risk assumption exacerbates the phenomenon, implying a significant reduction of the total gas offered to final consumers in the "Risk FLEX" cases (see Fig. 5.13). Only the residential/commercial sector maintains a relative adequate supply level, even though lower than in the corresponding "Risk No FLEX" and "Risk FLEX" cases, whereas industries and power generators face a significant curtailment. These two sectors are not even supplied when the $\Pi_{nm}^{SWNI_2}$ risk applies.

The mid-streamer behaves in this way because it wants to limit its exposure to risk, but mostly because it desires to mitigate its possible profit losses. This issue has

Table 5.8: Supplying countries that exchange gas and LNG with Italy under the "Risk" and "FLEX" assumptions

		NW	NL	RU	AL	LIB	QT
Gas LTCs	**NO Risk**	**No**	Yes (14%)	Yes (54%)	Yes (25%)	Yes (8%)	-
	Risk Π_{nm}^{HHI}	**No**	Yes (62%)	**No**	**No**	Yes (38%)	-
	Risk $\Pi_{nm}^{SWNI_2}$	**No**	**No**	**No**	**No**	**No**	-
	Risk Π_{nm}^{GES}	Yes (15%)	Yes (24%)	**No**	Yes (50%)	Yes (11%)	-
	Risk Π_{nm}^{REES}	Yes (14%)	Yes (23%)	**No**	Yes (50%)	Yes (13%)	-
LNG LTCs	**NO Risk**	-	-	-	**No**	-	**No**
	Risk Π_{nm}^{HHI}	-	-	-	**No**	-	**No**
	Risk $\Pi_{nm}^{SWNI_2}$	-	-	-	**No**	-	**No**
	Risk Π_{nm}^{GES}	-	-	-	**No**	-	**No**
	Risk Π_{nm}^{REES}	-	-	-	**No**	-	**No**
Gas Spot	**NO Risk**	**No**	Yes (59%)	Yes (1%)	**No**	Yes (40%)	-
	Risk Π_{nm}^{HHI}	**No**	Yes (50%)	Yes (16%)	**No**	Yes (34%)	-
	Risk $\Pi_{nm}^{SWNI_2}$	**No**	Yes (84%)	**No**	**No**	Yes (16%)	-
	Risk Π_{nm}^{GES}	**No**	Yes (53%)	**No**	**No**	Yes (47%)	-
	Risk Π_{nm}^{REES}	**No**	Yes (54%)	Yes (5%)	**No**	Yes (41%)	-
LNG Spot	**NO Risk**	-	-	-	Yes (100%)	-	**No**
	Risk Π_{nm}^{HHI}	-	-	-	Yes (29%)	-	Yes (71%)
	Risk $\Pi_{nm}^{SWNI_2}$	-	-	-	Yes (29%)	-	Yes (71%)
	Risk Π_{nm}^{GES}	-	-	-	Yes (29%)	-	Yes (71%)
	Risk Π_{nm}^{REES}	-	-	-	Yes (29%)	-	Yes (71%)

already been detected in Section 5.5.1 when discussing the "NO Risk FLEX" case.

Table 5.9 reports supplying countries and the mid-streamer's profits, the final gas consumers' surplus, and the social welfare in the "NO Risk FLEX" and in the "Risk FLEX" cases. In all "FLEX" cases, the mid-streamer's profits are positive thanks to the set of strategies that it adopts. Note that the significant curtailment of the expensive gas volumes traded with LTCs under the risk assumption allows the mid-streamer to

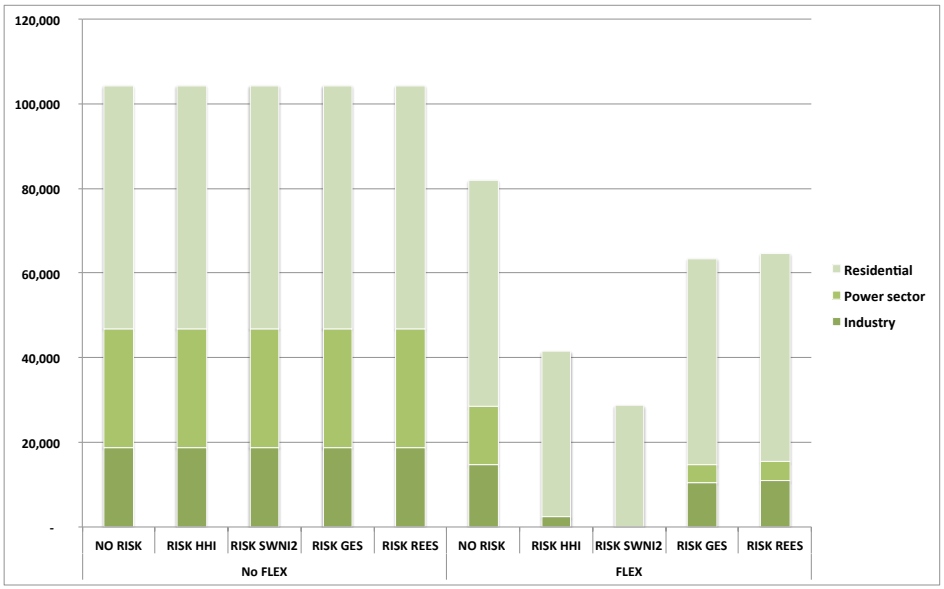

Figure 5.13: Yearly demand per consumer group (mcm/year)

Table 5.9: Supplying countries and mid-streamer's profits, final consumers' surplus, and social welfare under the "NO Risk" assumption (€/year)

FLEX						
		No Risk	**Risk Π_{nm}^{HHI}**	**Risk $\Pi_{nm}^{SWNI_2}$**	**Risk Π_{nm}^{GES}**	**Risk Π_{nm}^{REES}**
Supplying countries	Revenues	38,342	23,346	21,272	30,178	30,692
	Production costs	11,171	6,986	5,232	10,139	10,285
	Transportation costs	27,188	11,880	8,214	20,166	20,630
	Net Profits	**-17**	**4,480**	**7,825**	**-128**	**-223**
Mid-streamer	Revenues	52,550	49,877	45,647	52,481	52,464
	Distribution costs	9,895	6,247	4,471	8,472	8,579
	Purchase costs	38,342	23,346	21,272	30,178	30,692
	Regasification costs	53	185	185	185	185
	Injection costs	150	133	79	160	161
	Net Profits	**4,110**	**19,966**	**19,640**	**13,486**	**12,846**
Final consumers	Industry's surplus	13,962	961	-	7,436	7,934
	Power Sector 's surplus	4,899	-	-	945	1,122
	Residenatial's surplus	159,711	86,322	47,453	133,285	135,427
	Total surplus	**178,572**	**87,283**	**47,453**	**141,666**	**144,483**
Social welfare		**182,664**	**111,728**	**74,918**	**155,024**	**157,107**

increase its net profit compared to the "NO Risk FLEX" case. This is also due to the fact that the prices imposed to final consumers are higher than under the "NO Risk FLEX" assumption (see Table 5.11). This is particular evident when the $\Pi_{nm}^{SWNI_2}$ risk is implemented, since no gas/LNG is purchased with LTCs, but also when applying the Π_{nm}^{HHI} where the amount of gas/LNG bought on spot is proportionally higher than that imported with LTCs. This indeed has a negative impact on final consumers that see their surplus reducing with respect to the "NO Risk FLEX" assumption. In fact, the lowest consumers' surplus is registered when the $\Pi_{nm}^{SWNI_2}$ risk is applied. The effects

of the risk implementation on supplying countries' profits vary according to the risk indicator analyzed. In particular, supplying countries globally face losses when the risk indicators Π_{nm}^{GES} and Π_{nm}^{REES} are considered, while they gain with the Π_{nm}^{HHI} and $\Pi_{nm}^{SWNI_2}$ measures. Note that these losses are higher than in the "NO Risk FLEX" case. In this latest case, it is true that their revenues are lower, but also the associated production and transportation costs are limited. This allows supplying countries to gain from the situation.

Table 5.10 reports the LTC prices for gas under the "NO Risk FLEX" and "Risk FLEX" assumptions. One can note that the risk leads to the a slight increase of these prices.

In conclusion, the "FLEX" strategy is more protecting for the mid-streamers, but it does not result to be beneficial for the whole supply chain that registers a reduction of the social welfare. This phenomenon becomes more extreme with the application of the external supply risk measures.

Table 5.10: Prices of gas LTCs under the "Risk FLEX" assumptions (€/cm)

	FLEX					
	NW	**NL**	**RU**	**AL**	**LIB**	**QT**
NO Risk	n.s.	0.38	0.51	0.55	0.41	
Risk Π_{nm}^{HHI}	n.s.	0.39	n.s.	n.s.	0.43	
Risk $\Pi_{nm}^{SWNI_2}$	n.s.	n.s.	n.s.	n.s.	n.s.	
Risk Π_{nm}^{GES}	0.56	0.41	n.s.	0.56	0.43	
Risk Π_{nm}^{REES}	0.55	0.40	n.s.	0.56	0.42	

Table 5.11: Final consumers' prices under the "Risk FLEX" assumptions (€/cm)

	FLEX									
	NO Risk FLEX		**Risk** Π_{nm}^{HHI}		**Risk** $\Pi_{nm}^{SWNI_2}$		**Risk** Π_{nm}^{GES}		**Risk** Π_{nm}^{REES}	
	Low	**High**	**Low**	**High**	**Low**	**High**	**Low**	**High**	**Low**	**High**
Industry	0.57	0.60	1.05	1.13	n.s.	n.s.	0.74	0.77	0.73	0.76
Power Sector	0.55	0.58	n.s.	n.s.	n.s.	n.s.	0.65	0.75	0.65	0.73
Residenatial	0.65	0.68	1.18	1.21	1.56	1.59	0.82	0.86	0.81	0.84

5.6 Conclusions

In this work, we analyze the security of the external supply of the Italian gas market that mainly relies on imports to satisfy its gas demand. In particular, we develop an optimization problem model that describes the equilibrium state of a natural gas supply chain where supplying countries, mid-streamers and consumers exchange natural gas and LNG both with LTCs and on the spot market.

Mid-streamers who buy natural gas and LNG are assumed to be the market player mainly exposed to the external supply risk associated with the imports from foreign countries. In other words, mid-streamers define the amount of gas and LNG to be imported not only on the basis of the relative production and transportation costs, but also on the external supply risk associated with the countries from which the gas originates. The external supply risk is measured through indicators that we construct starting from those already existing in the literature. These indicators are then inserted in the volume balance constraints of the gas and LNG LTCs.

In addition to the impact of the external supply risk, we analyze different degrees of mid-streamer's flexibility. In particular, we consider both a situation where the mid-streamer fully satisfies the LTCs quantity clause and a case where the mid-streamer behaves in a more flexible way and it is not obliged to fulfill the LTC volume requirements.

Our analysis shows that, if the mid-streamer have to comply with the LTCs quantity clause ("No FLEX" assumption), it does not significantly change its supplying choices even when the risk is considered. Under this assumption, the mid-streamer faces significant losses, while the supplying countries gain. In contrast, these mid-streamers' losses disappear when it is not obliged to fully satisfy the LTCs requirements ("FLEX" case) because it is able to modify its supply mix. In particular, compared to the "No FLEX" case, it reduces the amount of gas imported with LTCs because it is more expensive and increases the quantity of cheaper spot gas. In addition, it increases its imports from less risky countries when possible. However, this flexible mid-streamer's behaviur has several drawbacks compared to the "No FLEX" case: the suppliers can face losses because of the significant drop in their revenues; the total amount of gas and LNG purchased drops because the decrease of the quantity of gas imported via LTCs is not fully compensated by the increase of the spot gas or LNG. This also leads to a reduction of gas availability for final consumers. In particular, the mid-streamer still guarantee the gas supply to the residential/commercial sector, but it decreases the supply to the power companies and to industries with respect to the "No FLEX" case. Considering these results, it turns out that LTCs are necessary to maintain the stability and to guarantee the security of supply, even though this may incur in losses for the mid-streamers. The "FLEX" strategy is more protecting for the mid-streamers, but it does not result to be beneficial for the society. This phenomenon becomes more extreme with the application of the external supply risk measures.

Chapter 6

Closure

6.1 Summary

This thesis can be seen as an attempt to study relevant issues related to the decarbonization of electricity and gas markets. Renewable energy generation is seen as one of the most effective ways to curb climate change, and intermittent sources like wind and solar are considered to be those with the highest potential. Anyway, renewable generation implies dealing with issues related to the variability and predictability of these sources, which represent a challenge for the power system. Possible solutions include integrating storage units to provide flexibility and use gas-fired plants as backup capacity. Because of the crucial role played by gas market in achieving the decarbonization targets, issues related to gas procurement in Europe are also analyzed. In particular, we investigate the re-negotiation of the LTCs required by European mid-streamers to make LTC gas prices more aligned with those resulting from the spot trading at the hubs. Moreover, we consider the issue of the risk of external supply, with a particular focus on the Italian gas market. The need of investigating this topic arises from the fact that most of the European Member States, and especially Italy, relies on imports from politically and economically unstable countries to cover their demand.

6.2 Conclusions

In this section, we briefly recall the main conclusions derived from the work developed in this thesis. Please refer to chapter related conclusions for additional details.

Policy mechanisms are needed to internalize the societal cost of carbon and address the transformation of the electric power system required by the decarbonization process. Onshore wind represents the best option to reach immediate emission reduction. Anyway, if CSP achieves its projected cost decrease and efficiency gains, it can become

an extremely competitive alternative. Moreover, the role of storage is fundamental in a renewable-dominated electric power system because it provides flexibility and allows for costs saving by serving electricity during peak hours. Electricity should also contribute to the decarbonization of the transport sector by facilitating the integration of electric vehicles. Benefits in terms of carbon emission reduction deriving from the EVs' usage are already tangible with the actual electricity generation mix, but these are expected to grow with the progressive increase of the renewable energy penetration expected in the years to come.

As indicated in the Energy Roadmap 2050, natural gas is the cheapest fossil fuel, and combined cycle power plants represent the most convenient electricity generation units in terms of both cost/efficiency ratio and emission rate. From a technological point of view, our analysis shows that the integration of the CCS mechanism in gas-fired power plants is a plausible option for the future in order to completely abate their carbon emissions. This is a general outcome that could be valid for all gas markets. However, considering our analysis of the European gas market, we can conclude that the LTCs need to be re-negotiated by also including, among the oil-based underlying assets, spot prices of gas traded at the hubs. Under this framework, introducing spot gas indexation might help mid-streamers' to compensate for possible losses caused by the accomplishment to quantity clause that anyway it is important to maintain the security of gas supply. The quantity clause is also a key issue in the analysis of the risk associated with external gas supply. Our analysis shows that, if the mid-streamer have to comply with the LTCs quantity clause, it does not significantly change its supplying choices even when the risk is considered. Under this assumption, the mid-streamer faces significant losses, while the supplying countries gain. In contrast, these mid-streamers' losses disappear when it is not obliged to fully satisfy the LTCs requirements because it is able to modify its supply mix.

6.3 Future Research

The models developed in the thesis project could be improved and further developed under different aspects. For this reason, we provide future research suggestions in the following:

- To extend the model proposed in Chapter 2 by developing a multi-stage stochastic optimization planning investment model with decarbonization targets.

- To consider alternative clustering methods, such as hierarchical agglomerative clustering using Ward's method, which has been shown to perform well when

dealing with a combination of renewable sources with atypical pattern (wind) and storage.

- To increase the number of operating conditions and scenarios and adopt a Bender's decomposition approach for the solution of the model investigated in the Chapters 2 and 3.
- To apply the models proposed in Chapter 2 to a realistic case study on the European electricity market and include pumped hydro storage as standalone storage unit.
- To compare the solutions of a stochastic optimization approach with those of an adaptive robust optimization approach by applying these two methodologies on the same problem.
- To consider smart charging strategies and vehicle-to grid systems in the planning of a SSEES as possible development of model investigated in Chapter 3.
- To develop the model formulated in Chapter 5 by introducing stochasticity in the demand by considering future consumption evolution by sector in the equilibrium problem on the gas supply chain.

Bibliography

Aas, K., Czado, C., Frigessi, A., and Bakken, H. (2009). Pair-copula constructions of multiple dependence. *Insurance: Mathematics and Economics*, 44:182–198.

Abada, I., Ehrenmann, A., and Smeers, Y. (2017). Modeling gas markets with endogenous long-term contracts. *Operations research*, 65(4):856–877.

Accioly, R. M. S. and Aiube, F. A. L. (2008). Analysis of crude oil and gasoline prices through copulas. *Cadernos do IME- Série Estatìstica*, 24:5–28.

ACER (2015). *European Gas Target Model review and update*. Agency for the Cooperation of Energy Regulators, Trg republike 3, 1000 Ljubljana, Slovenia.

Ackermann, T., Andersson, G., and Söder, L. (2001). Distributed generation: a definition1. *Electric power systems research*, 57(3):195–204.

AEEGSI (2016). *Relazione annuale sullo stato dei servizi e sull'attività svolta*. Autorità per l'Energia Elettrica il Gas e il Sistema Idrico, Corso di Porta Vittoria, 27 - 20122 Milano.

Aloui, R., Aïssa, M. S. B., and Nguyen, D. K. (2013). Conditional dependence structure between oil prices and exchange rates: a copula-garch approach. *Journal of International Money and Finance*, 32:719–738.

Barbour, E., Mignard, D., Ding, Y., and Li, Y. (2015). Adiabatic Compressed Air Energy Storage with packed bed thermal energy storage. *Applied Energy*, 155:804–815.

Baringo, A. and Baringo, L. (2017). A stochastic adaptive robust optimization approach for the offering strategy of a virtual power plant. *IEEE Transactions on Power Systems, 32(5)*, pages 3492–3504.

Baringo, L. and Baringo, A. (2018). A stochastic adaptive robust optimization approach for the generation and transmission expansion planning. *IEEE Transactions on Power Systems, 33(1)*, pages 792–802.

Baringo, L. and Conejo, A. (2013). Correlated wind-power production and electric load scenarios for investment decisions. *Applied energy*, 101:475–482.

Barnes, F. S., Budd, D. A., Lim, M., and Freeman, E. R. (2015). Compressed Air Energy Storage (CAES). In Cabeza, L. F., Sioshansi, R., and Yan, J., editors, *Handbook of Clean Energy Systems*, volume 5, Energy Storage, chapter 19, pages 2717–2742. John Wiley & Sons Ltd, West Sussex, United Kingdom.

Bassetti, F., De Giuli, M. E., Nicolino, E., and Tarantola, C. (2018). Multivariate dependence analysis via tree copula models: An application to one-year forward energy contracts. *European Journal of Operational Research*, pages 1–15.

Bedford, T. and Cooke, R. M. (2001). Probability density decomposition for conditionally dependent random variables modeled by vines. *Annals of Mathematics and Artificial Intelligence*, 32:245–268.

Bedford, T. and Cooke, R. M. (2002). Vines: A new graphical model for dependent random variables. *Annals of Statistics*, pages 1031–1068.

Bekiros, S., Hernandez, J. A., Hammoudeh, S., and Nguyen, D. K. (2015). Multivariate dependence risk and portfolio optimization: An application to mining stock portfolios. *Resources Policy*, 46:1–11.

Ben-Tal, A., El Ghaoui, L., and Nemirovski, A. (2009). *Robust optimization*, volume 28. Princeton University Press.

Bertsimas, D. and Brown, D. B. (2009). Constructing uncertainty sets for robust linear optimization. *Operations Research, 57(6)*, pages 1483–1495.

Bertsimas, D., Brown, D. B., and Caramanis, C. (2011). Theory and applications of robust optimization. *SIAM Review, 53(3)*, pages 464–501.

Bertsimas, D. and Sim, M. (2003). Robust discrete optimization and network flows. *Mathematical Programming, 98 (13)*, pages 49–71.

Bertsimas, D. and Sim, M. (2004). The price of robustness. *Operations Research, 52*, pages 35–53.

Bilgili, M., Yasar, A., and Simsek, E. (2011). Offshore wind power development in europe and its comparison with onshore counterpart. *Renewable and Sustainable Energy Reviews*, 15(2):905–915.

Birge, J. R. and Louveaux, F. (1997). *Introduction to Stochastic Programming*. Springer-Verlag, New York, NY.

Blair, N., Dobos, A. P., Freeman, J., Neises, T., Wagner, M., Ferguson, T., Gilman, P., and Janzou, S. (2014). System Advisor Model, SAM 2014.1.14: General Description. Technical Report NREL/TP-6A20-61019, National Renewable Energy Laboratory.

Blyth, W. and Lefevre, N. (2004). *Energy Security and Climate Change: An Assessment Framework*. International Energy Agency & Organisation for Economic Co-operation and Development.

BP (2016). *Statistical Review of World Energy 2016-Natural gas*. 1 St James's Square, London, United Kingdom.

Brechmann, E. C. and Czado, C. (2013). Risk management with high-dimensional vine copulas: an analysis of the euro stoxx 50. *Stat. Risk Model*, 30:307–342.

Calderón, S., Alvarez, A. C., Loboguerrero, A. M., Arango, S., Calvin, K., Kober, T., Daenzer, K., and Fisher-Vanden, K. (2016). Achieving CO_2 reductions in Colombia: Effects of carbon taxes and abatement targets. *Energy Economics*, 56:575–586.

Chekhlov, A., Uryasev, S., and Zabarankin, M. (2005). Drawdown measure in portfolio optimization. *International Journal of Theoretical and Applied Finance*, 8:13–58.

Chyong, C. K. (2015). Markets and long-term contracts: The case of russian gas supplies to europe. Working Paper 1524, EPRG.

Clarke, K. A. (2007). A simple distribution-free test for nonnested model selection. *Political Analysis*, 15:347–363.

Cohen, G., Joutz, F., and Loungani, P. (2011). Measuring energy security: Trends in the diversification of oil and natural gas supplies. *Energy policy*, 39(9):4860–4869.

Conejo, A. J. and Baringo, L. (2018). *Power System Operations*. Springer.

Conejo, A. J., Carrión, M., and Morales, J. M. (2010). *Decision making under uncertainty in electricity markets*, volume 1. Springer.

Conejo, A. J., Morales, L. B., Kazempour, S. J., and Siddiqui, A. S. (2016). *Investment in Electricity Generation and Transmission: Decision Making Under Uncertainty*. Springer.

Correljé, A. (2016). The european natural gas market. *Current Sustainable/Renewable Energy Reports*, 3(1-2):28–34.

Czado, C., Min, A., Baumann, T., and Dakovic, R. (2009). Pair-copula constructions for modeling exchange rate dependence. Preprint.

Czado, C., Schepsmeier, U., and Min, A. (2012). Maximum likelihood estimation of mixed c-vines with application to exchange rates. *Statistical Modelling*, 12(3):229–255.

Dalla Valle, L., Giuli, M. E. D., Tarantola, C., and Manelli, C. (2016). Default probability estimation via pair-copula constructions. *European Journal of Operational Research*, 249:298–311.

Das, T., Krishnan, V., Gu, Y., and McCalley, J. D. (2011). Compressed Air Energy Storage: State Space Modeling and Performance Analysis. In *2011 Power and Energy Society General Meeting*, San Diego, CA. Institute of Electrical and Electronics Engineers.

Denholm, P., Ela, E., Kirby, B., and Milligan, M. R. (2010). The Role of Energy Storage with Renewable Electricity Generation. Technical Report NREL/TP-6A2-47187, National Renewable Energy Laboratory.

Di Sbroiavacca, N., Nadal, G., Lallana, F., Falzon, J., and Calvin, K. (2016). Emissions reduction scenarios in the Argentinean Energy Sector. *Energy Economics*, 56:552–563.

Dickey, D. and Fuller, W. (1981). Likelihood ratio statistics for autoregressive time series with a unit root. *Econometrica*, 49:1057–1072.

Dirkse, S. P. and Ferris, M. C. (1995). The path solver: a nommonotone stabilization scheme for mixed complementarity problems. *Optimization Methods and Software*, 5(2):123–156.

Dißmann, J., Brechmann, E., Czado, C., and Kurowicka, D. (2013). Selecting and estimating regular vine copulae and application to financial returns. *Computational Statistics & Data Analysis*, 59:52–69.

Divya, K. and Østergaard, J. (2009). Battery energy storage technology for power systemsâĂŤan overview. *Electric Power Systems Research*, 79(4):511–520.

Dobrota, D., Lalić, B., and Komar, I. (2013). Problem of boil-off in lng supply chain. *Transactions on maritime science*, 2(02):91–100.

Domínguez, R., Conejo, A. J., and Carrión, M. (2015). Toward fully renewable electric energy systems. *IEEE Transactions on Power Systems*, 30(1):316–326.

Draxl, C., Clifton, A., Hodge, B.-M., and McCaa, J. (2015a). The Wind Integration National Dataset (WIND) Toolkit. *Applied Energy*, 151:353–366.

Draxl, C., Hodge, B.-M., Clifton, A., and McCaa, J. (2015b). Overview and Meteorological Validation of the Wind Integration National Dataset Toolkit. Technical Report NREL/TP-5000-61740, National Renewable Energy Laboratory.

Drury, E., Denholm, P., and Sioshansi, R. (2011). The Value of Compressed Air Energy Storage in Energy and Reserve Markets. *Energy*, 36:4959–4973.

Durante, F. and Sempi, C. (2015). *Principles of copula theory*. London, Chapman and Hall/CRC.

Egging, R. (2013). Benders decomposition for multi-stage stochastic mixed complementarity problems–applied to a global natural gas market model. *European Journal of Operational Research*, 226(2):341–353.

Egging, R., Gabriel, S. A., Holz, F., and Zhuang, J. (2008). A complementarity model for the european natural gas market. *Energy policy*, 36(7):2385–2414.

Egging, R. and Holz, F. (2016). Risks in global natural gas markets: investment, hedging and trade. *Energy Policy*, 94:468–479.

Egging, R., Holz, F., and Gabriel, S. A. (2010). The world gas model: A multi-period mixed complementarity model for the global natural gas market. *Energy*, 35(10):4016–4029.

Egging, R. G. and Gabriel, S. A. (2006). Examining market power in the european natural gas market. *Energy Policy*, 34(17):2762–2778.

El Khatib, S. and Galiana, F. D. (2007). Negotiating bilateral contracts in electricity markets. *IEEE Transactions on Power Systems*, 22(2):553–562.

ENTSO-G (2012). *Balancing tools-product definition and deployment*. European Network of Transmission Systsem Operator for Gas, Avenue de Cortenbergh 100 / Kortenberglaan 100, Bruxelles, Belgium.

EU Commission (2011a). *Communication from the Commission to the European Parliament, the Council, The European Economic and Social Committee, the Committee of the Regions and the Committee of the Regions. Energy Roadmap 2050*. European Commission, COM(2011) 885 final edition.

EU Commission (2011b). *White Paper, Roadmap to a Single European Transport Area-Towards a competitive and resource efficient transport system*. European Commission, COM(2011) 144 final edition.

EU Commission (2016). *Communication from the Commission to the European Parliament, the Council, The European Economic and Social Committee, the Committee of the Regions and the Committee of the Regions. A European Strategy for Low-Emission Mobility.* European Commission, COM(2016) 501 final edition.

Facchinei, F. and Pang, J.-S. (2007). *Finite-dimensional variational inequalities and complementarity problems.* Springer Science & Business Media.

Fischer, R., Serra, P., Joskow, P. L., and Hogan, W. W. (2000). Regulating the electricity sector in latin america [with comments]. *Economia*, 1(1):155–218.

Fisher, T. J. and O. Gallagher, C. M. (2012). New weighted portmanteau statistics for time series goodness of fit testing. *Journal of the American Statistical Association*, 107(498):777–787.

Flavin, C. and Kitasei, S. (2010). *The role of natural gas in a low-carbon energy economy.* Worldwatch Institute Washington, DC.

Franza, L. (2014). Long-term gas import contracts in europe. *CIEP paper*, 8.

Frisch, M. (2010). Current european gas pricing problems: solutions based on price review and price reopener provisions. Research paper Series, No 3, International energy law and policy.

Frondel, M. and Schmidt, C. M. (2008). Measuring energy security-a conceptual note. *Ruhr Economic Paper*, No. 52.

Fu, R., Feldman, D., Margolis, R., Woodhouse, M., and Ardani, K. (2017). U.S. Solar Photovoltaic System Cost Benchmark: Q1 2017. Technical Report NREL/TP-6A20-68925, National Renewable Energy Laboratory.

Gabriel, S. A., Conejo, A. J., Fuller, J. D., Hobbs, B. F., and Ruiz, C. (2013). Optimality and complementarity. In *Complementarity Modeling in Energy Markets*, pages 31–69. Springer.

Gaupp, F., Pflug, G., Hochrainer-Stigler, S., Hall, J., and Dadson, S. (2017). Dependency of crop production between global breadbaskets: a copula approach for the assessment of global and regional risk pools. *Risk Analysis*, 37(11):2212–2228.

Genest, C. and Favre, A. C. (2007). Everything you always wanted to know about copula modeling but were afraid to ask. *Journal of Hydrologic Engineering*, 12:347–368.

Genest, C. M. G. and Bourdeau-Brien, M. (2009). The advent of copulas in finance. *The European Journal of Finance*, 15:609–618.

Gibbins, J. and Chalmers, H. (2008). Carbon capture and storage. *Energy policy*, 36(12):4317–4322.

GIIGNL (2018). *The LNG industry*. International Group of Liquefied Natural Gas Importers.

GME (2009). *Vademecum della borsa elettrica*. Gestore Mercati Energetici, Viale Maresciallo Pilsudski, 122/124 Roma, Italia.

Gomez-Exposito, A., Conejo, A. J., and Canizares, C. (2018). *Electric energy systems: analysis and operation*. CRC press.

Graf, C. and Marcantonini, C. (2017). Renewable energy and its impact on thermal generation. *Energy Economics*, 66:421–430.

Graves, F., Jenkin, T., and Murphy, D. (1999). Opportunities for Electricity Storage in Deregulating Markets. *The Electricity Journal*, 12:46–56.

Greenblatt, J. B., Succar, S., Denkenberger, D. C., Williams, R. H., and Socolow, R. H. (2007). Baseload wind energy: modeling the competition between gas turbines and compressed air energy storage for supplemental generation. *Energy Policy*, 35:1474–1492.

Grégoire, V., Genest, C., and Gendron, M. (2008). Using copulas to model price dependencies in energy markets. *Energy Risk*, 5:58–64.

Grubb, M., Butler, L., and Twomey, P. (2006). Diversity and security in uk electricity generation: The influence of low-carbon objectives. *Energy policy*, 34(18):4050–4062.

Gupta, E. (2008). Oil vulnerability index of oil-importing countries. *Energy policy*, 36(3):1195–1211.

GWEC (2016). *Global wind energy outlook 2016*. Global Wind Energy Council, 80 Rue d'Arlon, 1040 Brussels, Belgium.

GWEC (2017). *Global Wind Report: Annual market up date 2017*. Global Wind Energy Council, 80 Rue d'Arlon, 1040 Brussels, Belgium.

Hartmann, N., Vöhringer, O., Kruck, C., and Eltrop, L. (2012). Simulation and analysis of different adiabatic Compressed Air Energy Storage plant configurations. *Applied Energy*, 93:541–548.

Hasan, M. F., Zheng, A. M., and Karimi, I. (2009). Minimizing boil-off losses in liquefied natural gas transportation. *Industrial & engineering chemistry research*, 48(21):9571–9580.

Heather, P. (2012). Continental european gas hubs: Are they fit for purpose? Technical Report 63, NG: Oxford Institute for Energy Studies.

Heather, P. (2015). The evolution of european traded gas hubs. Technical report, Oxford Institute for Energy Studies Oxford.

Heather, P. and Petrovich, B. (2017). European traded gas hubs: an updated analysis on liquidity, maturity and barriers to market integration. Technical report, The Oxford Institute for Energy Studies paper-Energy Insight.

Hernandez, J. A. (2014). Are oil and gas stocks from the australian market riskier than coal and uranium stocks? dependence risk analysis and portfolio optimization. *Energy Economics*, 45:528–536.

Herrero, I., Rodilla, P., Batlle, C., et al. (2018). Enhancing intraday price signals in us iso markets for a better integration of variable energy resources. *The Energy Journal*, 39(3).

Hofert, M., Kojadinovic, I., Maechler, M., and Yan, J. (2017). *Copula*. R package.

Holz, F., Engerer, H., Kemfert, C., Richter, P. M., and von Hirschhausen, C. (2014). *European natural gas infrastructure: The role of Gazprom in European natural gas supplies. Study Commissioned by The Greens/European Free Alliance in the European Parliament*. Number 81. DIW Berlin: Politikberatung kompakt.

Holz, F., Richter, P., and Egging, R. (2013). The role of natural gas in a low-carbon europe: Infrastructure and regional supply security in the global gas model.

Holz, F., Richter, P. M., and Egging, R. (2016). The role of natural gas in a low-carbon europe: Infrastructure and supply security. *Energy Journal*, 37.

Honoré, A. (2013). The italian gas market: Challenges and opportunities. Technical Report 76, Oxford Institute for Energy Studies Oxford.

Hull, J. C. and Basu, S. (2016). *Options, futures, and other derivatives*. Pearson Education India.

IEA (2007). *Energy Security and Climate Change; assessing interactions*. International Energy Agency, 9 rue de la Fédération, 75739 Paris Cedex 15, France.

IEA (2013). *Developing a Natural Gas Trading Hub in Asia-Obstacles and Opportunities*. International Energy Agency, 9 rue de la Fédération, 75739 Paris Cedex 15, France.

IEA (2014a). *Techology Roadmap: Solar Photovoltaic Energy*. International Energy Agency, 9 rue de la Fédération, 75739 Paris Cedex 15, France.

IEA (2014b). *Techology Roadmap: Solar Thermal Electricity*. International Energy Agency, 9 rue de la Fédération, 75739 Paris Cedex 15, France.

IEA (2016a). *Annual Gas Statistic Database*. International Energy Agency, 9 rue de la Fédération, 75739 Paris Cedex 15, France.

IEA (2016b). *Medium-Term Renewable Energy Market Report 2016*. International Energy Agency, 9 rue de la Fédération, 75739 Paris Cedex 15, France.

IEA (2016c). *Updated Capital Cost Estimates for Utility Scale Electricity Generating Plants*. International Energy Agency, 9 rue de la Fédération, 75739 Paris Cedex 15, France.

IEA (2016d). *World Energy Outlook 2016*. International Energy Agency, 9 rue de la Fédération, 75739 Paris Cedex 15, France.

IEA (2017). *Annual Energy Outlook 2017*. International Energy Agency, 9 rue de la Fédération, 75739 Paris Cedex 15, France.

IEA (2018). *Annual Energy Outlook 2018*. International Energy Agency, 9 rue de la Fédération, 75739 Paris Cedex 15, France.

IEA/OECD (2001). *Toward a sustainable energy future*. International Energy Agency & Organisation for Economic Co-operation and Development, Paris.

IRENA (2018a). *Global Energy Transformation: A Roadmap to 2050*. International Renewable Energy Agency, Masdar City, P.O. Box 236, Abu Dhabi, United Arab Emirates.

IRENA (2018b). *Renewable Power Generation Costs in 2017*. International Renewable Energy Agency, Masdar City, P.O. Box 236, Abu Dhabi, United Arab Emirates.

Jabr, R. A. (2013). Robust transmission network expansion planning with uncertain renewable generation and loads. *IEEE Transactions on Power Systems, 28(4)*, pages 4558–4567.

Jäschke, S. (2014). Estimation of risk measures in energy portfolios using modern copula techniques. *Computational Statistics and Data Analysis*, 76:359–376.

Jess, M. (1997). Restructuring energy industries: lessons from natural gas. *Natural Gas Monthly Special Report*.

Jiang, M., Zhang, G. L., and Guan, Y. (2014). Two-stage network constrained robust unit commitment problem. *European Journal of Operational Research, 234(3)*, pages 751–762.

Joe, H. (1996). Families of m-variate distributions with given margins and m(m-1)/2 bivariate dependence parameters. *IMS lecture notes*, 76:359–376.

Joe, H. (1997). *"Multivariate model and dependence concepts"*. Monographs on Statistics an Applied Probability, 73, Chapman, Hall, London.

Jónsson, T., Pinson, P., and Madsen, H. (2010). On the market impact of wind energy forecasts. *Energy Economics*, 32(2):313–320.

Kall, P., Wallace, S. W., and Kall, P. (1994). *Stochastic programming*. Springer.

Karan, M. B. and Kazdağli, H. (2011). The development of energy markets in europe. In *Financial Aspects in Energy*, pages 11–32. Springer.

King, J., Clifton, A., and Hodge, B.-M. (2014). Validation of Power Output for the WIND Toolkit. Technical Report NREL/TP-5D00-61714, National Renewable Energy Laboratory.

Konno, H., Shirakawa, H., and Yamazaki, H. (1993). A mean-absolute deviation-skewness portfolio optimization models. *Annals of Operations Research*, 45(1):205–220.

Krohn, S., Morthorst, P.-E., and Awerbuch, S. (2009). The Economics of Wind Energy. Technical report, European Wind Energy Association.

Kruyt, B., van Vuuren, D. P., de Vries, H. J., and Groenenberg, H. (2009). Indicators for energy security. *Energy policy*, 37(6):2166–2181.

Krzemienowski, A. and Szymczyk, S. (2016). Portfolio optimization with a copula-based extension of conditional value-at-risk. *Annals of Operations Research*, 237(1-2):219–236.

Kurowicka, D. and Cooke, R. (2006). *"Uncertainty analysis with high dimensional dependence modelling"*. Chichester, Wiley.

Kwiatkowski, D., Phillips, P. C. B., Schmidt, P., and Shin, Y. (1992). Testing the null hypothesis of stationarity against the alternative of a unitroot. *Journal of Econometrics*, 54:159–178.

Laing, T., Sato, M., Grubb, M., Comberti, C., et al. (2013). Assessing the effectiveness of the eu emissions trading system. *Centre for Climate Change Economics and Policy Working Paper*, 126.

Le Coq, C. and Paltseva, E. (2009). Measuring the security of external energy supply in the european union. *Energy Policy*, 37(11):4474–4481.

Lee, W.-W. (2004). Us lessons for energy industry restructuring: based on natural gas and california electricity incidences. *Energy Policy*, 32(2):237–259.

Li, X. and You, Y. (2014). A note on allocation of portfolio shares of random assets with Archimedean copula". *Annals of Operations Research*, 212(1):155–167.

Lilliestam, J., Labordena, M., Patt, A., and Pfenninger, S. (2017). Empirically observed learning rates for concentrating solar power and their responses to regime change. *Nature Energy*, 2:1–6.

Liu, J.-L. and Wang, J.-H. (2016). A comparative research of two adiabatic compressed air energy storage systems. *Energy Conversion and Management*, 108:566–578.

Liu, Y., Sioshansi, R., and Conejo, A. J. (2018a). Hierarchical Clustering to Find Representative Operating Periods for Capacity-Expansion Modeling. *IEEE Transactions on Power Systems*, 33:3029–3039.

Liu, Y., Sioshansi, R., and Conejo, A. J. (2018b). Multistage Stochastic Investment Planning with Multiscale Representation of Uncertainties and Decisions. *IEEE Transactions on Power Systems*, 33:781–791.

Lu, X. F., Lai, K. K., and Liang, L. (2014). Portfolio value-at-risk estimation in energy futures markets with time-varying copula-GARCH model. *Annals of Operations Research*, 219:333–357.

MacQueen, J. (1967). Some methods for classification and analysis of multivariate observations. In *Proceedings of the Fifth Berkeley Symposium on Mathematical Statistics and Probability*, volume 1, pages 281–297.

Madaeni, S. H., Sioshansi, R., and Denholm, P. (2012). How Thermal Energy Storage Enhances the Economic Viability of Concentrating Solar Power. *Proceedings of the IEEE*, 100:335–347.

Mandelbrot, B. B. (1963). The variation of certain speculative prices. *The Journal of Business*, 36:394–419.

Markowitz, H. (1952). Portfolio selection. *The journal of finance*, 7(1):77–91.

Mauritsen, T. and Pincus, R. (2017). Committed warming inferred from observations. *Nature Climate Change*.

Melling, A. J. (2010). Natural gas pricing and its future-europe ad the battleground. Technical report, Carnegie Endowment for international peace.

Mínguez, R. and García-Bertrand, R. (2016). Robust transmission network expansion planning in energy systems: Improving computational performance. *European Journal of Operational Research, 248 (1)*, pages 21–32.

Morales, J. M., Conejo, A. J., Madsen, H., Pinson, P., and Zugno, M. (2013). *Integrating renewables in electricity markets: operational problems*, volume 205. Springer Science & Business Media.

Morales-Napoles, O. (2010). Counting vines. *Dependence modeling: vine copula handbook*, pages 189–218.

Nagurney, A. (1999). Network economics: A variational inequality approach (revised second edition) kluwer academic publishers.

Nair, N.-K. C. and Garimella, N. (2010). Battery energy storage systems: Assessment for small-scale renewable energy integration. *Energy and Buildings*, 42(11):2124–2130.

Neises, T. W. and Turchi, C. S. (2014). A Comparison of Supercritical Carbon Dioxide Power Cycle Configurations with an Emphasis on CSP Applications. *Energy Procedia*, 49:1187–1196.

Nelsen, R. B. (1999). *An introduction to copulas*. Springer-Verlag Lecture Notes in Statistics, 139, New York.

NERA (2014). *Updated Macroeconomic Impacts of LNG Exports from the United States*. NERA economic consulting.

Neumann, A. (2004). Security of supply in liberalised european gas markets. *Europa-University Viadrina Frankfurt/Oder*, pages 17–20.

Pandžić, H., Wang, Y., Qiu, T., Dvorkin, Y., and Kirschen, D. S. (2015). Near-optimal method for siting and sizing of distributed storage in a transmission network. *IEEE Transactions on Power Systems, 30(5)*, pages 2288–2300.

Phillips, P. C. B. and Perron, P. (1988). Testing for unit roots in time series regression. *Biometrika*, 75:335–346.

Pickard, W. F., Shen, A. Q., and Hansing, N. J. (2009). Parking the power: Strategies and physical limitations for bulk energy storage in supply–demand matching on a grid whose input power is provided by intermittent sources. *Renewable and Sustainable Energy Reviews*, 13(8):1934–1945.

Prékopa, A. (2013). *Stochastic programming*, volume 324. Springer Science & Business Media.

Qi, T., Weng, Y., Zhang, X., and He, J. (2016). An analysis of the driving factors of energy-related CO_2 emission reduction in China from 2005 to 2013. *Energy Economics*, 60:15–22.

Quemada, J. M. M., García-Verdugo, J., and Escribano, G. (2012). *Energy security for the EU in the 21st century: markets, geopolitics and corridors*. Routledge.

Rademaekers, K., Slingenberg, A., and Morsy, S. (2008). Review and analysis of eu wholesale energy markets–historical and current data analysis of eu wholesale electricity, gas and co2 markets. *Final Report prepared for the European Commission DG TREN, Rotterdam*.

Raftery, A. E., Zimmer, A., Frierson, D. M., Startz, R., and Liu, P. (2017). Less than 2° C warming by 2100 unlikely. *Nature Climate Change*.

Reboredo, J. C. (2011). How do crude oil prices co-move?: A copula approach. *Energy Economics*, 33:95–113.

Rockafellar, R. T. and Uryasev, S. (2000). Optimization of conditional value-at-risk. *Journal of risk*, 2:21–42.

Ruiz, C. and Conejo, A. J. (2015). Robust transmission expansion planning. *European Journal of Operational Research, 242(2)*, pages 390–401.

Saida, A. B. and Prigent, J. (2018). On the robustness of portfolio allocation under copula misspecification. *Annals of Operations Research*, 262(2):631–652.

Schepsmeier, U. (2016). A goodness-of-fit test for regular vine copula models. *Econometric Reviews*, pages 1–22.

Schepsmeier, U. and Czado, C. (2016). Dependence modelling with regular vine copula models: a case-study for car crash simulation data. *Journal of the Royal Statistical Society: Series C (Applied Statistics)*, 65(3):415–429.

Schepsmeier, U., Stoeber, J., Brechmann, E. C., Graeler, B., Nagler, T., and Erhardt, T. (2018). *VineCopula: statistical inference of vine copulas*. R package.

Sciacovelli, A., Li, Y., Chen, H., Wu, Y., Wang, J., Garvey, S., and Ding, Y. (2017). Dynamic simulation of Adiabatic Compressed Air Energy Storage (A-CAES) plant with integrated thermal storage - Link between components performance and plant performance. *Applied Energy*, 185 Part 1:16–28.

Sengupta, M., Habte, A., Gotseff, P., Weekley, A., Lopez, A., Anderberg, M., Molling, C., and Heidinger, A. (2014a). A Physics-Based GOES Product for Use in NREL's National Solar Radiation Database. Technical Report NREL/CP-5D00-62776, National Renewable Energy Laboratory.

Sengupta, M., Habte, A., Gotseff, P., Weekley, A., Lopez, A., Molling, C., and Heidinger, A. (2014b). A Physics-Based GOES Satellite Product for Use in NREL's National Solar Radiation Database. Technical Report NREL/CP-5D00-62237, National Renewable Energy Laboratory.

Shahidehpour, M., Yamin, H., and Li, Z. (2003). *Market operations in electric power systems: forecasting, scheduling, and risk management*. John Wiley & Sons.

Sijm, J., Neuhoff, K., and Chen, Y. (2006). Co2 cost pass-through and windfall profits in the power sector. *Climate policy*, 6(1):49–72.

Silva, R. A., West, J. J., Lamarque, J.-F., Shindell, D. T., Collins, W. J., Faluvegi, G., Folberth, G. A., Horowitz, L. W., Nagashima, T., Naik, V., et al. (2017). Future global mortality from changes in air pollution attributable to climate change. *Nature Climate Change*.

Sioshansi, F. P. and Pfaffenberger, W. (2006). *Electricity market reform: an international perspective*. Elsevier.

Sioshansi, R. and Denholm, P. (2010a). The Value of Concentrating Solar Power and Thermal Energy Storage. Technical Report NREL/TP-6A2-45833, National Renewable Energy Laboratory.

Sioshansi, R. and Denholm, P. (2010b). The Value of Concentrating Solar Power and Thermal Energy Storage. *IEEE Transactions on Sustainable Energy*, 1:173–183.

Sioshansi, R., Denholm, P., and Jenkin, T. (2011). A Comparative Analysis of the Value of Pure and Hybrid Electricity Storage. *Energy Economics*, 33:56–66.

Sioshansi, R., Denholm, P., and Jenkin, T. (2012). Market and Policy Barriers to Deployment of Energy Storage. *Economics of Energy & Environmental Policy*, 1:47–63.

Sklar, M. (1959). Fonctions de repartition an dimensions et leurs marges. *Publ. inst. statist. univ. Paris*, 8:229–231.

Smith, M. and Castellano, J. (2015). Costs Associated With Non-Residential Electric Vehicle Supply Equipment: Factors to consider in the implementation of electric vehicle charging stations. Technical report, U.S. Department of Energy.

Snam (2016). *Annual Report*. Piazza Santa Barbara, 7 San Donato Milanese, Milan, Italy.

Stern, J. and Rogers, H. V. (2014). The dynamics of a liberalised european gas market: Key determinants of hub prices, and roles and risks of major players. Technical report, The Oxford Institute for Energy Studies.

Succar, S., Greenblatt, J. B., Denkenberger, D. C., and Williams, R. H. (2006). An Integrated Optimization Of Large-Scale Wind With Variable Rating Coupled To Compressed Air Energy Storage. In *Windpower 2006*, Pittsburgh, Pennsylvania. American Wind Energy Association.

Succar, S. and Williams, R. H. (2008). Compressed Air Energy Storage Theory, Resources, And Applications For Wind Power. Technical report, Princeton Environmental Institute.

Sun, K., Sarker, M. R., and Ortega-Vazquez, M. A. (2015). Statistical characterization of electric vehicle charging in different locations of the grid. *2015 IEEE Power & Energy Society General Meeting*.

Theisen, N. (2014). Natural gas pricing in the eu: From oil-indexation to a hybrid pricing system. Technical report, Regional Centre for Energy Policy Research.

Tissot, B. and Welte, D. (2012). *Petroleum formation and occurrence: a new approach to oil and gas exploration*. Springer Science & Business Media.

Tran, H. D., Pham, U. H., Ly, S., and T. Vo-Duy, T. (2017). Extraction dependence structure of distorted copulas via a measure of dependence. *Annals of Operations Research*, 256(2):221–236.

Turchi, C. S., Ma, Z., Neises, T. W., and Wagner, M. J. (2013). Thermodynamic Study of Advanced Supercritical Carbon Dioxide Power Cycles for Concentrating Solar Power Systems. *Journal of Solar Energy Engineering*, 135:041007.

UNFCCC (2015). *Paris Agreement*. United Nation Framework Convention on Climate Change.

Vaillancourt, K. (2014). Electricity Transmission and Distribution. Energy Technology Systems Analysis Program E12, International Energy Agency.

Vengosh, A., Warner, N., Jackson, R., and Darrah, T. (2013). The effects of shale gas exploration and hydraulic fracturing on the quality of water resources in the united states. *Procedia Earth and Planetary Science*, 7:863–866.

Von Meier, A. (2006). *Electric power systems: a conceptual introduction*. John Wiley & Sons.

Vuong, Q. H. (1989). Ratio tests for model selection and non-nested hypotheses. *Econometrica*, 57:307–333.

Wen, X., Wei, Y., and Huang, D. (2012). Measuring contagion between energy market and stock market during financial crisis: a copula approach. *Energy Economics*, 34:1435–1446.

Xunpeng, S. (2016). Gas and lng pricing and trading hub in east asia: An introduction. *Natural Gas Industry B*, 3:352–356.

Yafimava, K. (2014). Outlook for the long term contracts in a globalizing market (focus on europe). Technical report, The Oxford Insitute for Energy Studies.

Young, M. R. (1998). A minimax portfolio selection rule with linear programming solution. *Management science*, 44:673–683.

Zeng, B. and Zhao, L. (2013). Solving two-stage robust optimization problems using a column-and-constraint generation method. *Operation Research Letters, 41(5)*, pages 457–461.

Zhang, H., Baeyens, J., Degrève, J., and Cacères, G. (2013). Concentrated solar power plants: Review and design methodology. *Renewable and Sustainable Energy Reviews*, 22:466–481.

Zhang, X. and Conejo, J. A. (2018). Robust transmission expansion planning representing long- and short-term uncertainty. *IEEE Transactions on Power Systems, 33(2)*, pages 1329–1338.

Zugno, M. and Conejo, J. A. (2015). A robust optimization approach to energy and reserve dispatch in electricity markets. *European Journal of Operational Research, 247*, pages 659–671.